

AD-765 489

CRASHWORTHY LANDING GEAR STUDY

Norman S. Phillips, et al

Beta Industries, Incorporated

Prepared for:

Army Air Mobility Research and Development
Laboratory

April 1973

DISTRIBUTED BY:



National Technical Information Service
U. S. DEPARTMENT OF COMMERCE
5285 Port Royal Road, Springfield Va. 22151

AD 765489

AD

USAAMRDL TECHNICAL REPORT 72-61

CRASHWORTHY LANDING GEAR STUDY

By

Norman S. Phillips

Richard W. Carr

Richard S. Scranton

April 1973



EUSTIS DIRECTORATE

U. S. ARMY AIR MOBILITY RESEARCH AND DEVELOPMENT LABORATORY
FORT EUSTIS, VIRGINIA

CONTRACT DAAJ02-70-C-0055

BETA INDUSTRIES, INC.

DAYTON, OHIO

Approved for public release;
distribution unlimited.



Reproduced by
NATIONAL TECHNICAL
INFORMATION SERVICE
U.S. Department of Commerce
Springfield VA 22151

Unclassified

Security Classification

DOCUMENT CONTROL DATA - R & D

(Security classification of title, body of abstract and indexing annotation must be entered when the overall report is classified)

1. ORIGINATING ACTIVITY (Corporate author) Beta Industries, Inc. 2763 Culver Avenue Dayton, Ohio		2a. REPORT SECURITY CLASSIFICATION UNCLASSIFIED
3. REPORT TITLE CRASHWORTHY LANDING GEAR STUDY		2b. GROUP
4. DESCRIPTIVE NOTES (Type of report and inclusive dates)		
5. AUTHOR(S) (First name, middle initial, last name) Norman S. Phillips, Richard W. Carr, Richard S. Scranton		
6. REPORT DATE April 1973	7a. TOTAL NO. OF PAGES 206 202	7b. NO. OF REFS 42
8a. CONTRACT OR GRANT NO DAAJ02-70-C-0055	9a. ORIGINATOR > REPORT NUMBER(S) USAAMRDL Technical Report 72-61	
8b. PROJECT NO. 1F162203A529	9b. OTHER REPORT NO(S) (Any other numbers that may be assigned this report) BII 214-6	
10. DISTRIBUTION STATEMENT Approved for public release; distribution unlimited.		
11. SUPPLEMENTARY NOTES	12. SPONSORING MILITARY ACTIVITY Eustis Directorate U. S. Army Air Mobility Research and Development Laboratory Fort Eustis, Virginia	
13. ABSTRACT The purpose of the reported effort was twofold: (1) to develop rotary-wing landing gear concepts and criteria which, when applied, would lessen the magnitude of crash forces transferred to occupiable areas of helicopters involved in severe yet survivable accidents; (2) to use the concepts and criteria to design, fabricate, and test an experimental prototype skid landing gear system. Landing gear design criteria, crash criteria, energy-absorbing design criteria, and applicable specifications were collected and analyzed to establish the state of the art in the landing gear design and energy absorber design. Once this was accomplished, the data were used to develop preliminary design criteria and concepts for three classes of rotary-wing aircraft. The concepts were selected to be compatible with combined loads and various attitudes. The compilation of existing landing gear design criteria and the selection of practical energy-absorbing hardware provided data necessary to develop realistic concepts. Concepts were developed for medium cargo, utility, and light observation class vehicles. A concept compatible with the UH-1 was selected for design, fabrication, and test. The "additional" skid energy attenuation system and a test vehicle were fabricated and impact tested. The failure of the energy absorbers and structure to perform as predicted negated the results of the first test and eliminated further testing.		

DD FORM 1 NOV 65 1473

Unclassified

Security Classification

1a

Unclassified
Security Classification

14 KEY WORDS	LINK A		LINK B		LINK C	
	ROLE	WT	ROLE	WT	ROLE	WT
Helicopter Landing Gear Crashworthiness Energy Absorption Devices						

1b

Unclassified

Security Classification

3586-73



DEPARTMENT OF THE ARMY
U. S. ARMY AIR MOBILITY RESEARCH & DEVELOPMENT LABORATORY
EUSTIS DIRECTORATE
FORT EUSTIS, VIRGINIA 23604

This report was prepared by Beta Industries, Inc., under the terms of Contract DAAJ02-70-C-0055. The Eustis Directorate technical monitor for this contract was Mr. G. T. Singley III of the Military Operations Technology Division.

The objectives of the effort described herein were to:

1. Develop helicopter landing gear concepts and criteria which, when applied to Army helicopters, will serve to lessen the magnitude of crash forces transferred to the occupiable area of helicopters involved in survivable accidents without producing failure loading of the airframe.
2. Design, fabricate, and test a skid-type, crashworthy landing gear suitable for installation on the UH-1H helicopter, based on the development of the aforementioned criteria and concepts. The feasibility of the UH-1 crashworthy landing gear, as conceived, was not validated, primarily because of its failure to pass the dynamic (drop) test.

This report has been reviewed by the Eustis Directorate, U.S. Army Air Mobility Research and Development Laboratory and is published for information and the stimulation of ideas relative to crashworthiness design.

Project 1F162203A529
Contract DAAJ02-70-C-0055
USAAMRDL Technical Report 72-61
April 1973

CRASHWORTHY LANDING GEAR STUDY

Final Report

Beta Industries Report BII 214-6

By

Norman S. Phillips
Richard W. Carr
Richard S. Scranton

Prepared by

Beta Industries, Inc.
Dayton, Ohio

for

EUSTIS DIRECTORATE
U.S. ARMY AIR MOBILITY RESEARCH AND DEVELOPMENT LABORATORY
FORT EUSTIS, VIRGINIA

Approved for public release;
distribution unlimited.

SUMMARY

The purpose of the reported effort was twofold: (1) to develop rotary-wing landing gear concepts and criteria which, when applied, would lessen the magnitude of crash forces transferred to occupiable areas of helicopters involved in severe but survivable accidents; (2) to use the concepts and criteria to design, fabricate, and test an experimental prototype skid landing gear system.

The program was conducted in several phases. Landing gear design criteria, crash criteria, energy-absorbing design criteria, and applicable specifications were collected and analyzed to establish the state of the art in landing gear design and energy-absorber design.

Once this was accomplished, the data were used to develop preliminary design criteria and concepts for three classes of rotary-wing aircraft. The concepts were selected to be compatible with combined loads and various attitudes. The final phase consisted of fabricating and drop testing a skid-type crash force attenuation landing gear system.

The compilation of existing landing gear design criteria and the selection of practical energy-absorbing hardware provided data necessary to develop realistic concepts. Concepts of energy-absorbing landing gear were developed for medium cargo (CH), utility (UH), and light observation (LOH) class vehicles. Because it appeared conceptually better to add more independent energy attenuation capability rather than incorporate that capability into the existing skid configuration, the UH-1 concept selected for design, fabrication, and test was that of an "additional" skid beneath the fuselage.

The UH-1 energy attenuation system and test vehicle were fabricated and impact tested. The failure of the energy absorbing system to perform as predicted and a consequent structural failure of the vehicle negated the results of the first test and resulted in discontinuance of further testing. A trade-off study using impact criteria and hardware design data led to the conclusion that this energy-absorbing landing gear skid concept is practical only at higher impact velocities than originally assumed.

FOREWORD

This report was prepared for the Eustis Directorate of the U.S. Army Air Mobility Research and Development Laboratory, Fort Eustis, Virginia, by Beta Industries, Inc., Dayton, Ohio. The research was conducted under Contract DAAJ02-70-C-0055, Project 1F162203A529.

The effort was concerned with the improvement of landing gear design criteria as a portion of the overall problem of improved helicopter crashworthiness. Many individuals contributed to the initial phase of the program. Landing gear, airframe, and energy-absorber manufacturers, Governmental agencies concerned with landing gear systems and criteria, and many others concerned with crash safety contributed to the collection of the initial criteria.

TABLE OF CONTENTS

	<u>Page</u>
SUMMARY	iii
FOREWORD	v
LIST OF ILLUSTRATIONS	x
LIST OF TABLES	xiii
LIST OF SYMBOLS	xiv
CHAPTER 1. INTRODUCTION	1
CHAPTER 2. PHASE I -- STATE OF THE ART SURVEY	2
2.1 INTRODUCTION	2
2.2 INITIAL RESEARCH AND DATA SURVEY	2
2.2.1 Review of Crash Survival Design Guide	2
2.2.2 Literature Surveys	3
2.2.3 Government and Industry Survey	3
2.2.4 Periodicals and Research Reports Researched	4
2.2.5 Personal Contacts	4
2.3 LANDING GEAR DESIGN AND DESIGN CRITERIA	4
2.3.1 Industrial Survey Results	4
2.3.2 Landing Gear Design	8
2.3.2.1 Oleo-Strut Wheel Landing Gear Design	12
2.3.2.2 Skid Landing Gear Design	16
2.3.3 Landing Gear Design Summary	19
2.4 ENERGY-ABSORBER DESIGN ANALYSIS	19
2.4.1 Energy-Absorber Criteria	19
2.4.2 Survey Results	20
2.4.2.1 Energy-Absorber Manufacturers	20
2.4.2.2 Government Agencies	20
2.4.2.3 Design and Analytical Techniques	20
2.4.2.3.1 Compressible Tube Energy Absorber	21
2.4.2.3.2 Tube Flare	22
2.4.2.3.3 Frangible Tube Energy Absorber	25
2.4.2.3.4 Crushable Honeycomb Energy Absorber	25
2.4.2.3.5 Invertube Energy Absorber	25
2.4.2.3.6 Liquid Spring Energy Absorber	26
2.4.2.3.7 Cyclic Strain Energy Absorber	28
2.4.2.4 Energy-Absorber Data Summary	29
2.5 CRASH KINEMATICS	29
2.5.1 Crash Impact Accelerations and Velocities	30
2.5.2 Aircraft Impact Attitudes	33
2.6 PHASE I -- SUMMARY	34

Table of Contents (Cont'd)

	<u>Page</u>
CHAPTER 3. PHASE II ENERGY ABSORBING LANDING GEAR	
CRITERIA AND CONCEPTS	35
3.1 INTRODUCTION	35
3.2 ENERGY-ABSORBING LANDING GEAR DESIGN CRITERIA	35
3.3 HELICOPTER CONFIGURATION DATA	41
3.4 CONCEPT DEVELOPMENT	45
3.4.1 Medium-Cargo Configuration	45
3.4.1.1 Baseline Design	45
3.4.1.2 Concepts for Attenuation of Vertical Crash Loads	49
3.4.1.3 Energy Absorption Techniques	51
3.4.1.3.1 Collapsible Tube	53
3.4.1.3.2 Cyclic Strain Device	53
3.4.1.3.3 Liquid Spring	56
3.4.1.3.4 Comparative Data	56
3.4.1.4 Concept Variations	59
3.4.1.5 Drag and Side Load Effects	67
3.4.1. Summary	69
3.4.2 Utility-Class Configuration	71
3.4.2.1 Baseline Design (Figure 18)	71
3.4.2.2 Concepts for Attenuation of Vertical Crash Loads	73
3.4.2.2.1 Concept 1 (Figure 19)	73
3.4.2.2.2 Concept 2 (Figure 20)	73
3.4.2.2.3 Concept 3 (Figure 21)	73
3.4.2.2.4 Concept 4 (Figure 22)	78
3.4.2.2.5 Concept 5 (Figure 23)	78
3.4.2.3 Loading Condition Effects on Design	78
3.4.2.4 Plasticity Effects and Skid Stiffness	93
3.4.3 LOH Class Concepts	97
3.4.4 Concept Development Summary	100
3.5 COMPUTER PROGRAM DEVELOPMENT	100
3.6 PHASE II SUMMARY	109
CHAPTER 4. PHASE III ENERGY-ABSORBING UH-1 LANDING	
GEAR DESIGN, FABRICATION, AND TEST	112
4.1 INTRODUCTION	112
4.2 FAILURE ANALYSIS	112
4.3 SKID LANDING GEAR DESIGN	113
4.3.1 Skid Design for Normal Landing Conditions	113
4.3.2 Skid Design for Crash Impact	116
4.4 DATA REQUIREMENTS	130
4.4.1 Calibration Procedures	130
4.4.2 Multiple Oscillographs	130

Table of Contents (Cont'd)

	<u>Page</u>
4.4.3 Data Reduction	131
4.5 DYNAMIC TESTS	131
4.5.1 General Procedure	131
4.5.2 Test Results	132
4.6 TRADE-OFF STUDIES	133
4.6.1 Parameter Selection	133
4.6.2 Trade-Off Data Required	135
4.6.2.1 Conventional Skid	135
4.6.2.2 Energy-Absorbing Landing Gear Skid	139
4.6.2.3 Energy-Absorber Weight	146
4.6.2.4 Structural Weight of Fuselage	146
4.6.2.5 Seat Structure and Attenuators	148
4.6.3 Calculation Techniques and Resulting Data	148
4.6.4 Trade-off Data Analysis	152
CHAPTER 5 CONCLUSIONS AND RECOMMENDATIONS	160
5.1 CONCLUSIONS	160
5.1.1 Landing Gear Specifications	160
5.1.2 Energy-Absorbing Devices	160
5.1.3 Energy-Absorbing Landing Gear Concepts	160
5.1.4 Trade-Off Analysis	161
5.2 RECOMMENDATIONS	162
LITERATURE CITED	163
APPENDIX I TEST VEHICLE DESIGN	167
APPENDIX II TEST PARAMETERS MEASURED	174
APPENDIX III COMPUTER PROGRAM DESCRIPTION	181
DISTRIBUTION	192

LIST OF ILLUSTRATIONS

<u>Figure</u>		<u>Page</u>
1	Distribution of Average Acceleration in the Vertical, Longitudinal, and Lateral Directions	32
2	Distribution of Vertical, Longitudinal, and Lateral Impact Velocity Changes for Survivable Rotary and Light Fixed-Wing Aircraft Accidents (from Crash Survival Design Guide)	32
3	Basic Helicopter Dimensions	43
4	Medium-Cargo Configuration	48
5	Configuration Prior to Energy Absorption	50
6	Compressed Upper Strut Concept	52
7	TOR-SHOK Data, ARA Design Curves	54
8	TOR-SHOK Data, ARA Design Curves	55
9	Parallel and Series Hardware Designs	57
10	Extended Lower Strut Concept	60
11	Extended Middle Strut Concept	61
12	Extended Attachment Point Concept	63
13	Compressed Upper Attachment Point Concept	64
14	Multiple Energy Paths Concept	65
15	Developed Forces Concept	66
16	Developed Force Concept - Both Element, Stroke	68
17	Combined Loads Distribution	70
18	Utility Class Configuration	74
19	Rigid Link Concept	75
20	Energy-Absorbing Strut Concept	76
21	Crushable Skid Concept	77
22	Lever Mechanism Concept	79
23	Cantilever Energy Absorbers Concept	80

LIST OF ILLUSTRATIONS (Cont'd)

<u>Figure</u>	<u>Page</u>
24 UH-1F Configuration Approximation	83
25 Statically Determinate Structure	85
26 Applied Redundancies	86
27 Variation of Fuselage Bending Moment With Location of Applied Vertical Force of 1,000 Pounds	87
28 Secondary Configuration Determinate Reaction	88
29 Loads Due to Vertically Applied 1000 Pounds	90
30 Effects of Drag Force	91
31 Effects of Combined Loads at the Tip	92
32 Vertically Loaded Tip Distribution	94
33 LOH Configuration	98
34 Compressible Strut Concept	99
35 Helicopter Landing System Model	101
36 Landing Component Vector System	103
37 Pure Vertical Response Symmetrical Stiffness	107
38 Pure Vertical Drop Asymmetrical Stiffness	108
39 Load vs. Deflection	117
40 Vertical Impact	127
41 Energy Absorbing System	129
42 Energy Dissipation Curves	138
43 Skid Weight vs. G Limit	140
44 E/A Skid Weight vs. E/A Force (Total)	143
45 E/A Force (Total on Added Structure)	145
46 E/A Force vs. Stroke	147

LIST OF ILLUSTRATIONS (Cont'd)

<u>Figure</u>		<u>Page</u>
47	Calculation Procedure	149
48	Weight Variations vs. Attitude	153
49	Weight Variations of Minimum Weight Systems	154
50	Weight Penalty vs. Velocity and Attitude	156
51	Truss Configuration	171
52	Final Vehicle Configuration	172
53	Instrumentation System	179

LIST OF TABLES

<u>Table</u>		<u>Page</u>
I	Survey Results	5
II	Landing Gear Design Criteria (Limit Loads)	9
III	Material Properties	23
IV	Compilation of Data	24
V	Impact Criteria for Energy Absorbing Landing Gear	41
VI	Data on Helicopter Landing Gear	44
VII	Typical Values of Moments of Inertia	45
VIII	Comparative Data for Energy Absorber Techniques	58
IX	Element Loads, Selected Inputs	70
X	Planned Impact Tests	131

LIST OF SYMBOLS

A_h	hydraulic area, in. ²
C	slope of elastic load deflection curve, lb/in. ²
C_1	slope of plastic load deflection curve, lb/in. ²
D	drag, lb
D	diameter, in.
E	Young's Modulus, lb/in. ²
E_α	absorbed energy, ft-lb
E_τ	tire energy, in.-lb
F_B	bearing force, lb
F_F	frictional force, lb
F_H	hydraulic force, lb
F_v	vertical force, lb
G_d	orifice coefficient
H	average slope of the stress-strain curve in the plastic region, lb/in. ²
J	moment of inertia, lb-ft-sec
K	stiffness, lb/in.
L	lift, lb
M	moment, in.-lb
N_Z	vertical load factor, body axis system
N_v	vertical load factor, earth axis system
P	pressure lb/in. ²
P	angular velocity about the X axis, rad/sec
Q	angular velocity about the Y axis, rad/sec

List of Symbols (Cont'd)

q	influence coefficient
R	angular velocity about the Z axis, rad/sec
S	stroke, in.
T	time duration of a pulse, sec
t	wall thickness, in.
U	energy, in.-lb
V	impact velocity, ft/sec
V	specific volume, in. ³ /lb-mass
V _A	auxiliary gear vertical force, lb
V _M	main gear vertical force, lb
W	weight, lb
W	frequency, rad/sec
X	dimension along longitudinal axis
V	dimension along lateral axis
β	tube bending factor
ΔT	pulse duration, sec
ΔV	velocity change, ft/sec
δ	deformation
δ _g	deformation due to oleo movement, in.
δ _m	deformation of vehicle, in.
δ _y	deformation at elastic limit, ft
η	efficiency
θ	pitch angle, rad

List of Symbols (Cont'd)

μ	coefficient of friction
ρ	density, lbm/in. ³
σ	stress, lb/in. ²
σ_y	yield stress, lb/in. ²
ϕ	roll angle, rad
ψ	yaw angle, rad

CHAPTER 1 INTRODUCTION

The objective of the total program was twofold. First, it was desired to develop rotary-wing landing gear concepts and criteria which, when applied to Army helicopters, will lessen the magnitude of the crash forces transferred to the occupiable areas of helicopters involved in severe but survivable accidents without producing failure loading on the airframe. Secondly, based upon the developed concepts and criteria, a skid-type landing gear was to be designed, fabricated and tested to demonstrate the validity of the approach.

The program consisted of three phases. The first phase investigated and evaluated the state of the art of landing gear design and design criteria, and design and design criteria of energy-absorbing devices. Before improvements are made in the crashworthiness of helicopters by improved landing gear concepts, it is necessary to be knowledgeable about current landing gear design criteria and design practices. Several questions need to be answered. How many conditions influence the design of the landing gear? Does a landing load generate the most severe stress with least margin of safety? What type of device is a landing gear? Is the design of an elastic tire, viscoelastic shock strut and elastic wing amenable to simplified analysis? What initial conditions exist before a landing? What is a reasonable sink rate at touchdown? What force levels are permissible with a given energy-absorber type for a specific stroke length? In order to develop practical energy-absorbing landing gear designs and concepts, reasonable and realistic quantitative data must be available to infer the practical and theoretical limits of the concepts.

The purpose of the second phase was to develop feasible design criteria and concepts for energy-absorbing landing gear designs for three classes of U.S. Army helicopters. The results of Phase I were applied to develop skid type concepts for LOH and UH helicopter classes, and one wheel-type concept was developed for the CH class helicopter. The concepts developed were capable of attenuating crash forces transmitted in upward, aftward, and sideward directions. Additional design factors such as simplicity, weight, and cost were considered during this phase.

The last phase required demonstration of the feasibility of one concept by designing, fabricating, instrumenting, and testing a skid-type crash force attenuating landing gear system for the UH-1H helicopter. The data developed were used to examine the established criteria and to conduct a trade-off study of weight versus performance for that skid concept.

CHAPTER 2
PHASE I - STATE-OF-THE-ART SURVEY

2.1 INTRODUCTION

The specific goals of Phase I were:

1. Review the Crash Survival Design Guide.
2. Conduct a literature search and investigation into the state of the art of landing gear design and criteria, and characteristics of load-limiting devices.
3. Consider landing gear operational and crash environments.
4. Evaluate five types of load-limiting devices: rolling torus, liquid spring, compression of honeycomb, inverted tubes, tube flaring.
5. Consider seven sources of information: The U.S. Army Agency for Aviation Safety (USAAAVS), airframe manufacturers, load-limiting device manufacturers, appropriate governmental agencies, military standards and specifications, and landing gear manufacturers.

2.2 INITIAL RESEARCH AND DATA SURVEY

2.2.1 Review of Crash Survival Design Guide¹

The Crash Survival Design Guide was reviewed as a means of becoming familiar with the subject of energy-absorbing landing gear and becoming aware of the crashworthiness philosophy that is the basis for improving landing gear design. Reference 1 notes that the landing gear is an important means of attenuating vertical impacts and that there is the potential ability to dissipate impact velocities far greater than currently considered; however, it is not pointed out how a landing gear system behaves as a function of input conditions nor is it pointed out for what conditions a landing gear is designed relative to a crash design consideration. It is possible to say that improvements can be made, but difficult to say whether the improvement is significant and acutely dependent upon the input conditions.

The primary results of the review were to recognize that human tolerance data are available and statistical information is available for crash input accelerations and velocities. Analysis methods are recommended, and the philosophy of crashworthiness design is presented.

One of the most important results of the review was the recognition that a significant amount of research must yet be done in the area of energy-absorbing landing gear in order to realistically evaluate the potential that exists.

2.2.2 Literature Surveys

Several literature searches were initiated at the beginning of the program. Fifty-six reports were compiled from the Defense Documentation Center (DDC) in the area of landing gear and approximately eight hundred relative to energy-absorbing devices. The Department of Commerce Clearinghouse supplied 15 landing gear and 7 energy-absorber reports, and 47 current research projects on landing gear and 12 on energy absorbers were supplied by the Smithsonian Information Exchange.

The data collected were reviewed and pertinent reports were ordered through the appropriate agency.

2.2.3 Government and Industry Survey

Letters were sent to the following landing gear manufacturers, energy-absorber manufacturers, airframe manufacturers, and governmental agencies. The companies and agencies contacted were:

Major Airframe Manufacturers

Beech Aircraft Corp.
Bell Helicopter Company
Del Mar Engineering Labs
Fairchild Hiller Corp.
Gates Learjet Corp.
Gyrodyne Company of America
Hughes Tool Co., Aircraft Div.
Kaman Aircraft Corp.
Lockheed California Co.
Piasecki Aircraft Co.
Sikorsky Aircraft Division
Vertol Division, Boeing Co.

Energy-Absorber Manufacturers

Aerospace Research Assoc.
All American Engineering
American Chain & Cable
Arde
Engineering Design Services
General Motors Research Lab
Hardman Aerospace
Houdaille, Hydraulics Div.
Integrated Dynamics, Inc.
Mechanical Research, Inc.
Taylor Devices, Inc.
U.O.P., Aerotherm Div.

Landing Gear Manufacturers

All American Engineering
Bell Helicopter Company
Bendix Energy Control Div.
Cleveland Pneumatic Tool Co.
Goodyear Aerospace Corp.
Houdaille, Hydraulics Div.
I.C.C. Special Corp.
Menasco Manufacturing Co.
Royal Industries, Inc.
Vertol Division, Boeing Co.

Governmental Agencies

Federal Aviation Agency
NASA, Ames Research Center
(Energy Absorbers)
National Transportation Safety
Board
Naval Air Development Center
USAF Aeronautical Systems Div.
USAF Flight Dynamics Laboratory
U.S. Army Aeromedical Research
Laboratory
U. S. Army Agency for Aviation
Safety

2.2.4 Periodicals and Research Reports Researched

All post World War II NASA and NACA reports were scanned for pertinent data. The Journals of the American Helicopter Society were reviewed, as were the International Aerospace Abstracts and the Engineering Indexes.

2.2.5 Personal Contacts

At the beginning of the program it was realized that good technical quantitative data would be difficult to obtain for Army helicopters. Since the helicopters were designed under ANC-2, or were direct purchase items, there were no reports necessarily required to prove the design and present the analysis. For this reason, contacts were made at Wright-Patterson Air Force Base to locate reports which are required for Air Force helicopters purchased under MIL-S-8698. These efforts led to the review of CH-53, UH-1F, and HH-43 reports at Warner-Robins Air Force Base.

2.3 LANDING GEAR DESIGN AND DESIGN CRITERIA

2.3.1 Industrial Survey Results

Twelve airframe and nine landing gear manufacturers were surveyed. At the end of Phase I, eight airframe manufacturers and seven landing gear manufacturers had responded. Of these, two airframe companies indicated they could not or would not help, and two landing gear manufacturers did not provide quantitative data. The results of the survey are shown in Table I.

Several manufacturers indicated areas where the questions did not apply (DNA). As an example, a manufacturer of landing gears was not concerned with a dynamic analysis since the major airframe contractor supplied all design specifications. No dynamic analysis by the landing gear subcontractor was required. Similarly, if no dynamic analyses were conducted, no comparisons could be made. Lastly, cost guidelines would not influence the design specifications of the landing gear manufacturers, if the design were that of the prime airframe manufacturer.

The overall results are rather surprising considering the state of the art of landing gear analysis techniques. The specifications called out establish helicopter design criteria, landing gear criteria, and test requirements. Additionally, there are general information types of specifications such as the HIAD and U.S.N. SD-24J. The surprising aspects are those related to the dynamics aspects of the helicopter/landing gear system. In only one case was the landing gear force displacement profile considered as an input requirement. In only two cases were crash loads considered; one of these was the FAA requirement for fuselage crash accelerations which is so low that they are unrealistic for crash acceleration inputs to the landing gear. As an example, the emergency landing conditions of Federal Aviation

TABLE I. SURVEY RESULTS

	Manufacturer							
	1	2	3	4	5	6	7	8
1. Criteria								
(a) What specifications were followed?								
MIL-A 8860 Series	x							x
MIL-S-8698	x	x		x	x		x	x
MIL-S-8552	x						x	x
MIL-E-5272	x							
MIL-T-8679		x						
FAR 29	x		x		x	x		
HIAD		x						
SD-247 (Navy)		x						
AR-56 (Navy MIL S-8698)		x						
(b) Were force-displacement or force-time profiles specified?	No	No	No	No	Yes	No	No	No
(c) Were crash loads specified?	No	No	No	No	Yes	Yes	No	No
2. Design and Analysis								
(a) Was a complete dynamic analysis conducted?	DNA	No	No	Yes	Yes	No	No	No
(b) If not, were dynamics considered?		No	No		Yes	Yes	Yes	Yes
(c) Was there crash analysis?		No	No	No	Yes	Yes	No	No
3. Test Data								
(a) Was a full-scale test conducted?	Yes	Yes	No	Yes	Yes	Yes	Yes	Yes
(b) How did data compare with analysis, favorably?	Yes	DNA		Yes	Yes	Yes	Yes	Yes
4. Cost Information								
(a) Are cost guidelines available?	DNA	DNA	None	None	None	None	Yes	Yes
NOTE: DNA - Questions did not apply								

Regulations Part 29 states that the design downward deceleration level is 4.0G. Only two manufacturers conducted a complete dynamic analysis to determine the mutual response of vehicle and landing gear. The others who considered dynamic response used the techniques suggested in ANC-2 and MIL-A-8862 to evaluate spin-up and spring-back. Apparently, the acceptability of the landing gear system is based upon the full-scale test. The peak acceleration of the payload must fall below a specified limit, and the efficiency of the force-displacement profile must be greater than a specified limit. The end product always provided data indicating a conservative design. Cost information is limited primarily because the manufacturer emphasizes that the weight of the landing gear is the dominant factor. Some trade-off may have been made in preliminary design, but generally weight overshadows cost consideration.

Several of the primary specifications will be briefly reviewed to indicate their scope.

1. MIL-S-8698, Structural Design Requirements, Helicopters.
Definitions are established for strength, factor of safety, gross weights, and load factors. Ground loading conditions are specified in terms of landing parameters, landing conditions, taxiing and ground handling, and crash landing. Most of the conditions to be examined are directly related to ANC-2 requirements. The ultimate inertia-load factors for crash landing are not specified, but it is inferred that they will be specified by the procuring agency.
2. ANC-2, Ground Loads
This bulletin is the basis for all subsequent ground loads data and its content is similar to that of MIL-S-8698. However, ANC-2 also presents acceptable means of calculating dynamic landing loads. The analyses are based upon a specified maximum inertial load factor and a half-sine acceleration pulse input.
3. MIL-A-8862, Airplane Strength and Rigidity Landplane Landing and Ground Handling Loads.
Definitions and ground load conditions are similar to previous specifications, and included within this is the dynamic analysis technique specified in ANC-2.
4. MIL-L-8552-C, Landing Gear Aircraft Shock Absorber (Air-Oil Type).
The primary contribution of this specification to this effort is the definition of landing gear efficiency. The percent efficiency is the total energy absorbed divided by the product of peak force and peak stroke. The load factor produced during testing is not to be greater than that specified for the particular aircraft.

5. MIL-T-6053B, Tests, Impact, Shock Absorber, Landing Gear, Aircraft

The purpose of this specification is to standardize impact testing procedures on landing gear shock absorbers. Design landing tests, miscellaneous landing tests, airplane growth tests, and reserve energy tests are specified. Each helicopter has a specified weight, sink rate, attitude, wheel speed, strut pressure, and oil volume. The "adjusted mass" method of testing is defined in this specification.

6. Federal Aviation Regulations, Part 27, Normal Category Rotorcraft, and Part 29, Transport Category Rotorcraft.

Strength requirements and design and construction considerations are specified for wheel and skid-type landing gear. Assumptions, landing conditions, and test requirements are defined.

The specifications listed impose many design conditions upon the landing gear. These can be categorized into towing, taxiing, jacking, securing, and landing loads. The first four conditions are found in Table III of MIL-A-8862 and appropriate chapters of ANC-2.

The criteria that dictate the design of a landing gear for landing loads are so extensive that it is necessary to tabulate the many conditions as shown in Table II. Two conditions may be redundant. That is, the obstruction loads are in place of the drift loads if MIL-S-8698 is followed. If we consider the first 7 conditions as being those specified (the CH-46D was so designed), there are 36 different sets of forces assuming only one sink rate, one gross weight, and one strut extension length for each condition.

The specifications examined to this point indicate that there are 92 conditions that dictate the design limit loads for one landing gear. Not to be ignored are the criteria for skid-type landing gear. The detailed criteria come from ANC-2 (Chapter 6), FAR 29.501, and FAR 27.501. The former requires examination of a level landing with a vertical component and a rearward component acting through the center of the skid's contact area. The rearward component is one-half the magnitude of the vertical. Another condition has similar forces, but the rearward component is replaced by a lateral force. The last condition is a 15-degree nose down with ground reactions applied through the most forward point suitable for application of the force.

The Federal Air Regulations are most extensive in that they specify one skid landing loads and two special conditions. Side loads are one-quarter instead of one-half of the vertical force, and the forces are distributed over the surface of one skid only. The special conditions are an oblique load at 45 degrees to the longitudinal axis acting up and aft, and an examination of the vertical ground reaction applied at the skid tube fuselage

attachment and the midpoint of the skid. The ultimate loads are dictated by a drop height of 1.5 times that of the conventional landing gear specification and an assumed rotor lift limit of not more than 1.5 times the conventional requirement.

2.3.2 Landing Gear Design

It appears that there is a vast amount of direction for calculating the loads generated in a landing gear. There are strut extensions, gross weights, sink rates, rotor lift values, orientations, and many other specified aspects. However, they are all still not sufficient to calculate the first landing impact load. The specifications always referred to a maximum vertical reaction, or a maximum inertial load factor, or an acceleration maximum that would initiate the analysis. Where does this key quantity come from? The answer is within the specifications, but not quantitatively. ANC-2 states that "the ground reaction factors, N_{\dots} shall be specified by the procuring service . . .". This is not clarified in MIL-S-8698. The Federal Air Regulations state that "the landing inertial load factor . . . must be substantiated by tests"; the load factor is not specified.

The basic problem was that of determining the forces and accelerations throughout an elastic system without conducting a dynamic analysis. The results of the industrial survey indicated that a dynamic analysis was generally not conducted, and the dynamic analysis techniques of ANC-2 (Chapter 7) are not capable of defining impact inputs. However, essentially three approaches are currently taken and one other exists.

The first approach is that of accepting a specified acceleration level. In the detailed specification for a helicopter procurement, the manufacturer or the procuring agency may specify that an inertial acceleration level is realistic based upon previous test results and design experience. If the acceleration level is specified and the mass of the vehicle is known, the force the landing gear carries is easily calculated, and this is the maximum force that provides the basis for all other drag and side forces.

Another similar approach is to use the fuselage design load factor. MIL-S-8698 specifies a maximum acceleration of 3.5 for Class 1 helicopters. If this is used to specify the peak fuselage acceleration permitted by the landing gear, then the dynamics have again been eliminated from the design. The landing gear manufacturer again knows the weight supported by the landing gear and therefore can calculate the peak force that the strut must carry.

An energy approach is also used. The relation between potential energy and kinetic energy before and after a given drop condition can provide an acceleration level if an oleo efficiency is assumed. Since the oleo must, by specification, eventually achieve a given level, it is reasonable to assume that a value can be specified. The basic equation is

No.	IA	IB	IC	IIA	IB	IIIC	IIIA	IIIB	IIIC	IV A										
	Level Landing, Two Wheel (1)			Three Point Landing (1) (10)			One Wheel Landing													
Condition	Max. Spin-Up	Dynamic Spring-Back	Max. Vertical Reaction	Max. Spin-Up	Dynamic Spring-Back	Max. Vertical Reaction	Max. Spin-Up	Dynamic Spring-Back	Max. Vertical Reaction											
Ref. Spec. & Para.	ANC-2 2.21 2.312	ANC-2 2.22 2.312	ANC-2 2.23 2.312	ANC-2 2.21 2.311	ANC-2 2.22 2.311	ANC-2 2.23 2.311	ANC-2 2.21 2.314	ANC-2 2.22 2.314	ANC-2 2.23 2.314	Fwd.										
Main Gear V_M Loading D_M (Each S_M Gear) (5)	(2)	(2)	nWg $1/4 V_M$ and zero	(2) and (8)	(2) and (8)	$n/2 W_L^b$ $1/4 V_M$ and zero	(2)	(2)	nWg $1/4 V_M$ and zero	nWg $-1/2 V$										
Nose V_A Loading D_A (5) S_A				(2) and (8)	(2) & (8)	$nW_L^b + \frac{e}{4d}$ $1/4 V_A$														
Load is applied at	$\frac{C}{A}$ Axle	$\frac{C}{A}$ Axle	$\frac{C}{A}$ Axle	$\frac{C}{A}$ Axle	$\frac{C}{A}$ Axle	$\frac{C}{A}$ Axle	$\frac{C}{A}$ Axle	$\frac{C}{A}$ Axle	$\frac{C}{A}$ Axle	$\frac{C}{A}$ Axle										
Ship Attitude	Auxiliary Gear Just Clear of Ground			Three Point			Auxiliary Gear Just Clear of Ground													
SYMBOLS:																				
a = distance between c. g. and main gear reaction parallel to ground line.																				
b = distance between c. g. and auxiliary gear reaction parallel to ground line.																				
d = distance between main and auxiliary gear reaction points parallel to ground line.																				
e = distance between c. g. and axle center line perpendicular to ground line.																				
V_M or V_A = vertical gear load (main or auxiliary) perpendicular to ground line, positive up.																				
D_M or D_A = drag gear load (main or auxiliary) in the forward or aft direction parallel to the ground line, positive aft.																				
S_M or S_A = side gear load (main or auxiliary) in the lateral direction parallel to the ground line, positive when outboard.																				
n = Landing gear load factor; the ratio of the vertical ground reaction on any gear to the effective weight over the gear during landing impact.																				
W_L = Landing gross weight or alternate design.																				
W_g = Effective weight over any gear during landing impact.																				
NOTES:																				
1. FAR 27 h FAR 29 d of opti																				
2. The inertial MIL-S 6 ft/sec height drop h																				
3. DM and S																				
4. Auxiliary positio																				
5. All loads back 1																				

B

TABLE II. LANDING GEAR DESIGN CRITERIA (LIMIT LOADS)

(Ref. Para. 3.4 of MIL-S-8698, Chapter 2 of ANC-2
and FAR 27, Para. 27.485)

IV B	IV C	IV D	VA	VB	VC	VI	VII	VIII A	VIII B	VIII C
Main Gear Obstruction Loads (Notes 3 and 6)	Nose Gear Obstruction Loads (Notes 4 and 6)				Tail (6) Down	Nose (6) Down		Max. Spin- Up	Drift Lan	
	Aft	Inboard	Outboard	Fwd.	Aft.				Dynamic Spring Back	Max. (6) Vertical Reaction
MIL-S-8698 3.4.5.1			MIL-S-8698 3.4.5.2			ANC-2 2.313	MIL-S-8698 3.4.5.3	ANC-2 2.315	ANC-2 2.315	ANC-2 2.315
V_M	nWg $1/2 V_M$	nWg	nWg				nWg (9)	(9)	nWg Zero $0.6V_M(O)$ $0.8V_M(I)$	nWg zero $0.6V_M$ outbd. $0.8V_M$ inbd.
				$nW_L \frac{a}{d}$ $-.5V_A$	$nW_L \frac{a}{d}$ $.5V_A$	$nW_L \frac{a}{d}$ $\pm .5V_A$		$nW_L \frac{a}{d}$		
	\underline{C} Axe	Ground Line	Ground Line	\underline{C} Axe	\underline{C} Axe	\underline{C} Axe or G. L	\underline{C} Axe	\underline{C} Axe	Ground Line	Ground Line
Auxiliary Gear Just Clear of Ground			Main Gear Just Clear of Ground			Max. Nose Up	Main Gear Just Clear of Ground	Main Gear Contact Ground	Level Main Gear Contact Ground	

NOTES: (Cont'd.)

6. Unbalanced moments
7. Critical center-of-gravity for each landing gear
8. The rate-of-descent envelope with one load factor vs horizontal acting thrust. There is some conflict, but it appears the forward zero drag force, and ground reactions.
9. If there should be two, would require examination.
10. If there should be two, would require examination.

has neither a spin-up or dynamic spring-back condition.

does recognize spin-up loads and requires use of a ground speed that is 75 percent optimum forward speed for minimum rate of descent in autorotation.

ital loads are calculated based upon specified sink rates and rotor life values.

-S-8698 states 8 ft/sec, rotor lift of 2/3 basic design gross weight and alternately 8 sec with rotor lift of 2/3 design alternate gross weight. FAR 27 requires a drop test of 13 inches with 2/3 gross weight rotor lift. FAR 29 requires at least 8 inches height.

S_M are applied to one gear at a time. The opposite gear is loaded with V_M .

ny gear are swiveled in the direction of the transverse loads or locked in the aft position.

Is are applied throughout the entire vertical travel except that spin-up and spring-back loads are combined with the vertical load at the time of max forward or aft load.

A (LIMIT LOADS)

MIL-S-8698, Chapter 2 of ANC-2

ca. 27.485)

VC	VI	VII	VIII A	VIII B	VIII C	VIII D	VIII E
ands 3) ide	Tail (6) Down	Nose (6) Down	Max. Spin- Up	Dynamic Spring Back	Max. (6) Vertical Reaction	Drift Landing	
8	ANC-2 2.313	MIL-S-8698 3.4.5.3	ANC-2 2.315	ANC-2 2.315	ANC-2 2.315	FAR 27 27.485 FAR 29 29.485	FAR 27 27.485 FAR 29 29.485
	nWg (9)	(9)	nWg Zero 0.6V _M (O) 0.8V _M (I)	nWg zero 0.6V _M outbd. 0.8V _M inbd.			
^a W _{Ld}		^a nW _{Ld}				nWg zero 0.8V _m	
5V _A							
Axle or L	<u>C</u> Axe	<u>C</u> Axe	Ground Line	Ground Line	Ground Line	Ground Line	Ground Line
ast d	Max. Nose Up	Main Gear Just Clear of Ground	Level Main Gear Contact Ground		Three Point	Aux. Just Clear	

NOTES: (Cont'd.)

6. Unbalanced moments are reacted by helicopter inertia.
7. Critical center-of-gravity locations are to be investigated for each landing gear unit.
8. The rate-of-descent energy is apportioned in accordance with one load factor vertical and one-quarter load factor horizontal acting through the vehicle center of gravity.
9. There is some conflict between MIL-S-8698 and ANC-2 but it appears the forward velocity should be zero with zero drag force, and autorotating velocity for the three ground reactions.
10. If there should be two wheels forward, FAR's 27 and 29 would require examination of 60% and 40% load distribution.

condition.
e of a ground speed that is 75 percent
cent in autorotation.

sink rates and rotor life values.
design gross weight and alternately
s weight. FAR 27 requires a drop
FAR 29 requires at least 8 inches

posite gear is loaded with V_M.
ansverse loads or locked in the aft

ravel except that spin-up and spring-
the time of max forward or aft load.

$$\frac{WV^2}{2G} = W\delta_m - \frac{2}{3}W\delta_m - E_\tau - W\delta_g \eta N_z \quad (1)$$

where

W is the weight of the vehicle (lb)

δ_m is the total deflection of the vehicle (in.)

E_τ is the tire energy (in. - lb)

δ_g is the vertical displacement due to oleo movement (in.)

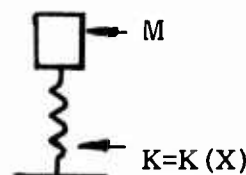
N_z is the load factor (dimensionless)

$\frac{2}{3}W$ is rotor lift (lb)

η is the efficiency of the landing gear (dimensionless)

The use of efficiency implies that there is a constant force stroke of the oleo during impact. A square wave is assumed, but the dynamic response of the system due to a square wave is ignored. This provides some means of calculating a load factor from a sink rate, rotor lift, and gross weight.

The possible final approach in generating landing loads is to calculate the dynamic response as it would naturally occur. The best example of this is the skid-type device. The skid behaves as an elastic-plastic element. There are established procedures for calculating the plastic bending curve of a beam and then the load deflection due to both the elastic and plastic deformation. The load-deflection curve is then used as a nonlinear spring element in a dynamic system.



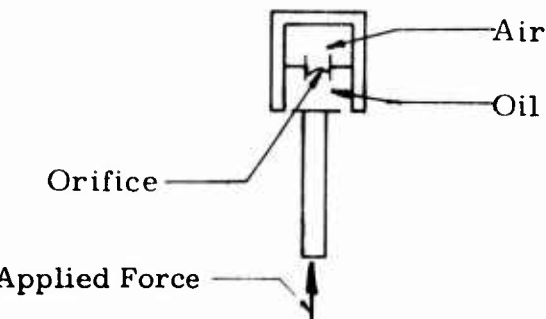
The system has a given weight, sink rate, rotor lift, and stiffness. The equations of motion are placed in a digital program and the accelerations, load factors, and deflections are calculated by an iterative process.

These are the four methods of deriving maximum force or acceleration response of a helicopter to an impact condition. The techniques used vary from manufacturer to manufacturer, but the primary method is evidently

to proceed, based upon specified values, and then later test to the design limits.

2.3.2.1 Oleo-Strut Wheel Landing Gear Design

The oleo strut wheel landing gear is essentially an air-oil hydraulic cylinder. The system is shown below:



The cylinder is pressurized with an air pressure that acts to balance the static loads of the vehicle and the dynamic loads during taxi. The air trapped within the cylinder follows the laws governing compressibility of a gas in a closed container and is simply described by

$$P_1 V_1^n = P_2 V_2^n \quad (2)$$

where P is the pressure of the gas, (lb/in.²)
 V is the specific volume (in.³/lb m)
the subscripts 1 and 2 define the initial and final states of the gas respectively.

During taxi, the vehicle rides on an air cushion as the strut strokes through the cylinder. In some cases, the pressure-volume curve has been specified as a design criterion to provide a desired "ride quality". Since the heat transferred to and from the gas is small under taxi conditions, the process is essentially isothermal. This is not quite true for impact conditions, and values of 1.06 have been used for n .

The hydraulic portion of the cylinder is for impact conditions. As the fluid is forced through an orifice, the pressure in the piston is defined by Bernoulli's principle for an ideal fluid. The hydraulic force becomes

$$F_h = \frac{\rho A_h^3 (S)^2}{2 (G_d A_n)^2} \quad (3)$$

where ρ is the density (lbm/in.³)

A_h is the hydraulic area of the piston (in.²)

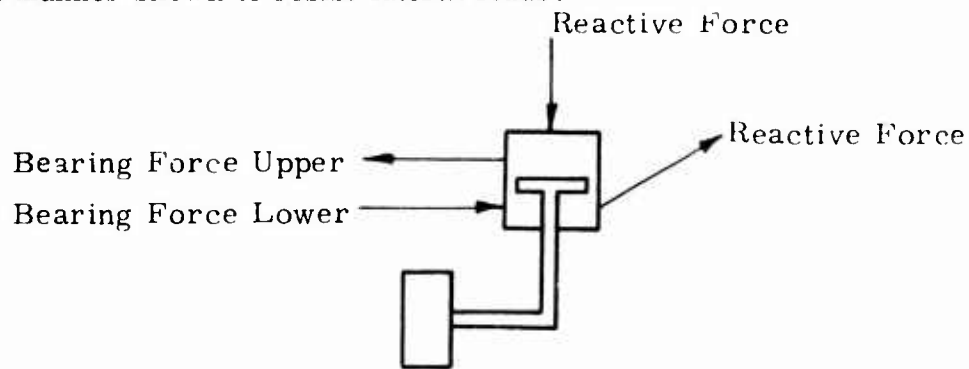
S is the stroke velocity (in./sec)

G_d is the orifice coefficient

A_n is the orifice area (in.²)

The basic equation indicates why landing gear units on crash tests have failed in the initial instants of impact without absorbing significant energy. If the vehicle impacts with a high velocity, the relative velocity across the strut is very large and the force is proportional to the square of the relative velocity. The strut quickly becomes a "rigid" link between the ground and the fuselage, and the extreme forces remove the landing gear from its attachment points.

The landing gear cylinder also resists compression through bearing frictional forces that act upon the piston. The piston is supported in the manner shown to resist lateral loads.



The frictional forces (F_F) are:

$$F_F = \sum_i \mu F_{Bi} \frac{\dot{S}}{|S|} \quad (4)$$

where

μ is the coefficient of sliding friction

F_B is the bearing force

The landing gear systems reviewed all have the design features mentioned. Many variations are possible. The orifice usually is combined with a metering pin to adjust the orifice area with stroke length. Orifice and relief valve combinations are used to introduce orifice variation as a function of force. Some liquid springs have been used where the function of the air pressure is replaced by compression of a fluid. These are a few of the possible variations that produce desirable refinements of the response but

do not alter the basic characteristics of the landing gear.

The approach to the design of a particular landing gear will now be discussed to demonstrate the various steps that lead to a finished piece of hardware. The major airframe manufacturer generates a set of criteria for the landing gear design subcontractor. These are the appropriate military specifications, preliminary weight estimates, moments of inertia, center-of-gravity location, landing gear stroke requirements, and vehicle attitude.

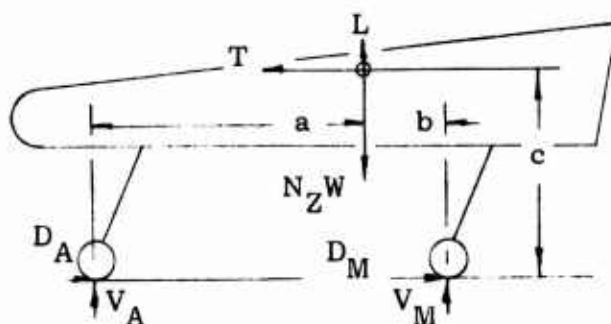
If the energy relation is used, the sink rate, gross weight, and oleo efficiency are used to calculate a load factor. This is calculated for forward and aft centers of gravity, as well as selected attitudes such as level-two point, level-three point, and tail down. The attitude is important because it modifies the stroke of the oleo. It's assumed the vehicle falls vertically, but the strut compresses along its axis. The output from the energy equation (1) is load factor.

The load factor is multiplied by the gross weight and a summation of forces and moments calculated for each landing condition. For the level-three point condition with maximum vertical reaction, it is assumed that each landing gear will have its dynamic vertical force apportioned according to the static distribution. The drag forces are one-quarter of the vertical forces, and the side forces are zero (Table II).

$$\text{Therefore } \sum F_v = V_A + V_M + \frac{2}{3} W - N_Z W = 0 \quad (5)$$

$$\begin{aligned} \sum M &= V_A (a+b) - N_Z W (b) \\ &\quad - T_c + \frac{2}{3} W b + M_s = 0 \end{aligned} \quad (6)$$

$$\sum D = D_A + D_M - T = 0 \quad (7)$$



M_s = moment contribution due to landing gear drag

$$L = \frac{2}{3} W$$

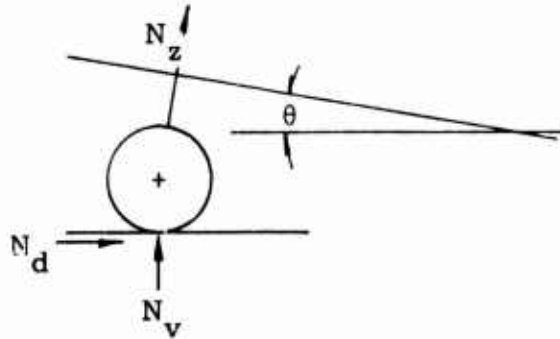
$$D = \frac{1}{4} V_A$$

and the system is solved for the reactions V_A , V_M , D_A , and D_M .

The next step is to calculate the loads in the landing gear axes. This is done by the equations of the form

$$N_z = N_v \cos \theta + N_d \sin \theta \quad (8)$$

where N_v and N_d are the load factor in the earth axis and θ is the attitude of the strut from configuration drawings of the various landing conditions as shown in the next diagram.



The strut load factors N_v , N_d , and N_z are then used to calculate the forces that each landing gear must carry. The forces are tabulated and analyzed to determine those conditions that are critical.

The airframe manufacturer then supplies the landing gear manufacturer with the critical design conditions along with gross weight, maximum load factor, static load, stroke, piston diameter, attachment point locations, overall length, and tire type. The landing gear manufacturer examines each condition and calculates the reaction loads due to each.

The design is significantly influenced by pressure considerations. The air pressure within the cylinder must support the vehicle in a static configuration. The design specification indicates that the piston is of a given diameter to carry the maximum forces and strokes from full extension to full compression. Additional guidance is provided in MIL-L-8552C. From the various design conditions, the maximum axial force is selected for static conditions. It is desired to have static pressure reasonably low (200 to 500 lb/in.²), although the specifications permit 2500 lb/in.². The difficulty lies in that decreased pressures dictate large pressure areas, whereas high pressures dictate very great stresses during full compression and necessitate increased material thicknesses.

The cylinder must be designed to stroke the designed full stroke plus an amount sufficient to alleviate bottoming. Reference 7 indicates that the additional stroke is sufficient to create a compression ratio of 4. Since the static to full stroke dimension is known, a compression ratio of 4 then dictates an additional stroke calculated by

$$\frac{(\text{Full stroke} - \text{Static stroke}) + \text{Additional stroke}}{\text{Additional stroke}} = 4.0$$

The relation $p_1 v_1^{1.1} = p_2 v_2^{1.1}$ is then used to calculate the full extended pressure which must be sufficient to insure full extension, and to determine the fully compressed pressure which is approximately a limit of 2500 psi.

The hydraulic operation of the strut is a function of orifice size and metering pin design. There have been analytical investigations to define the orifice area-stroke relation based upon a desired constant force response. However, it appears that the design is more a function of previous experience. Landing gear manufacturers have orifice and metering pin data available with orifice coefficients that will enable them to design a preliminary configuration. Since the configuration is selected based upon a worst condition, it remains for test results to generate a measure of how the strut responds to various inputs. That is, the design is from empirical data known to generate the proper efficiency for a given payload and drop height. Other conditions are apparently not evaluated analytically but only through test. By examining the measured data, the metering pin is modified to reduce undesirable peak forces and improve the efficiency.

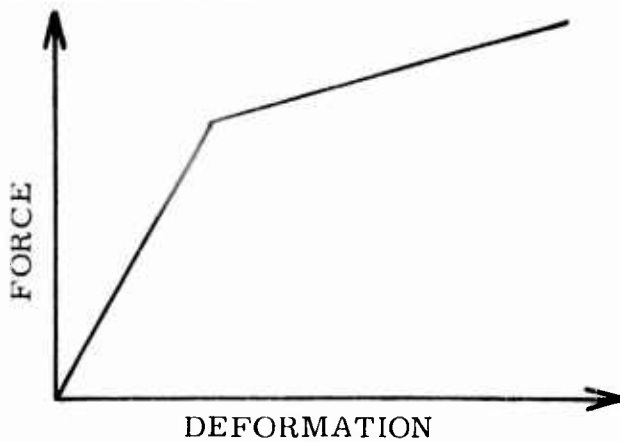
At this point, the preliminary data are compiled and the structural design is initiated. Overall lengths are known, externally applied forces are available, and internal pressure can be specified. These collectively dictate the necessary wall thicknesses and pivot point lug sizes. The remainder of the design is then a stress analysis problem using classical techniques.

2.3.2.2 Skid Landing Gear Design

The skid type landing gear has been used for many years on lightweight helicopters. It is a low cost means of creating small static deflections during normal landings, while providing energy dissipation efficiencies comparable to those of the oleo strut at impact velocities. The design problem associated with skids is that they are nonlinear structural elements. The skid has linearly related applied force and resulting deformation over a small amount of stroke. This stroke is that necessary to provide elastic deformation over the range of normal landing impact velocities. Beyond that point it is necessary to consider the plastic deformation of the skid.

The simplest design technique is that of Chernoff². It is assumed that the vehicle is supported by tubular members that cross horizontally at the bottom of the fuselage. The vehicle impact is in a horizontal attitude and dissipates all energy by the strain energy of bending in the tube.

The skid stiffness is idealized as a bilinear curve to duplicate the load deflection curve as shown below:



This is derived from an idealized stress versus strain curve for the particular material used.

Since the load-deflection curve is piecewise linear, it is easily integrated to determine the potential energy as a function of skid deflection. For the linearly elastic portion of the curve, the energy absorbed is:

$$E_{\alpha} = \int_{0}^{\delta} \rho(d\delta) = \frac{c}{2} \delta \quad (9)$$

where E_{α} is energy absorbed (ft-lb)

ρ is applied load (lb)

δ is deformation of skid (ft)

c is the slope of the elastic range of the load deflection curve

For the plastic portion of the curve

$$E_{\alpha} = \frac{c_1 \delta^2}{2} + (c - c_1) \delta \delta_y - \frac{1}{2} (\delta_y)^2 (c - c_1) \quad (10)$$

where c_1 is the slope of the plastic range

δ_y is the deformation at the elastic limit of the skid.

By equating kinetic and potential energies, equations are developed to relate applied loads, elastic limit, mass of the vehicle, weight applied per skid, and impact velocity. From Reference 2,

$$\delta = \frac{\frac{\delta y}{2} + \left\{ \frac{mW}{(c-c_1)\delta y} \right\} \frac{6}{mg} V^2}{1 + \left\{ \frac{mW}{(c-c_1)\delta y} \right\}} \quad (11)$$

is the equation for a perfectly plastic material,

where m is $\{ 1 - \frac{\text{lift}}{\text{weight}} \}$

W is the effective weight (lb)

g is the gravitational constant (ft/sec²)

V is the impact velocity (ft/sec)

Therefore, for varying impact velocities, rotor lift values, and desired effective weight on the skids, the deformation can be calculated. The load factor applied is then the ratio of applied force to effective weight.

$$n = \frac{P}{W} \quad (12)$$

The procedure available requires approximating the stress-strain curve of a material, and then the approximation of the resulting load-deflection curve for the integration process in the energy equations. The results of this type of approach have been compared with test data and have shown reasonable results¹⁰. Calculated center-of-gravity accelerations were within 6 percent of the measured.

The procedure shown has several distinct steps:

1. Establish the stress-strain characteristics of the tube material.
2. Calculate the force-displacement characteristics of the tube.
3. Incorporate the force-displacement characteristics into an energy relation or set of dynamic response equations.
4. Calculate the vehicle response.

2.3.3 Landing Gear Design Summary

Helicopter landing gear are designed primarily from specifications that do not consider crash environments. Many conditions that contribute to the design and several methods of determining the maximum inertial response need to be considered. The only design that is presently known to have been conducted from a truly dynamic analysis was for the UH-1 skid. With the shock strut device, some means of circumventing a dynamic analysis is available, but with a skid that can go into the plastic region it is necessary to examine the effects of force-displacement.

2.4 ENERGY-ABSORBER DESIGN ANALYSIS

2.4.1 Energy-Absorber Criteria

A multitude of devices and techniques exist that will dissipate energy by providing an acceptable force that reacts over a given distance. Most of the existing energy absorbers or load limiters are mechanical in nature, and an optimum device to be used on aircraft should be selected on the basis of the criteria listed below:

1. The device should be of minimum weight.
2. The device should operate satisfactorily and reliably with a minimum of maintenance.
3. Cost of the unit should be low.
4. The volume of the device should be at a minimum.
5. The force levels generated by the unit should be independent of velocity.
6. The stroke efficiency should be a maximum.
7. The device should maintain a constant load over the stroking distance.
8. The device should operate in both tension and compression.
9. The device should be capable of performing its intended function not only when loaded uniaxially but also when subjected to omni-directionally combined loading.

The above requirements are for an optimum energy absorber. Existing energy absorbers do not satisfy all the requirements, and selection

of a particular device will depend on the application and what trade-offs are acceptable.

2.4.2 Survey Results

2.4.2.1 Energy-Absorber Manufacturers

The list of manufacturers enumerated on page 3, engaged in the production of energy dissipation devices, was compiled using References 1 and 11, and the product catalogs.

The manufacturers' information and data were utilized in the following section where it was applicable. Generally, the devices available today are designed using empirical formulas and past experience to provide a force-deflection curve that approaches a square wave in shape.

2.4.2.2 Government Agencies

Government agencies were contacted and asked to supply any available data. It appeared that the National Aeronautics and Space Administration had conducted numerous investigations in the area of energy absorption. Their primary application of energy absorbers was for spacecraft cushioning devices. Since spacecraft have a size and weight limitation, NASA investigated numerous techniques in an effort to obtain an optimum energy absorber. Several of the devices developed by NASA¹² were patented as discussed by a recent report by the University of Denver¹². Additional energy-absorber patents are also discussed in the report which gives a good survey of the state of the art in energy-absorbing techniques.

2.4.2. Designs and Analytical Techniques

Chapter 3 of the Crash Survival Design Guide²³ describes and evaluates some of the more promising, simple, lightweight, "one-shot" energy absorbers. The types of devices studied were

1. Honeycomb compression
2. Tube flare
3. Inversion tube
4. Rod through tube
5. S-shaped bar
6. Standard cable
7. Metal tube
8. Strap/rod
9. Tension pulley
10. Bar through die
11. Wire through platten
12. Rolling-torus

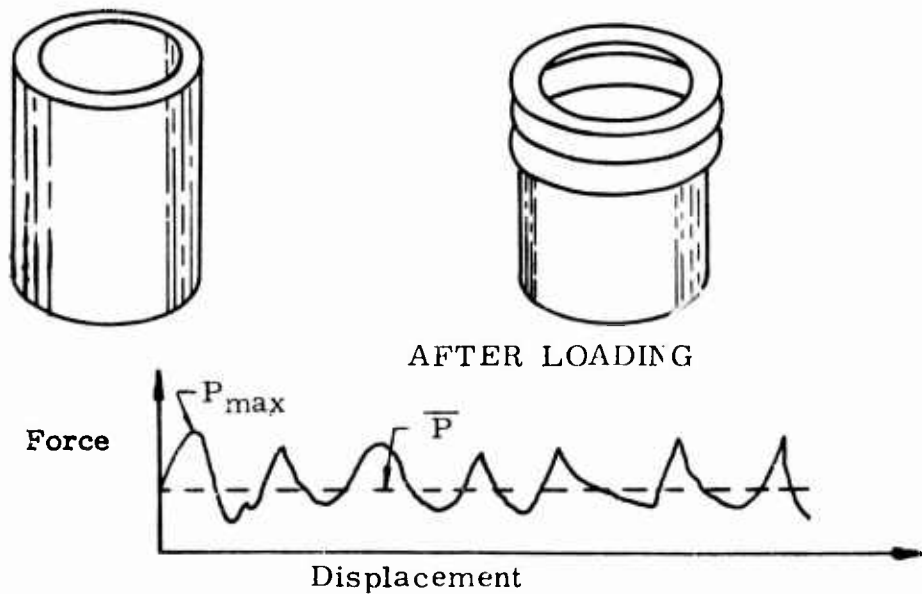
The majority of energy absorbers used today depend on complex mechanisms such as metal fracture, plastic deformation of a metal, and fluid flow through an orifice for dissipating impact energy. The

exact analysis of these techniques is extremely difficult, and normally, energy absorbers are designed using empirical relations and design equations derived from an analysis using simplifying assumptions. These equations and empirical formulas are used to select initial sizes and materials for a given energy absorber. Prototype units are then built, using the initial design values, and tested. Some adjustment or change is usually necessary. These are incorporated into the unit and it is retested. This cyclic process is then repeated as many times as necessary to meet the original specifications. The technique outlined above appears to be universal in the design of energy absorbers, since the mechanism which actually dissipated the impact energy in most cases is difficult to analyze.

The operation and simplified analysis for several energy absorbers are presented in the following sections. The design equations which theoretically predict operating characteristics, and experimental data show the relation between calculated and measured parameters and indicate why energy-absorber design is as much an art as it is a science.

2.4.2.3.1 Compressible Tube Energy Absorber¹³

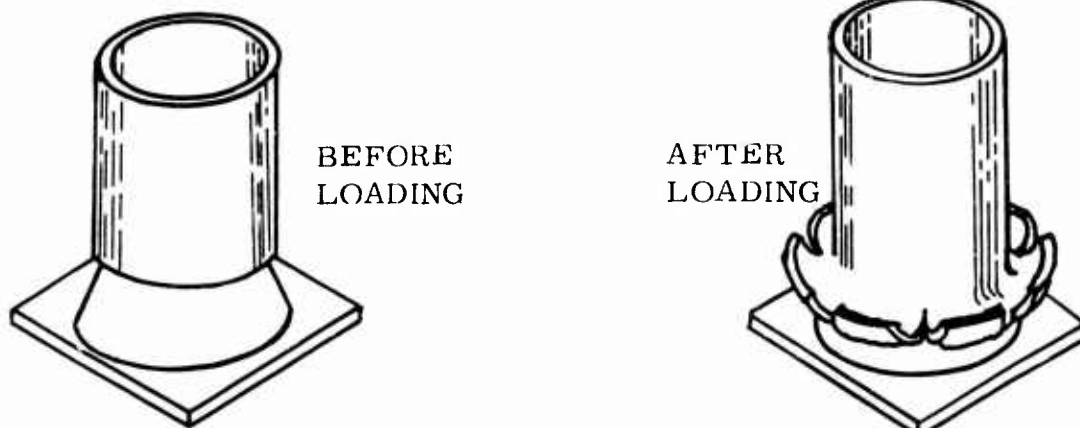
The compressible or folding tube energy absorber dissipates the applied energy by plastically deforming, through folding, the wall of a cylindrical thin-walled tube as an axial force is applied in compression. This device, along with a typical force-displacement curve, is illustrated as follows:



There is an initial peak force P_{\max} followed by a semi-regular variation in force level about some average value \bar{P} . Each cycle fluctuation corresponds to the formation of a single fold, and since the geometry of the tube changes with the stroke, the force level is not constant. The operating average force P is primarily determined by the tube diameter and wall thickness, the yield strength of the material, and the work-hardening characteristics of the material. The axial length of the tube also becomes a factor if the strut is long enough to consider buckling effects. Detailed analyses and design data are contained in Reference 13.

2.4.2.3.2 Tube Flare¹³

An energy absorber that utilizes the tube flare or tube and mandrel technique dissipates energy by fracturing or splitting a metal tube as it is forced over a mandrel. This type of device was developed by NASA for the space program and is very similar to a frangible tube energy absorber invented by J.R. McGehee.¹⁴ This type device is illustrated as follows:



Experiments were conducted at the University of Denver to establish a design equation applicable to tube flare attenuators. An empirical equation for determining the average force developed during compression was

$$\bar{P} = 8(\sigma_y + 0.25H) t^{3/2} D^{1/2} \quad (13)$$

where

\bar{P} is the average force (lb)

σ_y is the yield stress (psi)

H is the average slope of the stress-strain curves in the plastic region (psi)

t is the tube wall (in.)

D is the outer diameter (in.)

Tests were conducted to evaluate the properties required and are shown in Table III.

The experimental data quoted for a range of materials, tube diameter and thickness is shown in Table IV. P_{max} is the initial force spike that is typical of this type absorber.

TABLE III. MATERIAL PROPERTIES

Material	σ_y	H
ALUMINUM		
2024-0	11, 000	70, 000
3003-H14	21, 000	7, 000
5050	31, 000	60, 000
5052-0	13, 000	50, 000
6061-0	8, 000	33, 000
6061-T4	21, 000	55, 000
6061-T6	40, 000	30, 000
STEEL		
1015	45, 000	60. 000
4130	75, 000	80, 000

TABLE IV. COMPILED OF DATA

Alloy	D (in.)	t (in.)	P _{max} (lb)	\bar{P} (lb)
STEEL	4130	1	.035	12,240
		1	.035	12,350
		1	.035	12,325
		1	.035	12,080
		1	.035	12,060
		1	.065	23,000
		1	.049	16,300
				11,500
STEEL	1015	1	.035	7,800
		1	.035	8,000
		1	.035	8,000
		1	.065	15,900
		1	.049	12,300
		2	.035	17,000
				5,100
ALUMINUM	5050	1	.035	5,200
		1	.065	10,700
		1	.049	9,000
ALUMINUM	5052-0	1	.035	2,430
		1	.035	2,420
		1	.035	2,450
		1	.049	3,810
		1	.065	5,140
		2	.035	3,880
ALUMINUM	3003-H14	1	.035	2,270
		1	.035	2,250
		1	.035	2,290
		1	.049	3,365
		1	.065	4,780
		2	.035	4,790
ALUMINUM	6061-0	1	.035	1,380
		1	.035	1,345
		1	.065	3,480
ALUMINUM	6061-T6	1	.035	4,640
		1	.035	4,625
		1	.035	4,640
		1	.049	6,970
		1	.065	8,440
		2	.035	9,050

An energy absorber of this type is simple and easy to manufacture since it consists of only two parts, a tube and mandrel. The tube can be easily obtained from commercial suppliers, and the mandrel can be readily machined from standard metal stock. During the first part of the stroke, a high force spike may appear due to initial cracking of the tube. Notches cut into the tube and a beveled inside edge will eliminate this effect. Force levels for the tube and mandrel are basically determined by the tube diameter, wall thickness and mandrel configuration, and therefore can be changed by adjusting the two tube parameters or the mandrel design. Since this type of device can use the majority of its length to dissipate the energy applied, it has a high stroke to length ratio which can be utilized when available space is at a premium, such as in aerospace vehicles. Detailed data are contained in Reference 12.

2.4.2.3.3 Frangible Tube Energy Absorber^{14,16}

Energy is absorbed or dissipated by a frangible tube energy absorber as a thin-walled tube is pressed over a die and breaks into fragmented pieces. The die is formed so that a portion of the tube is forced over the die. A fluctuating force is developed by the splitting process, but the average force about which the actuation force varies is approximately constant once stroking of the device has been initiated. An initial peak force, higher than the average load, is usually necessary to begin the fragmenting process; but through special techniques discussed later, this initial force spike can be reduced. As the frangible tube is pressed over the die, the tube elements break off and disperse, permitting the entire length of the working element to be used as the working stroke. This type of device was investigated as part of a landing gear system for manned spacecraft by J.R. McGehee, the inventor. Extensive testing of the frangible tube technique has been performed, with the results of these tests contained in the referenced reports.

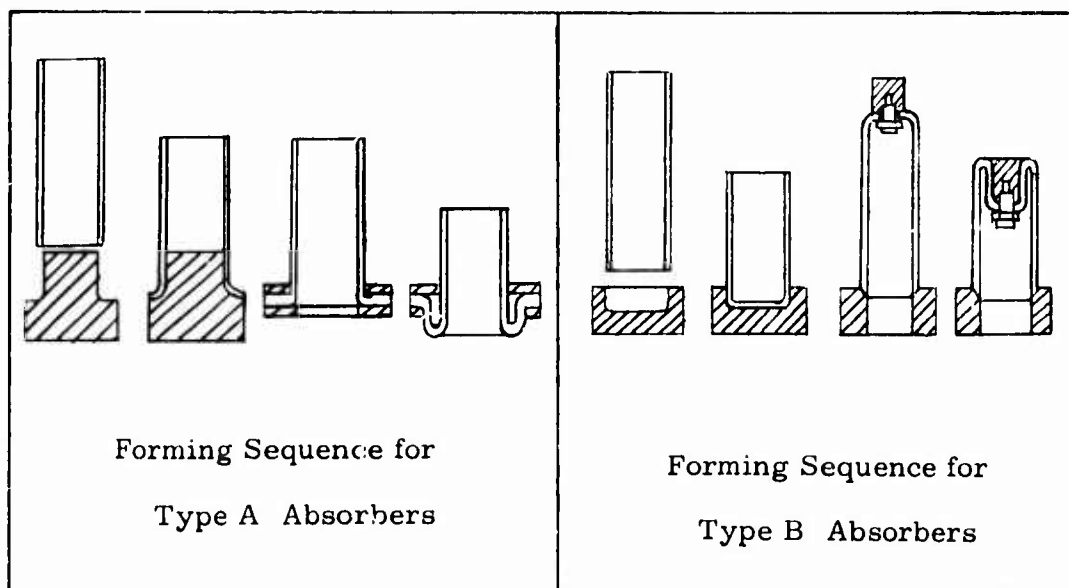
2.4.2.3.4 Crushable Honeycomb Energy Absorber¹⁵

Energy-absorption devices employing crushable honeycomb are generally used when large kinetic energies are to be dissipated at a uniform acceleration (a constant force deflection system). This type of device has been used to cushion large loads that are air dropped with or without parachutes. A procedure for selecting a particular type honeycomb that will protect cargo under specified conditions is given in Reference 15.

2.4.2.3.5 Invertube Energy Absorber^{16,17}

The invertube or tube inversion type of energy absorber absorbs energy through a process that simply turns a thin-walled tube inside out. Experimental results indicate that tube inversion is only feasible for certain ductile materials and a certain range of tube diameter and

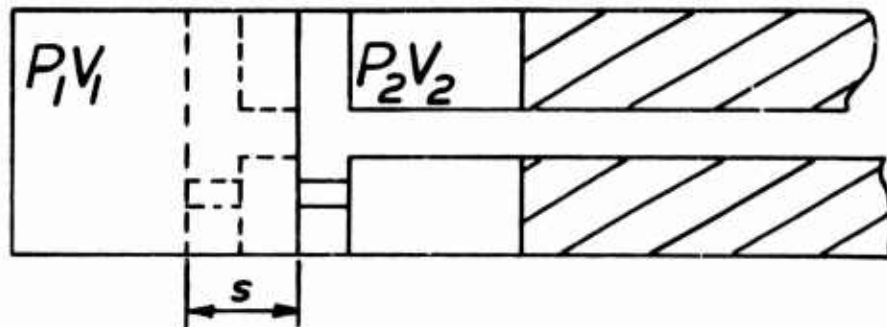
wall thickness ratios. The actual inversion of the energy-absorbing units or capsules can be accomplished by several different techniques. One method, Type A, turns the tube inside out while a second method, Type B, inverts the tube by turning the outside in. Devices of both types are preformed by flaring one end of a length of tubing, clamping a neck or ring around the periphery of the flare, and applying an axial compressive load. At a sufficiently high force level, yielding within the flair radius occurs, this results, through progressive transformation, into a fully developed roll radius. The figure below illustrates the forming sequence of Type A and Type B inversion tubes.



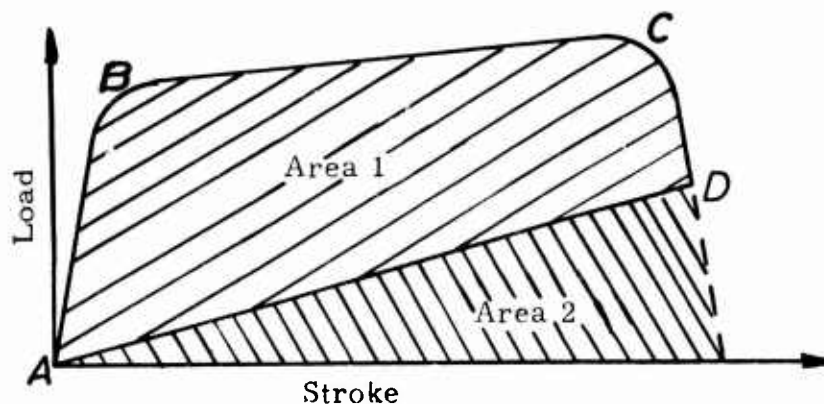
Another type of inversion tube that has been developed, Type C, is essentially a Type A without a clamping ring attached to the initial flare. The Type C device allows the initial flaring to just continue, and the tube inverts by turning inside out. The Type C inversion tube requires a higher stroking force than Type A and generates a larger roll radius. Detailed analyses and empirical data are contained within the cited references.

2 4.2.3.6 Liquid Spring Energy Absorber¹⁸

A liquid spring energy or shock attenuator is a device that absorbs energy by compression of a fluid and by control of the fluid flow through an orifice. Since the compression of a liquid is involved, these devices inherently have short stroke lengths. The construction of a liquid spring is essentially the same as a hydraulic cylinder except the bore of the cylinder is completely enclosed and there is an orifice in the piston. The simple geometry of a liquid spring is illustrated below:



Operation of the liquid spring depends primarily on two parameters: the compressibility of the fluid, and the pressure drop across the orifice due to the velocity of the piston. The fluid compressibility is a function of the bulk modulus of the fluid which usually varies linearly with pressure over the operating range of the device. If a liquid spring is actuated very slowly, with essentially zero velocity, the fluid is compressed by an amount equal to the stroking distance times the rod area, which creates a restoring force that varies linearly with the stroke. When the velocity of the liquid spring's piston is not zero, an additional restoring force is generated by the pressure drop across the orifice due to the fluid velocity through it and due to physical characteristics. The resulting load-stroke curve is therefore velocity sensitive and in general has the following appearance:



The straight line from A to D represents the spring force due to the fluid compressibility, and the curved line ABCD represents the force caused by a difference in pressure across the orifice which is proportional to piston velocity. At a higher stroking velocity, the force level will be greater. The energy absorbed by a liquid spring is the sum of Areas 1 and 2, where Area 1 is the energy dissipated by the orificing action and Area 2 is the energy stored by compressing the fluid. The initial slope of the velocity effect curve, the portion from A to B, is directly proportional to velocity until the effects of fluid compres-

sibility are noticed. At this point the slope of the curve is a function of the bulk modulus of the fluid and area of the piston. When higher velocities occur, the pressure or force increases but the slope remains the same.

The exact shape of the curve ABCD where the piston velocities are greater than some minimum value depends primarily on the orifice characteristics such as area and surface finish. These characteristics can be adjusted so that the load-stroke curve approximates a rectangular pulse making the liquid spring highly efficient in the sense of providing maximum energy dissipation with the minimum stroke.

2.4.2.3.7 Cyclic Strain Energy Absorbers^{19,20}

Energy absorbers have recently been developed which employ the technique of cyclic plastic straining of a material. These devices have advantages over most mechanical devices (i.e., tube flare, crushable honeycomb) of being reusable and having very high specific energy-absorption (SEA) capacity.

SEA is a parameter commonly used for comparing energy-absorption mechanisms. The SEA of a particular energy absorber is the amount of energy the unit dissipates divided by the weight of the device. The SEA for materials and techniques commonly employed in energy attenuators is given below:

<u>Attenuator</u>	<u>SEA (ft-lb/lb)</u>
Balsa Wood	24,000
Metal Honeycomb	12,000
Frangible Tube	31,000

The SEA value for a cyclic strain energy device is a function of the number of cycles required to produce failure. For example, if pure titanium metal is cycled in the plastic strain range so that failure occurs in 100 cycles, the total SEA at failure is approximately 350,000 ft-lb.¹⁹ An SEA of approximately 800,000 ft-lb/lb can be obtained from the same unit if the plastic strain range is reduced so that failure occurs in 1,000 cycles.¹⁹ The cyclic strain energy absorber is therefore capable of greatly reducing the weight required to absorb a given amount of energy.

A cyclic strain energy attenuator absorbs energy through cyclic deformation of a working metal. In these types of devices, working elements are cycled through tension and compression states and produce essentially constant resisting forces. In the torus device, rolling of the toroidal elements produces¹⁹ cyclic tension and compression of the longitudinal fibers of the element. Similarly, rolling of the compressed tube causes¹⁹ cyclic bending deformation of the tube wall in the circumferential direction.

2.4.2.4 Energy-Absorber Data Summary

Reference material collected for all types of energy absorbers has been compiled and is sufficient to design an absorber based upon any selected absorption concept. The equations usually combine empirical materials data within functional relations having a theoretical basis. Because of this, it is necessary to recognize the limits of the data in evaluating any particular design. Based upon the data collected, it appears that the liquid spring and cyclic strain concepts are the most attractive considering "commercial" capability for the ranges of loads, strokes, and energy dissipation anticipated for the landing gear systems to be designed during this effort.

Crushable honeycomb has been incorporated within landing gear struts as discussed by Rich.²¹ This was successfully accomplished for a particular gross weight vehicle and designed to permit additional strokes of a landing gear at approximately the original impact force level. Hence, there has been honeycomb within a column attenuation demonstrated by an airframe manufacturer.³⁰ The OH-6A also possesses a crushable honeycomb landing gear system.

2.5 CRASH KINEMATICS

In addition to the design criteria collected it was necessary to conduct analyses to determine better energy-absorbing landing gear criteria using a digital routine (see section 3.5). The digital program developed had to have some input information that would reflect a survivable crash condition. The concepts to be developed could then be examined to calculate the loads to the airframe when the applied loads are loaded simultaneously in an upward, aftward, and sideward direction at the landing gear. The current applied force criteria do not quantitatively specify the attitude, nor do they define a survivable crash. It is possible to use the FAR "crash" conditions for fuselage design, but these numbers are unrealistic for the purposes of this program because of their small values. It was apparent that it would be necessary to quantitatively define a set of crash conditions.

A computer program was developed to permit the analysis of a "crashing" helicopter. A rigid body supported at the corners by viscoelastic elements was the model for the program. For this model it was necessary to have input conditions that would reflect the crash impact. One approach is to assume a rigid earth and let the elasticity, mass, and viscous components of the system determine accelerations from initial conditions. The second approach is to use measured crash acceleration data as input to the landing gear and calculate the response which would then reflect to some degree the elasticity of the soil. The two approaches indicate the necessity for pursuing not only initial conditions (altitude, sink rate, etc.), but measured response, accelerations, and forces.

The analysis of the crash input data collected indicates that aircraft

attitude and acceleration-time curves are important parameters for use in the computer program. The acceleration-time data must include longitudinal, lateral, and vertical accelerations and pulse shape, as the input to the landing gear.

2.5.1 Crash Impact Accelerations and Velocities

Crash accelerations as the input to the landing gear were not available explicitly in any of the data surveyed. However, the Crash Survival Design Guide¹ did contain acceleration-time pulse data pertaining to survivable U.S. Army aircraft accidents for the period 1 July 1960 30 June 1965. Controlled crash tests²² indicate that the landing gear does not appreciably decelerate helicopter aircraft, and therefore, the floor accelerations as compiled in the Crash Survival Design Guide should be indicative of crash input data for current aircraft designs.

The aircraft accelerations presented are accelerations at the floor near the center of gravity of the aircraft and are based on comparative data (see paragraph 1.1.1.3 of Reference 1) with calculations using the equation

$$G_{AVG} = \frac{V^2}{2 g S} \quad (14)$$

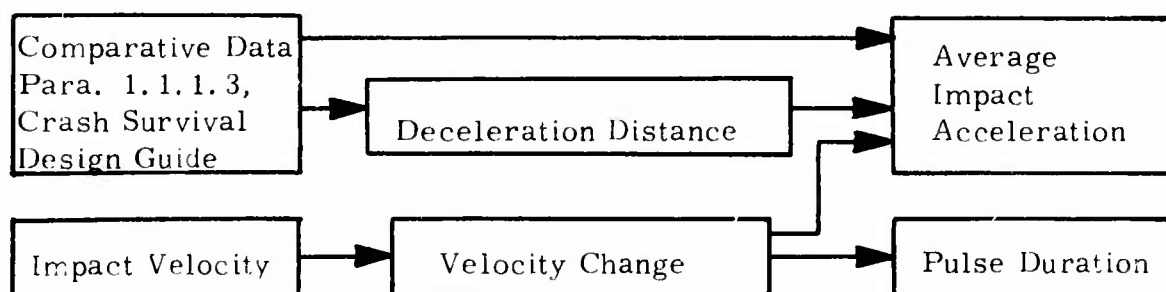
where G_{AVG} is the average load factor of the pulse

V is the impact velocity (ft/sec)

g is the gravitational constant (ft/sec²)

S is the displacement (ft)

The chart below summarizes the procedure by which acceleration versus time data at the input to the landing gear is determined.



Velocity change was estimated from known impact velocities and comparative data, and the average impact accelerations were estimated from velocity changes, comparative data, and known deceleration distances. The average impact acceleration is that for the major impact. The pulse duration for a given probability of occurrence of accident is given by the equation

$$T = \frac{2V}{gG_{\text{peak}}} \quad (15)$$

where T is the time duration of the pulse (seconds)
 G_{peak} is twice the average G

Therefore, the pulse duration can be computed from corresponding percentile points on the distribution curves of velocity change and average acceleration. The result is an acceleration-time pulse at the floor of the helicopter for the vertical, longitudinal, and lateral directions.

Figures 1 and 2 show the distributions of velocity changes and accelerations in the vertical, lateral, and longitudinal directions as determined by the accident study.

Data were insufficient to plot distribution curves of lateral impact acceleration and lateral velocity change; however, upper limits on these parameters were estimated to be 16G peak and 25 fps.*

Although these data represent floor accelerations and velocity changes, they can be used to estimate inputs at the landing gear. For example, in one test ²² an H-25 helicopter was dropped from a moving crane so that it attained a vertical impact velocity of 45 fps, a vertical impact acceleration peak of 115G and a pulse duration of approximately 25 milliseconds. Substituting 45 fps and 25 millisecond into the equation

$$\Delta V = \frac{A \Delta T}{2} \quad (16)$$

where ΔV is the velocity change (ft/sec)

A is the peak acceleration of a triangular pulse
 (ft/sec^2)

ΔT is the pulse duration (sec)

* These values have been updated to 18G peak and 30 fps for rotary-wing aircraft. (Reference 23.)

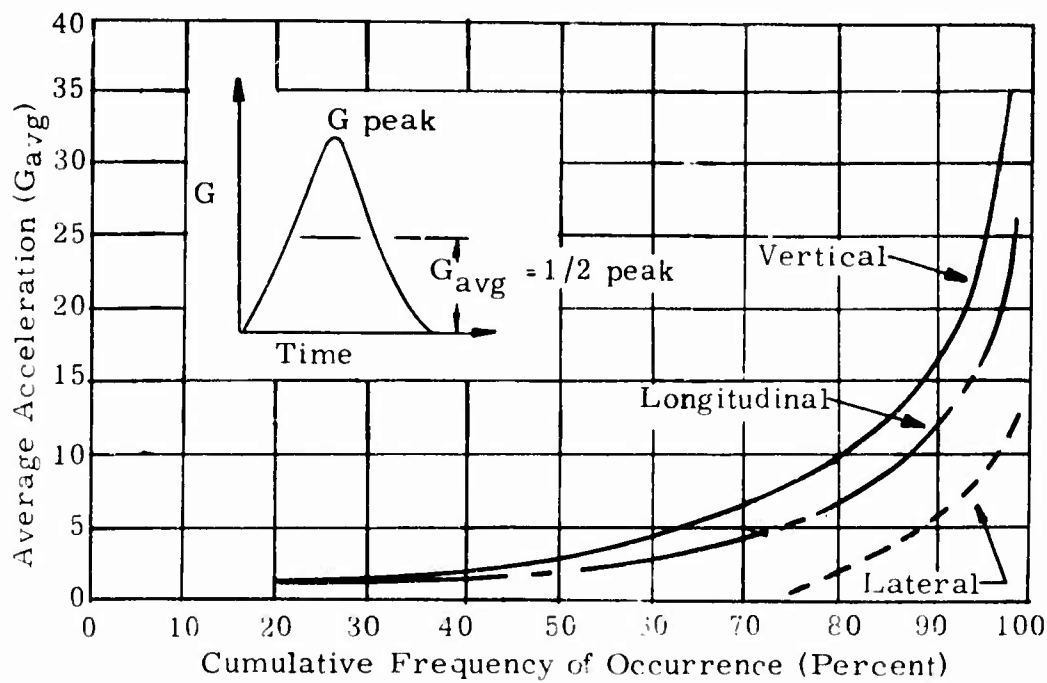


Figure 1. Distribution of Average Acceleration in the Vertical, Longitudinal, and Lateral Directions.

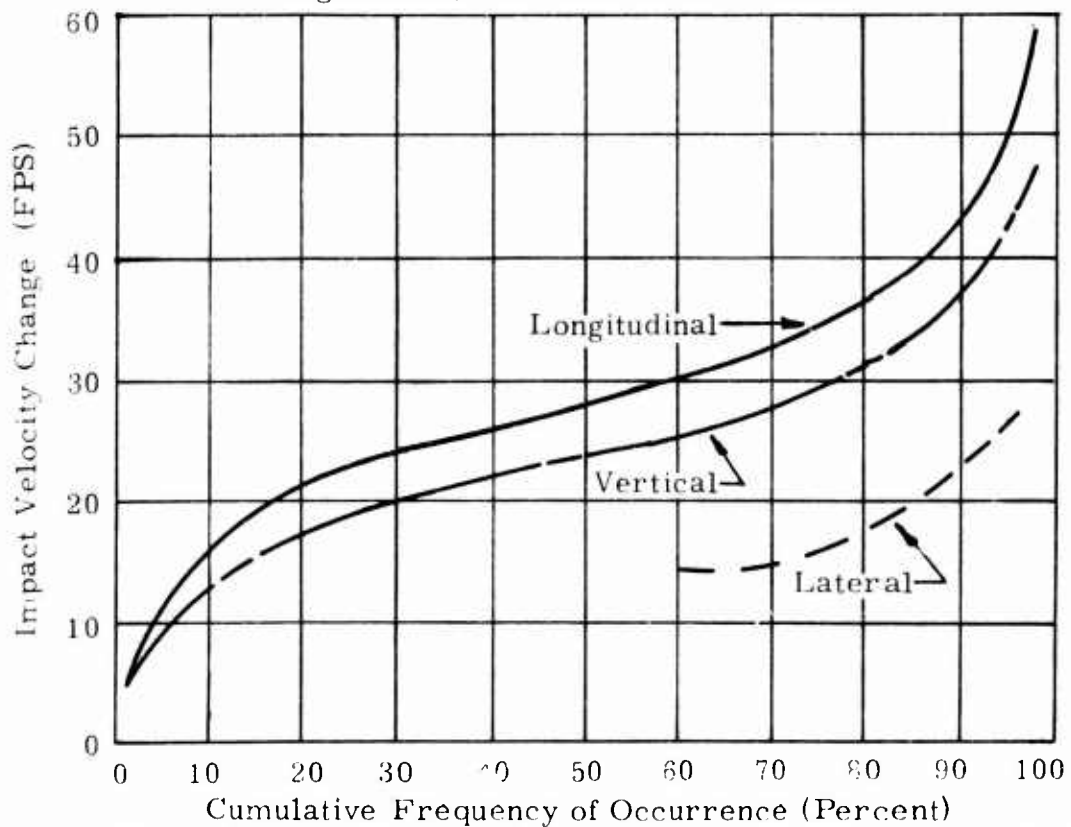


Figure 2. Distribution of Vertical, Longitudinal, and Lateral Impact Velocity Changes for Survivable Rotary and Light Fixed-Wing Aircraft Accidents (from Crash Survival Design Guide).

results in a peak acceleration of approximately 112G, which is nearly the value of peak acceleration that was measured directly at the floor (115G). This procedure was repeated for five other crash tests^{24,25} where the measured peak vertical acceleration at the floor of the aircraft was compared with the calculated peak acceleration using values of vertical impact velocity and pulse duration. Two of the tests resulted in measured accelerations which were 34% and 6.5% higher than the calculated values, and the remaining tests resulted in measured accelerations which were 34%, 14%, and 26% lower than the calculated values. Although these results vary, some of this can be attributed to experimental errors as well as some energy absorption by the landing gear. In addition, the peak vertical accelerations in all but one of these tests were significantly higher than the peak vertical acceleration (48G) corresponding to the 95th percentile accident as computed in Table 1.1 of the Crash Survival Design Guide in which only survivable accidents are considered. As a result, the vertical accelerations shown in Figure 1 will be used as the best estimates of input accelerations where pulse duration will be computed as described above.

Referring to Figures 1 and 2, the longitudinal impact velocities are slightly higher than the vertical velocities, but the longitudinal accelerations are slightly lower than the vertical accelerations. Therefore, we can conclude that the landing gear did decelerate the aircraft to some extent in the longitudinal direction. This probably is indicative of the energy dissipated by frictional forces in skidding of the landing gear, the fuselage and to some extent in the wheel bearings. Since these effects do act as a landing gear energy absorber, as a first estimate, the curves represent longitudinal crash input data for the purpose of designing landing gear energy absorbers.

The Crash Survival Design Guide¹ estimates that lateral floor accelerations rarely exceed peaks of greater than 16G. If this is assumed to be the 95th percentile case and the lateral accelerations are proportional to the longitudinal accelerations, the distribution of lateral accelerations can be assumed, for design purposes, to be as shown by the dashed lines of Figures 1 and 2. Also for reasons similar to those given in the longitudinal case, these lateral floor accelerations can be used as landing gear input data.

2.5.2 Aircraft Impact Attitudes

Little data on helicopter attitude on crash landings are available. The Crash Survival Design Guide contained none*, and although a report prepared by the Boeing Company, Vertol Division²⁶ did contain some attitude data, this was limited to attitudes while in flight and when a survival escape system could be activated. Several crash test reports

*At the time this was written the USAAMRDL 70-22 did not contain attitude data. This has since been incorporated into the latter issue, Reference 23.

indicate that for potentially survivable helicopter crashes, the attitude varies only a few degrees from level for pitch, roll and yaw. One crash test report²⁷ states that the average crash condition from successful auto-rotation following power failure would result in an impact with a pitch of 9 degrees nose up and 6 degrees roll left. Several other crashes were surveyed and the results showed that the aircraft pitch was nearly 0 degrees with respect to horizontal flight path.

2.6 PHASE I SUMMARY

1. The criteria for the design of helicopter landing gear are to be found in the specifications of three agencies:
ANC-2 Ground Loads (U.S. Army)
MIL-S-8698 (U.S. Air Force)
Federal Aviation Regulations Parts 27 and 29 (Civilian)
2. The design procedure for wheel-oleo strut type landing gear is to examine the conditions required in the specification, calculate the reaction forces, determine the structure required to carry these forces, and then select hydraulic areas and orifice sizes to generate an acceptably efficient shock strut.
3. The design procedure for the skid-type landing gear is to establish the stress-strain characteristics of the tube material, develop the force-displacement characteristics from them, and then incorporate these into an energy relation or set of dynamic response equations.
4. There is no quantitative crash specification applicable to the landing gear.
5. The many types of energy absorbers available do, in general have some analytical basis for generating design information required. A great amount of information is available in test results. The theoretical design equations are based upon these data.
6. Some crash criteria information is available to define input conditions.
7. There is sufficient data available on the design and design criteria of landing gear and energy-absorbing devices to permit development of feasible design criteria and concepts for energy-absorbing landing gear designs.

CHAPTER 3
PHASE II - ENERGY-ABSORBING LANDING GEAR
DESIGN CRITERIA AND CONCEPTS

3.1 INTRODUCTION

The goal of Phase II was to develop feasible criteria and concepts for energy absorbing landing gear designs for the LOH, UH, and CH helicopter classes.

The concepts developed were to include a skid-type concept for both the LOH and UH, and a one-wheel-type concept for the CH. The concepts were to consider upward, sideward, and aftward loads when applied at either end of the gear or during pure vertical survivable impact. After concepts were selected, the following factors were considered:

- a. Operational and normal landing requirements
- b. Combined landing gear and airframe loading
- c. Environment
- d. Cost
- e. Reliability
- f. Maintainability
- g. Simplicity
- h. Weight

3.2 ENERGY-ABSORBING LANDING GEAR DESIGN CRITERIA

The purpose of design criteria is to establish enough information concerning the input and the response desired to design a system. A landing gear system is designed for given input velocities and orientations and must have sufficient strength and rigidity such that the impact acceleration generated will not exceed a specified level. Similarly, if the design is to be for an energy-absorbing landing gear, the criteria must specify how the system is acted upon and what levels of response must not be exceeded.

Data previously collected for landing gear criteria specified various conditions of attitude, sink rate, gross weight, load factor, forward velocity, load distribution, center-of-gravity location, moment balance, rotor lift, and methods of analysis. These are the necessary parameters but not necessarily those sufficient to define the new criteria.

First, let us consider the initial velocities as a means of introducing

the energy balance equations previously reported. The only curves available for impact velocity distribution for survivable accidents come from the Crash Survival Design Guide, (see Figure 2).

The question to be resolved is, over what levels of input velocity should the energy-absorbing landing gear system be operable? The intent of the system is to lessen the magnitude of the crash forces but not necessarily to reduce them to a minimum. The system is to perform attenuation of the impact, not elimination of it.

It will be assumed for this discussion that the vehicle is in a level attitude and that the body axis of the vehicle and the earth axis are coincident. Later discussions of attitude will establish their true relations at impact. The vertical velocity is the most important. At impact, the vertical velocity must be dissipated over a short distance; the stroke required from impact velocity to rest is relatively small. Longitudinal and lateral velocities could conceivably be dissipated over greater distances just as a fixed-wing vehicle does during landing. If the system were rigid, the lateral and longitudinal velocities would be dissipated by run-out friction, assuming the structure could withstand the vertical shock. If the vertical velocity cannot be attenuated, then the others are of lesser importance.

Vertical velocity as an input criterion alone tells us nothing about the accelerations or forces to be developed at impact. The characteristics of the system that impacts determine how these are developed. Hence, impact vertical velocity only specifies the available energy. This was pointed out in the Phase I discussion and was specifically mentioned in the energy approaches to landing gear design. We wanted to design for a maximum possible velocity, with a minimum stroke and yet not exceed certain limits on the airframe or crewmember. Without having selected a particular concept, the only approach practical is based upon energy dissipation.

If a mass impacts with an initial velocity and the energy is attenuated over a particular stroke, the relation between the variables is

$$\frac{V^2}{2g} = N\eta S \quad (17)$$

where V is the impact velocity (ft/sec)

g is the gravitational constant

N is the load factor

S is the stroke (feet)

η is the efficiency of the system

At this point it is necessary to rely on additional data collected. What are realistic velocities, strokes, and efficiencies?

A recent work, "Design Criteria for Energy Absorption Systems,"²⁸ shows that for an optimum energy-absorber waveform, helicopter crash input, a stroke of 18 to 20 inches was required to dissipate 44 feet per second. The 18 inches were between input and seat pan regardless of where the stroke was physically achieved.

Another effort by J.R. Turnbow²⁹ indicated that it was desirable to have a structural capability of surviving 25-foot-per-second impacts. After having conducted full-scale tests on a helicopter, it was suggested that an 8G deceleration over 1 foot was desirable. Smith and McDermott³⁰ of Hughes Aircraft proposed 30-foot-per-second impact survivability for occupants, and Army experience in Vietnam suggested improved³¹ crashworthiness up to 25 feet per second (Watson and Dunham).³¹ The survey letter received from the U.S. Army Agency for Aviation Safety indicated that 10 to 15 foot-per-second impacts could currently be sustained prior to ground contact of the fuselage and that additional attenuation capacity should be investigated.

From this data it appears that there are some theoretical and practical limits that have been alluded to by many different sources:

Vertical Velocity (v): $15 < v < 44$ feet per second

Load Factor (N): $3 < N < 18G$

Stroke (S): $8 < S < 18$ inches

The load factor of 18 is approximate since the referenced report²⁸ assumed that the limit of 18 was a dynamic response index of the seated subject rather than seat accelerations. However, the two are considered approximately equal at this point.

The assumption was made that 25 feet per second would be a reasonable criterion. Inserting this into the energy equation (17),

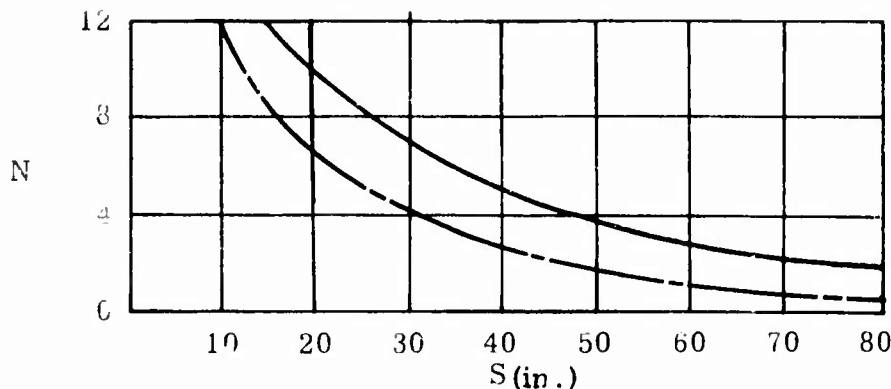
$$N\eta S = 9.7 \quad (18)$$

From empirical data the efficiencies of liquid spring, oleos, honeycomb and plastic materials range from 0.9 down to 0.7. Assuming a value of:

$$\underline{\underline{\eta}} = 0.7 \quad NS = 13.9$$

$$\underline{\underline{\eta}} = 0.9 \quad NS = 10.8$$

This is plotted on the following page.



The curve indicates that it is possible to limit the acceleration levels while keeping the stroke below 18 inches. If we attempt to raise the impact velocity to 30 feet per second, an 18-inch stroke with 70 percent efficiency would generate 13.3G acceleration. Since the crew-member is an elastic system with approximately a 0.25 damping ratio, the structural input of 13.3G can generate a subject response of greater than 18 Lynamic Response Index (DRI). This implies a spinal injury probability of more than 5 percent, the current Air Force ejection seat limit. It may easily be argued that the definition of survivable permits greater levels, but it should also be remembered that the efficiency of a complex landing gear-absorber-structural system will probably not be as great as assumed.

The magnitude of 25 feet per second has been selected as the vertical impact velocity for crash design criteria based on the objective and subjective data available. It is conceivable that the level could be much higher without severely penalizing the stroke, but it soon becomes an evaluation, or estimation, of how many possible survivable crashes are to be absolutely protected against, versus how probable is the combination of velocity, resulting acceleration, and injury. The 25-foot-per-second magnitude is greater than half of the survivable aircraft accidents level, as shown in Figure 2. It represents a doubling of current drop specifications and therefore an increase in energy by a factor of 4.

The corresponding fiftieth (50th) percentile longitudinal and lateral velocities are 29 feet per second and 15 feet per second respectively, assuming the Crash Survival Design Guide distribution. As a means of comparing this to velocities that could be dissipated, assume that a 15G impact is permitted over 18 inches. A friction coefficient of 0.5 would cause a translational deceleration of 7.5G, and the velocity change would be approximately 19 feet per second. Two thirds of the longitudinal velocity could therefore be theoretically dissipated by the energy-absorbing landing gear system prior to fuselage impact. The remainder could easily be removed by fuselage sliding friction.

Although the longitudinal and lateral velocities may be appreciable they only provide an indication of the energy that must be dissipated. The structure does not feel energy, only forces and accelerations which cause

the energy to be dissipated over some time interval. Consequently, of more importance than the velocity is the coefficient of friction that exists at the impact surface if it is assumed that the structure remains intact. If the structure can carry the impact and drag forces, the energy will be dissipated regardless of its magnitude.

The next aspect to be considered is attitude. As mentioned in the previous chapter, very little attitude data is available. Crash data collected indicates that attitudes of ± 5 degrees in roll, pitch, and yaw are possible during drop tests. Of course, this does not necessarily relate directly to operational conditions. One skid specification does specify a 15-degree nose-down attitude, but this is not known to be dictated by crash experience. Considering the lack of data, but realizing the possible effect that may result by tip loading a skid, it seems reasonable to assume that 10 degrees of attitude variation is certainly probable during autorotation maneuvers.

Another aspect that is related to the nature of previous specifications is load factor. It has been shown, by the simplest energy relation, that the load factor is truly a result of system response and as such cannot really be specified except as a limit. In order to make load factor applicable, it is necessary to consider a magnitude that can be related to the survivability of the crewmember. If we assume that it is desirable to keep the impact acceleration below 20G (Eiband³²), or below a DRI of 18³³, the input must be approximately 15G. This is based upon the existing biodynamic model of seated subjects exposed to vertical accelerations. The subject is a system of 8 to 10 Hz natural frequency and 0.22 to 0.30 damping ratio. For a step input acceleration, perfect square wave, the overshoot of such a system is approximately 30 percent, and hence 15G is a realistic value for fuselage limit acceleration.

The load factor of 15G is compatible with the previously discussed vertical impact velocity criteria, assuming that stroke and efficiency can be obtained as required and assuming no injurious failure of the aircraft structure. This is significantly greater than the current fuselage maximum acceleration of 3.5G magnitude and is strictly only applicable to the load path that exists between impact surface and crew seat. If the energy-absorbing system creates a 15G acceleration at the seat by decelerating 25 feet per second over 18 inches, then it theoretically is unimportant whether or not the rest of the fuselage has survived beyond 3.5G. Practically, this is not so because care must be taken to insure that a survivable environment exists in the occupiable areas and material damage should be minimized. This is as specifically mentioned in the Crash Survival Design Guide whenever reinforcement of the cabin area is discussed. However, it is now possible to quantitatively indicate the acceleration level to be considered.

Rotor lift should also be discussed. The more exact energy relation is

$$\frac{WV^2}{2G} = WN\eta S + \frac{2}{3} WS \quad (19)$$

where the additional term assumes a rotor lift of two-thirds of the weight. At an impact velocity of 25 feet per second, the initial kinetic energy is nearly 10 times greater than the rotor contribution. This is in comparison with the conventional sink rate ratio of two to one. Therefore, although the effect of rotor lift is necessary for the conventional landing design criteria, it is of lesser importance for crash criteria.

Several other parameters are gross weight, center-of-gravity location, and methods of analysis. It is assumed that gross weights assumed for normal landing loads will still be utilized; that is, design gross weight or alternate gross weight, depending upon which was the more critical. Center-of-gravity locations should also be varied as in normal analyses. And lastly, a dynamics analysis should be conducted to reflect the elastic and plastic deformation of the landing gear system. If the analysis is conducted using systems of differential equations with nonlinear capability, there will be no need for inertial load factors or landing gear load factors. These will simply become outputs due to the system characteristics and the initial conditions specified.

The criteria selected for the energy-absorbing landing gear concepts development can be summarized by an array of conditions. Roll, pitch, and yaw may vary within ± 10 degrees. It is assumed that the asymmetric conditions of positive roll and negative yaw cannot exist. This assumes the standard convention of nose up, right wing down, and nose right being positive. The number of possible unique loading attitudes due to the 27 combinations is 9. That is nose up and positive roll and yaw produce the same impact conditions as nose up and negative roll and yaw. The velocity combinations are 25 feet per second vertical, 29 feet per second longitudinal, and 15 feet per second lateral. These provide four more combinations to examine, assuming that the vertical velocity always exists and that the lateral velocity is always in the direction of the roll.

These conditions are shown in Table V.

TABLE V. IMPACT CRITERIA FOR ENERGY-ABSORBING LANDING GEAR

ATTITUDE ANGLE (DEGREES)				IMPACT VELOCITY (FT/SEC)		
Condition Number	Roll	Pitch	Yaw	Vertical	Longitudinal	Lateral
1	0	0	0	25	0	0
3	+10	+10	0	25	0	0
.
.
.
35
36	-10	-10	-10	25	29	15

By examining the 36 conditions tabulated, all previously desired conditions of simultaneous load application and attitude are automatically included. Condition 1 is pure vertical drop, whereas Condition 36 is the most unusual attitude possible with maximum velocity input.

Additional criteria are:

1. The occupiable structure should be crashworthy through a 15G limit acceleration and should provide sufficient structural integrity between the impact point and cockpit floor to carry any loads generated by the above conditions and the energy-absorbing landing gear.
2. Rotor lift is relatively insignificant.
3. The critical design weight should be used.
4. The critical center-of-gravity position should be used.
5. A coefficient of friction at the impact point must be used that is representative of the ground condition. In the absence of friction data, a coefficient of 0.5 may be assumed to be consistent with the value specified in ANC-2 for normal landing conditions.

The criteria specified are sufficient to develop design concepts provided basic data of the helicopter configuration are available. Such data are presented in the next section.

3.3 HELICOPTER CONFIGURATION DATA

Before concepts could be developed, it was necessary to have some means of estimating the approximate size of the configuration desired. It would be possible to just select a vehicle of each type and utilize its characteristics.

However, it is more advantageous to collect dimensional data on all possible vehicles and then see if there is any significant trend in dimensions as a function of gross weight.

A survey of helicopter aircraft data was undertaken to determine typical values of the locations of the landing gear with respect to the aircraft center of gravity, and to determine the three moments of inertia. Fifty-two aircraft were considered. The primary source of data was the latest copy of Jane's "All the World's Aircraft" ³⁴. Data were taken directly from this source or estimated from pictures or drawings and overall aircraft dimensions. The center of gravity was estimated on the basis of location of engine and other components, and was generally taken to be directly under the rotor axis. Those dimensions shown in Figure 3 were recorded and plotted against the gross weight of the aircraft. Typical dimensions were taken from these graphs for various combinations of the three aircraft weight categories and the landing gear type (see Table VI).

The landing gear fuselage attachment locations are generally the same distance fore and aft of the center of gravity, as are the ground touch points for the tricycle and quadricycle landing gears. In almost all helicopters the landing gear are attached to the extreme lateral edge of the fuselage. Some of the Bell helicopters with skid landing gears were attached nearer to the center of the bottom of the fuselage. Nearly all of the Sikorsky (medium-cargo) helicopters and landing gear were attached to the extreme lateral edge and bottom of the fuselage through retractable wheels. These landing gear also have additional struts which attach 4 to 8 feet above the bottom of the fuselage.

Moments of inertia with respect to the pitch, roll, and yaw axes were calculated for the three helicopter weight categories. Weights and their positions relative to the center of gravity were estimated or obtained directly from References 34 and 35. The weight of the engine, fuel tanks, and transmission were, in most cases, lumped together at the center of gravity and assumed to be a sphere or uniform mass. The remainder of the mass, which included the cargo and the fuselage, was assumed to be evenly distributed throughout a cylinder centered at the center of gravity and with the approximate dimensions of the fuselage. The three moments of inertia were calculated using these two approximations and, as expected, the moments of inertia with respect to the pitch and yaw axes were larger than the moment of inertia with respect to the roll axis. From the calculated moments of inertia and the gross weight of the aircraft, the radius of gyration was calculated and cross-checked with the known helicopter fuselage dimensions. The three moments of inertia are shown in Table VII for each of the three helicopter weight categories.

The plotted dimensional data indicates that there is no apparent strong linear weight dependence. The scatter was very great because of the many types of landing gear systems used and the variations that are inherent because of manufacturer design philosophy. The moment of inertia data, although approximate, agree favorably with limited available data. UH1 data for the

LEGEND

A_{xa} - Distance from horizontal C. G. to aft attachment point
 A_{xf} - Distance from horizontal C. G. to front attachment point
 A_y - Distance from horizontal C. G. to side attachment point
 A_z - Distance from horizontal contact point to attachment point
 G_{xa} - Distance from horizontal C. G. to aft contact point
 G_{xf} - Distance from horizontal C. G. to front contact point
 G_y - Distance from horizontal C. G. to side contact point
 G_z - Distance from vertical C. G. to contact point
 F - Fuselage width

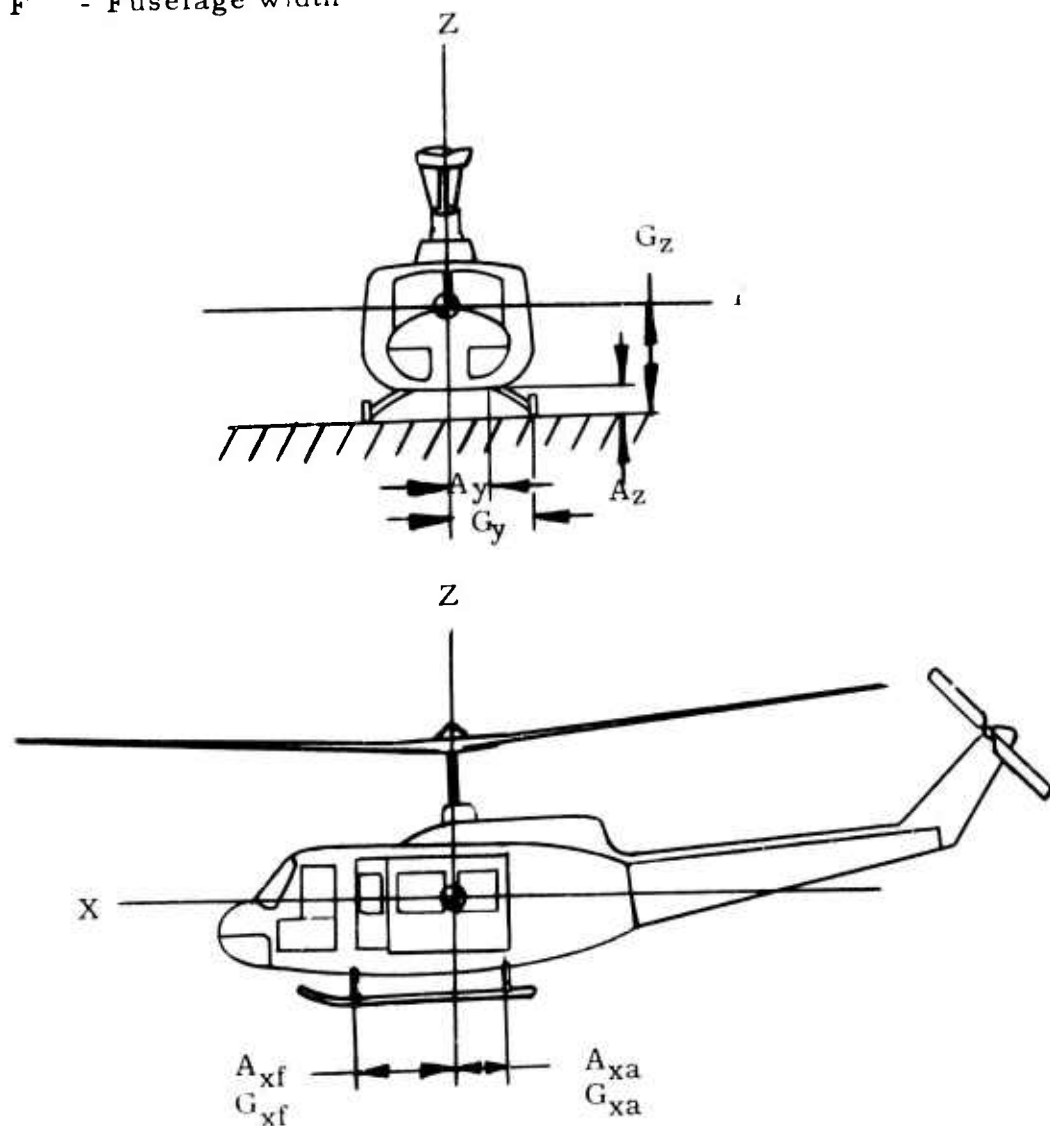


Figure 3. Basic Helicopter Dimensions.

TABLE VI. DATA ON HELICOPTER LANDING GEAR (REF. FIG. 3)

Descriptor	G_y	G_{xf}	G_{xa}	G_z	A_y	A_{xf}	A_{xa}	A_z	F
Type _{cf} Helicopter & Landing Gear									
LOH skid	3-4. 5	4-9	2. 5-9	4-5. 5	2-3. 7	2-3. 5	2. 8-3. 5	0. 9-1. 8	4-7. 5
UH, skid	3. 5-5	7. 5	3. 5	4-7	3. 5-4. 5	3. 5-6	1. 6-2. 5	1. 3-1. 9	7-9
CH, tricycle with single wheel toward nose	6. 5-7	21-22. 5	4. 5	10	3. 7-4	G_{xf}	G_{xa}	1	7. 5-8
UH, tricycle, with single tail wheel	5. 5-6	2. 5-5	17	8	2. 7-4	G_{xf}	G_{xa}	1-2	5. 5-8
CH, quadricycle	11. 3	5	16. 5	10-5	3. 7	G_{xf}	G_{xa}	1. 7	7. 5

heaviest gross weight reported 3.06×10^4 , 1.41×10^5 and 1.22×10^5 in.-lb-sec² for roll, pitch, and yaw respectively. The maximum difference is then 16 percent and the minimum, less than 1 percent.

TABLE VII. TYPICAL VALUES OF MOMENTS OF INERTIA				
Helicopter	Gross Weight Range (lb)	Moments of Inertia (in-lb-sec ²)		
		I _{Roll}	I _{Pitch}	I _{Yaw}
LOH	2,100 - 1,700	1.5×10^3	3.5×10^3	3.5×10^3
UH	8,500 - 11,000	2.5×10^4	1.4×10^5	1.4×10^5
CH	33,000 - 39,000	3.7×10^5	8.3×10^6	8.3×10^6

3.4 CONCEPT DEVELOPMENT

Three concepts are required to reflect the effects of weight class upon configuration, energy absorption, hardware, costs, etc. The procedure followed is to establish a configuration that first satisfies the normal landing loads requirement and then to establish the forces and energy levels that are developed because of the crash energy absorption criteria. In each case the vertical response is calculated first to determine a concept capable of attenuating the primary impact parameter. This is done primarily because of the difficulties encountered in examining combined loads and unusual attitudes. In order to develop reasonable concepts it is necessary to progress from the simplest, analytically, to the most difficult. To do otherwise would be to become lost in variations of load applications, load locations, and structural redundancies with their necessary mixtures of dynamic and structural analyses.

3.4.1 Medium-Cargo (CH) Class Configuration

The CH vehicle is defined as a helicopter having a gross weight range of 33,000 to 39,000 pounds. The first step was to define a wheel-type landing gear system that will satisfy the normal landing loads criteria.

3.4.1.1 Baseline Design

The stroke required for an air-hydraulic cylinder and tire system has been empirically shown to be

$$\frac{h}{r_1} = 0.8N - 0.469N^{0.23} + 0.47N^{1.9}K \quad (20)$$

where h is the drop height required (ft)

r is the ratio of vertical movement to strut closure

l is the stroke (ft)

N is the vertical load factor

$$K = \left(\frac{\delta_{\max}}{rl} \right) \left(\frac{W}{P} \right)$$

where δ_{\max} is the maximum tire deflection (ft)

W is the burst load of the tire (lb)

P is the static weight carried by one tire (lb)

The tire is assumed to be a low pressure tire of 6 to 9 inches width and capable of carrying a maximum load three times greater than its

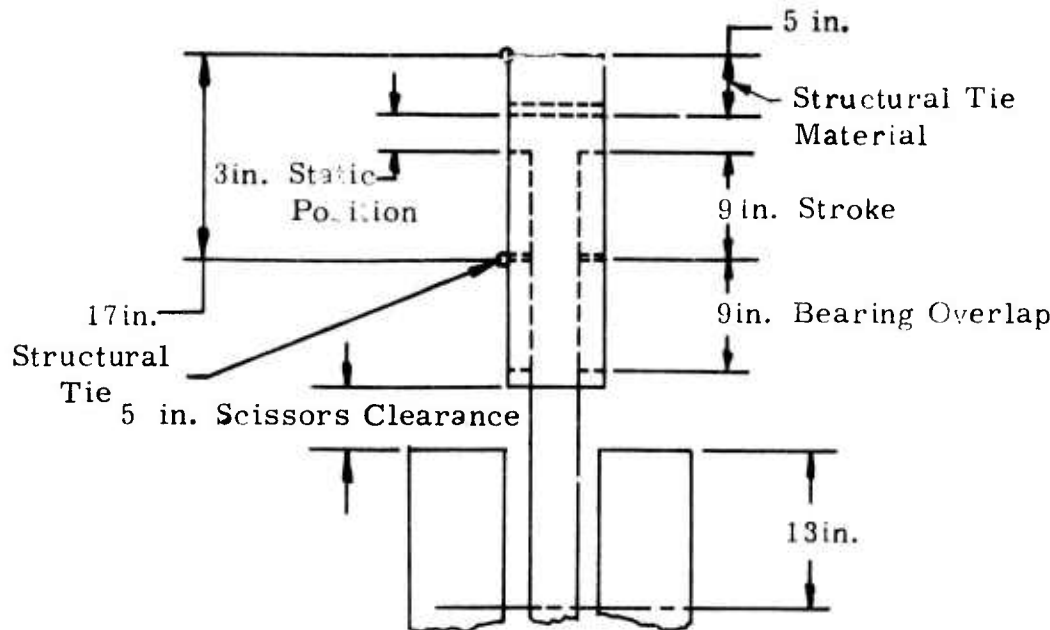
static design pressure ($\frac{W}{P} = 3$). Maximum tire deflection, δ_{\max} , is approximately two-thirds of the tire width. Drop height is 2.25 ft. corresponding to an impact velocity of 12 ft/sec, and maximum load factor desired is 3.5. Inserting these values into the stroke-required equation yields a stroke length of 8.5 inches. In order to provide a compression ratio of four, the clearance volume must be one-third of the stroke, and therefore, the total cylinder length required is approximately 12 inches. It is now necessary to determine the other dimensions required to locate the strut relative to the fuselage and ground.

The vehicle will be assumed to have tricycle landing gear with equal load distribution. The resulting 13,000 pounds per tire requires a multiple tire configuration per cylinder. By referring to MIL-T-5041E, a Type III MH-TL 8.50 x 10, 10-ply tire is necessary. The tire has a maximum height of 26.3 inches with a rim diameter of 10 inches and static deflection 35 percent of the sidewall depth.

The shock dimensions are finalized by assuming that the head of the piston requires 5 inches of depth for a structural tie, 9 inches of bearing overlap, and at least 5 inches beneath the strut for torque scissor mechanism and structure.

All of the above dimensions are, of course, based upon empirical equations as well as specification information and an appreciation for the structural material that must exist. The data are a set of basic design numbers indicative of the class being examined.

The landing gear system developed from these dimensions is shown on the following page.



The location of the landing gear relative to the fuselage must be established. If air pressure were lost in the oleo and the tire became flat, clearance would still be required between the fuselage and the ground. A 6-inch clearance is assumed. Adding the clearance, static oleo stroke, and static tire deformation, the upper attachment point of the strut must be 66 inches above the ground to provide an 18-inch static clearance above the ground. The resulting configuration is shown in Figure 4.

The original criteria of 3.5G permissible fuselage load factor and the 12-foot-per-second sink rate were used to arrive at the configuration found. The crash criteria must now be examined to determine the feasibility of using this system for energy-absorption purposes.

The oleo strokes 9 inches to get the vehicle up to 3.5G. The energy (U) dissipated is:

$$U = \eta NP \delta \quad (21)$$

using previous terminology.

Since the oleo efficiency is about 0.8 and the static weight per wheel is 13,000 pounds, the energy is 328,000 inch-pounds. The total energy to be dissipated based upon proposed criteria is

$$U = \frac{1}{2} MV^2 = 1,520,000 \text{ in-lb} \text{ when } V = 25 \frac{\text{ft}}{\text{sec}} \quad (22)$$

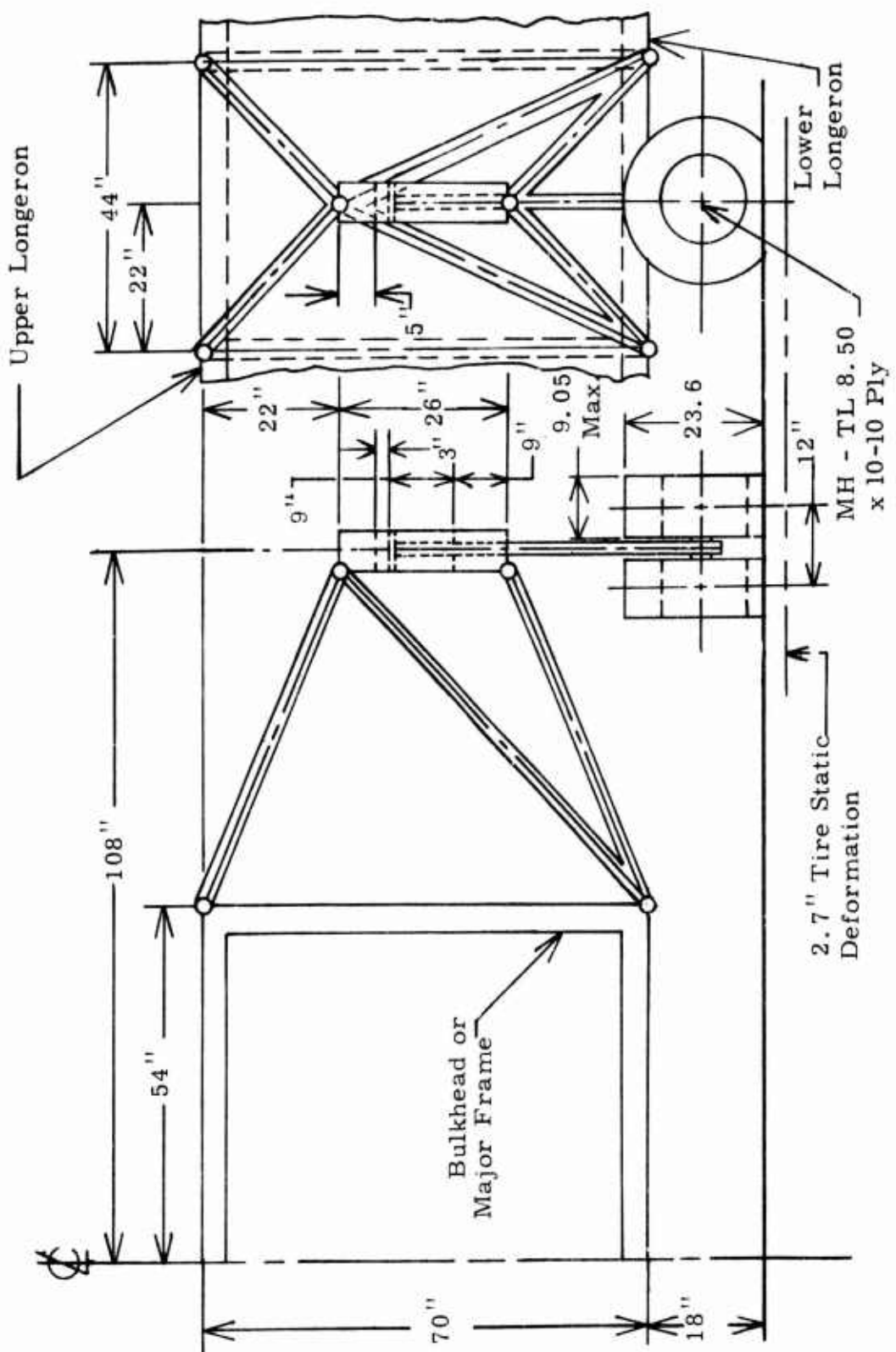


Figure 4. Medium-Cargo Configuration.

If the energy absorber is a liquid spring or equally efficient absorber, the energy relation would be

$$U_{ea} = \eta F \delta \quad \eta = 0.9$$

where F is the peak force developed at the end of a stroke of 8 inches.

The energy that must be absorbed after the $3.5G$ level has been surpassed is

$$1.52 \times 10^6 - 0.33 \times 10^6 = U_{ea} = 0.9 FS \quad (23)$$

where 1.52×10^6 = Total energy
 0.33×10^6 = Landing gear energy

The allowable vertical stroke is the difference between static clearance minus compression, and the remaining fuselage clearance. This results in a 9-inch vertical stroke. The peak force is then 0.147×10^6 pounds. If we examine the rigid body acceleration of the fuselage due to these forces acting on the fuselage, the load factor would be

$$\begin{array}{ll} 11.3G & \eta = 0.9 \\ 14.5G & \eta = 0.7 \end{array}$$

Therefore, it appears that even an inefficient absorber that can permit the proper energy to be dissipated over a 9-inch stroke will not cause the vehicle to exceed the $15G$ criterion established for fuselage structure.

Figure 4 shows the simplest structure possible to carry all applied forces at the wheel impact surface. Each member is a rigid link with pinned ends to permit only axial loads. The wheel span and fuselage size are assumed from the data of the previous section. The structural width was based only upon a symmetrical height to width dimension for upper and lower trusses.

3.4.1.2 Concepts for Attenuation of Vertical Crash Loads

It is assumed that the energy absorbed by the energy absorbers is dissipated after the oleo is fully stroked and the tire has ruptured. This is shown in Figure 5. This is a reasonable and conservative assumption. The tire fails at a burst pressure of four times the static weight, when the oleo has stroked and is on the clearance volume. The oleo contributes very little energy absorption beyond its design stroke since it is in that portion of the pressure-volume curve that it acts more nearly as a rigid link rather than an absorber. Hence, the 3 inches is conservative in that there is a greater stroking distance available than assumed.

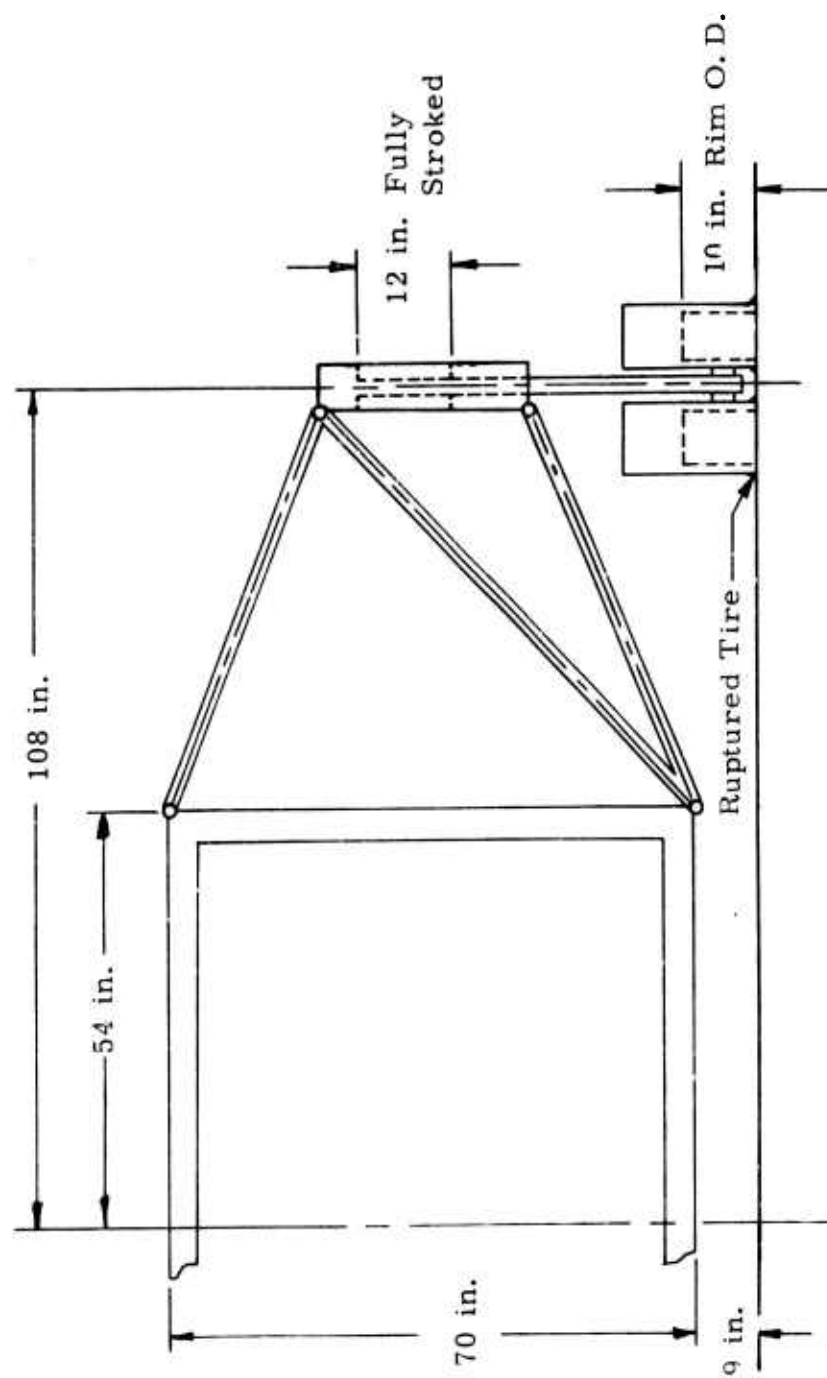


Figure 5. Configuration Prior to Energy Absorption.

The first concept shown (Figure 6) assumes that the lower elements of the truss remain rigid and that the upper elements are permitted to compress. Prior to compression, the forces build up to a level below the peak magnitude established in the previous section (147,000 pounds) and the absorber is then permitted to begin its stroke. The level that will balance the force at any particular instant will be determined by the operational nature of the energy absorber but will eventually approach the peak value. In order to determine conceptual forces, the peak value is used, realizing that this would be true only if a square wave device is actuated instantaneously when that level is reached. In the case of a liquid spring, the device would have to be mechanically in parallel with the existing strut. When the strut reaches a particular displacement, or fails, the spring would actuate and quickly establish the force levels required to dissipate the correct energy. The only point to be made is that ideally the vertical force strokes through several inches at the tire rim, while the energy absorber strokes at a constant force through the number of inches required. Practically, there are transient levels that will modify the results.

The applied force of 147,000 pounds acts vertically at 54 inches from the attachment points. As the landing gear system is raised, it rotates and the moment generated is altered by the change in orientation. However, the change is neglected. Hence, over the crushing of the upper element, the reaction is a constant value:

$$R = \frac{147,000 \times 54}{70.2} = 56,700 \frac{\text{in. lb}}{\text{attachment}}$$

Because of the orientation of the strut, the axial force in each is 65,200 pounds. The system rotates up as shown and the strut compresses 12.3 inches. This will dissipate 1.61×10^6 inch-pounds of energy. Since the original energy to be dissipated was less, and yet the deformation of the strut must be kinematically linked to the 9 inches of displacement, the peak force desired within the energy absorber must be 53,500 pounds. The vehicle impacts and begins to decelerate. The acceleration quickly exceeds the normal impact levels, and the impact force at the wheel reaches 121,000 pounds. The energy absorbers stroke as the landing gear system is raised, and the applied force of 147,000 pounds acts to accelerate the landing gear relative to the fuselage. The applied force peaks at a value greater than that necessary and the available and dissipated energy balance. This type of approach is the only means available to solve a kinematical and dynamics problem without using the true force-displacement characteristics of the elements.

3.4.1.3 Energy Absorption Techniques

The next aspect is whether these requirements can be met by any practical means. From the previous chapter it is possible to calculate the required dimensions for various types of energy-absorbing devices.

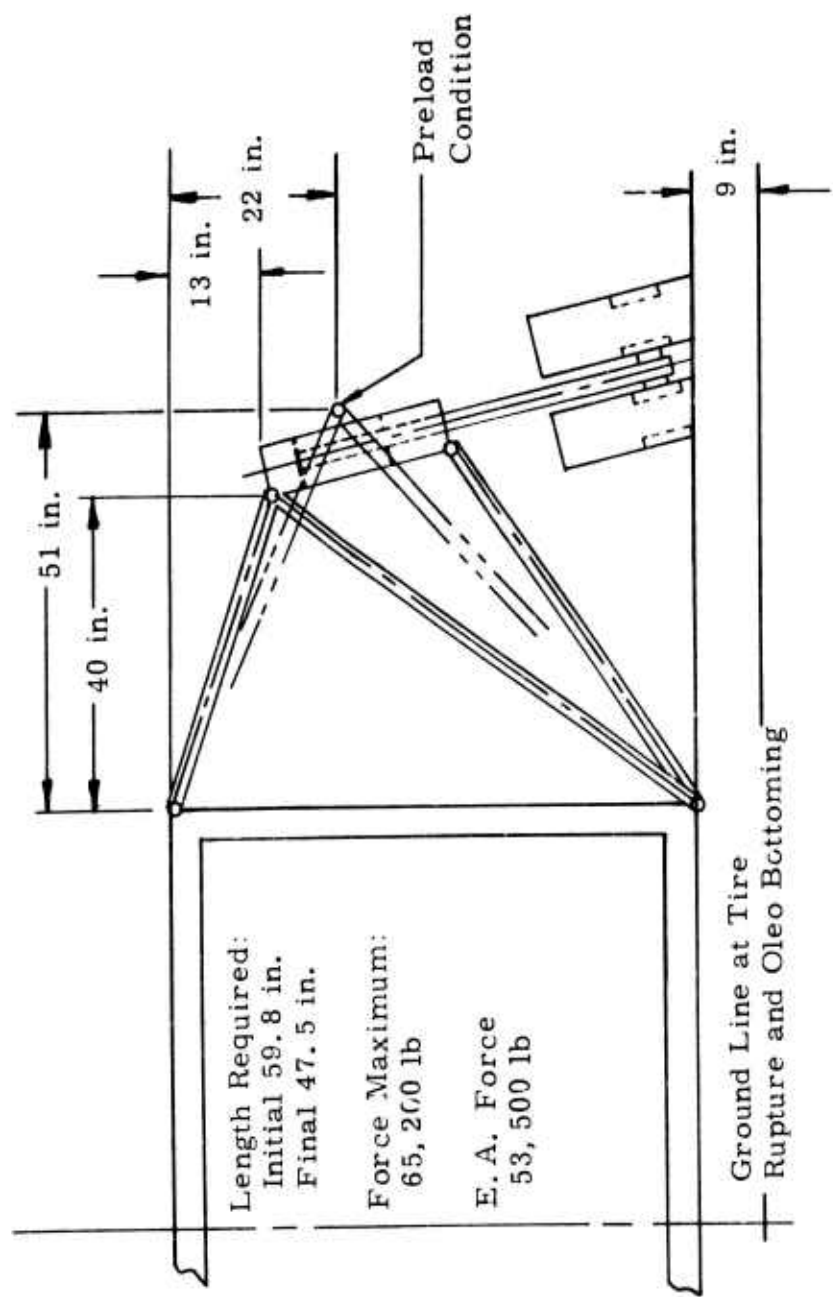


Figure 6. Compressed Upper Strut Concept.

3.4.1.3.1 Collapsible Tube

For the collapsible tube, the mean force is

$$\bar{P} = 8 (\sigma_y + 0.25H) t^{3/2} D^{1/2} \quad (12)$$

For 6061-T6 $\sigma_y = 40,000$ psi and $H = 30,000$ psi. Solving for a 53,000 pound capability yields a tube of 2.1 inch diameter. In order to be in the short column range, the effective slenderness ratio KL/r must be less than 63³⁷. A 2.0 inch-diameter tube with 3/16 inch wall thickness has a radius of gyration, r , of 0.644. Therefore, for a pinned-pinned column, $KL/r = 1.55L$. The critical column length is 40.7 inches. Therefore, it appears that it is conceptually feasible to have a compressible tube within the upper link of sufficient length to have end attachments and the 12.3 inches of stroke and not exceed a buckling length.

The load relation for an invertube is

$$P = \frac{A\sigma_p}{2} \left(\frac{1}{c} + \frac{2ct}{D} \right) \quad (23)$$

where A is cross sectional area of tube wall

σ_p is plastic yield stress

t is wall thickness

c is curvature parameter

Assuming a D/t of 10 and calculating a curvature parameter of 2 yields a tube of 4-inch outside diameter and 0.4-inch wall thickness for the same material as the compressible tube. A 4-inch OD and 3/8-inch wall tube has a radius of gyration of 1.289, and hence the critical column length is 81 inches. Again, conceptually, an invertube would function properly.

3.4.1.3.2 Cyclic Strain Device

Rolling torus type devices are available with appropriate characteristics. It is desirable to have the strut as a pinned element. Heavy-duty pinned-pinned elements have the capability of requiring 25,000 pounds actuation force and developing millions of inch-pounds of energy. It is desired to have units of one stage and approximately 50 inches in length, this would result in an extended length (L_{ext}) to compression length (L_{com}) ratio of less than 1.5 (Fig. 7). The Model H can develop 25,000 pounds provided the length is less than approximately 100 inches (Fig. 8). Fortunately, the element can be less for the concept application, and the energy is then dissipated over the stroke required. If two devices were placed in parallel, 50,000 pounds of retarding force would be available. The stroke is one-third of the total length, hence, a 37-inch, or greater, unit is required. Two heavy-duty Model H, small, TOR-SHOK devices of 37-inch total length would suffice.

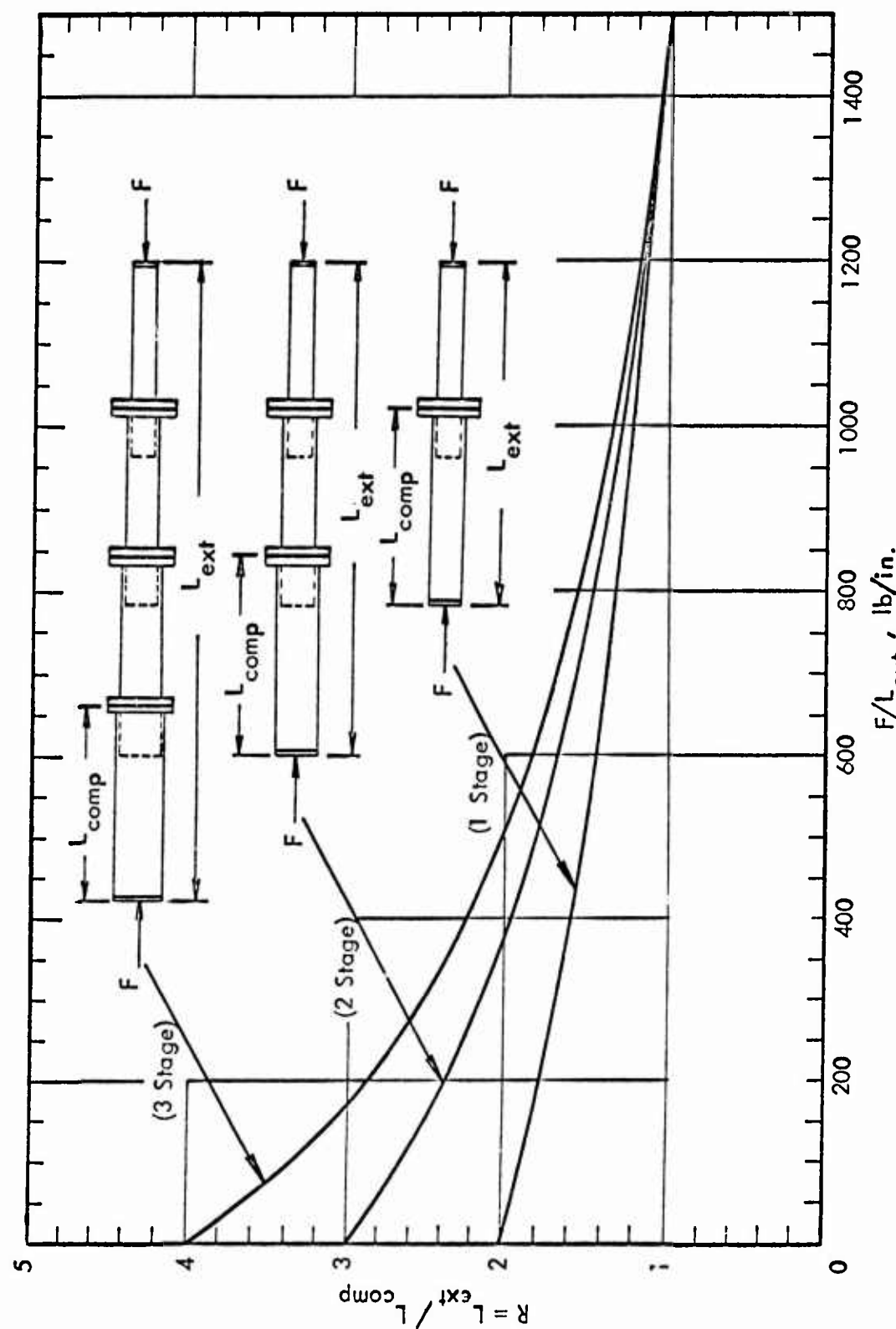


Figure 7. TOR-SHOK ARA Curves, Model H, Maximum Extended to Compressed Length Ratio.

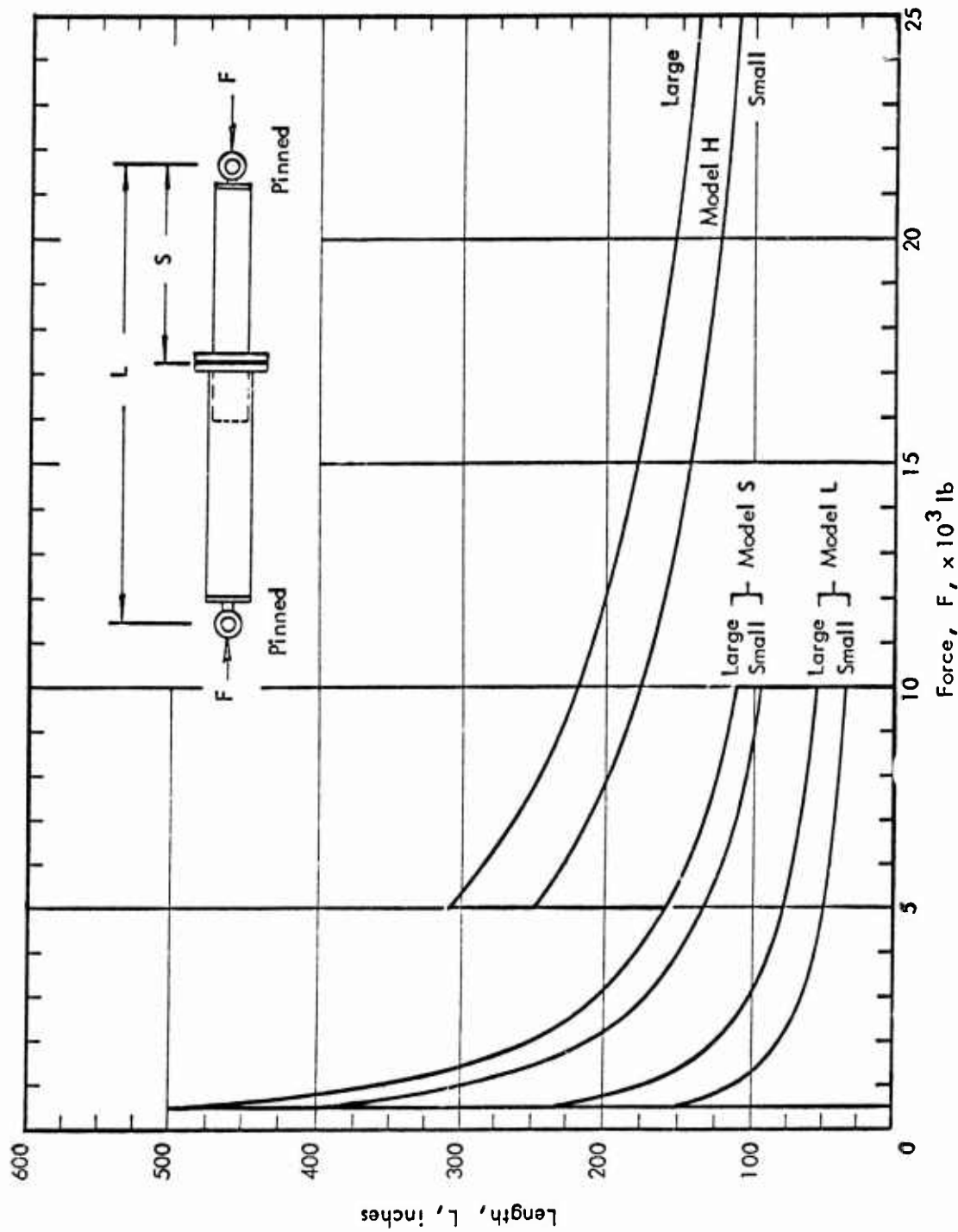


Figure 8. TOR-SHOK ARA Design Curves, Models S and L,
Maximum Extended to Compressed Length Ratio.

3.4.1.3.3 Liquid Spring

Liquid springs can be designed to provide just about any shock absorbing characteristic required. However, the specific design is a function of the compressible media used as well as the orifice and piston configuration. For this reason it is better, at least for a concept, to consider the application of known pieces of hardware. As an example, there is a commercially available "Fluidicshok" device that develops 46,000 pounds over 6 inches. The force is a long life value and can be increased by 30 percent for limited applications. This raises the capability to over 59,000 pounds and the energy capacity to 288,000 inch-pounds per actuator. By placing two in series, we have the capability of carrying 59,000 pounds over 12 inches and dissipating 1.15×10^6 inch-pounds of energy. Consequently, although the particular unit is not quite what is desired, it is very indicative of the unit that would be necessary. The 3-inch-diameter unit is 15 inches long, and two would fit between the attachment points of landing gear strut and fuselage.

The unique aspect of a liquid spring is that there must be some relative velocity across the device. If a liquid spring is slowly loaded, it will gradually stroke with very little force, neglecting preload. Therefore, structure that can carry normal static loads must be provided in addition to any energy-absorption hardware. A liquid spring cannot carry a large static load and still provide energy-absorption capability.

The two particular hardware designs are shown in Figure 9. These are shown primarily to establish the overall configuration of each and to demonstrate that particular designers would have to consider many practical design features in order to make the system operable. Both require a compression unit of approximately 60 inches length; this is achieved by either a series or parallel mechanical system. The end fittings must provide a swivel or ball joint capability, which is not particularly unusual for the truss arrangement shown. Similar fittings are currently contained in the truss arrangements of the CH-3.

3.4.1.3.4 Comparative Data

Before continuing into other concept problem areas, it is desirable to present some means of comparing the information considering aspects other than energy, force, and stroke requirements.

In general, the metal deformation techniques are the simplest considering the mechanism of achieving energy absorption. They are also the cheapest items if device cost alone is considered. There is no maintenance, and the weight is an absolute minimum since the device is capable of carrying all forces from normal loads through crash loads. However, there is some question concerning the reliability of the unit. Reliability can be considered acceptable only after many have been tested and evaluated over the range of forces, strain rates, and bending moment values possible. Hence, the material costs may be only a small portion of the development costs required. The basic problem in using

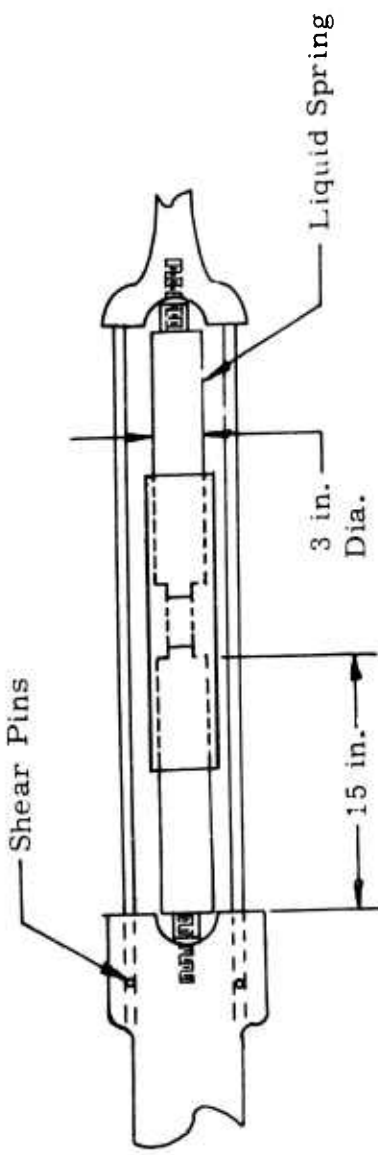
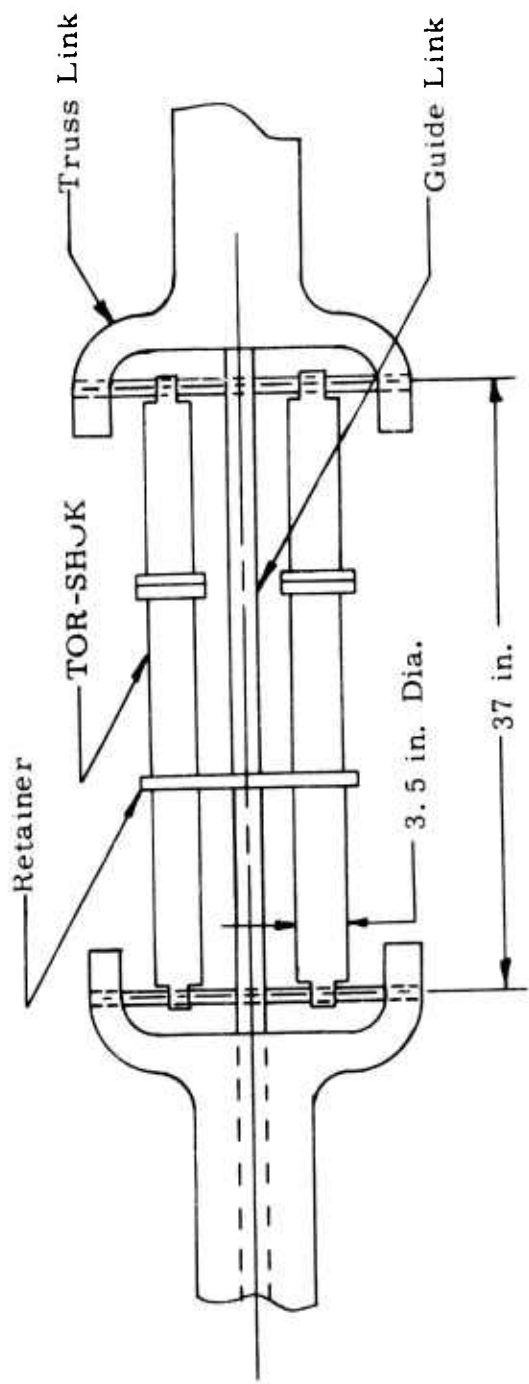


Figure 9 . Parallel and Series Hardware Designs.

metal deformation techniques is the lack of data at the conditions required for this particular application.

The cyclic strain devices, such as the TOR-SHOK or Mechanics Research Incorporated absorbers, can carry normal and impact forces without additional structure. They should not require excessive maintenance if properly protected from the environment. Some limited data have shown an environmental effect on the starting force which was caused by rusting of one tube¹¹. The costs of TOR-SHOK devices are approximately hundreds of dollars apiece, while MRI type devices have been an order of magnitude higher. The weight of the TOR-SHOK devices is about 20 pounds for a 25,000 pound unit of 30 inches length. Comparable MRI data are not available.

The liquid spring device has been used for many unusual environments and loading conditions. The unit has only a limited number of parts and proven reliability. The 46,000 pound unit weighs about 20 pounds and costs several hundreds of dollars per unit. The primary disadvantage is that additional structure must be provided to maintain any appreciable static load.

Qualitative information for the various concepts is compared in Table VIII.

TABLE VIII. COMPARATIVE DATA FOR ENERGY ABSORBER TECHNIQUES

	Metal Deformation	Cyclic Strain	Typical Liquid Spring
Capability to Carry Static Loads	Yes	Yes	No
Crash Load Capability	*Unproven	Proven	Proven
Environmental Effects	Possible	Possible	Negligible (-60°F to +200°F)

*The exception to this is the crushing of honeycomb which has been used successfully in several applications.

TABLE VIII. (CONTINUED)

	Metal Defor- mation	Cyclic Strain	Typical Liquid Spring
Reliability	Unknown	Some Basis Available	Proven
Maintainability	Limited	Limited	None Required
Simplicity (of the device)	Simplest	Most Complex	Ten Parts
Weight (of the device)	4.5-30lb/unit	30 lb/Unit	30 lb/Unit
System Weight (concept)	Least	Mean Value	Greatest

3.4.1.4 Concept Variations

Another means of dissipating the energy is to have the lower elements extend as the landing gear folds outboard under load (Figure 10). This method is not as efficient in that the loads contained in the tension members are smaller and require a greater stroke. It was assumed that an applied force at the outboard tire centerline would generate the extension initiating moment and require a balancing axial force of 19,300 pounds. As the applied force increases to the peak of 147,000 pounds, the average required (considering the change in orientation) becomes 51,000 pounds. Over a stroke of 17 inches, only 85 percent of the total energy is dissipated. If the fuselage were to crush without any significant resistance, a 20-inch stroke would be required, the energy would balance, and the vehicle would have crushed 5 inches.

Both dual acting hardware types previously mentioned could be used. The cyclic strain units can be made to variable lengths, and two 60-inch units in parallel would have the 20-inch stroke required with 50,000-pound capability. The liquid spring system would require three units in series and structurally in parallel with a strut capable of carrying the normal loads. Three in series would have 18-inch capability and require 45 inches of length. The other passive energy-absorption devices, compression tubes, invertubes, etc., would not provide the tension capability required. Another tension element concept is shown in Figure 11. The upper and lower elements are rigid, and the middle pair provide a means of pivoting the landing gear. The axial force levels are large, 79,200 pounds, and 8.5 inches of stroke will permit the

Length Required:
 Initial 59.8 in.
 Final 76.8 in.
 = 0.85 Required
 Force Average =
 51,000 lb

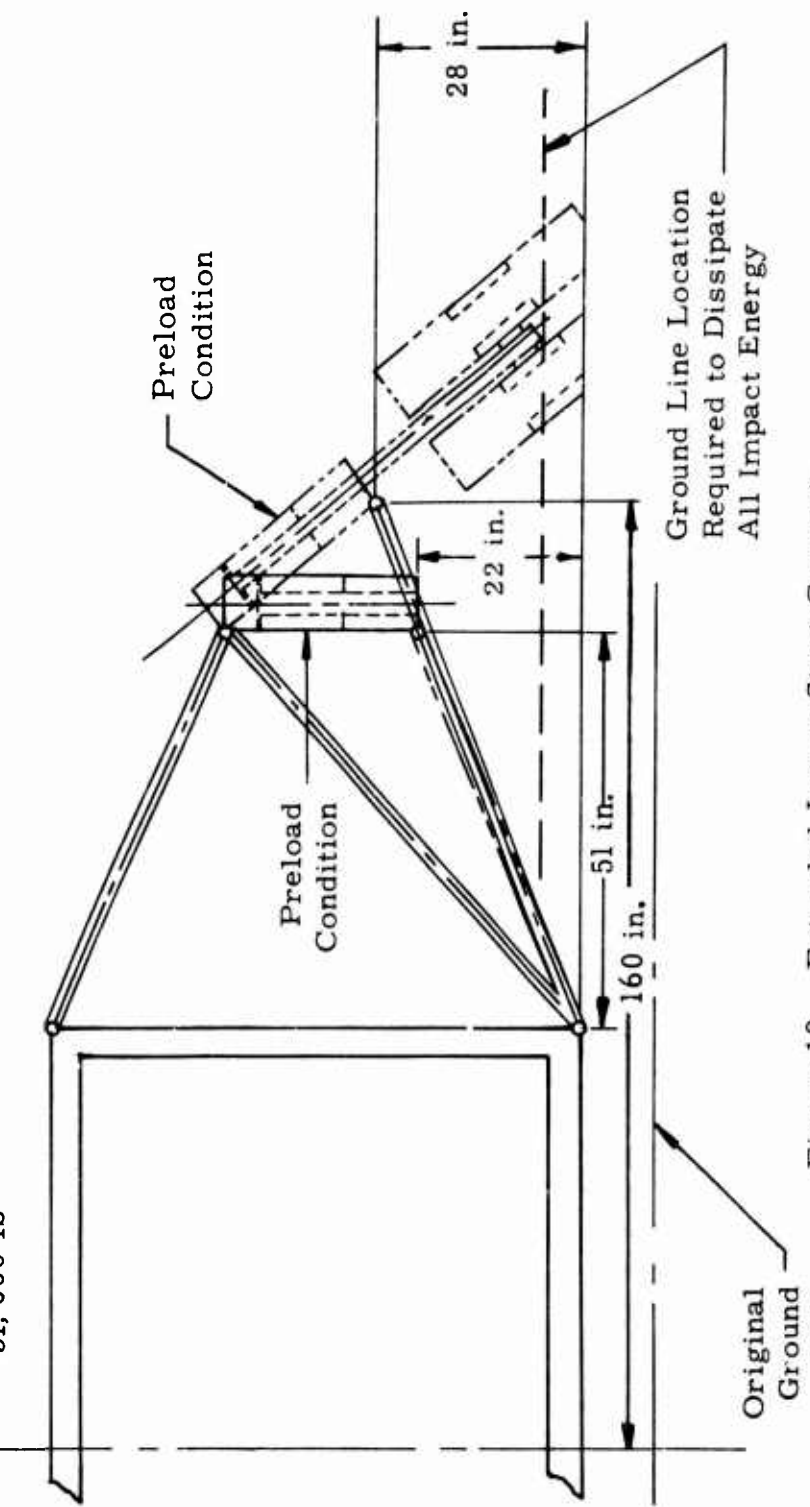


Figure 10. Extended Lower Strut Concept.

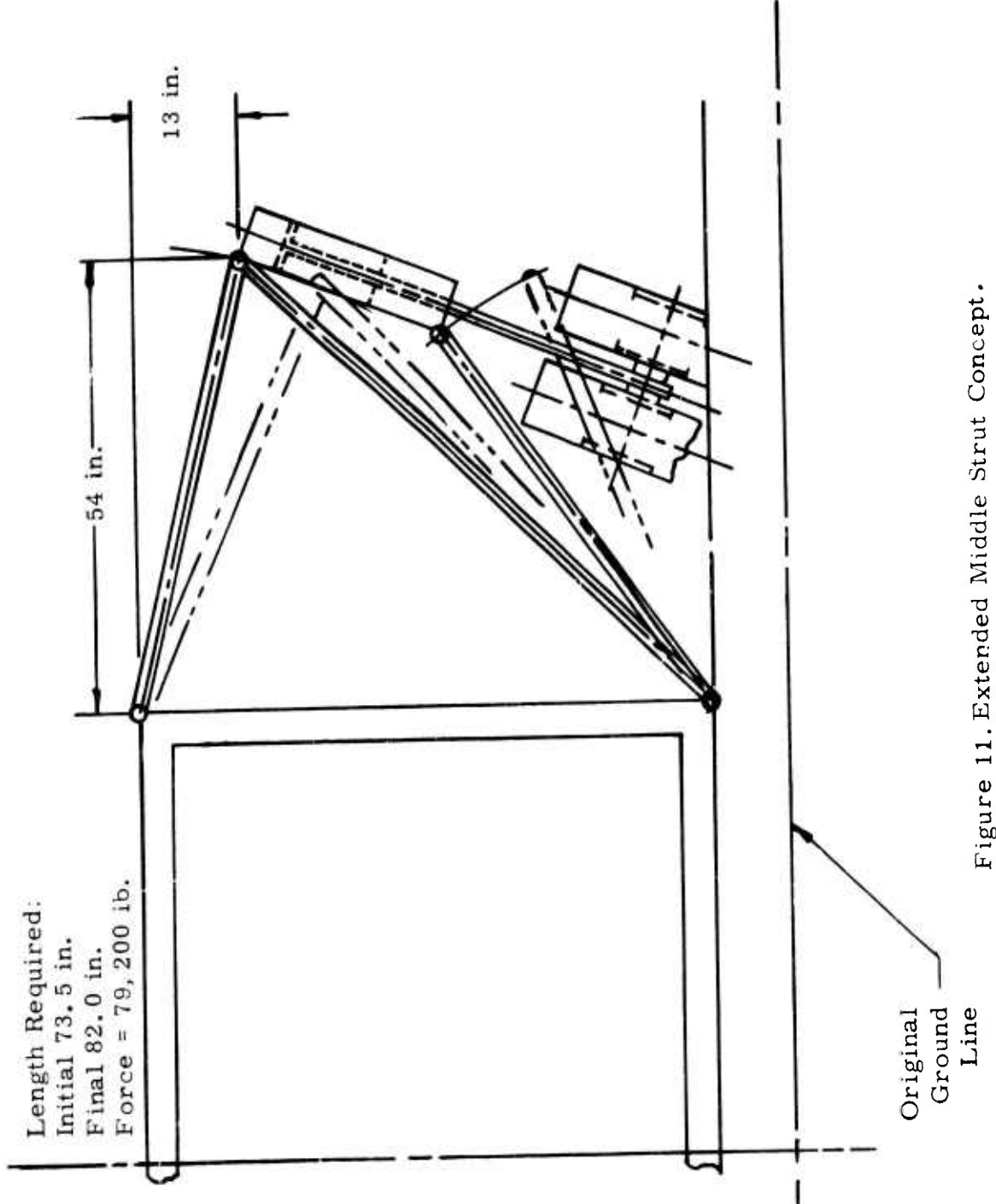


Figure 11. Extended Middle Strut Concept.

fuselage to bottom. The energy dissipated is within 2 percent of the available. Three cyclic strain devices could be used, or one liquid spring device. There is a commercially available liquid spring of 82,000 pound peak force with a 10 inch stroke. The unit is specifically a compression unit, but the liquid spring concepts are equally applicable for both compression and tension. Since this unit is available, a tension device can be provided.

Two other approaches are shown in Figures 12 and 13. Both rely on being able to maintain the configuration of the landing gear support structure and permitting the fuselage attachment points to be extended or compressed. Both configurations have many inherent difficulties not contained in the previous concepts. If the lower attachment point is to be withdrawn, a vertical force component must be carried by structure running from the lower attachment to the upper. This means that a portion of the frame must tear out, or separate structure must be provided, such that as the point swings out the vertical force is transferred to the upper attachment. Otherwise, the energy absorber must carry bending. The forces and strokes can be satisfied by cyclic strain or liquid spring devices.

If the upper attachment point crushes, the fuselage structure must be penetrated or additional structure must be provided above the frame. The stroke would have to be guided to provide reaction capability for the vertical components.

Another approach would be multiple energy dissipation paths. Figure 14 indicates an attempt to absorb the energy vertically in the frame. If the structure is permitted to rotate as the vertical force at the lower attachment strokes, the required length would crush the fuselage. If it is assumed that the upper strut can compress a small amount, 9 inches would be adequate clearance. The figure shows a 9-inch vertical displacement of the 50,500-pound vertical reactions, and a compression of 2.8 inches of the 65,200 pound axial force upper elements. This would provide the necessary absorption within 4 percent. The lower attachment would require a guide mechanism to react the horizontal component. Neither force nor stroke requirement is demanding for the current hardware previously mentioned.

The last concept (shown in Figure 15) is designed to eliminate any drag being carried through the energy-absorbing link. This will be shown to be important in the next section. The configuration has triangular trusses to carry the drag loads, and the vertical elements can balance any applied vertical or side load. The concept is similar to the CH-3 truss system. If the system rotates about the center attachment, the upper and lower elements carry 123,000 pound axial force over approximately a 5-inch stroke.

The simplified load paths create very large forces. This was done to demonstrate a concept that produces force levels that would tend to

Length of Stroke:
13 in.
Required: 11.7 in.
Force = 56,700 lb

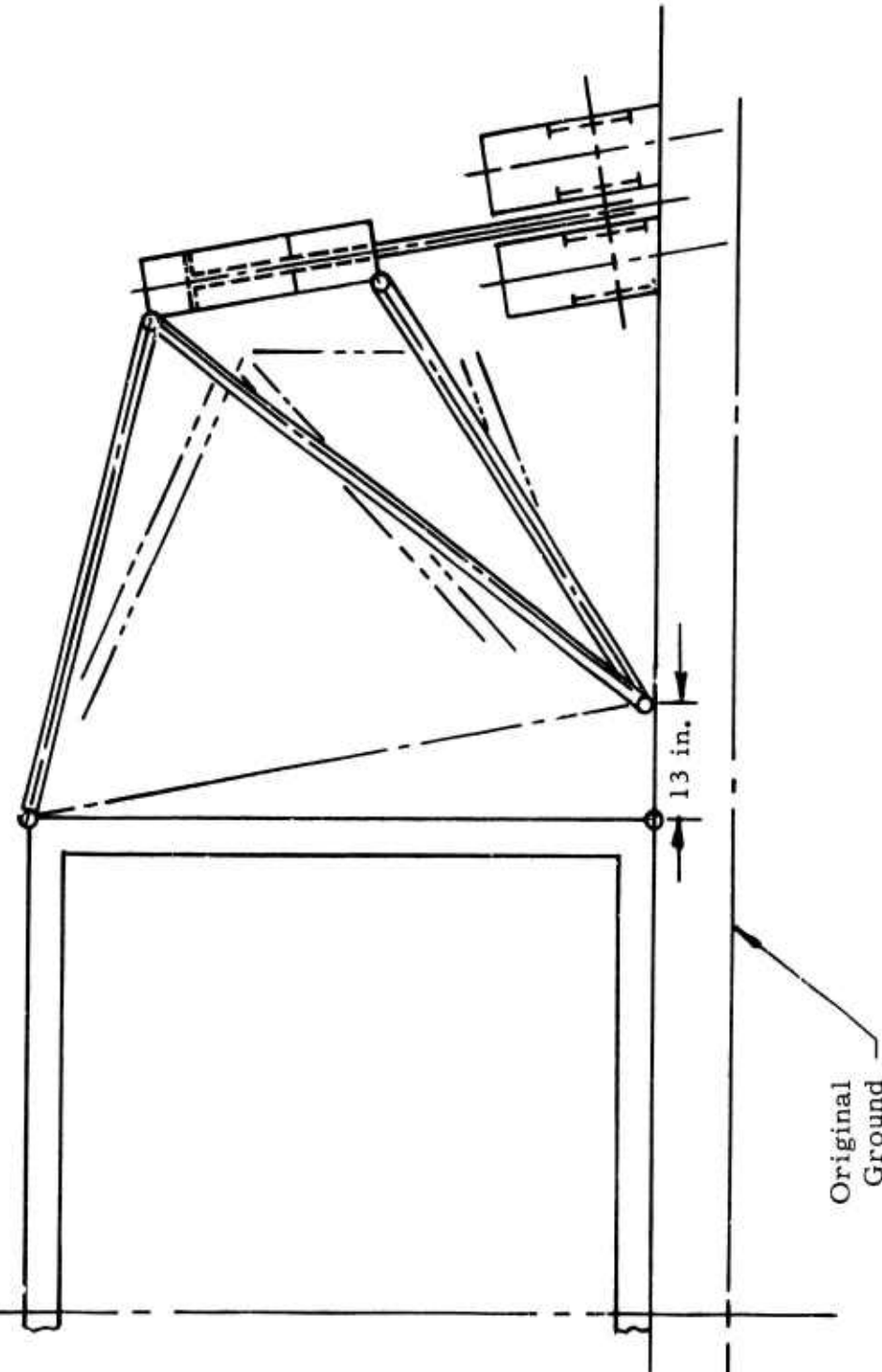


Figure 12. Extended Attachment Point Concept.

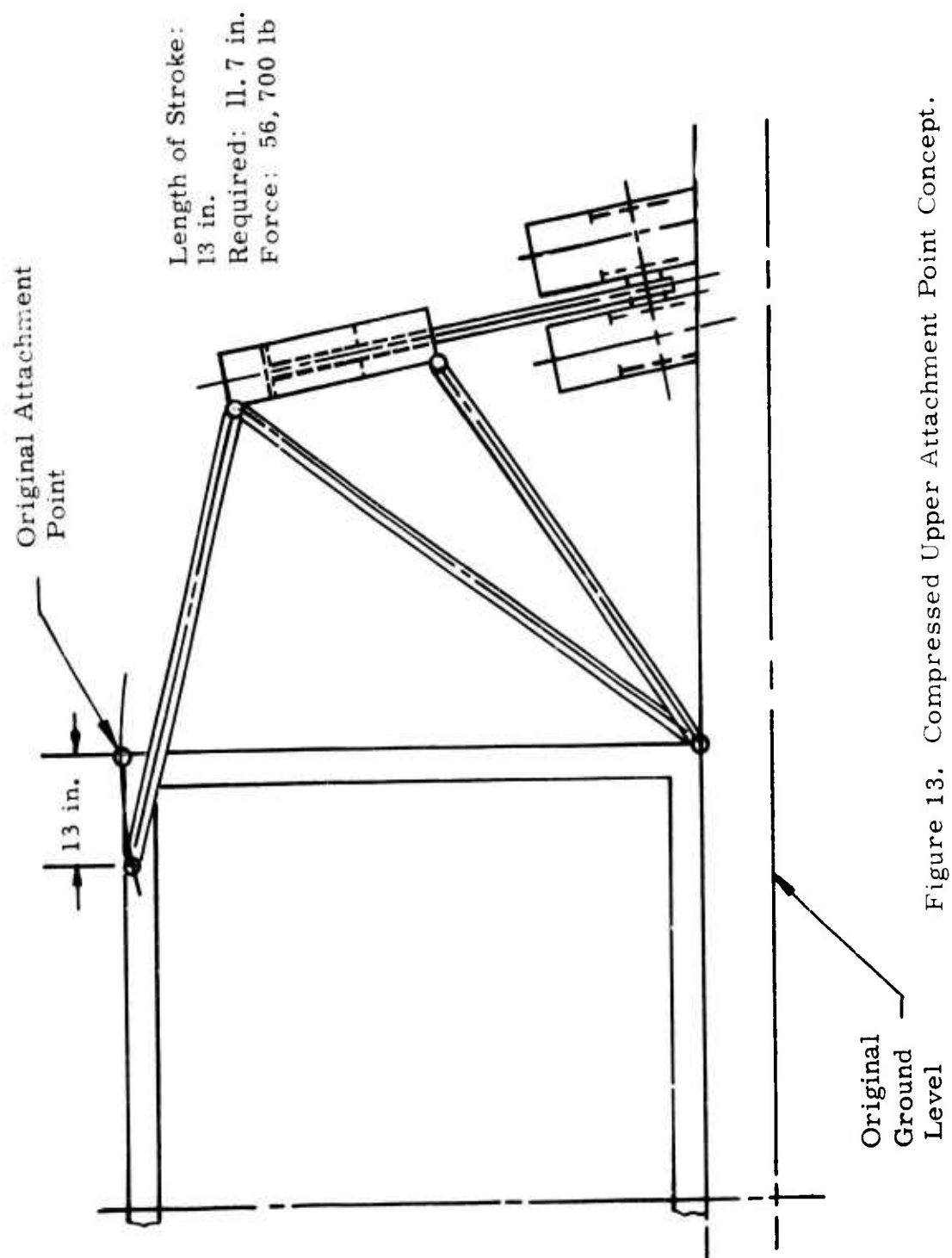


Figure 13. Compressed Upper Attachment Point Concept.

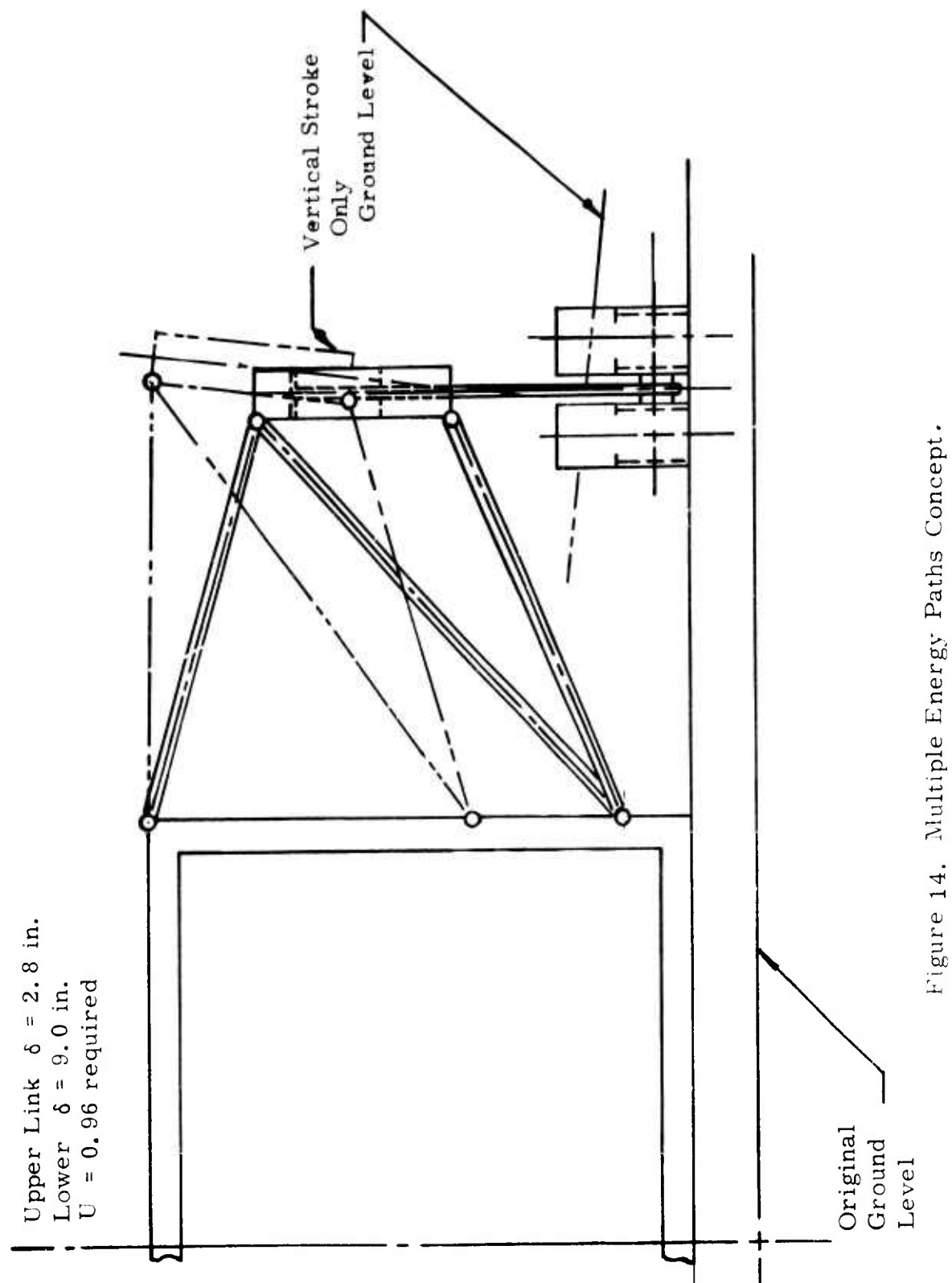


Figure 14. Multiple Energy Paths Concept.

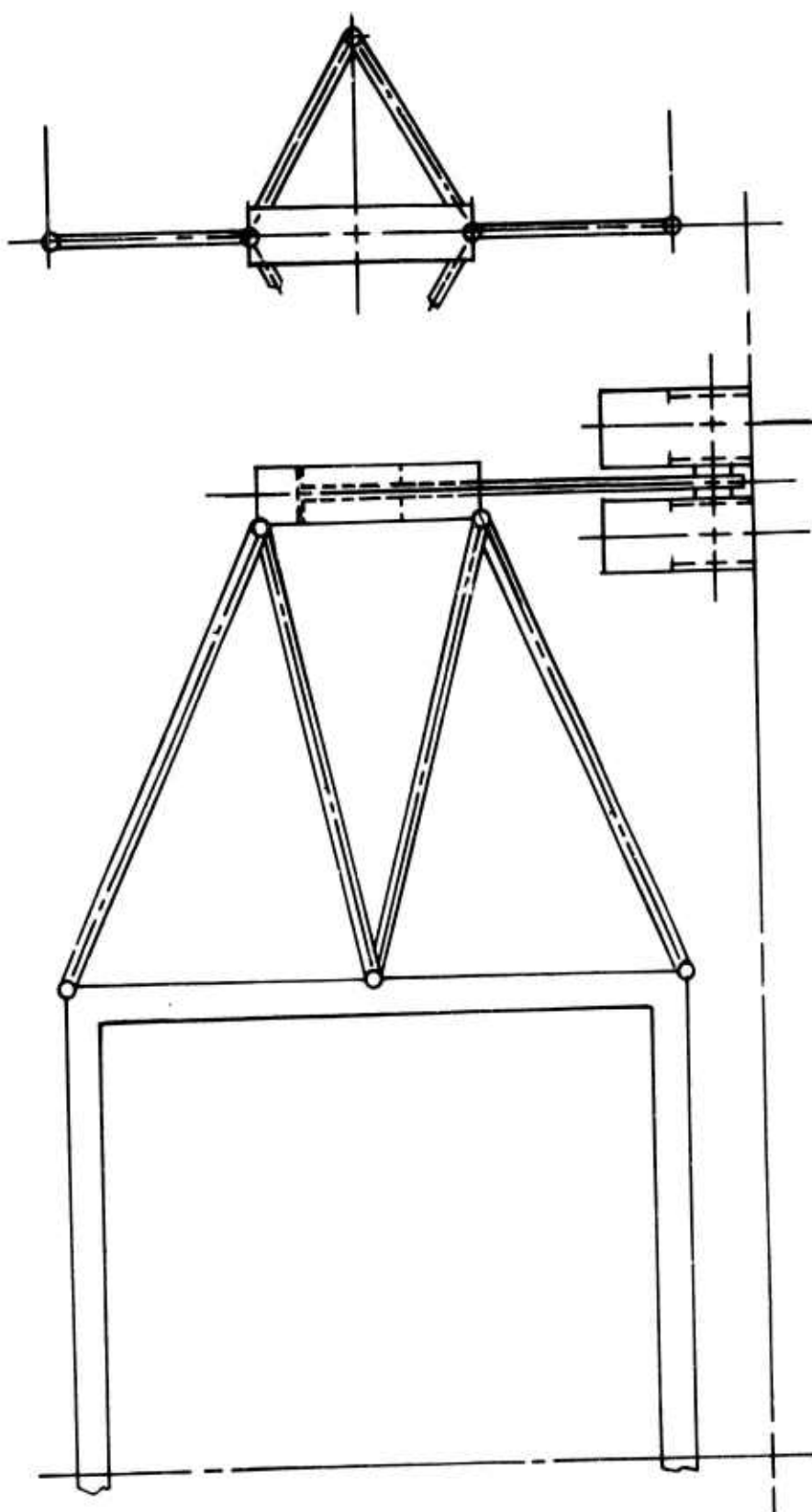


Figure 15. Developed Forces Concept.

eliminate available cyclic strain devices because of the number of units required. However, there is a commercially available liquid spring having 120,000 pound (nominal) capacity with 6-inch stroke. The concept is shown in Figure 16.

Several variations of the original concept have been presented to indicate that there are many possible means available to dissipate energy. The most direct method is to crush or elongate an axial load carrying member. This is accomplished by having truss arrangements and limiting the number of elements that can be solved by statically determinate methods. It is apparent that if variations of energy-absorbing capability were examined for all possible combinations of upper, lower, and middle strut compression and elongation, as well as attachment point motion there would be many pages of concepts. This could be further extended by considering the addition of beam elements rather than axial elements. However, several comments can be made about the limited concepts observed.

First, any motion tends to introduce forces or deformations not along the axis of the absorber. These must be taken out by appropriate pinned connections. Because of the practical aspects of achieving this and yet carrying large forces, it appears that the techniques of deforming metal have limited proven capability for this application. The compressible tube, invertube, and frangible tube techniques have not been tested for the configurations required. Empirical relations are available for each, but the relations must be used for extrapolation rather than interpolation. Additionally, any compression member is usually sensitive to the eccentricity of the applied load. Any introduced bending could, at operating levels, cause failure of the absorber.

Secondly, it appears as though the energy levels and force levels required are within the capabilities of current cyclic strain and liquid spring devices.

3.4.1.5 Drag and Side Load Effects

The drag and side forces have been calculated assuming a coefficient of friction of 0.5. This was based upon the value specified by ANC-2. The peak vertical force is assumed to be the original 147,000 pounds per strut. Fortunately, as the force builds, the moment arm decreases. The peak applied drag force (D) and resulting moment (M) are

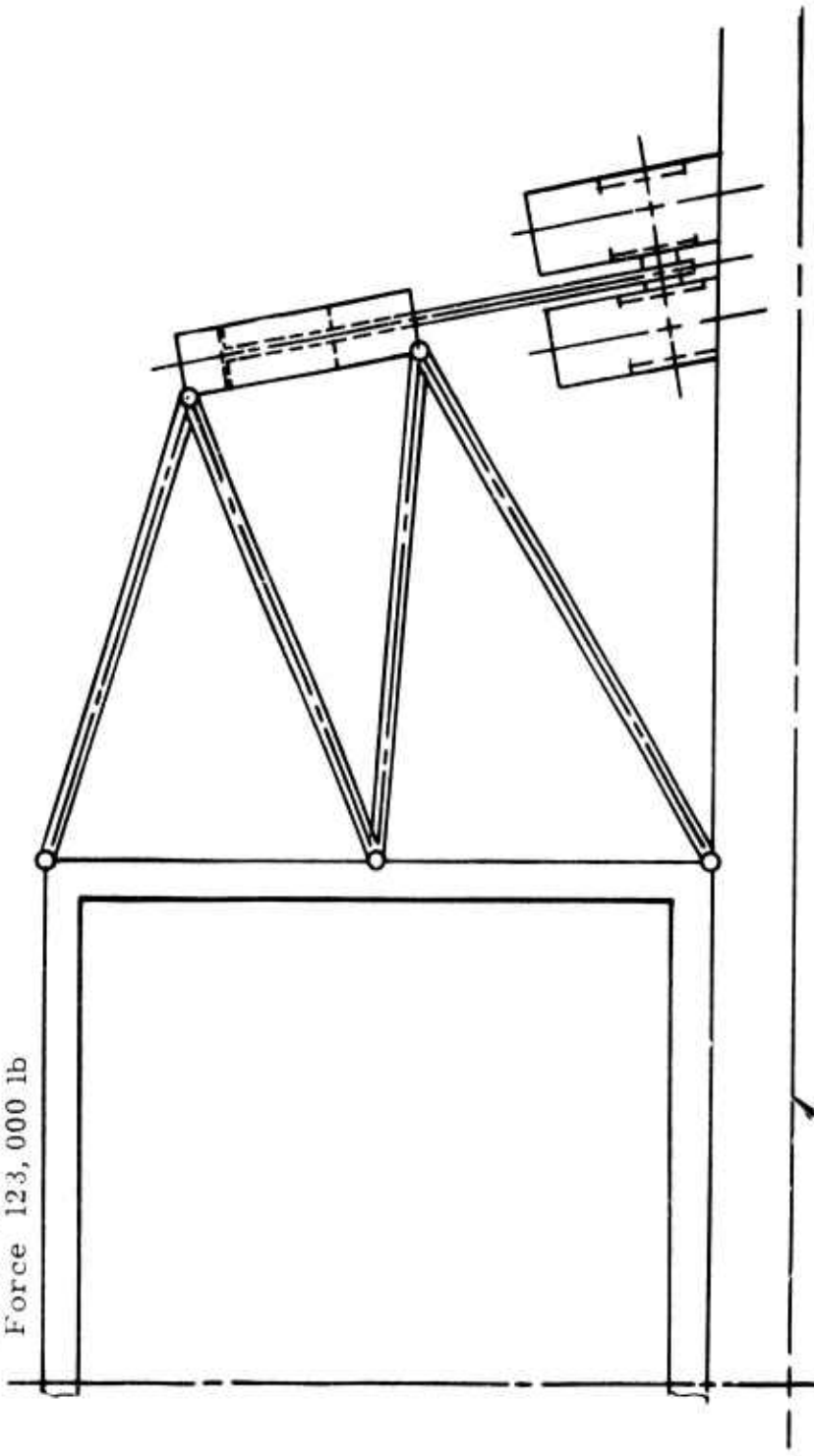
$$D = \mu F = 0.5 (147,000) = 73,500 \text{ lb} \quad (24)$$

$$M = 22D = 1,617,000 \text{ in.lb} \quad (25)$$

These result in axial forces of 60,500 pounds, 27,500 pounds, and 192,000 pounds in the upper, middle, and lower struts respectively.

The peak applied side force and moment introduce axial forces of

Length Required:
Initial 55.7 in.
Final 61.2 in.
Force 123,000 lb



Original
Ground
Line

Figure 16. Developed Force Concept - Both Element, Stroke.

24,700 pounds, 13,000 pounds, and 78,000 pounds into the same members in the same manner.

The summation of these is shown in Figure 17. It is quickly evident that the drag and side forces have significant effect. The immediate question is how to provide protection for the variations that may exist.

Table IX presents the possible combinations of forces to be absorbed. It is necessary that the absorbers work for the vertical drop, and it is only reasonable based upon the available accident data, that drag forces will be present. This seems realistic for an autorotation. Consequently, it is necessary to determine those links that are consistent with previously developed concepts. The only acceptable ones are elements 3 and 4 which extend during impact. If the drag is considered to be present whenever the impact occurs, it is necessary to lower the actuation level of the forward absorber from 79,000 to 51,500 pounds and maintain the other at 79,000 pounds. In this manner, when the impact builds to 65 percent of the pure vertical value, the forward link yields, dumping the load into the other elongating strut. At that instant, the rear strut is already at 69,500 pounds and the absorbing element has begun to stroke if a liquid spring device is used. If a cyclic device is used, the unit is only 11 percent beneath its starting force level. The other truss members would provide some stability to the system and enable both units to stroke over approximately the same distance. This would cause the required stroke to increase from a nominal 8.5 inches to 10.3 inches, which is possible for the unit discussed.

3.4.1.6 CH Summary

The original concept configuration was selected to show with easily defined load paths several means of absorbing energy while satisfying the crash criteria. Several concepts were shown with only a vertical velocity impact. The impact energy could be dissipated by several means, and each could be implemented by available techniques.

The addition of drag and side forces complicates the problem if the structural load paths are coupled for combined loads. It is always necessary to provide structure capable of carrying forces in every direction. Whether these structural elements can be decoupled during loading must be established by analysis of any particular original concept. The configuration examined in the previous section could, in fact, accomplish this. How many other approaches are capable of accomplishing this is unknown. A torque tube could be used to carry that drag force while adding little vertical stiffness, or beams could be placed to add negligible stiffness in particular places of loading.

If the concepts cannot provide decoupling because of other practicalities, then the combined loads analysis must be conducted and load paths found which have monotonically increasing forces with added loads. It is interesting that members are designed for maximum forces, whereas

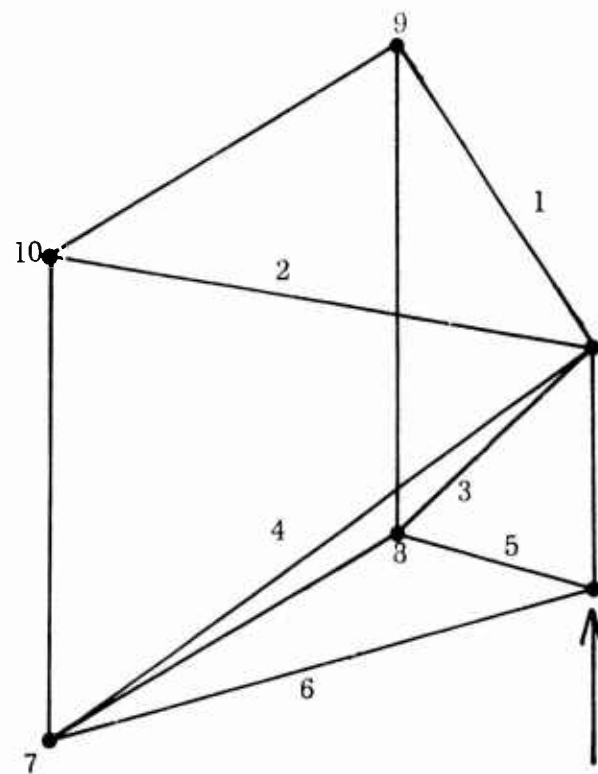


Figure 17. Combined Loads Distribution.

TABLE IX. ELEMENT LOADS (LB)				SELECTED INPUTS	
Force*	V	D	S	V + D	V + D + S
Element					
1	-65,000	60,500	24,700	-4,500	+20,200
2	-65,000	-60,500	24,700	-125,500	-100,800
3	79,000	27,500	13,600	106,500	120,100
4	79,000	-27,500	13,600	51,500	65,100
5	0	-192,000	-78,000	-192,000	-270,000
6	0	192,000	-78,000	192,000	+114,000
Joint					
7	56,700	147,000	-58,000	203,700	145,700
8	56,700	-147,000	-58,000	-90,300	-148,300
9	-56,700	52,500	21,400	-4,200	17,200
10	-56,700	-52,500	21,400	-109,200	-87,800

*V = Vertical Force (lb)
 D = Drag Force (lb)
 S = Side Force (lb)

energy absorbers must be designed to actuate under the minimum load. When the forces do not increase as desired, it is possible that the configuration can be changed to modify the component or axial forces of the members. Elongating a span, or increasing the height of the attachment points, can be used to adjust the force within a particular member in order to take advantage of the effects of combined applied forces.

The CH concepts shown indicate that the force levels developed by the structure and absorbers are carried by available techniques. The forces, energy, and stroke lengths required are satisfied without exceeding the crash criteria established. Commercially available devices are applicable, and hence it is reasonable to assume that crashworthy improvements can be made. The analyses have been approximate, since a true dynamic analysis was not conducted. But the techniques are consistent with current design practice and indicate sufficient flexibility in the hardware requirements to insure feasibility.

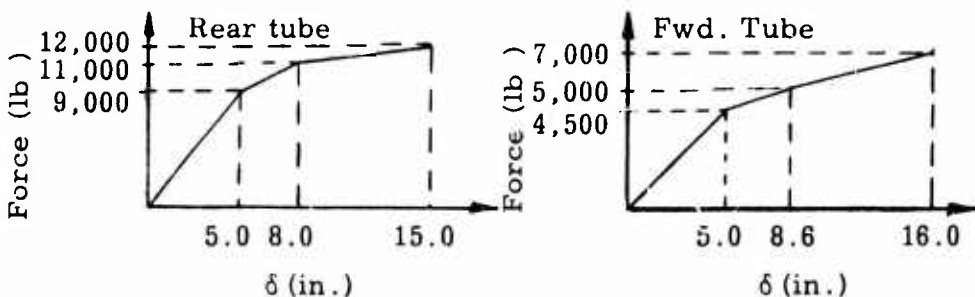
3.4.2 Utility (UH) Class Configuration

The UH class helicopter has a weight range of 8,500 pounds to 11,000 pounds.² The analysis will be restricted to a skid-type landing gear. The discussion follows that of the previous section in that energy relations are used to calculate realistic stroke and force levels, which are then used to determine realistic concepts.

3.4.2.1 Baseline Design (Figure 18)

The initial step is to examine the response of a skid configuration to determine how one is normally designed. In this manner the loads dictated by conventional criteria can be satisfied. A skid is assumed to be a rigid frame that relies upon the bending strength of the cross-members to carry the static weight and utilizes the strain energy of plastic bending to absorb impact energy.

Several curves are available indicating the force-deflection and energy dissipated by a skid. From a Bell report "Structural Analysis of UH-1F", there are two curves for large and small diameter tubes³⁸. Schematics of the curves are shown below:



Approximate analysis indicates that the efficiency of the large diameter tube up to ultimate is 74 percent and that of the smaller is 71 percent. The energy approximation is introduced to establish a design relation:

$$\frac{V^2}{2g} = N\eta s \quad (17)$$

From the same report it was possible to establish that at the design impact condition (9.8 feet per second), 3.28G was reached with a 12.9-inch stroke. Therefore, the design relation for the skid is

$$\frac{V^2}{2g} = \frac{N(67.5)s}{1.44} \quad (26)$$

indicating that over the design force range (not ultimate), a lesser efficiency is required to make acceleration and stroke balance.

If it is assumed that the normal design condition for impact is 12 feet per second and 3.5G, 16 inches of stroke is required. Available data indicate that the skid cross members are usually placed to carry two-thirds of the weight on the rear support. For the 11,000 pound UH weight, this means 7,320 pounds (mass) to be stroked over 16 inches. The energy dissipated is 277,000 inch-pounds. The crash condition generates because of the kinetic energy:

$$U_t = \frac{1}{2} \left(\frac{7320}{386} (2512) \right)^2 = 854,000 \text{ in.-lb} \quad (27)$$

The energy absorber must develop

$$U_{ea} = 577,000 \text{ in.-lb}$$

$$U_{ea} = F_{ea} \eta s \quad (28)$$

$$\eta = 0.9$$

The maximum force and stroke must equal 642,000 inch-pounds. If the structure is to feel 15G, the stroke should be 5.82 inches. Therefore, if 6 inches is provided, the resulting acceleration level should be 14.6G.

A balanced loading condition would create a force of 12,800 pounds applied to one skid at 3.5G. By referring to the Bell analyses for a similar configuration, the maximum aft tube bending moment calculated using a redundant analysis would be 323,000 inch-pounds. Aluminum tubing with a D/t ratio of 10 has a bending modulus 1.35 times greater than the ultimate tensile strength. Aluminum tubing of 7075-T6 will,

therefore, provide an allowable stress of 110,000 psi. The stress can be satisfied by a 3-3/4-inch-OD, 3/8 inch wall thickness tube. Such a tube cantilevered from a fuselage will deflect 0.9 inch under a static weight. This implies an effective stiffness of approximately 4,000 pounds/inch, which is about double that of the 6,600 pound UH-1 configuration. The result of this analysis is that the UH weight vehicle will appear as shown in Figure 18. Under static load it deflects 1 inch; 15 inches is necessary to reach the normal impact level, and an additional 6 inches is provided for the crash criteria.

3.4.2.2 Concepts for Attenuation of Vertical Crash Loads

The concepts that follow show the skid as an undeformed member at the 3.5G impact level. This is not completely accurate since the attachment point at the frame has some original angle with respect to the horizontal. Therefore, as the beam deflects it attempts to maintain that angle and curves along its length. The figures assume the curvature to be negligible.

3.4.2.2.1 Concept 1 (Figure 19)

The first concept indicates that a rigid link is provided to cover the skid as long as 3.5G or greater acceleration is developed. At levels less than 3.5G the link could rest against its supporting structure, or could be designed to continue to cover the strut. As a large impact develops, the link follows the strut on roller surfaces and is raised about its pivot point. Since the lower corner of the link is attached to an absorber, the absorber must be stroked in order for the strut to be raised. A tensile force of 107,400 pounds is developed over 3 inches. Two Series 12 fluidic shocks in parallel could approximate these requirements. Cyclic strain devices require greater stroke, and crushable tubes are again eliminated because of the high force levels required.

3.4.2.2.2 Concept 2 (Figure 20)

The second concept is more conventional in that a link, or links, can be added to stroke as the strut is raised. Figure 20 indicates that two link locations have been examined. The short link requires forces that restrict its usage. The longer link is feasible in that the load-deformation is the same as in the previous concept. The links would ride in slots in the struts in order to permit the energy absorber link to float until high enough deformations are reached.

3.4.2.2.3 Concept 3 (Figure 21)

The third concept is perhaps the most direct and yet the easiest to implement. Another strut is added below the fuselage at the fuselage mold line. The strut is supported by energy absorbers that stroke 6 inches and must collectively develop 53,700 pounds. Several compression tubes in parallel could provide the necessary energy, as could

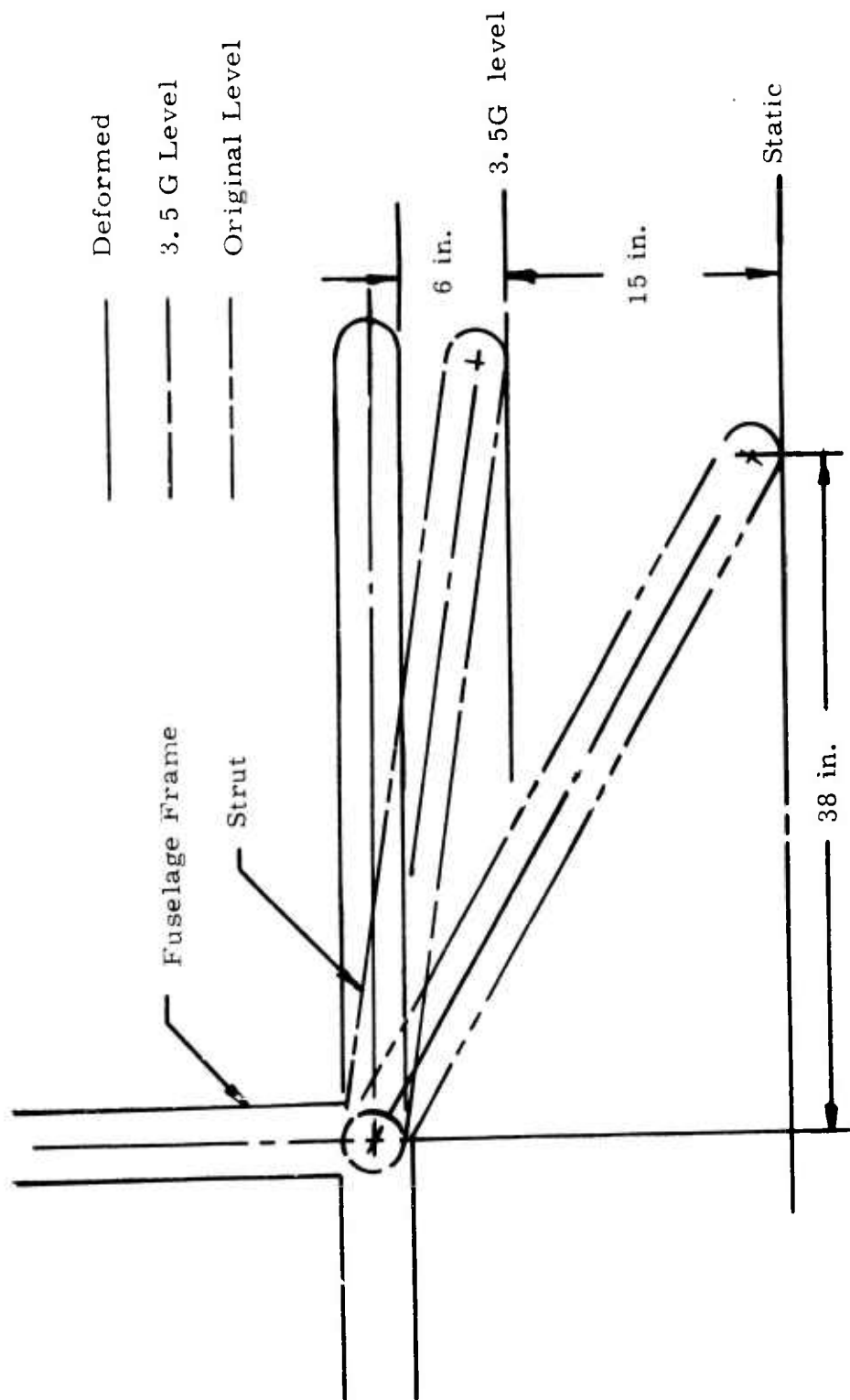


Figure 18. UH Baseline Configuration.

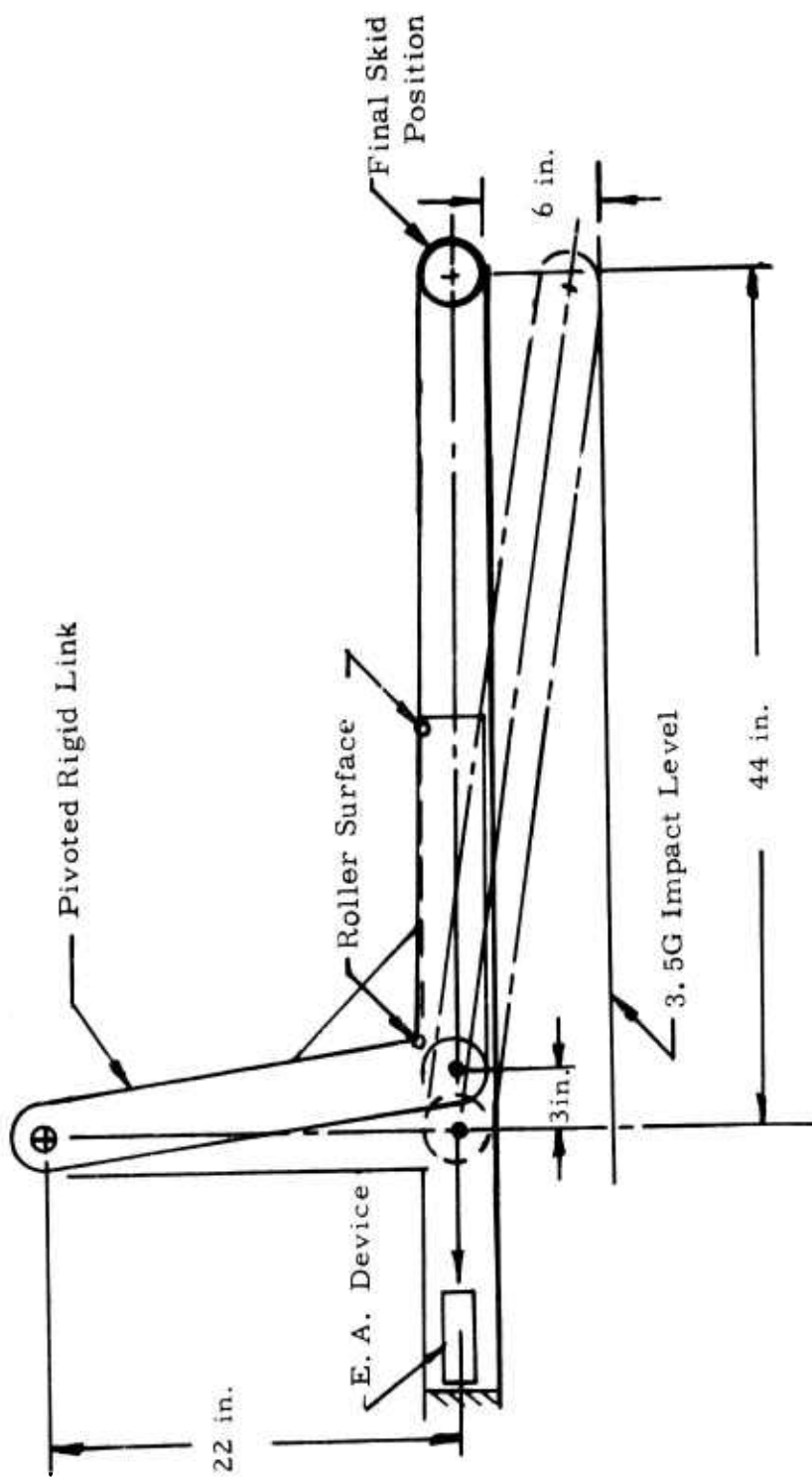


Figure 19. Rigid Link Concept.

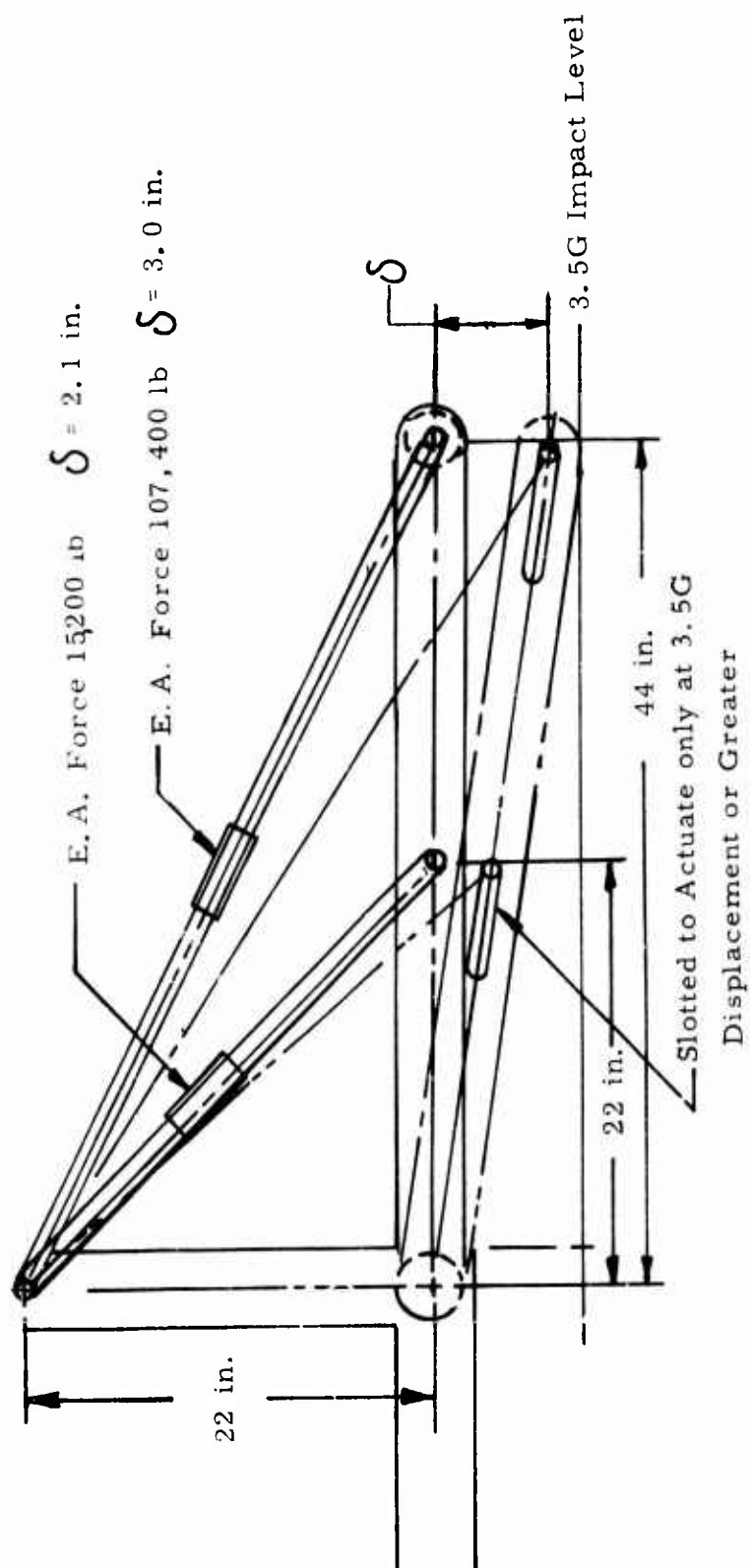


Figure 20. Energy-Absorbing Strut Concept.

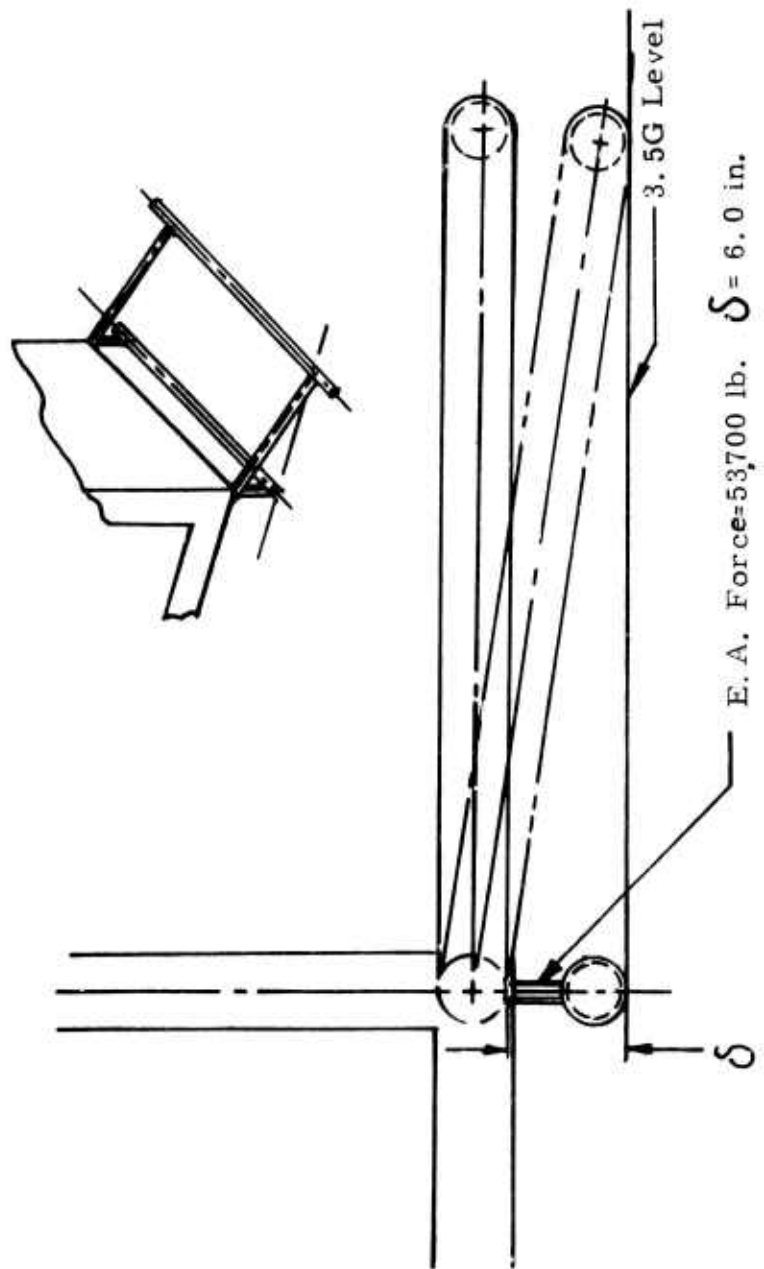


Figure 21. Crushable Skid Concept.

the cyclic strain or liquid spring device. The advantage of this concept is that the full 6 inches of stroke is available. There is no necessity for levers, pivots or guides, and the forces can be distributed over greater areas.

3.4.2.2.4 Concept 4 (Figure 22)

Another concept is to provide a lever and pivot arrangement that can be activated when the strut exceeds the 3.5G level. The lever is attached to an energy absorber on both sides, and a stroke of 1.5 inches acts on as many devices as necessary to develop the 214,800 pounds required. The small stroke and large force make this concept less desirable.

3.4.2.2.5 Concept 5 (Figure 23)

The last concept is another straightforward approach in that support structure is added about the skid to react the energy-absorber forces. This again appears to be undesirable because of the high forces that will be developed unless the structure extends well out over the strut.

3.4.2.3 Loading Condition Effects on Design

An interesting aspect of the skid-type analysis is the examination of the effects of upward, aftward, and sideward loads when applied at either end of the gear or when loaded purely in a vertical direction. All data available on skids assume that the inertial force acts through the center of gravity and is balanced by reactions at the struts. The question of end loading effects is not answered, and yet it is realized that the load distribution throughout a redundant frame is influenced by the location of the applied force. The distribution must be found if deformations of the skid are to be properly evaluated. Previous concepts indicated that the force distribution was known. The rear strut carried two-thirds of the weight, and the forward the remainder. This is not necessarily true. If the rear strut were very stiff and the skids had significant bending strength, it would be possible to cut out the forward struts and the vehicle would not topple over. Relative stiffness determines where the applied force is carried.

A skid configuration is shown on page 81.

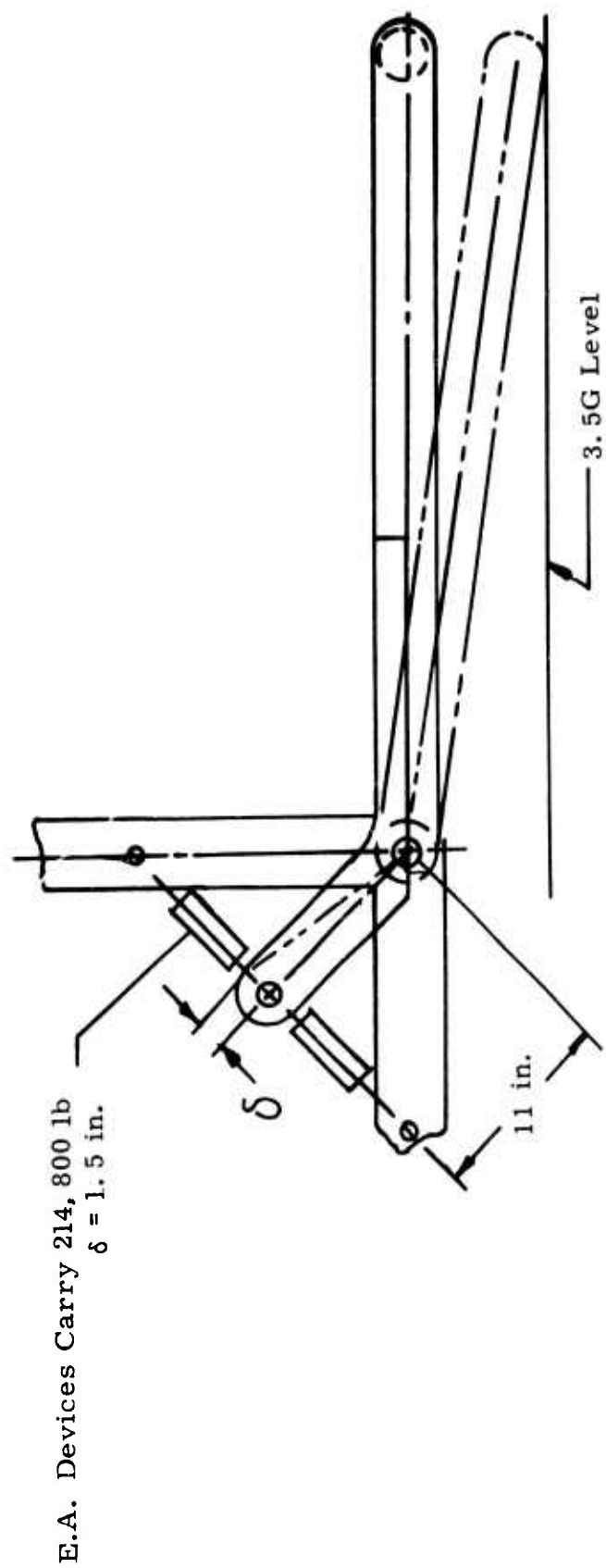


Figure 22. Lever Mechanism Concept.

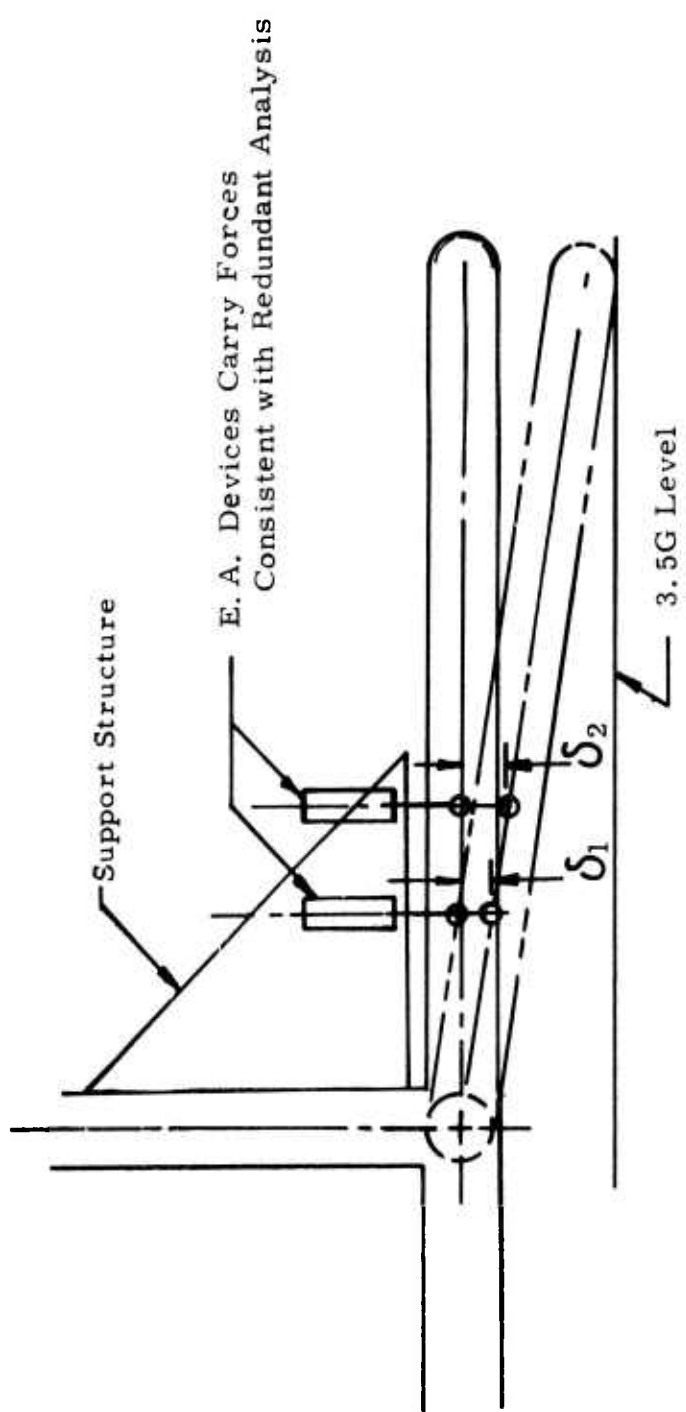
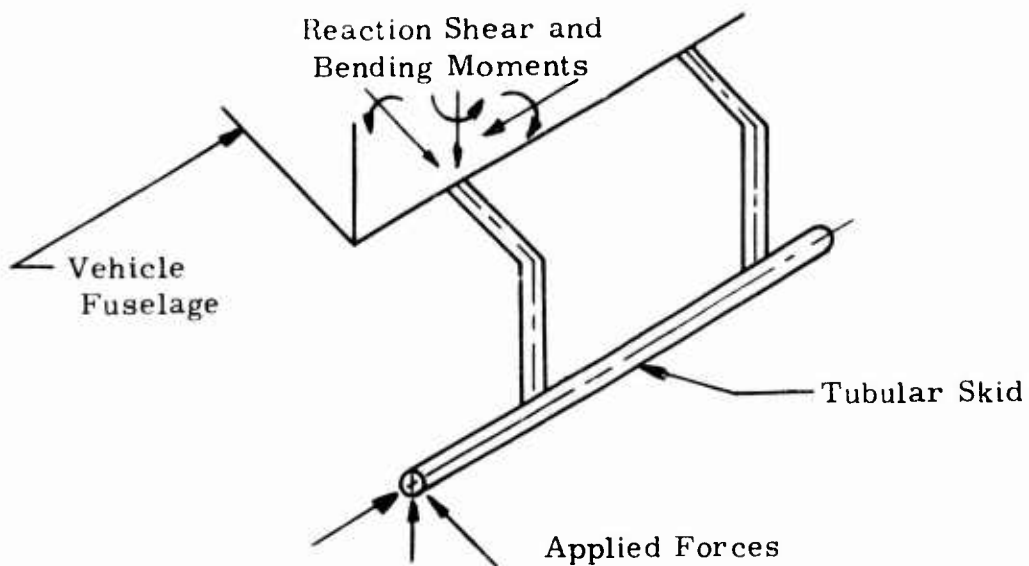
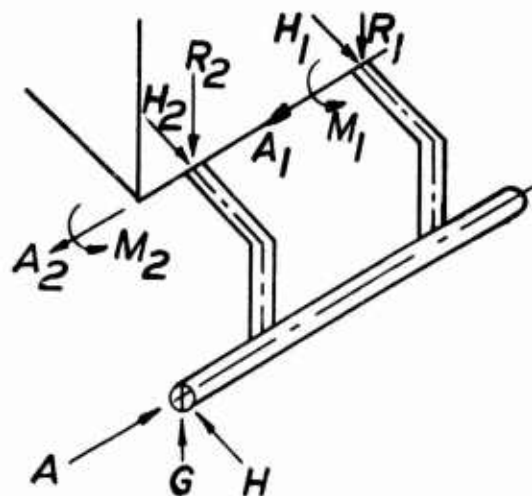


Figure 23. Centilever Energy-Absorber Concept



The struts are attached to the fuselage and may be capable of reacting forces and moments in all planes. In order to solve this system and calculate the reactions for given applied loads, it is necessary to use energy methods, that is, to reduce the redundant system to a determinate system and then evaluate the effects of the redundants. A determinate system for the skid configuration above is



where:

A , G , and H are the original axial, vertical and lateral forces respectively.

A_n , M_n , H_n , and R_n are the axial force, bending moment, horizontal force, and vertical force developed at the fuselage attachment point n .

For any given applied load, the reaction shown can be calculated by statics. There are enough independent equations available to solve for all reactions. If we assume that additional reactions exist (redundancies), these are accounted for by calculating the deformations that exist with the static and redundant forces and equating them to 0, a continuous structure. This is done numerically by equations of the

form

$$\delta q_0 + Q\delta q_1 + H_1\delta q_2 + R\delta q_3 + H_4\delta q_4 = 0 \quad (29)$$

where $\delta q_0 = \int \frac{M_0 m dx}{EI} + \int \frac{T_0 t dx}{JG}$

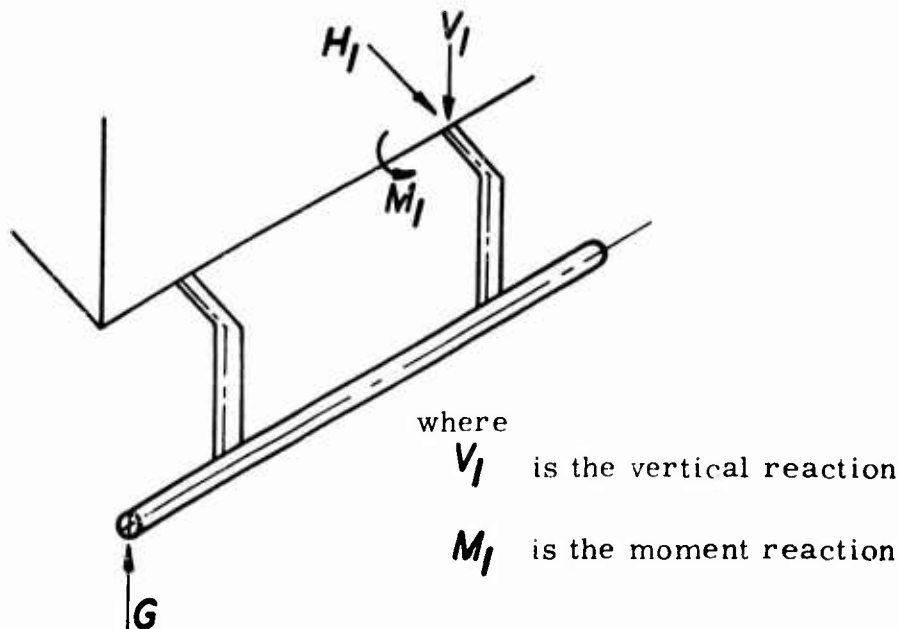
(30)

δq_i are influence coefficients

and Q, H_1, R , and H_4 are reactions measured at the fuselage.

Each coefficient is influenced by the length of each element, the moments applied, M_0, m , and the stiffnesses I and J. Therefore,

it is very difficult to establish with one particular configuration what the moment distribution will be if an element is longer, or of greater bending stiffness, with different torsional stiffness which does not vary linearly with either bending stiffness or cross-sectional area. A sample configuration was chosen in order to obtain results that would be meaningful to a UH weight vehicle. Specifically, the UH-1F configuration was approximated in order to study load application variation. The configuration is shown in Figure 24. The lengths, areas, and inertial characteristics are approximately those used in the original Bell Hardy-Cross analysis for the skid. The next step is to select a realistic and practical determinate structure. Each redundancy adds another equation and another term in each equation. The redundancies selected are shown below:



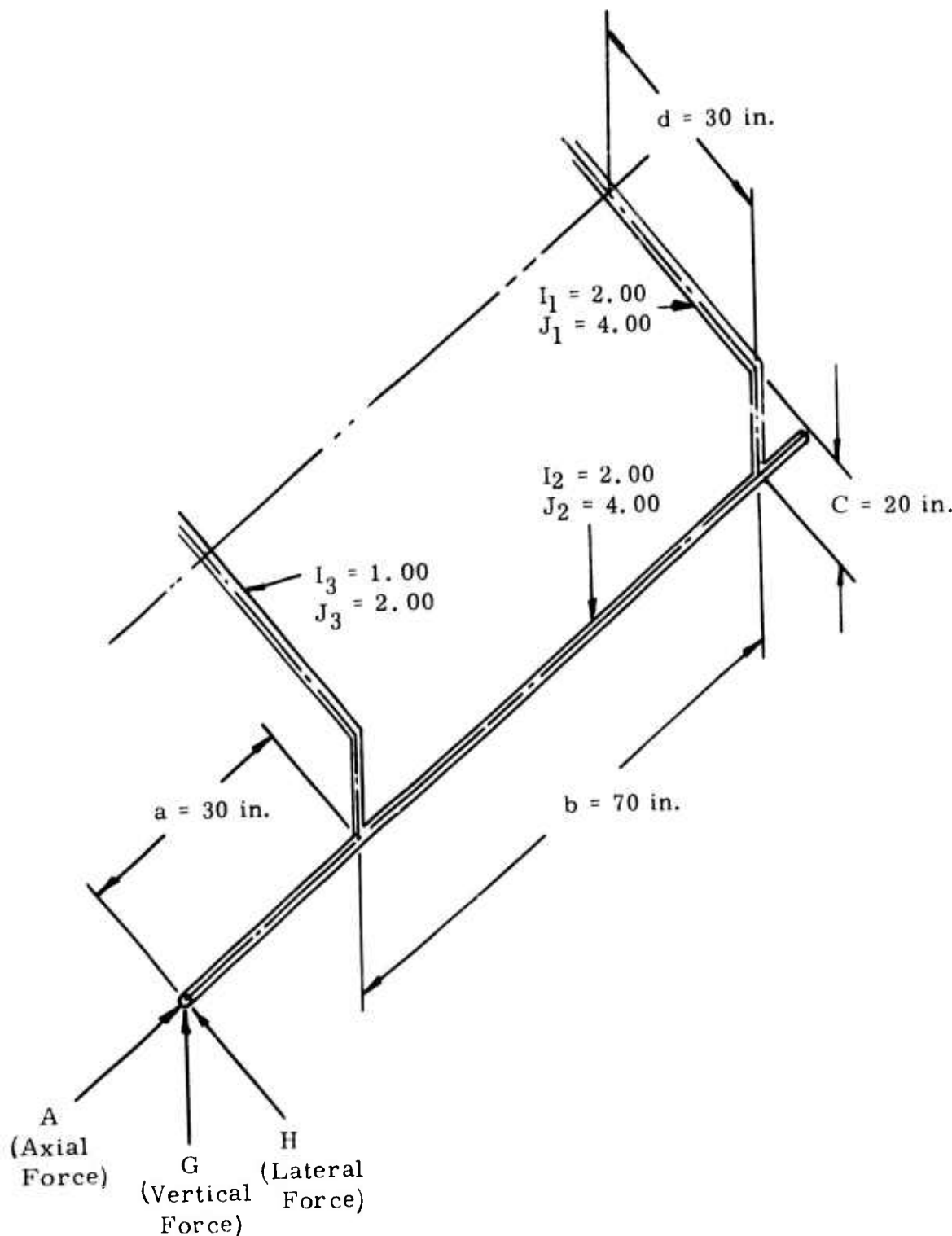


Figure 24. UH-1F Configuration Approximation.

The first analysis is for a forward tip load of 1,000 pounds vertically. The determinate structure is shown in Figure 25, and the redundancies are shown in Figure 26. The influence coefficients are found by semi-graphic integration to be

$$\delta H_1^o = 1,886 \quad (31)$$

$$\delta H_1 H_1 = 2,733 \times 10^{-3} \quad (32)$$

$$\delta H_1 M_1 = 0.147 \times 10^{-3} \quad (33)$$

$$\delta M_1 M_1 = -1,333 \times 10^{-5} \quad (34)$$

$$\delta M_1^o = -0.126 \quad (35)$$

The system

$$\delta H_1^o + H_1 \delta H_1 H_1 + M_1 \delta H_1 M_1 = 0 \quad (36)$$

$$\delta M_1^o + M_1 \delta H_1 M_1 + H_1 \delta M_1 M_1 = 0 \quad (37)$$

yields

$$M_1 = 4500 \text{ in.-lb} \text{ and } H_1 = -450 \text{ lb}$$

Since the redundant moment and applied moment must be balanced by the forward strut, 34,500 inch-pounds of bending moment is developed. The resisting moment is greater than the applied. If the two-third/one-third ratio had been used, the moment would have been 10,000 inch-pounds. Equally as surprising is the fact that the moment at the rear strut is in the same direction as the applied moment. This can be interpreted by realizing that as the frame is loaded, the rear strut is pulled downward from the fuselage. In order to resist this a vertical force (428 pounds) is required which causes a positive bending moment at the attachment. Since the joint is assumed fixed, a moment is necessary to return the strut to its original attitude.

Similar calculations were made for loads applied at the forward strut, midspan, rear strut, and rear tip of the skid. The results are plotted in Figure 27. The figure provides the magnitude of the bending moments developed at each fuselage intersection as a function of the location of an applied force of 1000 pounds. Since both moments are the only means of balancing the applied body the sum of both must equal the applied 30,000 inch-pounds at any location. The plot indicates bending moment in the struts as a function of applied force location, not bending moment in skid.

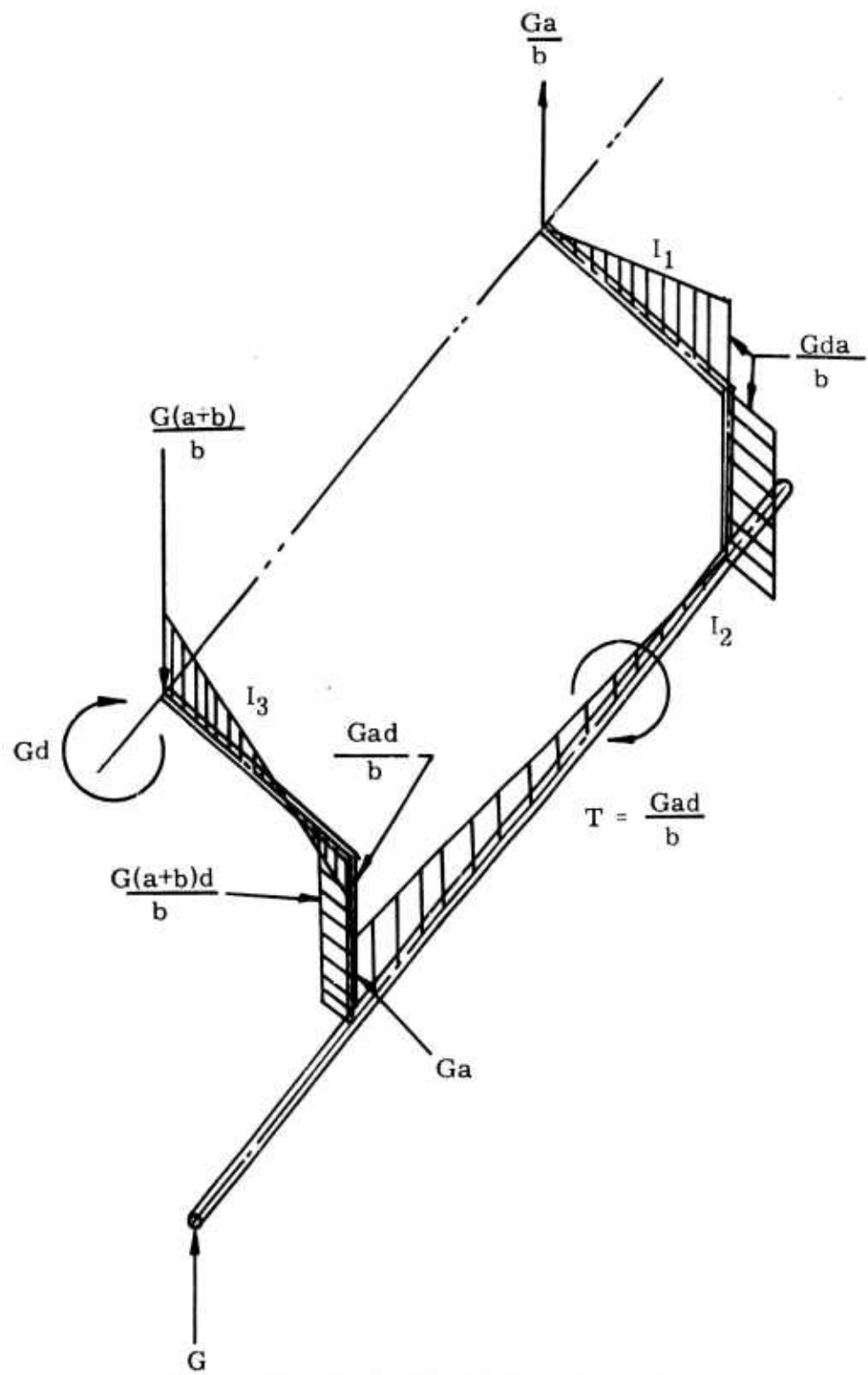


Figure 25. Statically Determinate Structure.

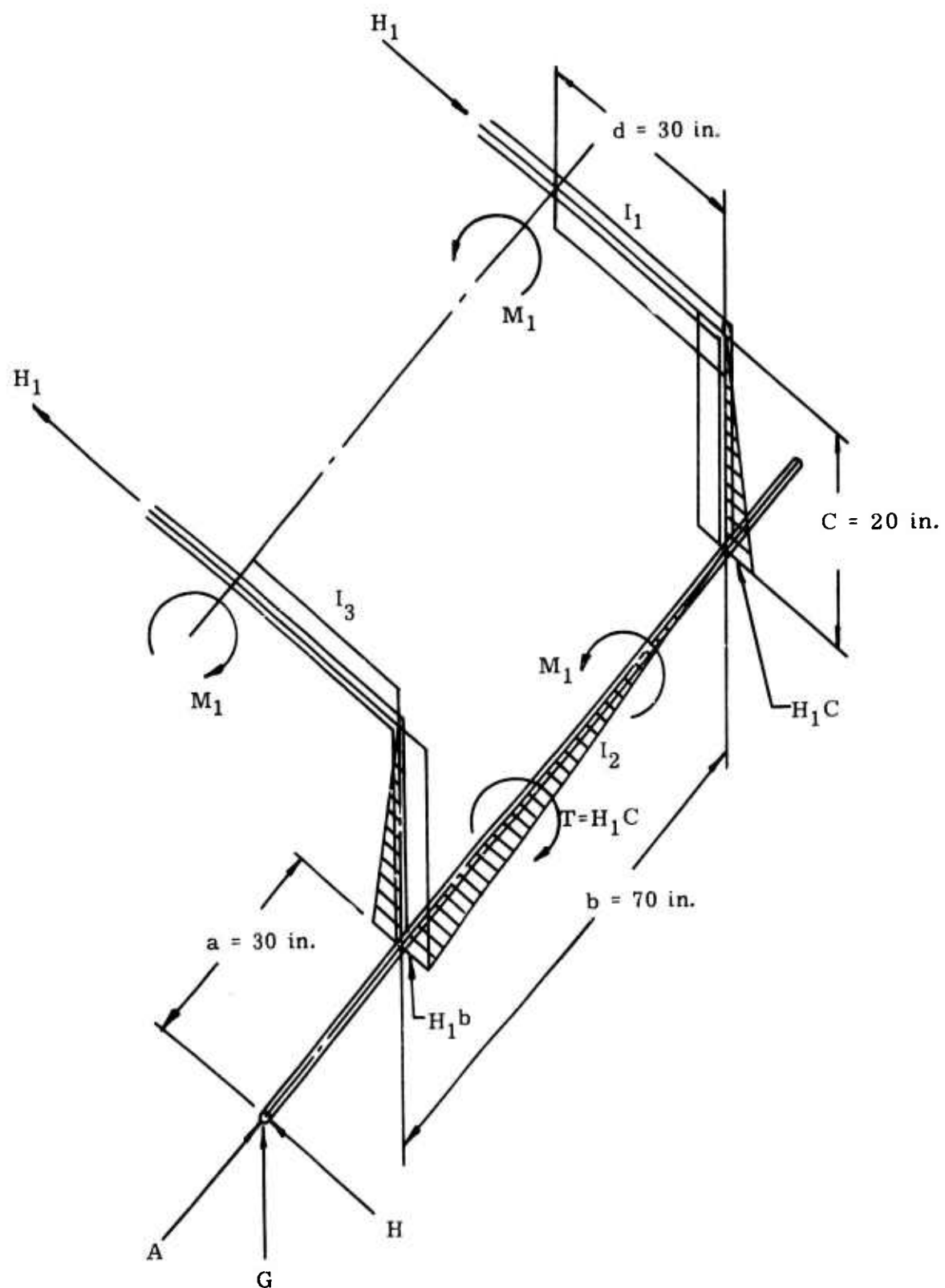


Figure 26. Applied Redundancies.

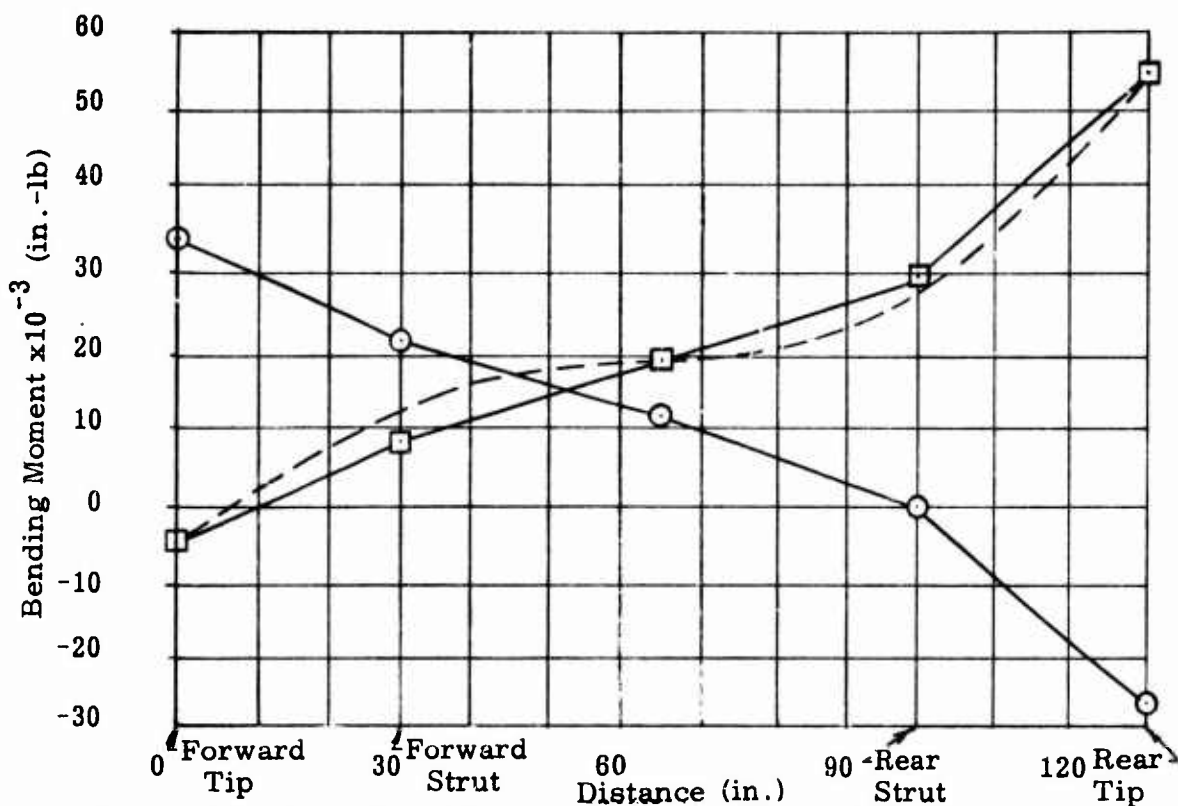


Figure 27 Variation of Fuselage Bending Moment With Location of Applied Force of 1,000 Pounds.

The plot indicates that the forward strut bending moment nearly reverses in going from forward loading to aft loading. When the load is applied beneath the rear strut, nearly all bending is taken out in that strut. It is only at a point aft of midspan that the two third/one third load distribution is correct. The dashed line is indicative of a more realistic curve that would exist under crash conditions.

As the vehicle impacts at a particular attitude, the load may act at a tip. However, as the tip deforms and the skid settles into the ground, the applied forces approach a more uniform distribution across the skid and would create a more nearly constant moment distribution between the supports.

Another configuration was examined to determine the effects of assuming different restraint conditions. The configuration is shown in Figure 28 with the statically determinate reactions. It is assumed that the vehicle does not have sufficient bending stiffness at the fuselage landing gear junction to act as a rigid joint. Instead, the tube continues across the fuselage, and vertical and horizontal reactions are permitted at the frame-longeron junction. The side forces are assumed to be balanced by shear forces acting along the struts.

The same analysis procedure is used. The redundancies, one vertical and two horizontal forces on the rear tube with a shear flow across the tube, are determined by evaluating the influence coefficients and calcu-

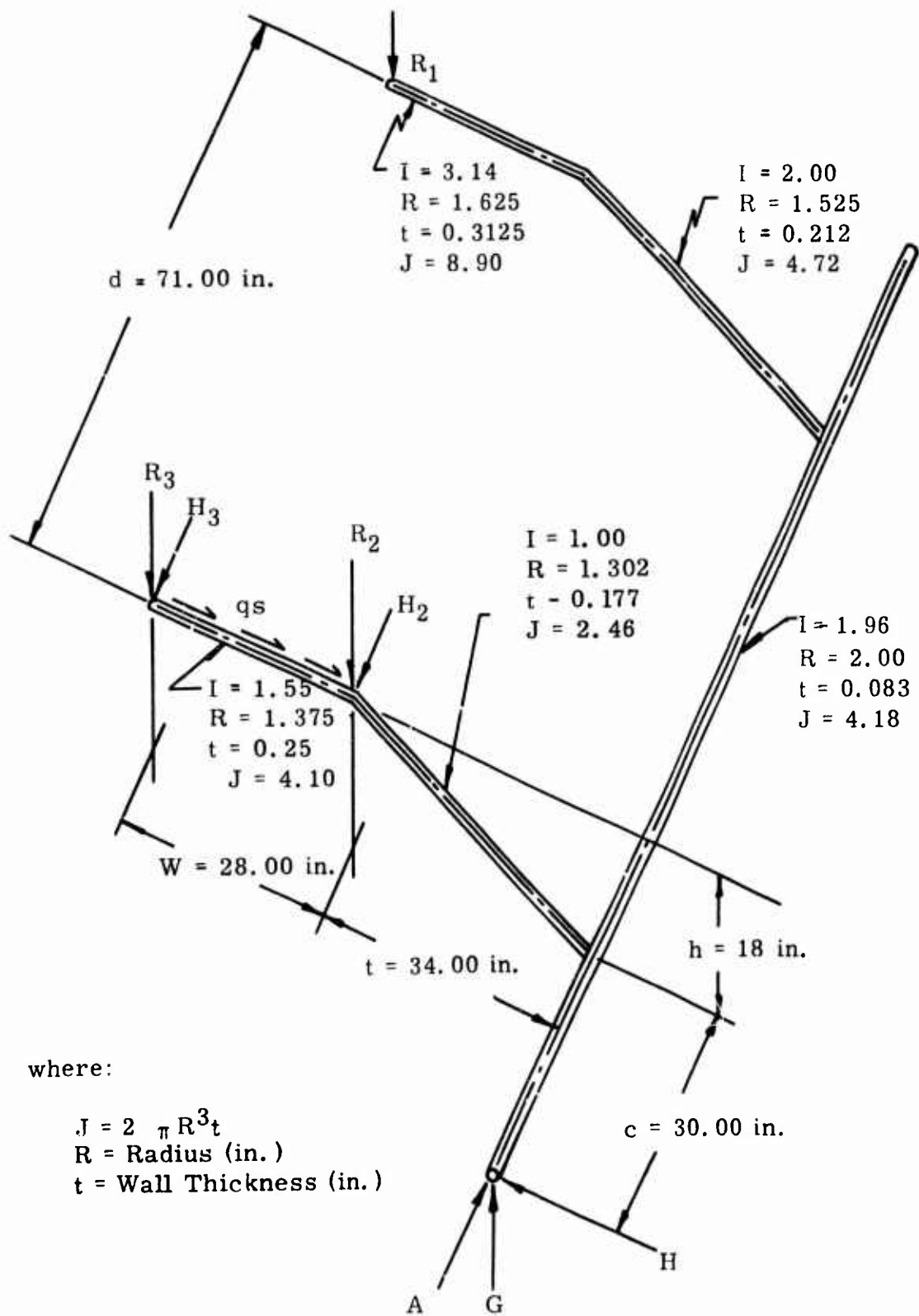


Figure 28. Statically Determinate Reactions of Second Configuration.

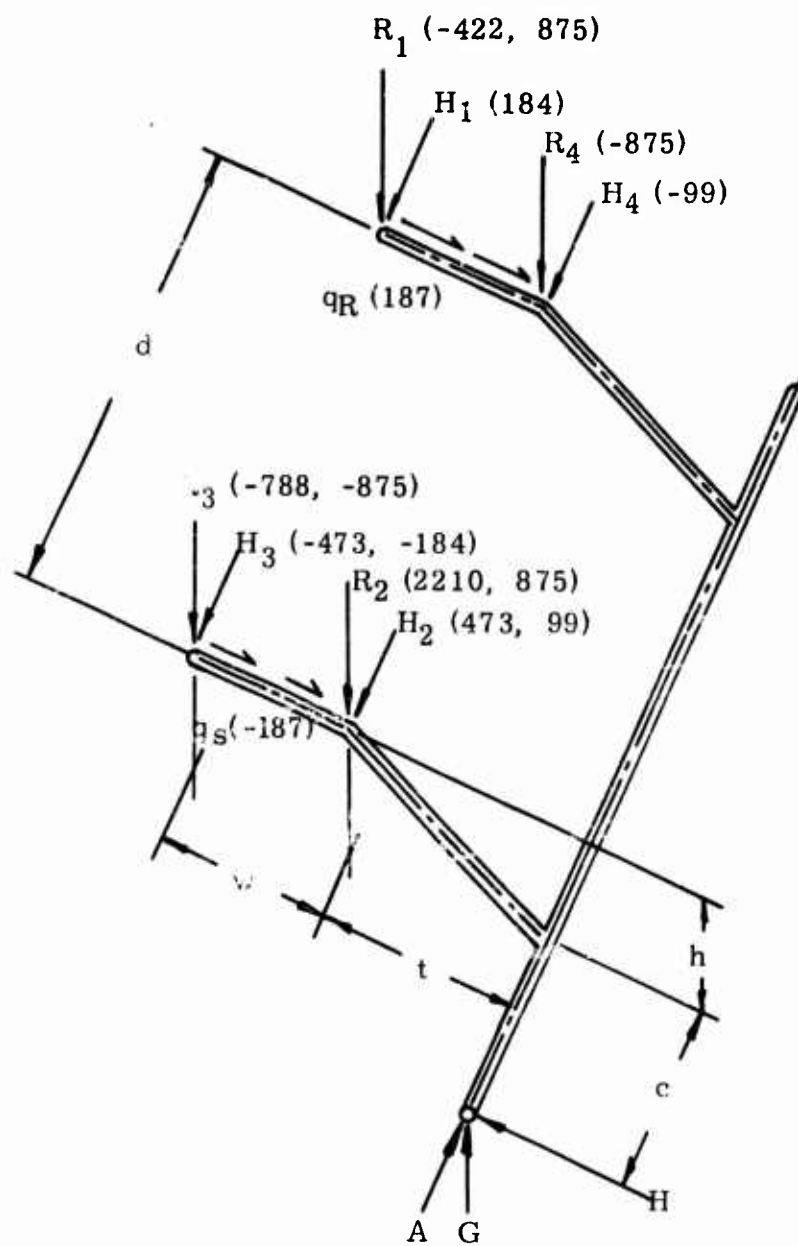
lating the solutions of a 5×5 matrix. The results are shown in Figure 29. The bending moments at the fuselage are 46,500 and -12,700 inch-pounds. Therefore, it appears that the moment distribution is characterized more by the frame and the point of load application than by the redundancies assumed. This implies that for the utility configuration being examined, the pattern of moment versus loading point should be the same regardless of how the skid is attached to the fuselage. Since the reactions of the latter configuration reflect pinned connections at the fuselage, it is reasonable to assume that these represent maximum values.

The results of the analysis indicate that as the vertically applied force shifts from forward to aft tip, the bending moment shifts according to a particular pattern and the bending moments by a particular strut can be 3-1/2 to 4 times greater than those assumed for a pure vertical loading condition.

This can have direct application to the problem of selecting the proper energy absorber when it is realized that the forces and moments introduced into a strut must be carried by both the strut and the energy absorber and must function properly at particular levels. The problem is further complicated in that it is difficult to determine how great the moment distribution effect will be. As the vehicle impacts, the strut and skid deform elastically up until plasticity effects become larger. At the same time, the vehicle rotates and approaches a uniform loading condition across the skid. When do plasticity effects occur? How long does it take for the uniform distribution to be satisfied? A helicopter impacting on skids acts as a rigid body falling on nonlinear springs (plasticity), where the nonlinearity is a function of the point of load application.

Additional load distribution data were collected for other loads. The drag load is calculated assuming that the skid is relatively inextensible along its axis. The loads carried by the struts are not changed as the drag is applied at the tip or along the bottom of the skid. The drag contributions are shown in Figure 30. The interesting aspect is that the drag does not appreciably change the bending moment in the vertical plane (1,430 inch-pounds). This would indicate that for the skid-type landing gear, the vertical energy absorption may be relatively independent of the applied drag and it is only necessary that the strut be capable of carrying drag bending moments. The skid would react the drag by deformation, and the energy absorbers would stroke vertically as required.

The other skid configuration was examined for both drag and side force effects. The same energy procedures were used assuming vertical and horizontal reactions at strut-longeron intersections. The results are shown in Figure 31. Note that the drag forces are assumed to be one-half the value of the vertical (500 pounds). All values are summed, the difference is found between vertical only and the summation, and the percent



R_1	R_2	R_3	R_4	H_1	H_2	H_3	H_4	q_R	q_s
473	3085	-1663	-875	184	572	-657	-99	187	-187

Figure 29. Loads Due to Vertically Applied 1000 Pounds.

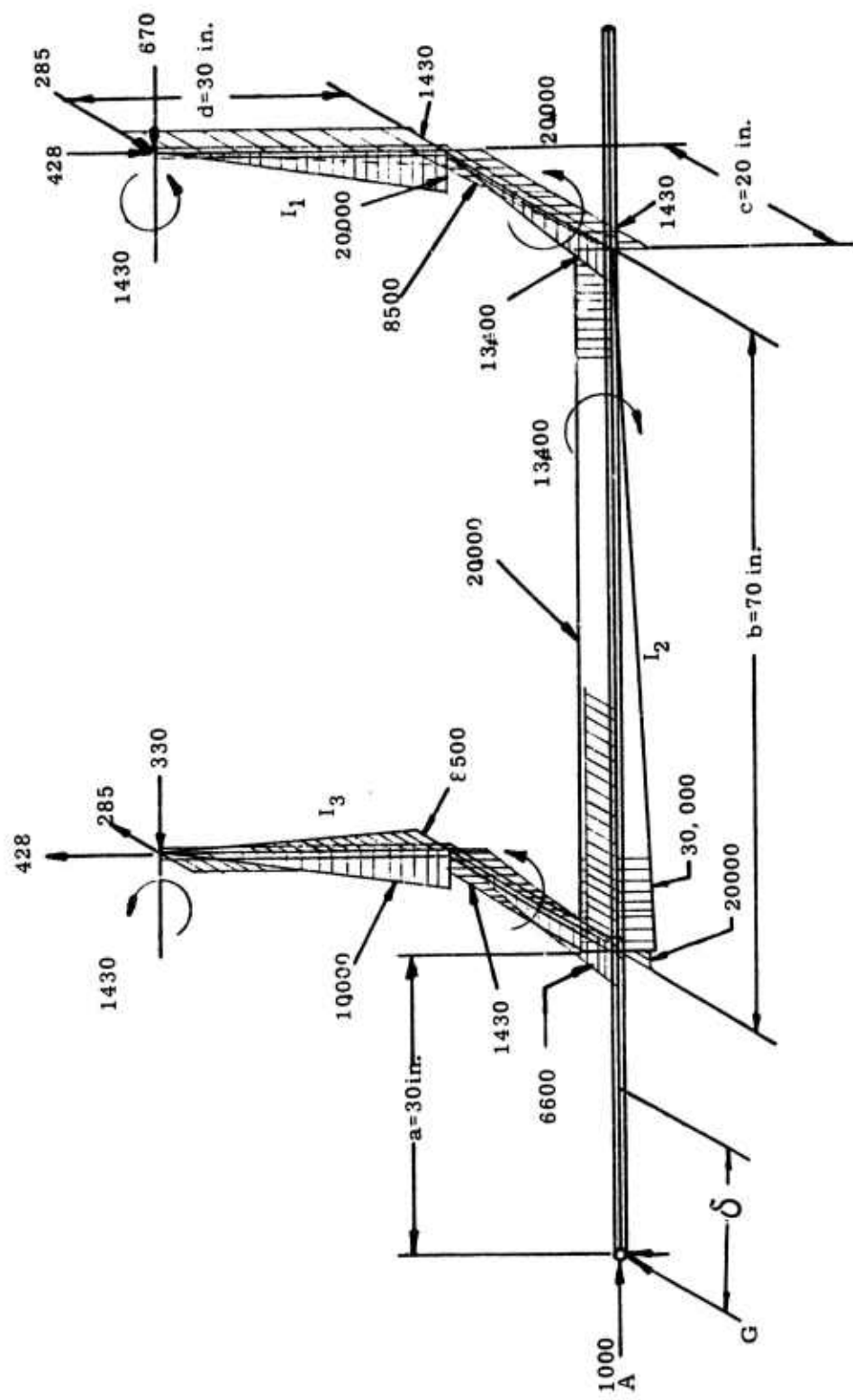
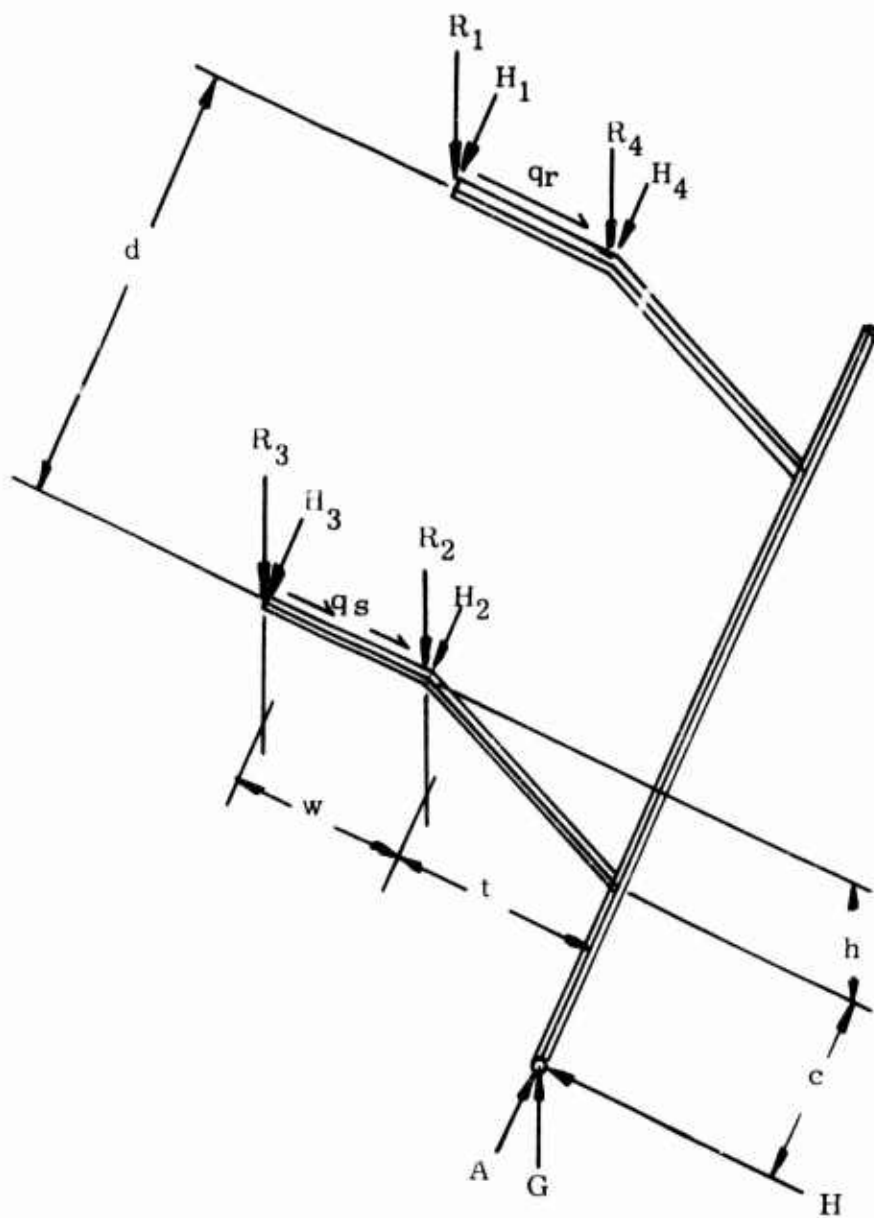


Figure 30. Effects of Drag Force.



	R_1	R_2	R_3	R_4	H_1	H_2	H_3	H_4	q_r	q_s
G	453	3085	-1663	-875	184	+572	-657	-99	187	-187
H	42	42	-42	-42	169	-438	377	-108	+ 5	495
A	-52	-179	52	179	196	924	-448	-172	-139	139
SUM	443	2948	-1653	-738	549	1058	-728	-379	53	+447
Δ	-10	-237	+10	+137	365	486	-51	-280	-134	+260
$\% \Delta$	2.2	8.3	0.6	18.6	66.6	45.8	7.0	74.0	252.	58.2

Figure 31. Effects of Combined Loads at the Tip.

difference is calculated. The table indicates that the vertical reactions are influenced mostly by the axial or drag force and little by the side force. The horizontal reactions are dictated by all three forces, as are the shear forces.

The moments and forces calculated are all based upon the configuration shown. Lengths of segments, torsional stiffness, bending stiffness, and end fixity all contribute to the values calculated. If it is assumed that the configurations shown are indicative of skid-type landing gear, then the following statements can be made:

1. The skid deformation useable for energy absorption will be primarily dictated by the vertical reactions and moments at the fuselage-strut junction.
2. The force and moments at junction can be altered by a factor of 3 to 4, and even the direction can be reversed as the applied vertical force is shifted fore and aft along the skid.
3. The drag and side forces do not contribute significant reactions in comparison with the effects of tip loading conditions.

There are many possible ideas that could be pursued, but it is difficult to calculate how plastically deforming, variable load path structures will respond. Consequently, a pure vertical drop attitude will be used for the following concepts. This can be justified in that since the skid does plastically yield over a large stroke, as shown in Section 3.4.2.1, the skid will deform and permit the location of the applied force to shift toward a more balanced position. Therefore, for reasonable attitude angles, $\pm 10^\circ$, where the attitude can be reduced by vehicle rotation, and the skid deforms plastically without strut failure or fuselage impact, the vertical attitude will be a reasonable assumption.

3.4.2.4 Plasticity Effects and Skid Stiffness

Previous sections have made reference to plasticity effects and the use of a computer program. If a program were available to calculate input responses, it would have to accept stiffness values as representations of the landing gear. These must provide a correct measure of the force-displacement relation over the entire range of displacement up to failure, i.e., include plasticity effects. This will provide additional energy which has not been included in the previous analysis. The assumption was conservative in that less energy in the energy absorber is required. From Section 3.4.2.3, the moment distribution of a skid for various loads is known. The stiffness is calculated by evaluating the deformation due to unit loads applied in the direction of the applied force. Figure 32 shows the applied force and resulting moments for a forward loaded tip. A unit load is applied and the equation

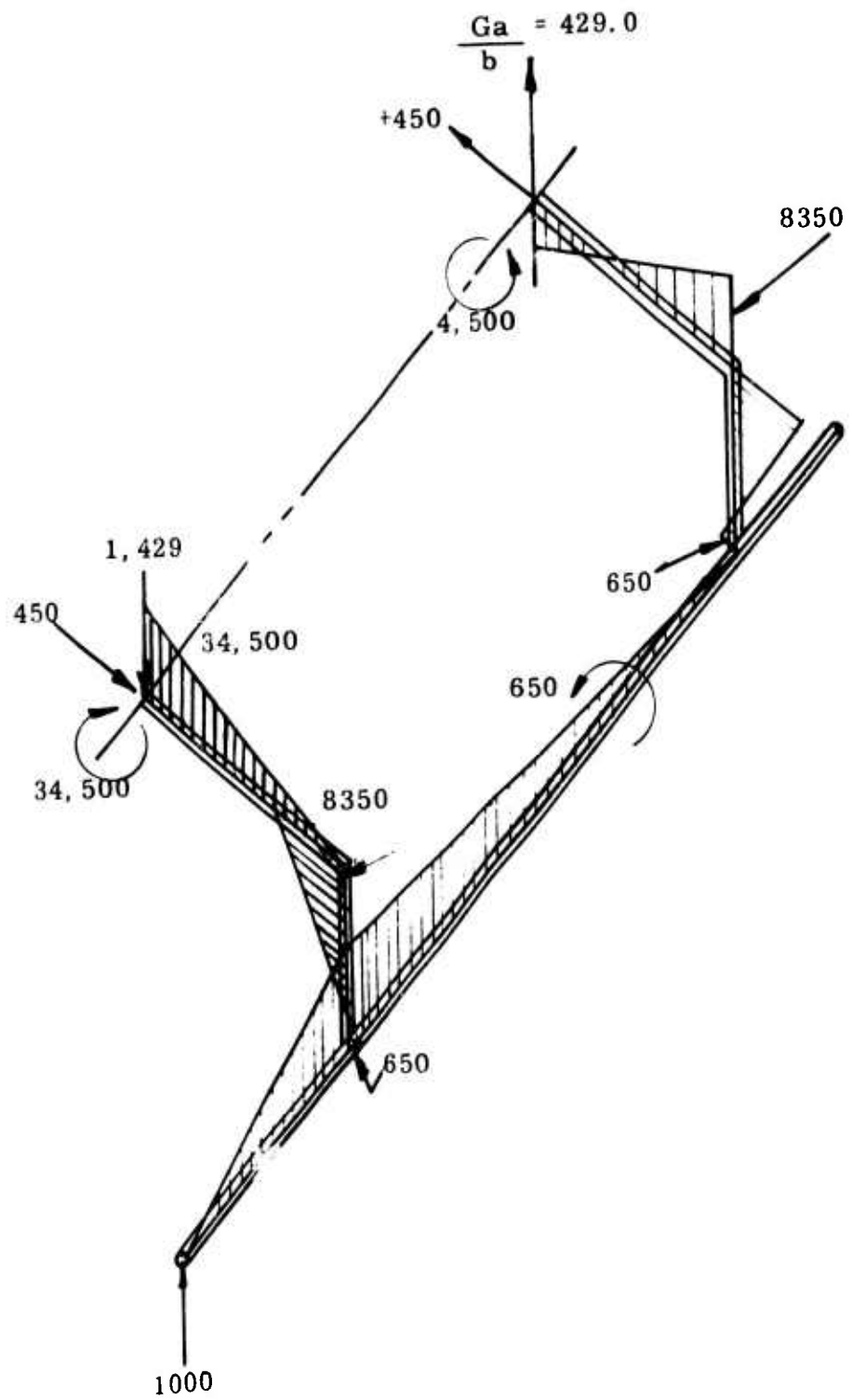


Figure 32 . Vertically Loaded Tip Distribution.

$$\delta = \frac{\sum M m ds}{EI} \quad (38)$$

evaluated. The displacement is 2.596 inches for 1,000 pounds or a stiffness of 385 pounds per inch in the elastic range. The plastic values are calculated using the techniques of Chernoff². The techniques rely on the assumption that the plane surfaces remain planar during deformation although the stress levels depend upon the failure characteristics of the material. The solution is implemented by evaluating a factor β , which would exist if all fibers extended elastically. The equation is

$$\beta = \left\{ \left(1 - \frac{E_1}{E} \right) \left(\frac{\theta_y}{\pi/2} + \frac{(\sin \theta_y) (\cos \theta_y)}{\pi/2} \right) \right\} + \frac{E_1}{E} \quad (39)$$

and is derived for a tube of $D/t \geq 10$

E_1 = slope of the stress-strain curve in the plastic region

E = Young's modulus

$\sin \theta_y = E_y / E_a$

E_y = strain at yield stress

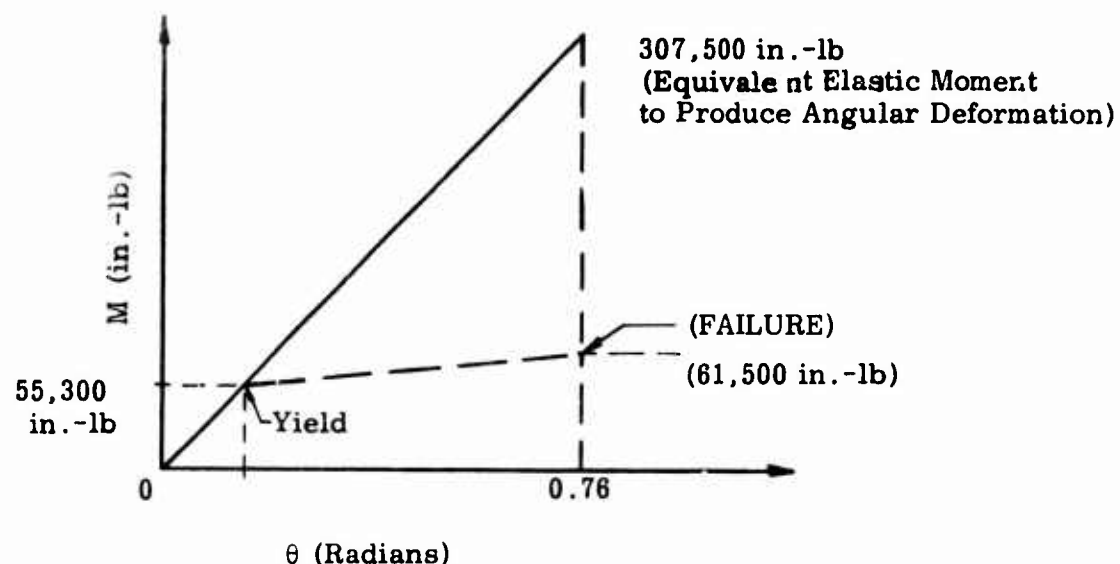
E_a = strain at outer fiber

Bell tube data³⁸ were used to gain realistic values. The values of strain used were $E_y = 0.0072$ and $E_a = 0.054$ corresponding to a yield stress 72,000 psi and an ultimate of 80,000 psi. Therefore, $\beta = 0.184$, which means the ratio of elastic to plastic bending moment at failure is approximately 5. A tube bent by an applied force and strained to its ultimate will carry 1/5 of the moment that would be necessary to elastically deform the tube to the same displacement. Beyond the yield stress, the tube carries very little additional moment but does deform appreciably.

The plastic deformation curve is calculated by equating the internal strain energy due to bending with the externally applied work. The internal strain energy is calculated by determining the integral of the moment and angular displacement of the tip. The work is the product of applied force and deformation.

The angular motion at the tip is calculated by applying a unit couple to the tip and calculating the angle due to the equivalent elastic moment at failure just found. The tube data used assumed an ultimate stress of 80,000 psi. For the strut, this implies an applied bending moment of 61,500 inch-pounds. The strain at ultimate is the equivalent of 5 times the elastic strain at ultimate, or 307,500 inch-pounds. Figure 32 shows that an applied tip force of 8,910 pounds is required. The rotation

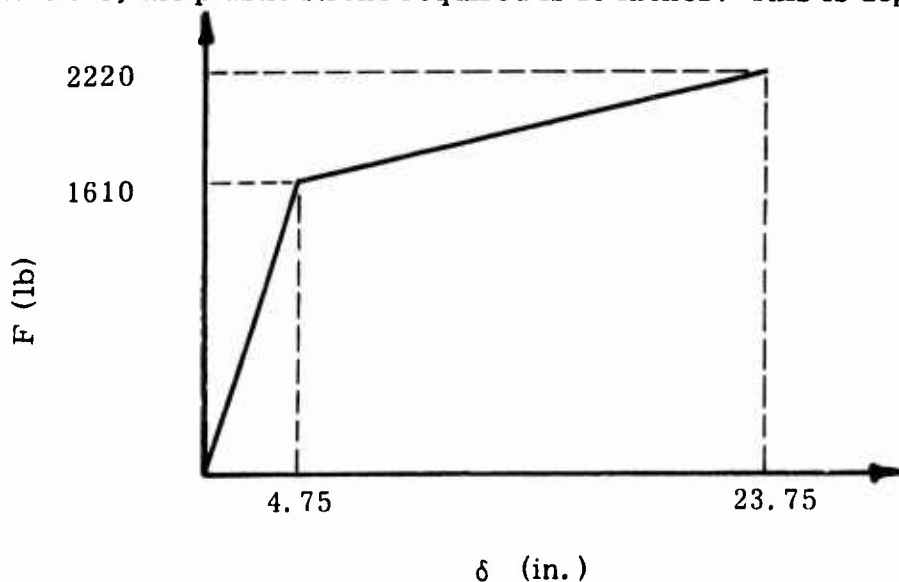
calculated is 0.76 radian. A figure depicting these results is shown below:



The strain energy of bending to ultimate is 40,360 inch-pounds.

The work generated is the product of the force through an unknown displacement. The elastic portion of the energy is 3,820 inch-pounds. The force at yield is 1,610 pounds, and hence the displacement is 4.75 inches. The plastic regime requires the dissipation of 36,540 inch-pounds of energy at force up to the ultimate of 2,220 pounds.

Therefore, the plastic stroke required is 19 inches. This is depicted below:



The stiffness in the elastic range is 340 pounds per inch, compared to 385 for the initial analysis, and the plastic stiffness is 32 pounds per inch.

The strut will stroke vertically 23.75 inches without failure and carry 2,220 pounds if the force is applied at the tip. The stiffness of the above figure is used in the computer program and it is now known that for the strokes previously discussed, the strut will be a continuous member throughout the energy-absorber stroke. The stiffness as the load is applied at the other point is different, since the moment distribution is different. Therefore, in order to obtain the correct stiffnesses over the range of attitudes possible, the present procedure should be used for both tips and midspan for vertical and side loads. The drag load is not influenced by the point of load application.

3.4.3 Light Observation Helicopter Class Concepts

The LOH class is defined as having a weight range of 2100 to 2700 pounds. For the 2700 pounds, assuming a 12 feet per second and 3.5G, the stroke required is 16 inches, the rear strut dissipates 68,000 inch-pounds, and the total energy at impact is 210,000 inch-pounds. If an efficient absorber is used, i.e. $\eta=0.9$, the product of peak force and stroke must be 157,000 inch-pounds. A 15G deceleration would be developed if the stroke were 5.8 inches. Therefore, an assumed 6-inch stroke is provided and the configuration must have 22 inches of unloaded clearance from fuselage to ground.

A balanced condition will create a force of 3,150 pounds applied to one skid at 3.5G. From the helicopter configuration data it is assumed that a fuselage width of 4-1/2 feet is representative, and that the landing gear will span 7 feet. Based upon the previous redundant analysis, it is assumed that it would be necessary to design for a bending moment 2.8 times a static weight distribution value. Therefore, a design value of $(3.50 \times 16 \times 2.8) 141,000$ inch-pounds is required. The tube required for 7075-T6 material is a 2-3/4-inch OD, 3/16-inch wall thickness. The static deflection is less than 1 inch. The resulting configuration is shown in Figure 33.

A typical concept is shown in Figure 34 to indicate the applicability of previous concepts. The compressible strut is shown positioned to provide a magnification ratio similar to that previously used. The force in the strut is significantly lower than in the UH configuration, and yet the displacements are comparable. The net effect is that the concepts are more compatible with available hardware. Any skid concept that has been previously shown is more readily accomplished with the LOH requirement. Therefore, all UH concepts automatically satisfy the LOH requirement.

The one feature of the LOH class that makes it more easily adapted to energy-absorbing devices is that compression tubes of tested capability are within the range of force-displacement levels required. This is particularly true if the additional skid along the bottom of the fuselage is

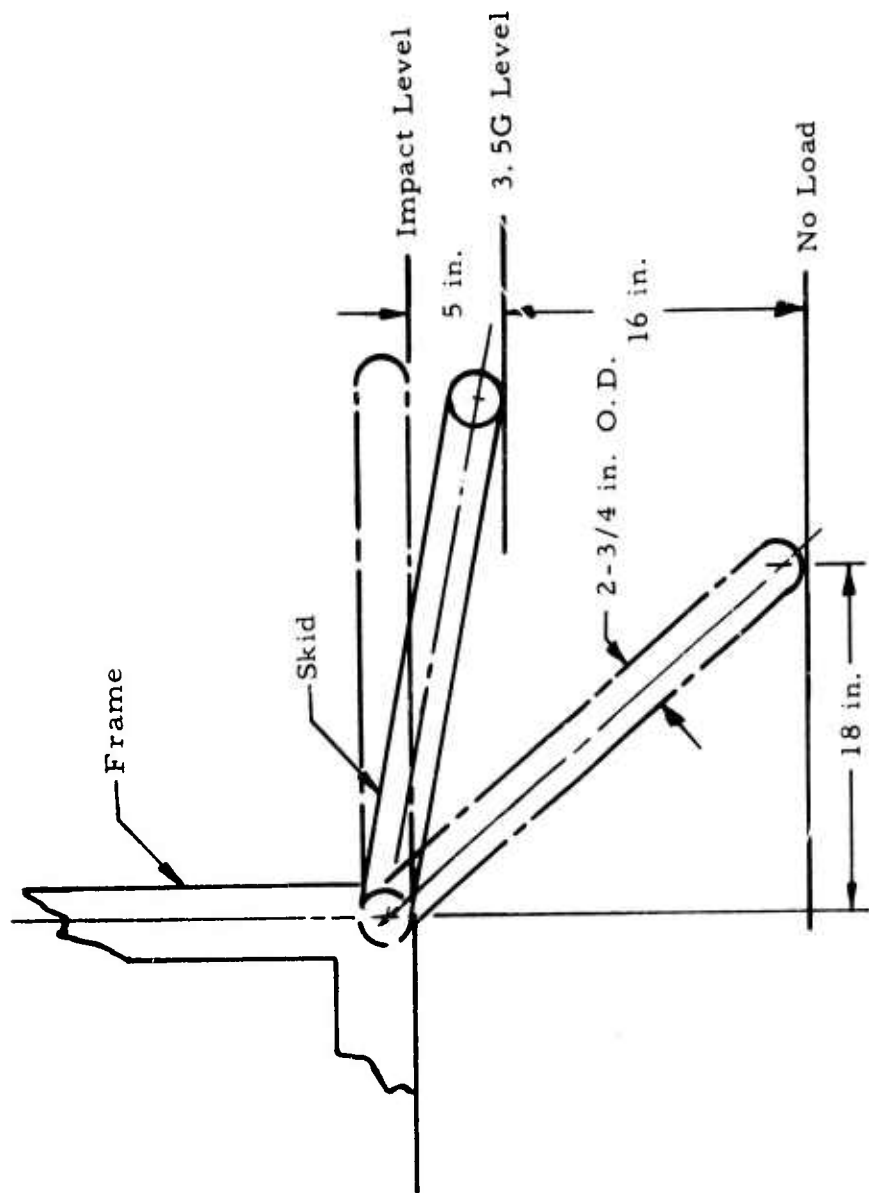


Figure 33. LOH Configuration.

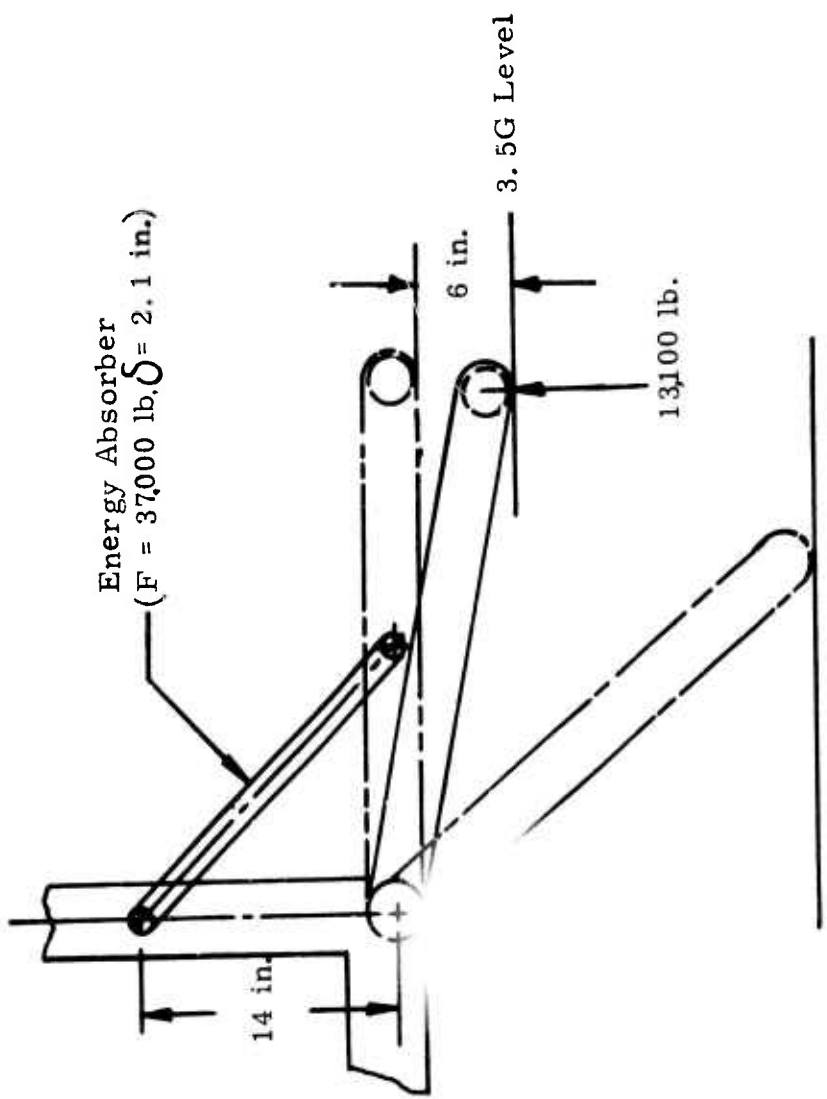


Figure 34. Compressible Strut Concept.

added.

3.4.4 Concept Development Summary

It appears that for the heavier weight vehicles, it is more advantageous to use commercially available types of energy absorbers with proven capability. The force levels are too great for tube or other metal deformation absorbers, but not incompatible with energy-absorbing struts incorporating precrushed honeycomb material²¹. The lightest vehicles can utilize either type of device, and consequently it appears that a particular concept will have the most economical device since their weights are comparable. If a cyclic strain device or liquid spring device is available with adequate force and stroke, it will probably be cheaper than the design and qualification of any tube-type device or honeycomb strut.

3.5 COMPUTER PROGRAM DEVELOPMENT

The development of design criteria and new concepts for an energy-absorbing landing gear system can be aided considerably by an analytical description or model of the total system-fuselage, struts, wheels or skids, and energy absorbers. The analytical model can then be used to better understand the important parameters of a landing gear system that dissipates energy in a crash environment. One method of analytically describing a landing gear system is to construct a lumped parameter model representative of the landing gear and derive the differential equations of motion from this model.

The analytical model selected for this program is shown in Figure 35 and consists of a rigid mass in the shape of a parallelepiped supported at each of the lower four corners by elements which represent the landing gear and energy absorbers. The configuration of the elements at each of the corners reflects three-dimensional motion by allowing motion in three translational coordinates and three rotational coordinates, resulting in a six-degree-of-freedom model that requires six coupled differential equations to describe the motion.

The program to be discussed was originally to be developed prior to designing a finalized concept. However, the routine was not completely defined and debugged soon enough to permit its usage. The program is presented to indicate the theory and its application in terms of a coded, operable program.

The analytical description of the helicopter landing gear system-fuselage, struts, wheels, and energy absorbers, shown in Figure 35, is a three-dimensional model having 6 degrees of freedom: 3 translational and 3 rotational. The elements at each corner represent the stiffness and damping characteristics in three directions of a landing gear component and are considered to be rigidly connected to a common point corresponding to a touchdown point of the landing gear system. The

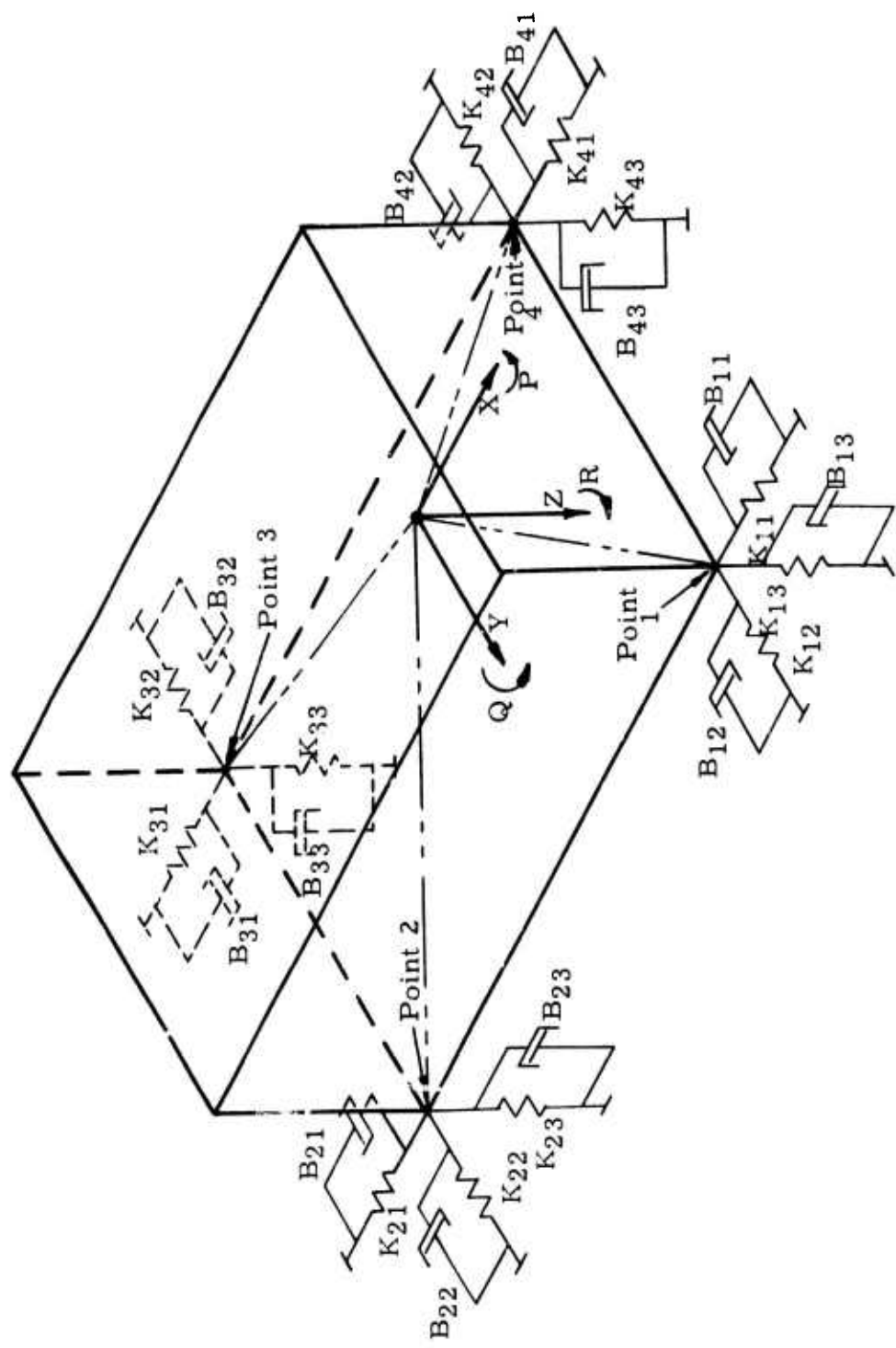


Figure 35. Helicopter Landing System Model.

initial placement of the elements is such that they are aligned with a rectangular coordinate system which describes a component of the landing gear.

For the model shown, there are 5 coordinate systems: 1 for the rigid body and 1 for each of the 4 components. The orientation of these coordinate systems with respect to each other is assumed fixed provided impact or contact with the ground has not occurred.

Impact with the ground is indicated when the origin of the component axis reaches some predetermined value. This requires a sixth coordinate system which is defined as the earth axis system, and impact occurs when the vertical dimensions of the component coordinate system become 0. At this time the component axis becomes "quasi-fixed" with respect to the earth axis while the body axis is free to translate and rotate depending on its initial velocities and the forces generated by the landing gear component elements. The "quasi-fixed" status of the component system implies that the axis will remain fixed for most conditions but could translate in the plane of the earth's surface. The condition which dictates motion of the component axis is an imbalance between the lateral forces applied to the rigid body and the forces due to friction between the landing gear component and the earth. Analytically, this frictional force can be determined by multiplying the force generated in the vertical element of the landing gear representation by a coefficient of friction.

The relation between the body axis coordinate system and the component axis coordinate system is shown graphically in Figure 36. At initial contact with the earth, the origin of the body axis system is at point A, the component coordinate system origin is at point B, and point 1 represents the attachment point of the landing gear. Sometime after the initial contact, relative motion between the body and the landing gear component will have occurred, causing point A to move to point A' and point 1 to move to point 1'. The movement of point 1 to 1' can be defined in the component axis system by the vector δ which will be a function of the translational and rotational motion of the rigid body. Using this vector and its time derivative, a force acting on the rigid body at that point can be calculated. This force will be a vector quantity expressed in the component coordinate system and must be transformed back into the body coordinate system to derive the motion equations. When this is done, the equations of motion expressed in body coordinates become

$$M\ddot{x}_r = F_{11} + F_{41} - F_{21} - F_{31} \quad (40)$$

$$M\ddot{y}_r = F_{12} + F_{22} - F_{32} - F_{42} \quad (41)$$

$$M\ddot{z}_r = F_{13} + F_{23} + F_{33} + F_{43} \quad (42)$$

$$J_p \ddot{P} = Y_3 F_{33} + Y_4 F_{43} - Y_1 F_{13} - Y_2 F_{23} + Z_1 F_{12} + Z_2 F_{22} - Z_3 F_{32} - Z_4 F_{42} \quad (43)$$

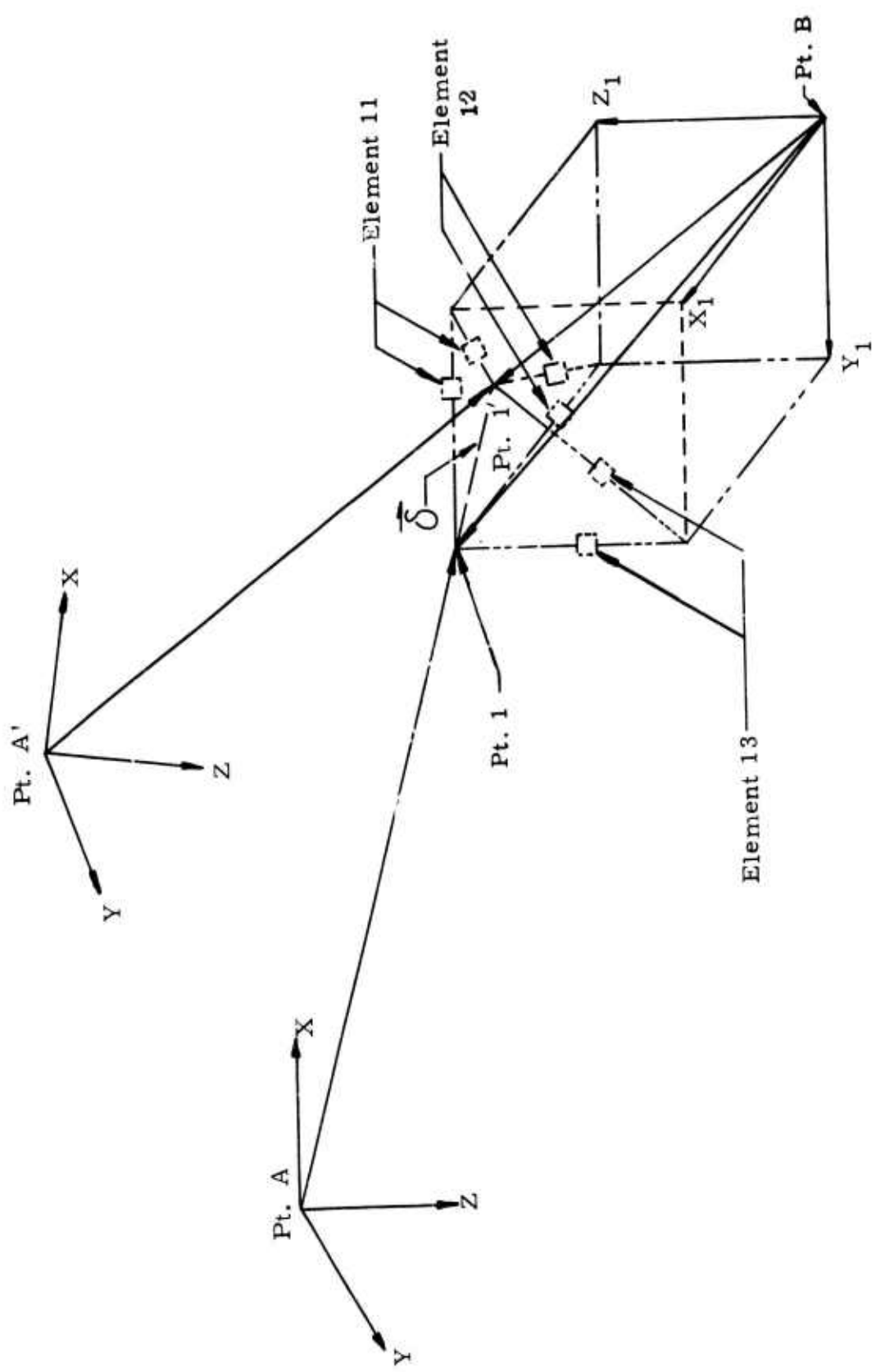


Figure 36. Landing Component Vector System.

$$\dot{J}_q Q = X_1 F_{13} + X_4 F_{43} - X_2 F_{23} - X_3 F_{33} + Z_2 F_{21} + z_3 F_{31} - Z_1 F_{11} - Z_4 F_{42} \quad (44)$$

$$\dot{J}_r R = Y_1 F_{11} + Y_3 F_{31} - Y_4 F_{41} - Y_2 F_{21} + X_2 F_{21} + X_4 F_{42} - Y_1 F_{12} - Y_3 F_{32} \quad (45)$$

where

M = mass of rigid axis

J_p = inertia about X axis

J_q = inertia about Y axis

J_r = inertia about Z axis

X_r = rigid body X coordinate

Y_r = rigid body Y coordinate

Z_r = rigid body Z coordinate

P = angular velocity about X axis

Q = angular velocity about Y axis

R = angular velocity about Z axis

X_j = X dimension to jth connection point

Y_j = Y dimension to jth connection point

Z_j = Z dimension to jth connection point

F_{ij} = F force in the jth element at ith connection point

The above equations have utilized notational simplifications that mask the subtle complexities involved in expressing the motion of a rigid body in three dimensions. The forces in each of the equations are functions of six body coordinates X_r, Y_r, Z_r, P, Q and R which all

depend on the relative motion of the rigid body and the landing gear components. This motion is best described by a vector and is expressed in the component coordinate system to determine the forces in each of the elements of a particular landing gear component. The forces in each of the elements can be combined into a resultant force vector acting at the attachment point of the component. Since this force vector is expressed on component axis coordinates, it has to be transformed into the body axis system to express the motion equations in terms of rigid body coordinates.

To transform one coordinate system into another requires that several specific angular rotations be performed. A standard method for describ-

ing a rotational transformation is to use a rotation matrix (λ) containing the three independent Eulerian angles Ψ, θ, ϕ . Using this method to transform the component axis system into the body coordinate system requires an additional transformation to relate roll, pitch, and yaw (P, Q, and R) velocities to the Euler angles, since they do not correspond directly.

By insuring that the coordinate transformations are handled in the correct manner, the forces generated in the component coordinate system can be transformed into the body axis system when they are used to find the motion of the rigid body.

The equations of motion for the rigid body and the coordinate transformation equations were programmed for solution using MIMIC^{3d}, which is a FORTRAN program designed to solve sets of ordinary differential equations. A complete listing of the program is given in Appendix III. The initial section of the program reads in system constants and parameters; these are lines 7 through 27. The constants are basically dimensions and inertial characteristics of the fuselage and landing gear. The parameters are the initial conditions for the various velocities, displacements, stiffness coefficients, and damping coefficients. The values can be easily changed between successive runs of the program so that the influence of any set of parameters can be determined. The next section of the program, lines 28 through 50, determines the landing configuration. By sensing the vertical location of a landing gear component, the program can determine whether or not that particular component is in contact with the ground and make the proper correction in the motion equations. In this fashion the program can handle initial impact orientations and rebound situations.

Next in the program listing, lines 52 through 137, are the equations of motion for the rigid body in the body axis system. These are the differential equations for the three linear coordinates (X, Y, Z) and three rotational coordinates (P, Q, R). Also included in this section of the program are the motion equations for each of the four landing gear attachment points. Following these equations come the rotation angle equations which transform the body axis angular velocities P, Q, R into the Euler angle rotations Ψ, θ, ϕ . The next two groups of equations, lines 163 through 193, are simply the velocities and displacements of the landing gear attachment points transformed from the body axis coordinate system to the component axis system using the Euler angles. The displacements are used in the succeeding section to determine the magnitude of the displacement vector. The following group of equations calculate the displacements and velocities of the landing gear attachment points in the component coordinate system.

The attachment point velocities and displacements are then used to determine the force in each element of the landing gear components. Following the force equations are the equations for the elements of the

transformation matrix which transform the landing gear element forces from the component axis to the body axis coordinate system (lines 292 through 345). This completes the equations necessary to determine the motion of the analytical model. The remaining statements in the program listing are output statements which dictate the parameters to be printed.

After programming the equations of motion for the analytical model and debugging, a series of test cases was run to verify that the computer selections were correct. A shortage of contract resources (time and money) prevented a thorough checkout of the program; however, test cases simulating vertical impacts were run, and the responses were those anticipated. One test case was a vertical drop with equal stiffness and damping at each of the four landing gear attachment points. Theoretically, this case should reduce to a single-degree-of-freedom spring mass damper system. The response of the model's vertical displacement is shown in Figure 37 which agrees with the anticipated results. A second test case was run with unequal stiffness of the fore and aft landing gear components and reduced damping. This case responds as a two-degree-of-freedom system with one linear displacement and one rotational displacement.

In Figure 38 the vertical time response of the landing gear attachment points and the angular displacement of the rigid body about the center of gravity are plotted. These results are in reasonable agreement with the expected responses of a two-degree-of-freedom system. Additional test cases involving higher degrees of freedom were not run due to the complexity of the checkout procedure and the shortage of time.

During the checkout of the program, some inherent difficulties in using the program were noticed. One difficulty is that displacements may extend beyond their physical limit due to unrealistic or wrong input data. A high input velocity and mass, together with weak springs, combine to give the rigid body large displacements which are meaningless. There is nothing in the program to detect this situation, so realistic input data are required to prevent it. Another small problem with the program is the error introduced in the coordinate transformations. The elements of the transformation matrices are trigonometric functions of angles expressed in radians. Since π and its multiples cannot be expressed in binary form, the computer introduces a small error into the elements of the transformation matrices. This error causes small, out of plane forces to appear in the equations of motion of the rigid body. Initially, this error is quite small and may be neglected for short duration runs. However, should long runs be required, this error may become sizeable. The previous difficulties could be eliminated through programming changes if required. In the interim, however, the program can be used taking account of the above conditions to investigate the impact response of an energy-absorbing landing gear system.

The program presented was debugged and operated using simplified impact conditions. Classical single and two-degree of freedom response calculations were made to compare with the computer output and validate the

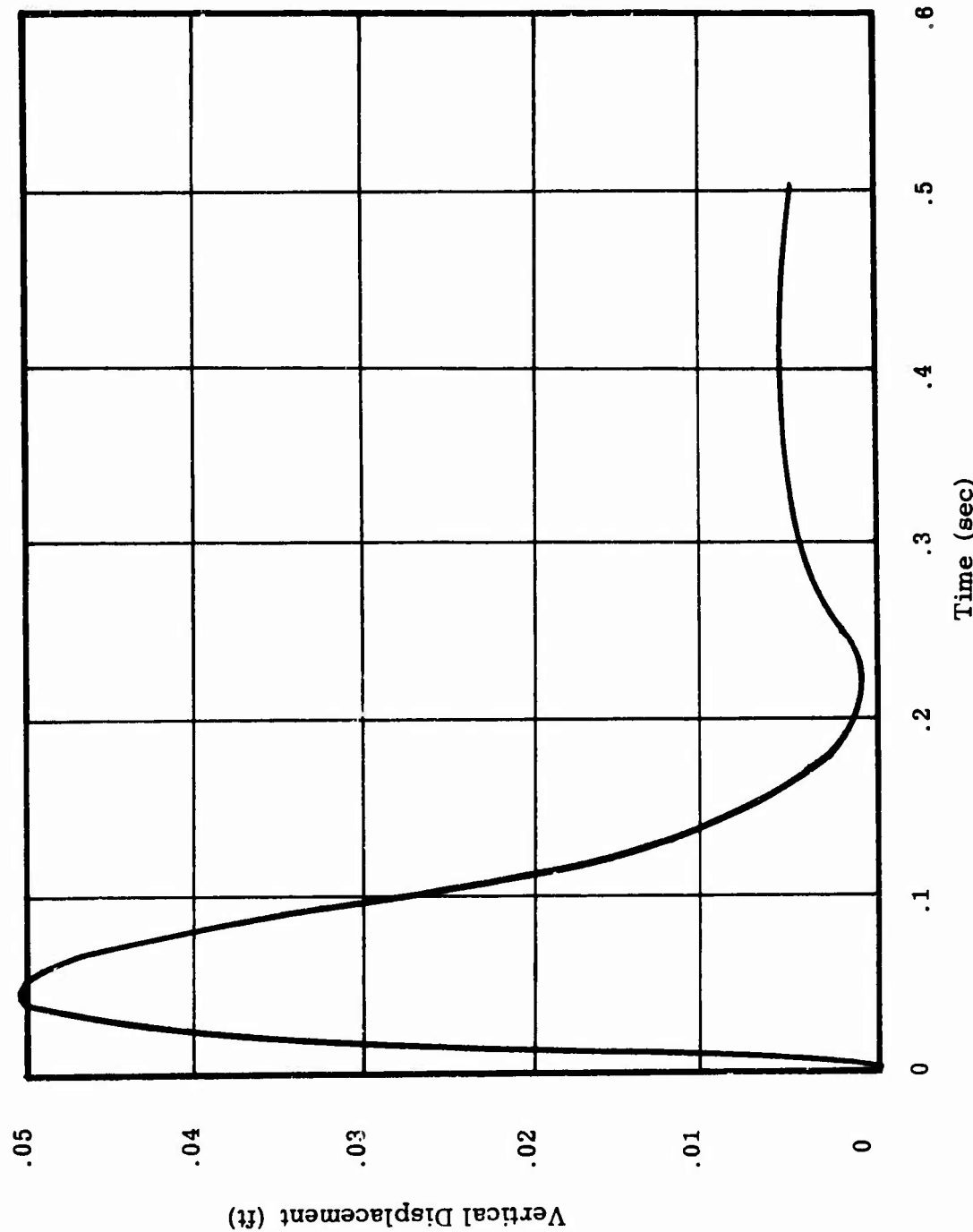


Figure 37. Pure Vertical Response Symmetrical Stiffness.

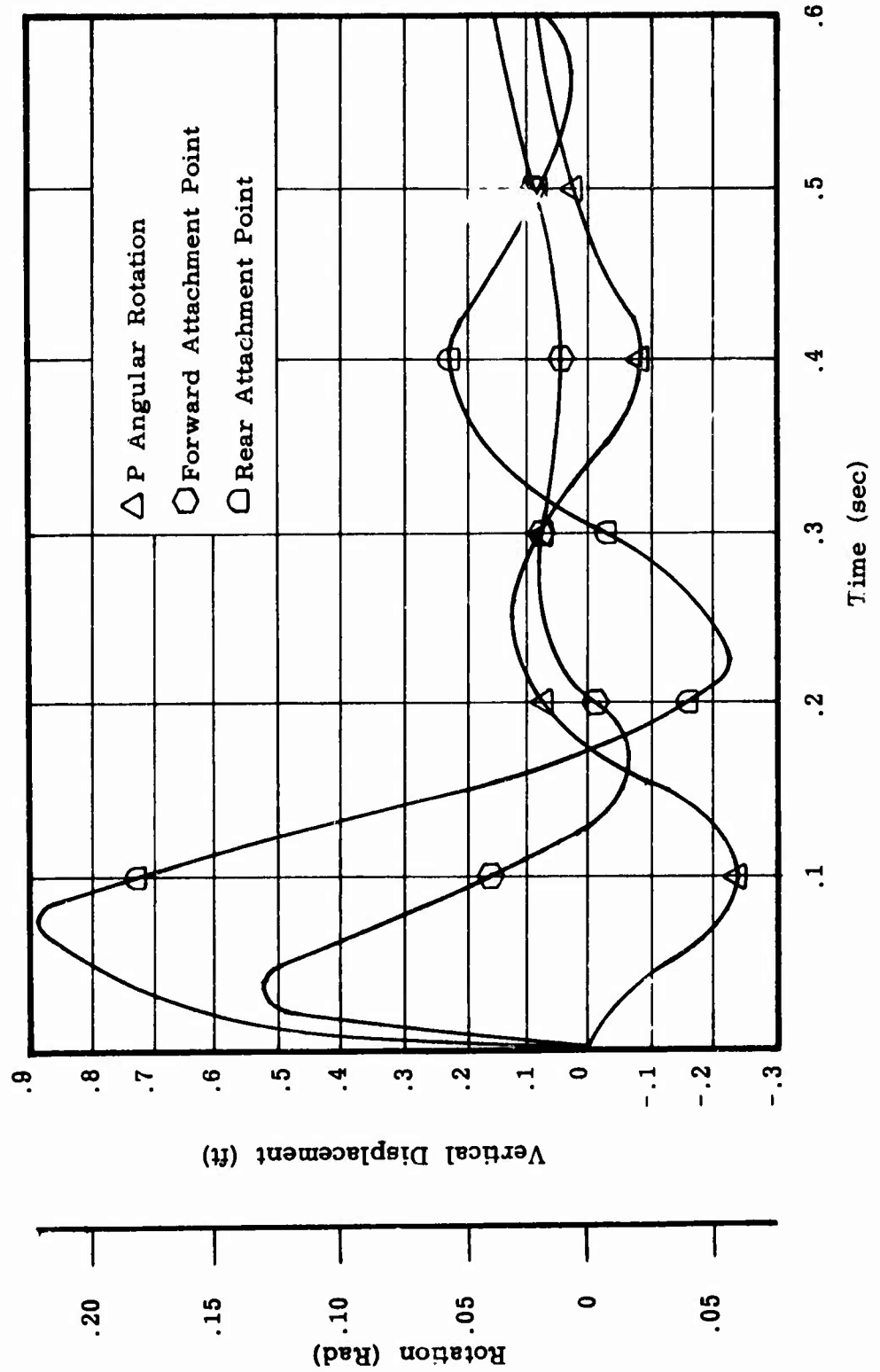


Figure 38. Pure Vertical Drop Asymmetrical Stiffness.

results. It was not possible during this effort to incorporate the additional logic required to recognize vehicle impact rather than landing gear attenuation. That is, the program is developed assuming that the landing gear attenuate the response and inhibits fuselage impact. Given that energy-absorbing landing gear coefficients are reasonably compatible with impact input conditions, the program is valid. If severe inputs are used with inadequate attenuation, the results are invalid just as are the original input data.

3.6 PHASE II SUMMARY

Results of this phase are as follows:

1. Design criteria for crash conditions were quantitatively defined as a set of 36 impact conditions that consider attitudes and velocities. In addition, the structural acceleration limit of 15G was established as a realistic criterion for improved fuselage crashworthiness.
2. Several concepts were examined to determine the feasibility of establishing energy-absorbing capability into landing gear systems. The concepts established using the criteria developed indicated that it is feasible to combine existing energy-absorbing devices into future or existing landing system designs.
3. The effects of combined loads and of the location of applied loads create significant variations in forces and moments carried by structural elements.
4. The truss concept shown in Figure 17 for the medium cargo class helicopter indicated that it is possible to select truss elements that can have energy absorbers incorporated within them that successfully operate with the combined loads.
5. The UH & LOH skid concepts were greatly influenced by the location of the applied load.
6. Skid configurations can be analyzed to evaluate the effects of plasticity and yield stiffness coefficients for a dynamic analysis.
7. A computer program that accepts nonlinear elements and computes a simulated helicopter response in three inertial degrees of freedom was completed, although not in time for concept development.

After weighing several design factors, one of the UH skid concepts was selected for Phase III evaluation. The first consideration was operational requirements, including normal landing loads. All UH skid concepts shown satisfy these requirements because all are designed not to actuate until the environment is more severe than "normally" designed for. The rigid link (Figure 19) rides over the existing strut and does not stroke until raised above a

particular level. The energy-absorbing strut (Figure 20) will not actuate until the slotted strut is sufficiently raised. The crushable skid (Figure 21) lever and cantilever (Figures 22, 23) concepts are also displacement activated.

The combined crash landing load of the landing gear and airframe does not occur if the concepts operate as anticipated. However, it is only realistic to consider what happens if that should occur during crashes that are more severe than designed for. All concepts except the crushable skid concept introduce additional forces and moments into the fuselage frame which tend to reduce its crashworthiness. Any concept which relies on carrying the force from some point on the skid back to the fuselage introduces moments that must be balanced by forces and moments in the frame. As the fuselage impacts, the bending capability of the frame is reduced because of these additional moments.

Environmental effects can be discussed for the systems. The rigid link concept (Figure 19) and lever mechanism concept (Figure 22) rely upon a pivot point within the fuselage, and yet actuation requires impact contact external to the fuselage. Therefore, the mechanism that ties the energy absorber and skid together must pass through some seal or expose the pivot to the environment. The energy-absorbing struts and cantilevered absorbers are both continually exposed to the environment, and this may or may not be a problem, depending upon the device. The mechanism required to cause the actuating displacement, such as a slot, does introduce another source of wear. The crushable skid can be rigidly attached to the fuselage and hence is only influenced inasmuch as the device is influenced.

Cost is meant to imply the cost of implementing the concept and not of retrofitting an old design. The rigid link and lever concepts require the fabrication of pivots that permit the change of direction of the applied forces. Additionally, the structure between the absorber and the strut must be fabricated and installed. The cantilevered absorbers require additional structure attached to the fuselage. The energy-absorbing strut and crushable skid are similar in that only the attachment structure is required.

The reliability of the concepts can be judged by the number of components required to actuate the absorber. Each component introduces another link that has a probability of failure.

Conceptually, the crushable skid has a minimum number of components in that it consists of energy attenuators that displace vertically within guides. The side and drag force effects are carried in the guides and the vertical forces are attenuated during the displacement. This also implies minimum weight and complexity in that no additional structural "hard points" are required other than within the lower frame structure.

Additional consideration was given to the fact that by coupling the crash attenuation to the skid, the effects of combined loads and tip loads severely

complicate the problem of generating a fixed configuration attenuation system. The skid deforms differently depending upon the point of load application. If the added attenuation is relative to skid displacement, it cannot sense whether or not greater attenuation at an extreme attitude is required.

Because of the aforementioned aspects, the "additional" skid concept was selected for hardware design. As glaringly pointed out in the following sections, this was shown to be a very suspect selection. The combined loads effects could not be carried by guides and the design evolved into a skid with additional linkages.

CHAPTER 4
PHASE III - ENERGY-ABSORBING UH-1
LANDING GEAR DESIGN, FABRICATION, AND TEST

4.1 INTRODUCTION

The final phase of the program consisted of several tasks:

1. Analyze the UH-1H helicopter landing gear system to identify any design deficiencies and hazards contributing to the incidents of injuries and fatalities.
2. Design an experimental prototype skid-type crash force attenuating landing gear utilizing the previous criteria and concepts.
3. Fabricate and test the designed landing gear in accordance with the established criteria using a full-scale test vehicle.

4.2 FAILURE ANALYSIS

The present UH-1H helicopter landing gear system was analyzed to identify design features which contribute to the incidence of injuries and fatalities sustained in severe but survivable UH-1H helicopter accidents.

The response of the skid to applied loads in the drag, side, and vertical directions at various points on the skid were examined. It has been shown that severe bending moments and shear reactions are created when the loads are applied at the forward tip of the skid. The magnitudes of the reactions are such that the bending moments vertically and horizontally are 46,200 inch-pounds and 20,400 inch-pounds respectively for applied loads of 1,000 pounds vertical and 500 pounds axial and side. The forward tube has a radius of 1.375 inches and a moment of inertia of 1.55. These provide bending stresses of 40,800 psi and 18,100 psi. The stiffness of the skid to an applied vertical tip load is approximately 385 pounds per inch. Therefore, at a load sufficient to develop a yield stress for 7075-T6 aluminum, the deflection is sufficient to rotate the tip up to nearly 10 degrees. Hence, even if the skid tips were a horizontal extension of the flat bottom skids, they would deform elastically up to a sufficient degree to load the vertical struts at impact.

Beyond the application of the tip yield load the struts carry the increased load while the tip remains fixed relative to the strut. The strut then carries proportionately less bending moment due to more being transferred to the rear strut. For loads applied at the strut, the bending moment carried is 21,740 inch-pounds per 1,000 pounds applied and has a stiffness of 1,900 pounds per inch. The strut deforms elastically up to 3,730 pounds and 1.96 inches. Plastic deformation then continues up to 4 to 5 times the elastic stroke. By this time the fuselage has been contacted and additional deformation of the skid relative to the fuselage is

not possible.

The results of the above plastic analysis for combined loading effects indicate that:

1. The conventional skid has sufficient plastic deformation to permit deformation without rupture up to fuselage impact.
2. Even with an extreme tip load application, the deformation is such that a skid segment would not be ruptured and torn free from mating components.
3. The tie-down attachments at the junction of the struts and skids are designed to carry a maximum of approximately 4G. At this level the critical bolt in any particular attachment saddle has only a 13 percent margin of safety. Others in the pattern are, of course, not under the severe load developed by both moment and shear. It was anticipated that several bolts would fail at critical locations, but that the skid and strut would not separate. The criticality depends upon the attitude and tip loading. At yield, the tip loading condition does not exist.

The general conclusion made is that because of the configuration, material type, and attachment means, the tubular, circular arc landing gear fails without creating hazardous flying objects or segments that tend to penetrate the fuselage.

4.3 SKID LANDING GEAR DESIGN

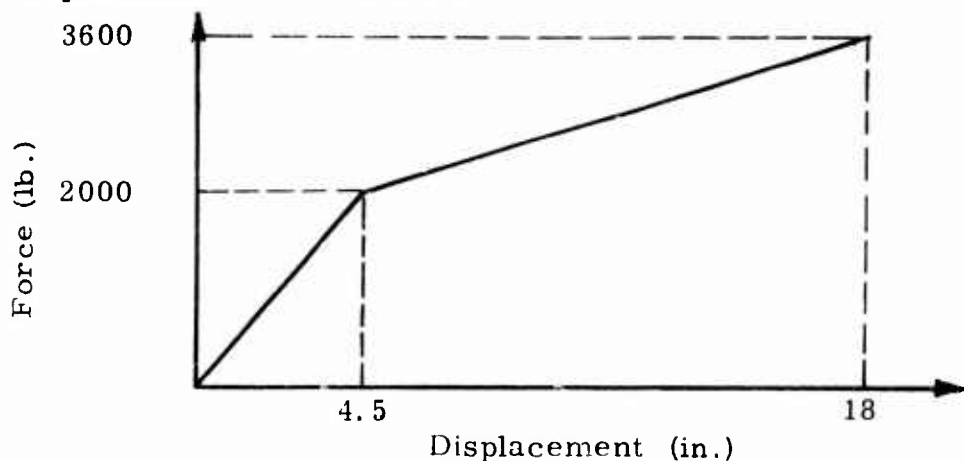
A requirement of the energy-absorbing landing gear system was that it meet or surpass the capabilities of the current UH-1 skid. By decoupling the energy attenuation system from the skid configuration, it was then possible to provide a skid which would duplicate the existing design. This simplified the design of the landing gear in that duplication alone could be considered rather than designing a system with both "normal" and "crash" criteria.

4.3.1 Skid Design for Normal Landing Conditions

Unsuccessful attempts were made to obtain a set of UH-1 skids that could be incorporated into the test vehicle. Also, it was determined that duplicating the skid, with its curvature, material type and internal chem-milled wall thickness, would be very time consuming and expensive. Consequently, it was desirable to find a skid configuration of commercially available stock with minimum forming or fabrication. A skid of particular wall thickness, material type, curvature and length that would duplicate force, energy and stroke in the elastic and plastic range was needed.

The forward cross-tube was examined first. The desired force-

displacement curve is shown below:



The deflection of a curved tube is calculated from

$$w = \int \frac{Mm ds}{EI} + \frac{2L_1 L_2 E}{D} \quad (46)$$

where the first integral is the elastic deformation and

$L_1 L_2$ = dimensions from attachment point to point of load

E = strain from an elastic-plastic bending curve

D = outside diameter of the tube

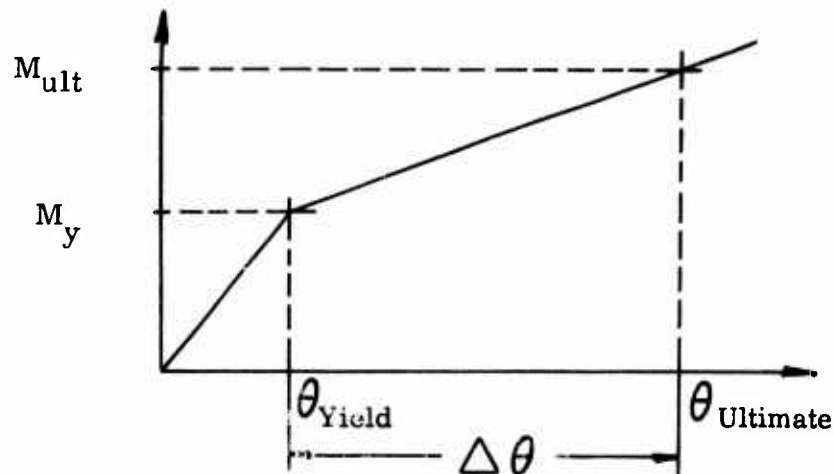
Mm = the product of applied moment (M) and virtual moment (m)

An analysis was conducted on several configurations of aluminum and steel. Aluminum tubing of the desired geometry has both a yield and ultimate deflection that are too low. That is, if a section property is selected to carry the design force at failure, the strain will not permit large enough displacements. Both low-carbon and annealed nickel-chrome steel were examined. The low-carbon steel has proper yield value but will not displace far enough at ultimate to generate the desirable energy. The annealed material is least desirable in that the deformations are considerably less than required.

A constant cross-section aluminum pipe was examined as a straight cantilevered beam to determine whether or not the section properties and free length could be varied to satisfy the criteria. The analysis was based upon the paper by Chernoff and the assumption that planes remain planar during bending; hence, strain energy in bending can be related to the translational energy dissipated by the load at the tip of the beam. The plasticity effect is incorporated into the analysis in that an effective or

equivalent elastic bending moment at failure can be calculated from material properties and incorporated into the otherwise linear analysis.

As the cantilever is bent, the strain energy due to bending can be represented by the area of curve shown below:



This must be equivalent to the energy of the applied load.

After several iterations of configurations, specific tubes were found. For the forward tube, the desirable yield and ultimate forces were 2000 and 3600 pounds respectively. If 6061-T6 tubing is used with an ultimate strength of 42,000 psi, then the bending stress is 59,000 psi for a section. For a 59,000 psi stress and 55-inch cantilever, it is necessary to have a 4-inch by 5/16-inch wall thickness tube. The applied force would be 3310 pounds ultimate and 1980 pounds yield.

The angular deformations due to the yield and ultimate load are .048 radian and .280 radian. This is based upon the curves of Chernoff which indicate that the ultimate and yield strain differ by a factor of 5.43. Equating the internal strain energy and applied energy, the strokes developed are

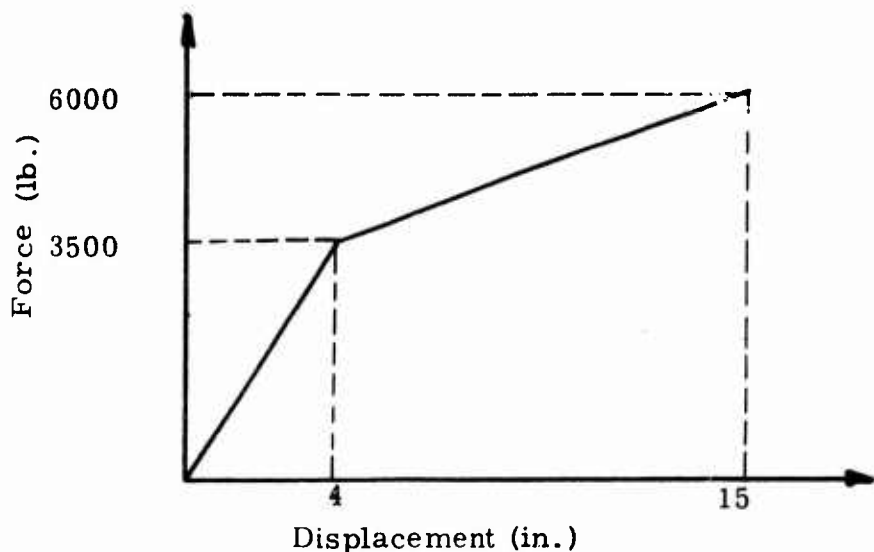
$$\delta_{yield} = 2.31 \text{ in.}$$

$$\Delta \delta_{ult} = 13.80 \text{ in.}$$

so that the total deformation at ultimate is 16.11 in. The Bell data³⁸ indicate about 3550 pounds at 16 inches. Therefore, the tubing selected

was a commercially available 3½-inch pipe (4 inch OD) with 0.318-inch wall thickness.

The rear strut selected was a 4-inch pipe (4.5 inch OD) with 0.337-inch wall thickness. The curve analytically anticipated is shown below. A 60-inch cantilever was required.



The fore and aft members of the UH-1 skids were fabricated from 2024-T3 4-inch OD by 0.085 inch wall thickness tubing. The strength required was duplicated by designing with 4½ inch OD by .125 inch-thick 6061-T6 tubing.

Two sample skid landing gear were fabricated and strain gaged to determine how close the designed tubular skids could duplicate the original UH-1 skids. The samples were sent to Bowser-Morner Testing Laboratories, Dayton, Ohio, to determine the force-deflection characteristics as well as strain data for later calculation of skid force during impact tests.

The curves generated are plotted with the desired Bell data to indicate the agreement (Figure 39). Although the skids are of different material, configuration and length, it was thought that their characteristics would sufficiently duplicate the maximum forces, stroke length, and energies required during failure of the skids.

4.3.2 Skid Design for Crash Impact

The results of the concept studies indicated that the concept of an additional energy-absorbing skid to absorb the crash energy of a simulated UH-1 vehicle is attractive. The energy-absorbing skid would

TEST DATA LEGEND

Aft Cross Tube, 6061-T6 Aluminum



Fwd Cross Tube, 6061-T6 Aluminum



Bowser - Morner Test Lab

Report No. 750404



Aft Cross Tube, 7075-T6 Aluminum



Fwd Cross Tube, 7075-T6 Aluminum

Bell Helicopter Company

Report No. 204-099-691

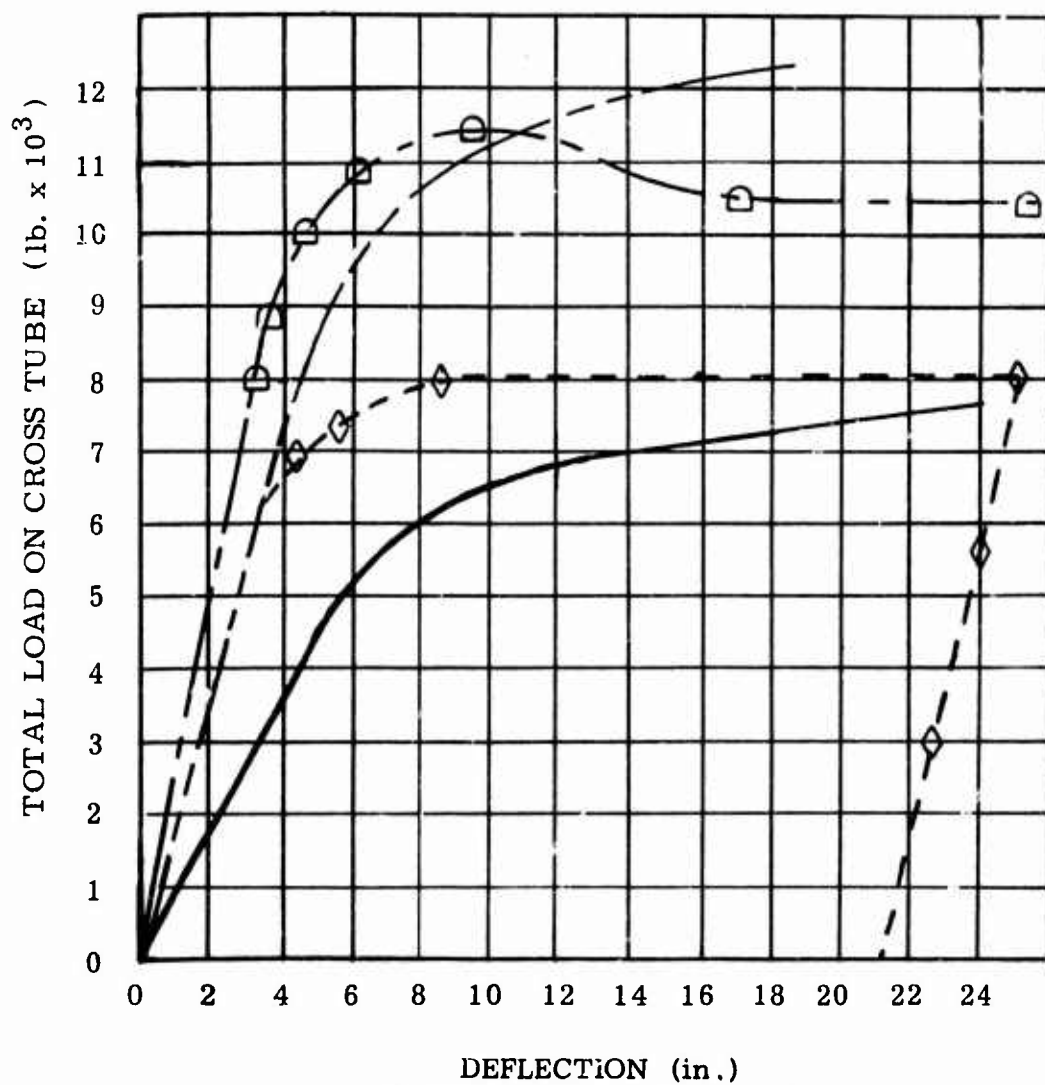
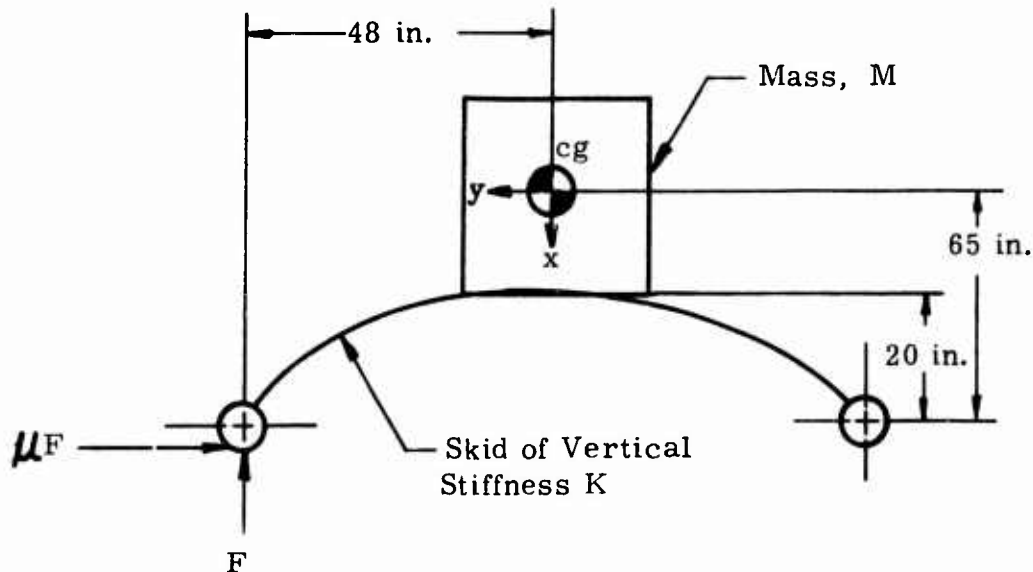


Figure 39. Load vs. Deflection.

supplement the capabilities of the existing skids in that the crash pulse of 25 feet per second vertical velocity was to be dissipated at attitudes of angles of up to 10 degrees without exceeding 15G on the fuselage. Additionally, side and drag velocities were to be considered.

Initially, an estimation of the impact response of a UH-1 vehicle due to initial conditions of attitude was sought. Test data collected previously on full-scale crash tests indicated that for large impact velocities, the conventional landing skid had been somewhat useless in changing the attitude of the vehicle. That is, if the vehicle were nose high at impact, the vehicle would remain in that attitude during crushing of the skids. This would be inferred from the inertial characteristics of the vehicle, but it was desirable to obtain a reasonable approximation of the vehicle response to indicate the criteria that would be applicable to the energy-absorbing skids.

The vehicle was approximated by the system shown below:



The first case examined was that of 10 degree roll only with combined vertical and horizontal velocity. The equations of motion were assumed to be decoupled so that the angular and translational motions could be easily calculated.

For translational lightly damped response,

$$M\ddot{X} + KX = 0 \quad (47)$$

where K is the stiffness of the skid.

The angular response is calculated from

$$\rho = I \ddot{\theta}$$

(48)

where I is the rolling moment of inertia

$\ddot{\theta}$ is the angular velocity

The problem is solved by calculating the translational equation and determining the time required to stroke through the range of the linear stiffness. The angular response for that time is evaluated, and then both equations are reevaluated for constant force failure of the skid.

For the nose down, 10 degree roll impact, the stiffness of only one skid is initially effective. From existing data, the stiffness would be 433 pounds per inch. Evaluation of the expression

$$X = \frac{V_0}{W} \sin \omega t + \cos \omega t \quad (49)$$

where

X is the vertical displacement

V_0 is the initial vertical velocity

$$W = \sqrt{\frac{K}{M}}$$

for a displacement of 6 inches (the linear range) yields a time required of .020 second. In this amount of time, the vehicle rolls only 0.01 radian. At that point the equations are reevaluated for a desired 10 degree of roll. The result is that one skid would crush 11.7 inches during the total 10 degrees. Therefore, the roll inertia is low enough that it is apparent the vehicle will be approaching a level attitude when the additional skid becomes effective. This was an important point because it means that it can be assumed that skids on both sides of the vehicle will be effective during the energy-absorbing stroke. If the inertia were too great, in relation to the forces, moments and stroke lengths required, then it would be necessary to consider the requirement of having large energy-absorption capability at each "corner" of the vehicle.

As an example, consider the effects of pitch attitude. For the same conditions as above (the softest skid impacting first) the inertia in pitching is nearly five times greater. This creates the need for 27 inches of stroke in order to rotate the nose up 10 degrees. This clearly indicates that a pitching attitude will remain virtually unchanged during the stroking of the conventional skid.

The yawed configuration is similar to the pitched attitude in that the moment of inertia is similar (11.9×10^4 versus 13.7×10^4) and the stiffness of the forward strut to side load is similar to the vertical used above. Side force stiffness of the forward skid is calculated at 360 pounds per inch as compared with 433 pounds per inch. Therefore, the vehicle

will attempt to continue at any initial yaw angle during the vertical energy attenuation process.

The simplified analysis indicates that it is now reasonable to assume that the existing skid configuration will provide sufficient force and stroke for the vehicle to roll during impact, but insufficient strength to modify the pitch or yaw attitude at impact. Therefore, in designing the energy-absorption system which is to supplement the skid, it will be necessary to examine the effects of a pitch attitude at impact.

The effects of the yaw attitude are ignored for the moment, since it is difficult to realistically evaluate how that particular "component" of the total energy is to be dissipated. It is possible to have no attenuation within the vehicle. Rollers could expend the energy in rolling laterally. This is true of the longitudinal velocity. The dissipation is accomplished through surface effects at the impact point or area, and not through stroking of an attenuator. This is not true of the vertical velocity at impact.

During the conceptual stages of energy-absorbing system design, it was necessary to determine how much force, energy, and stroke would be required to dissipate the total energy available. The assumed UH-1 configuration of 6,600 pounds impacting at 25 feet per second will generate 7.7×10^5 inch-pounds of energy. If the impact is purely vertical and the existing skids deform over their theoretical capability of about 16 inches, the energy dissipated by the skids will be

$$E = \eta F \delta = \{(.75)(19,200)\} 16 = 2.31 \times 10^5 \quad (50)$$

where $\eta = 0.75$ was chosen for a conservative efficiency

$F = 19,200$ pounds, is the total force developed by both skids

Therefore, the energy-absorbing landing gear must absorb 5.39×10^5 ($7.7 \times 10^5 - 2.31 \times 10^5$) inch-pounds. If a stroke of 6 inches is assumed with an efficiency of 90 percent (typical for an energy attenuator).

$$5.39 \times 10^5 = \eta F \delta \quad F = 100,000 \text{ pounds}$$

For equally loaded energy absorbers on the vehicle, this would require 25,000 pound units, and the acceleration of the fuselage would be

$$\frac{19,200 + 100,000}{6,600} = 18.1G$$

which is greater than desired.

Assuming the skids could operate out to 22 inches of stroke,

$$E = (.75)(20,200)(22) = 3.33 \times 10^5$$

and the landing gear must carry 4.37×10^5 inch-pounds. The energy absorber would then carry 20,250 pounds and generate a load factor of 15.3G. A ground clearance of 22 inches is necessary to satisfy the acceleration and energy levels required utilizing conventional skids.

If the attitude is changed to 10 degrees nose up, the rear skids will only provide 2.10×10^5 inch-pounds, and the energy to be dissipated is 5.60×10^5 inch-pounds. The absorber just found for the pure vertical impact is assumed to exist and would generate

$$E = 2.185 \times 10^5 \text{ inch-pounds}$$

An additional capability must exist to dissipate 3.415×10^5 inch-pounds. For the same stroke length (6 inches) the force required would be 63,200 pounds and the fuselage would feel

$$\frac{63,200 + 40,500 + 19,200}{6,600} = 20.1G$$

Similarly, for the nose-down condition, the fuselage will develop 19.2G and will require 78,500 pounds of additional force.

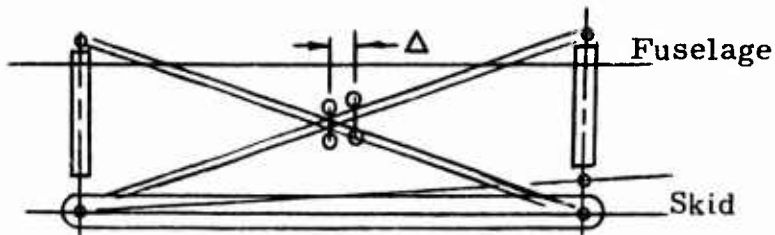
This indicates that if a given stroke length of energy absorber will satisfy the pure vertical drop, the effects of attitude will require additional energy absorbers, fore and aft, that will generate unacceptable G levels. It would be desirable to have an absorber system sensitive to attitude, one that would vary the force with the direction of application. As a first approximation to the system desired, it would be necessary to have a configuration with four 20,250-pound energy absorbers at the skid tie-down points, two 31,600-pound attenuators aft, and two 39,250-pound units forward.

The preliminary analysis is conservative in the sense that in a 10-degree attitude the forward and aft skids both dissipate energy. After approximately 12 inches of stroke, both skids are bending and dissipating energy which reduces the capacity and force level of additional energy absorbers.

At this point the problem was twofold. A system was necessary which could generate different force levels as a function of pitch attitude, and which was capable of carrying the side and drag loads developed by frictional forces.

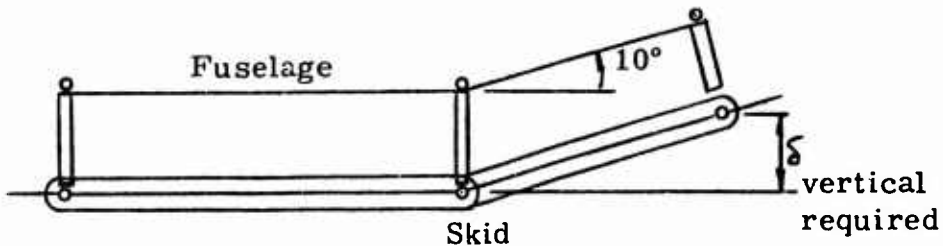
The first aspect was examined to determine if types of linkages with particular attachment points could be used. The addition of a linkage was not a desirable feature. Previous criteria had indicated that conceptually the additional skid would not need linkages to perform properly. However, more detailed examination into the problem indicated that attitude sensitivity was a significant problem. This problem is present regardless of the concept selected. The energy absorption system must passively detect an attitude at impact and have the capability to supply reacting forces that are "matched" to the requirements. Given that an attitude

angle exists between fuselage and impact surface, the relative motion must be recognized and utilized to alter the force levels developed. The only means found of accomplishing this was that of linkages which could create relative displacements if other than a vertical impact occurred. As an example, consider the linkage shown below.



If the skid is forced upward vertically, the intersection of the cross-members travels vertically and horizontally. If the rear end compresses at some attitude angle, the intersection point travels aft and another absorber tied to that point and the front of the fuselage has to be elongated. There are many practical difficulties in such a system as well as the problems of carrying large loads at large angles to develop significant component forces.

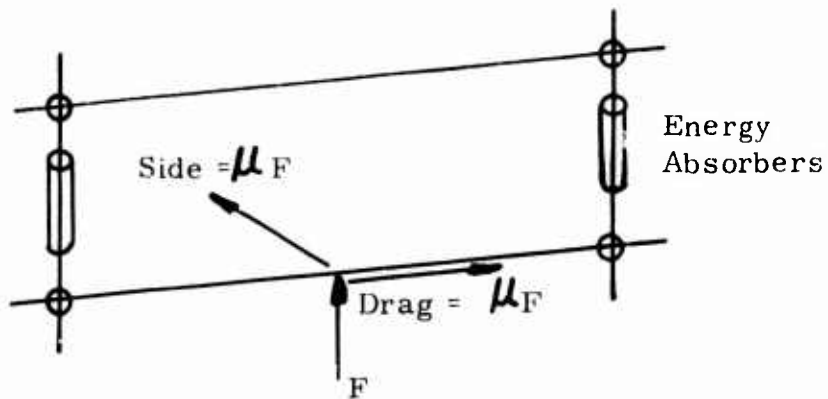
One method to be examined was to recess the additional absorbers by the attitude required.



If the attachment point of the "attitude" sensitive absorber is at the selected angle above the "pure vertical" absorbers, then the rear unit cannot stroke unless there is some attitude. At 10 degrees of nose-up pitch, both units would stroke simultaneously. At some in-between angle the "attitude" absorber would not stroke until the center units had stroked and the front skid dissipated additional energy.

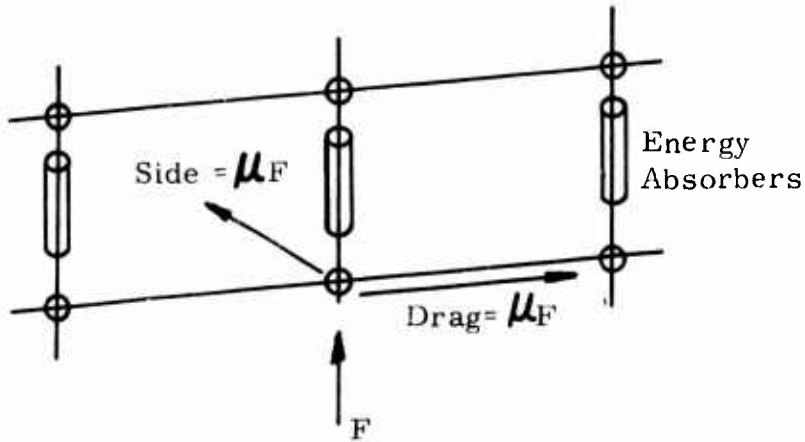
At the extreme attitude angle selected, the center units and the attitude units stroke simultaneously after the one conventional skid has stroked. For the pure vertical drop, both skids actuate and all center fuselage energy absorbers stroke. At any in-between attitude, one strut and a center attenuator act initially until the deformation gradually picks up energy from the other strut and then the "attitude" absorber.

The second aspect, side and drag force capability, proved to be more difficult to solve. Consider the schematic:



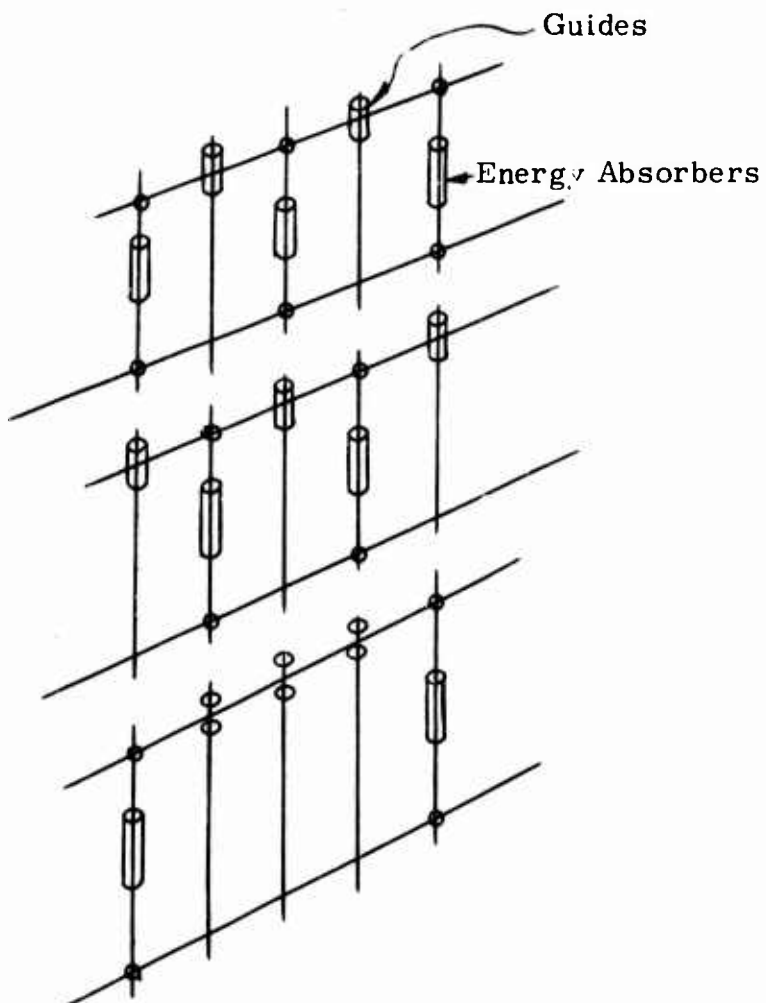
The energy absorbers stroke at a given force level and permit a side and drag force of one-half the vertical force. The schematic is indicative of the system to be used but not definitive in establishing where the attachment points are or how they function under load.

The system could be:



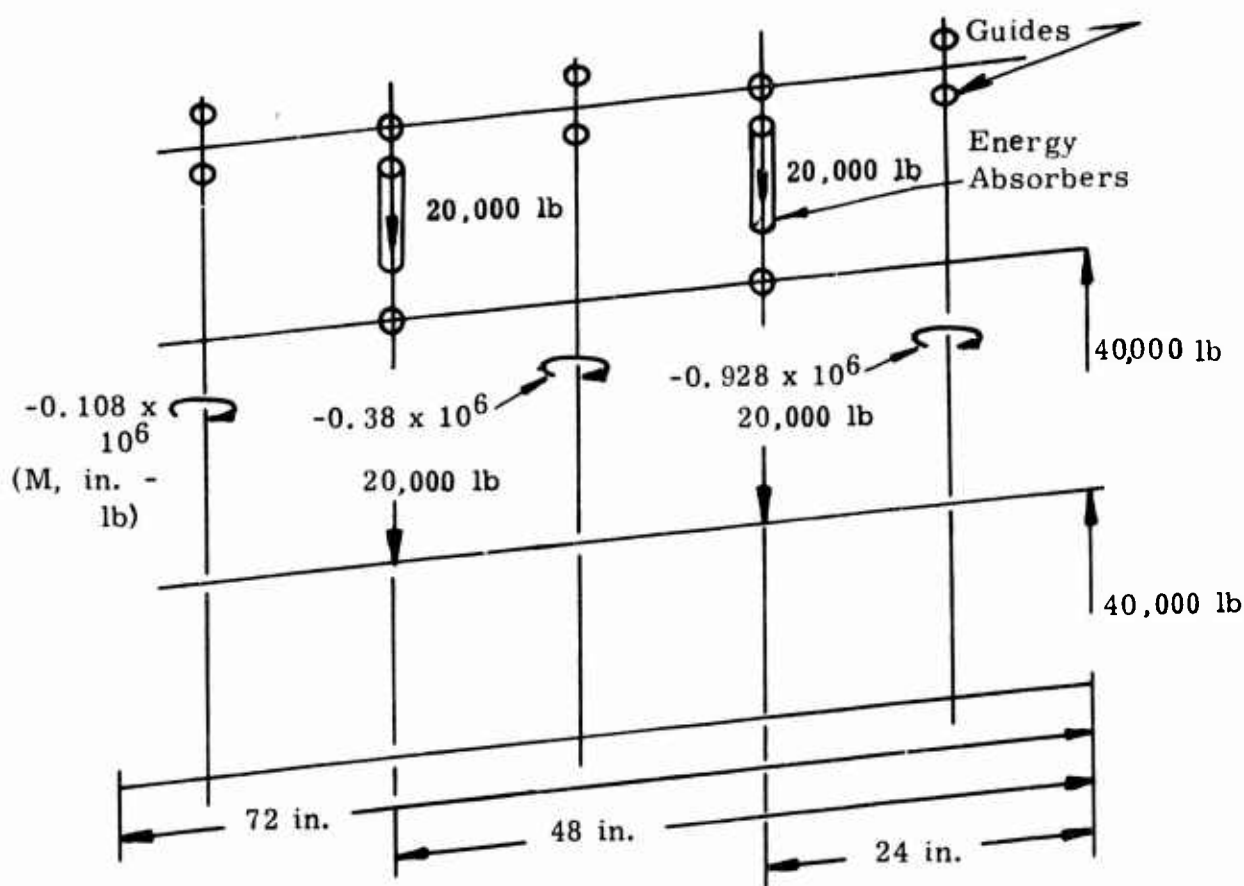
and would then reduce the force level required for any one absorber. The attachment points could be pin connections, assuming the side and drag

forces are carried elsewhere. However, if pinned to permit only axial variations of this arrangement were examined, such as



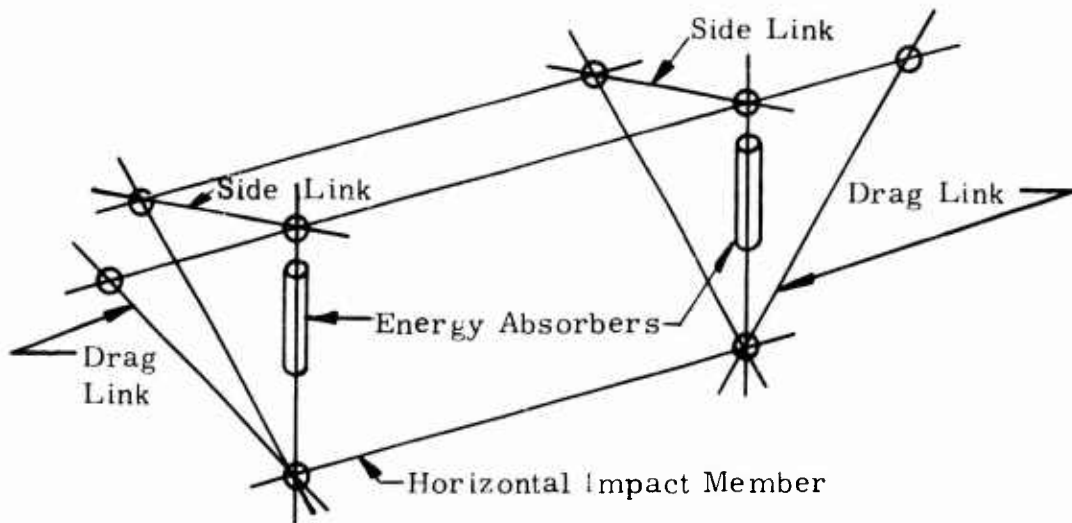
Multiple guides were examined in parallel with multiple energy absorbers to determine the loads that have to be carried in each structural element. It is necessary to insure that the bending moments generated by the side and drag forces are carried in the guides, not the absorbers. The conventional absorbers available cannot carry appreciable bending loads and are designed to act axially.

The analyses indicate that guides create large bending moments in order to carry the loads from impact point to absorber. As an example, the configuration shown below considers the condition where the energy-absorber skid has impacted at a small pitch attitude and must develop the forces of the center absorbers.



Notice that the guide nearest the applied load must carry nearly 1 million inch-pounds of moment without drag or side load effects. This leads to the question of whether or not the guides would even work under these conditions. The arrangement would be similar to the sides of a crib where the movement must be vertical without bending. The moments to be carried require enormous section properties and rigid supporting structure. A similar result was obtained for several variations of guide-absorber-link arrangements.

At this point the design reverted to the technique of providing structure in the direction of the applied load. That is, if a drag load is present, why not provide a drag link, an axial member that can efficiently carry a particular load? Similarly, if the side load exists, it must be carried by a side link. Therefore, the energy absorbing landing gear system becomes schematically



The impact loads are introduced into the horizontal members and carried into the drag and side links through pinned connections. To determine the loads carried in each member, vector diagrams were generated for various impact conditions. As the vehicle impacts at a 10-degree attitude, the linkage permits the skid to swing up into the proper attitude. Since it is assumed that the vehicle does not change attitudes during the stroking of the energy absorbers, the links connecting the energy absorbers remain at the same attitude and stroke through a given displacement. Figure 40 indicates a force balance diagram.

With the addition of side and drag forces, additional vertical components are added into the analysis. As shown in the figure, the addition of drag introduces additional vertical components which must be accounted for. The result is that it requires 27,000 pounds of vertical force to cause a 20,000 pound energy absorber to stroke over 6 inches. Several variations of input conditions were examined, and it was found that in order to have reasonable forces and stroke lengths the design forces would have to be

Midsection energy absorbers	16,000 pounds
Aft fuselage energy absorbers	24,000 pounds
Forward fuselage energy absorbers	30,000 pounds
Maximum stroke length required	8 inches

With this configuration the 15G design level could be achieved except for the nose down at 10 degree condition. For this condition, a theoretical

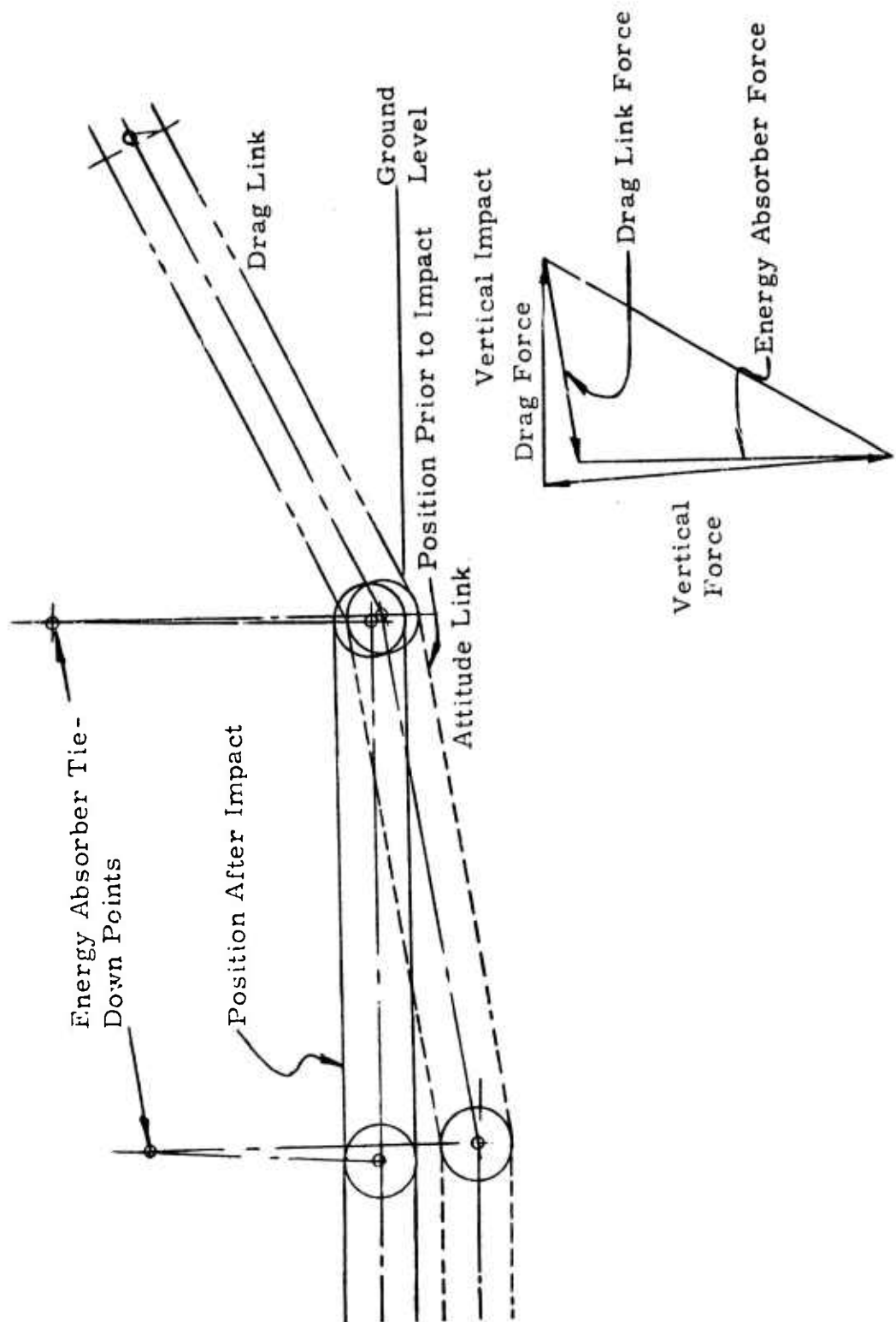
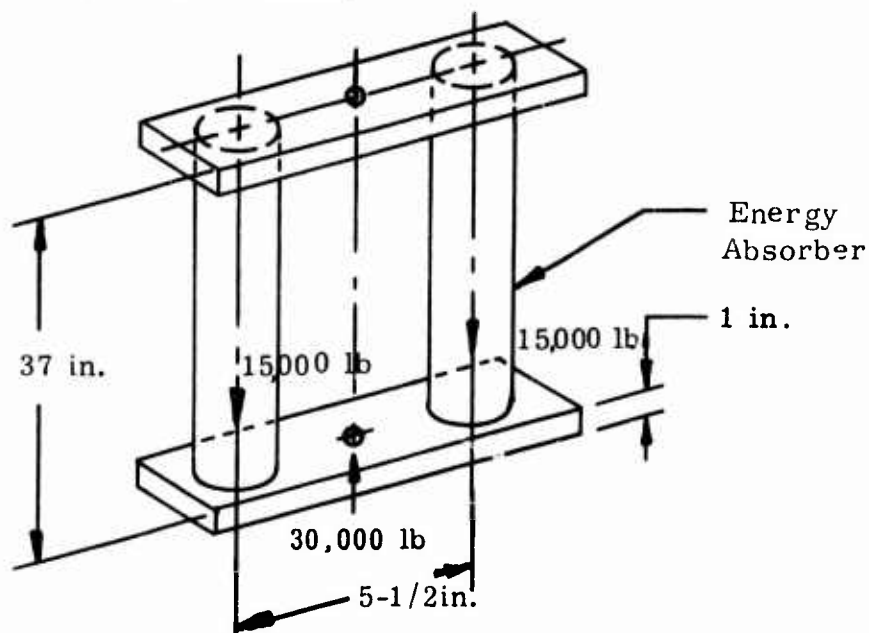


Figure 40. Vertical Impact.

18.2G level would be developed.

Several energy-absorber manufacturers had been contacted to obtain information that could be used to select currently available energy absorbers. ARA Products, Inc., was contacted to obtain the required energy absorbers. After initial specifications had been reviewed and analysis conducted, it was found that it would be necessary to use energy absorbers in parallel to generate forces greater than 16,000 pounds. A redundant analysis was conducted to calculate the type of structural tie needed to minimize any bending that might be carried within the energy absorbers during compression. For the arrangement shown below, a 1-inch-thick steel plate assures that the energy absorber tube carries less than 10 percent of its compression capability in bending.



The detailed design of the skid mechanisms was developed from the given criteria, and it was possible to design pinned joints having adequate strength and flexibility to transfer applied loads into the axial links. A drawing of the system is shown in Figure 41.

The system consists of several components. The large horizontal tubes across the middle have inner and outer segments with rollers between them. This is necessary in order to permit the free swing of the drag links during vertical impact. The entire tube is free to rotate so that side force could be partially dissipated by roll-out rather than pure sliding action along the ground surface. The inner tube with rollers weigh $23\frac{1}{2}$ pounds and the outer tube weighs 57 pounds. The stiffness required was based upon a running load along the tube balanced by pinned end connections.

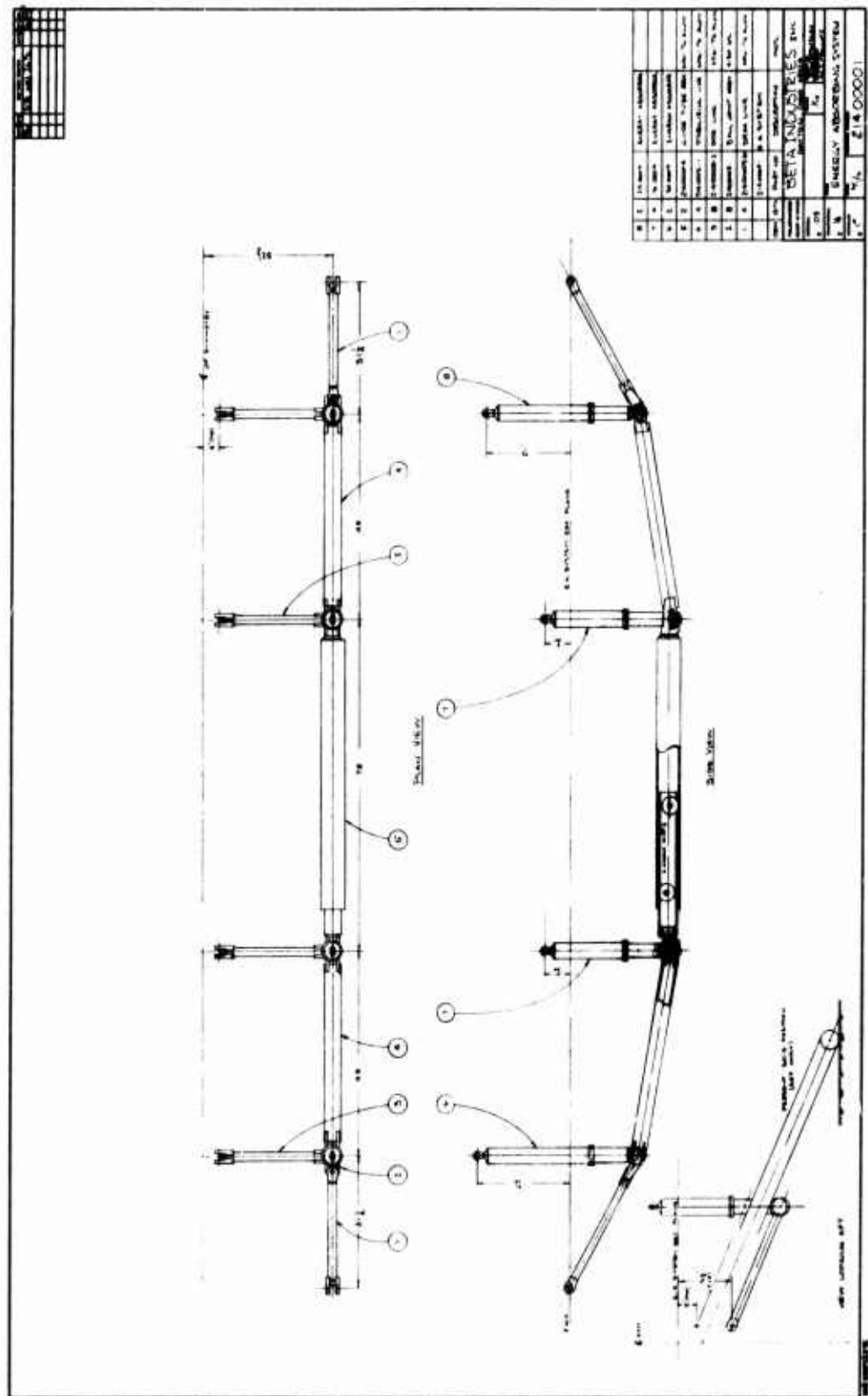


Figure 41. Energy-Absorbing System.

The stabilizing links with attached side links weigh $50\frac{1}{2}$ pounds, including all bearings and attachments. The drag link weighs $7\frac{1}{2}$ pounds.

The bearings and tie-ends are all commercially available hardware that was readily obtained.

The total weight of the skid system is 440 pounds. The energy absorbers required weigh a total of 304 pounds for a total system weight of 744 pounds. If it is assumed that the side and drag force requirements are removed along with the attitude restriction, the system weight would be:

	<u>Wt(lb)</u>	<u>% of Aircraft Gross Weight</u>
Total weight	744	11.27
Stabilizers & side links	202	3.06
Drag links	30	0.46
Energy absorber	216	3.27
	<u>448</u>	<u>6.79</u>
System weight for vertical loads only	296	4.48

This indicates the severity of imposing attitude and combined forces, particularly for this design concept.

One energy absorber has the capacity to carry 16,000 pounds over $8\frac{1}{2}$ inches at an efficiency of .95. The specific strain energy would be 5,860 inch-pounds per inch-pound. For the system, the SEA is 586.0 inch-pounds per inch-pound. Hence, the design creates an order of magnitude change in energy-absorption capability. If only vertical attenuation is required, the SEA is 1,480 inch-pounds per pound and a ratio of 4.

4.4 DATA REQUIREMENTS

4.4.1 Calibration Procedures

Basic calibration data were obtained and supplied for all pertinent components. In order to relate these to the test data obtained, a Honeywell bridge balance unit was used to provide a 4-point calibration. The resultant deviations, produced by shunting the strain gage bridge with known resistors, in conjunction with their associated calibration data, provided the necessary units (G's or pounds) per inch of galvanometer deflection. In addition, the 4-point calibration provided a means of checking the transducer linearity.

4.4.2 Multiple Oscillographs

The large number of data channels accommodated necessitated the use of 2 oscillographs. Oscillographs did exist with the required channel capacity, but it was felt that the confusion introduced by squeezing the data onto one record would greatly offset any advantages which might have

accrued. Identifying individual traces was made easier by spreading the data over two records; however this task was facilitated further by obtaining oscillographs which were equipped with light beam interrupter type trace identifiers. The use of two units did introduce a problem of time correlation between records. Time was correlated by noting the acceleration changes at the release time. The oscillographs were equipped with timing systems, capable of recording time lines at .01, 0.1, 1.0, and 10 second intervals, which facilitated this procedure.

4.4.3 Data Reduction

The resultant test data were manually reduced, i.e., the calibration pulses were measured, calibration factors determined, and the data traces scaled and logged together with their time of occurrence on data sheets. These data sheets serve as the source documents for determining the effectiveness of the energy-absorbing landing gear concept and for comparison with the results of the anticipated computer simulation.

4.5 DYNAMIC TESTS

4.5.1 General Procedure

The subject tests were conducted during the week of 6 September 1971 (at the Springfield Municipal Airport, Springfield, Ohio). Three drops from a moving crane and several low static check-out drops were planned.

TABLE X. PLANNED IMPACT TESTS

Test	Angle (Degrees)			Impact Velocity (Ft/Sec)		
	Roll	Pitch	Yaw	Vertical	Longitudinal	Lateral
1	0	0	0	25	0	0
2	0	0	0	25	15	0
3	+10	+10	+10	25	15	29

The test vehicle was attached to the crane using the release mechanism and suspension system previously described, properly oriented and raised to the drop height. A drop height of approximately 10 feet for each of the 3 orientations, which are level, 10 degrees nose up, and 10 degrees nose down, was required. The crane was then to proceed to a predetermined position on the runway which permitted the attainment of the desired 20 mile-per-hour release speed prior to reaching the impact area. There it was to be joined by the instrumentation truck. After attaching the umbilical cable and making the appropriate calibrations, the crane and truck would proceed toward the impact area where the cameras and associated control

equipment were set up. Upon reaching the impact area the release mechanism was manually actuated and data were collected. After each of the first two tests the test vehicle was to be repaired at the test site, since spare parts had been fabricated and delivered to the test site.

4.5.2 Test Results

Drop test number 1 was conducted on 9 September 1971. The vehicle was adjusted for a level attitude, within 1 degree in roll for the greatest deviation, and raised to 9 feet. At this height the vehicle interfered with the crane boom, and hence it was impossible to achieve the desired 9.7 feet. The tubular skids had been installed, accelerometers and displacement transducers located and calibrated, and photo coverage readied. At impact, the vehicle crushed the tubular skids in the same manner observed during the static tests. The energy absorbers, however, stroked only a small amount while their supporting bulkheads deformed.

The absorbers stroked only $2\frac{1}{4}$ to $1\frac{9}{16}$ inches while the remainder of the vertical displacement desired was provided by deformation of the lower portion of the bulkhead. At impact, the moment generated by the absorber force caused the reaction forces in the lower beam to shear the end attachments. Without the end restraints, the beam was free to bow as a simply supported beam and the attached absorber rotated upward.

The energy absorbers were sent to Bowser-Morner Testing Laboratories to determine the force levels that each required for compression loading. The design force level was 16,000 pounds, and it was found that the plateau levels of the absorbers were all within 4 percent. The starting levels for the absorbers were higher, between 1450 and 2800 pounds greater, but not sufficiently higher to explain the failures. The tests were run at very slow strain rates, machine limited to 2 inches per minute, but it is assumed that the starting forces measured are indicative of those achieved at impact.

Thirty-three channels of data were collected. Two channels of data, lateral acceleration on the side of the vehicle and the left rear strut strain gage, were lost. The remaining data did record, but the extreme translation of the channels and the high frequency content made the data nearly impossible to interpret and highly suspect in magnitude. The photo coverage had similar disastrous results in that the starting current was not supplied by the portable generator and both cameras failed to photograph the impact.

The vehicle could not be repaired in the field because of the nature of the damage. The need for replacement linkages and some attachment failures had been anticipated, but the vehicle damage was not. The vehicle was returned to Beta Industries, Inc., and no further testing was attempted.

The results of the test were disappointing in that the structural failure did not permit the energy-absorbing landing gear to function as designed.

The skids were later examined, and it was found that the linkages did carry the impact loads without any observable cracks or deformations.

4.6 TRADE-OFF STUDIES

The goal of this phase of the program was to develop an experimental prototype energy-absorbing landing gear system that would demonstrate that a linkage system in series with commercially available energy absorbers would attenuate the impact at various aircraft attitudes and velocities. The results of the test program were inconclusive in that the structural failure of the vehicle bulkheads did not permit an evaluation of energy-absorber response or linkage response for the environments selected. All attachment points of the energy-absorbing system, as well as bearing, rollers, tubes, devices, etc., did survive the impact that occurred. Additionally, test results on the absorber indicated that forces developed did generate the loads anticipated in the energy-absorbing system. Therefore, it was thought reasonable to assume that the size, weight, and strength requirements of a linkage-skid system as developed would provide baseline data for examining the effects of crash parameters on energy-absorbing landing gear of the type tested.

4.6.1 Parameter Selection

There are several parameters to be examined when considering energy attenuation: vertical velocity, drag and side forces, attitude, conventional skid configuration, energy-absorbing landing gear criteria, fuselage structure, and crew seat criteria. The first three quantities directly influence the energy attenuation required in that the velocity, combined forces, and attitudes dictate the strength requirements of the linkages and force levels of the energy absorbers. Inherent in establishing the force levels required is some level of fuselage structural strength required to carry the applied loads. If the fuselage cannot carry the 15G level of the attenuation system at the attachment points, then it is useless to design for 15G force level absorbers.

Another consideration is the conventional skid configuration. A skid designed for 3.5G and 8-foot-per-second impact velocity will absorb a given amount of energy. If these criteria are modified to 5G and 12 feet per second, the energy dissipated is significantly different. Similarly, if the energy-absorbing landing gear system is designed to achieve a force level of 9G instead of 15G with a greater stroke, this also influences the energy balance. Ultimately, the occupants' seats must absorb or transmit the remaining impact energy.

The trade-off problem can become very extensive if all possible combinations of configurations, environments, and energy levels are considered. At one extreme we have a helicopter with conventional skids and no other appreciable crash energy attenuation. At the other extreme we have a vehicle which could have a modified skid, energy-absorbing landing gear, crushable

fuselage, and energy-absorbing seat.

Consider some reasonable parameter variations:

Impact velocity	25, 37.5, 50 ft/sec
Drag force	Does or does not exist
Side force	Does or does not exist
Attitude (pitch only)	0°, 5°, 10°, 15°,
Conventional skids	3.5, 5.0, 7.5, 10.0G 8.0, 12.0, 16.0 ft/sec
Energy absorbing landing gear	50%, 75%, 100% (Percentage of energy to be dissipated) 7.5, 10.0, 12.5, 15.0G (force level to be reached)
Structural strength	3.5, 5.0, 7.5, 10.0G
Seat load limit	7.5, 10.0, 12.5, 15.0G

The total number of possible combinations to be investigated is approximately 111,000. In order to reduce the scope and place the emphasis properly on the energy-absorbing landing gear system, it was necessary to establish a more realistic set of boundary conditions for manual calculations.

At this point it is evident that the crash criteria proposed in Phase II can be tested to determine if modifications can be made, with variations in weight, cost, and performance, which would lead to improved criteria. It is not possible with the current data to establish improved criteria critically considering all aspects of the helicopter (skids, absorber, structure, and seat). However, reasonably accurate estimates can be made concerning the skids and energy-absorbing system.

For the trade-off study, the important parameters are those of the crash environment (velocity, combined forces, and attitude). The levels of these parameters chosen obviously influence the weight, cost, and performance of the helicopter. The weight can be estimated based upon the Phase III hardware design. The cost can be estimated similarly for the skid system and fuselage alterations, and the performance can be estimated based upon the ability of the attenuation system to protect the occupants.

With the input criteria established as 4 parameters having 11 values there are 48 combinations of input conditions. The conventional skids will be assumed to be 3.5G and 8-feet-per-second skids, and 7.5G with 16-feet-per-second. The latter was chosen based upon the result of Reference 40. It will be assumed that the energy-absorbing landing gear will absorb all of the energy that the landing gear skid does not attenuate,

provided that the forces do not generate acceleration levels greater than 15G. The fuselage is a nominal 3.5G fuselage, but this infers a bending capability rather than the level of force that can be carried into the structure. Based upon the data of Reference 40, it will be assumed that the structure has the capability to withstand a 15G whole body acceleration without failing if adequate strength is provided at the structural interface between the skids, the attenuators, and fuselage. The seat load limits indicated were estimates of levels that could be used to initiate energy absorption by the seat. This will only be examined if there is inadequate energy attenuation of the other components. Therefore, the tentative trade-off analysis will consider

Impact velocity	25, 37.5, 50 ft/sec
Drag force	Yes or no
Side force	Yes or no
Attitude (pitch)	0°, 5°, 10°, 15°
Conventional skids	3.5G & 8 ft/sec 7.5G & 16 ft/sec
Energy-absorbing landing gear	100% of unabsorbed energy, if possible
Fuselage strength	As required
Seat attenuation	100% of unabsorbed energy, if possible

This will require approximately 100 variations for the initial examination.

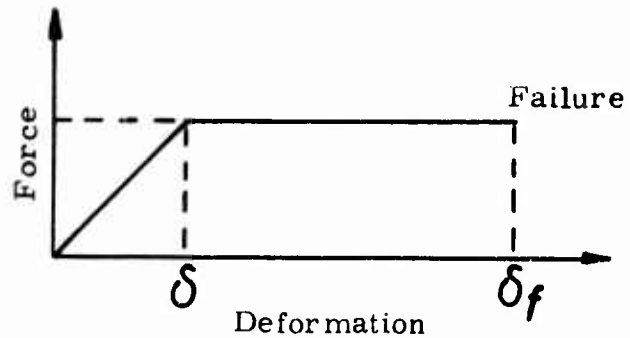
4.6.2 Trade-Off Data Required

4.6.2.1 Conventional Skid

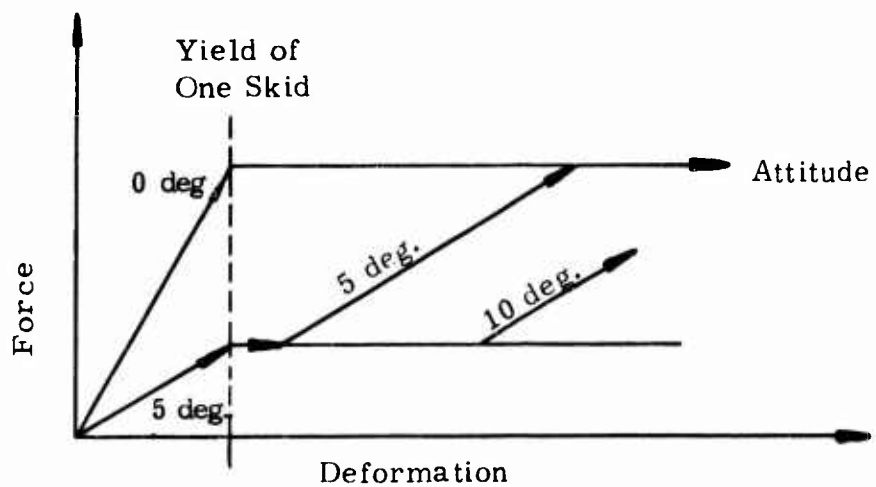
The first item requiring examination is the energy dissipated by the conventional skid as a function of G level, impact velocity, and pitch attitude. From the simplest equation relating impact kinetic energy to elastically stored energy:

$$\frac{1}{2} mv^2 = \eta N \delta \quad (51)$$

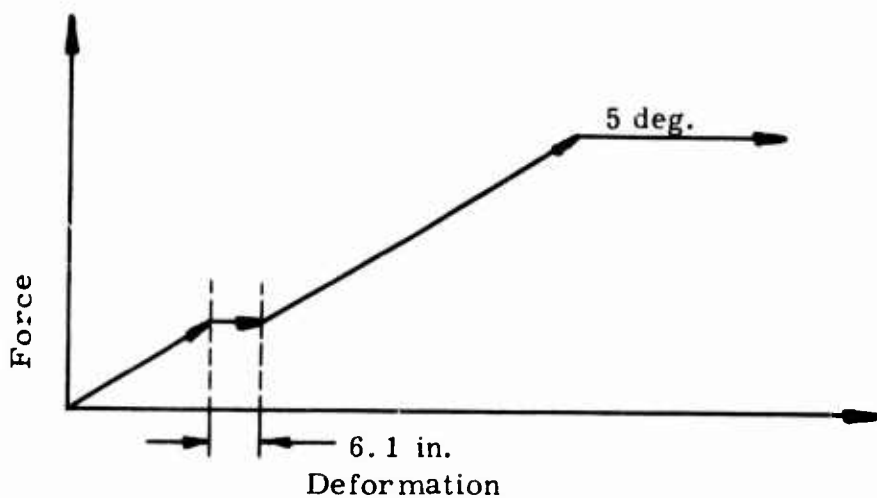
The displacement required to elastically absorb and restore the impact at a 3.5G level is 6.75 inches, which compares quite favorably with the existing skid configuration. If rotor lift is considered, the stroke is 4.92 inches. For a level attitude at impact, the skid response can be idealized as:



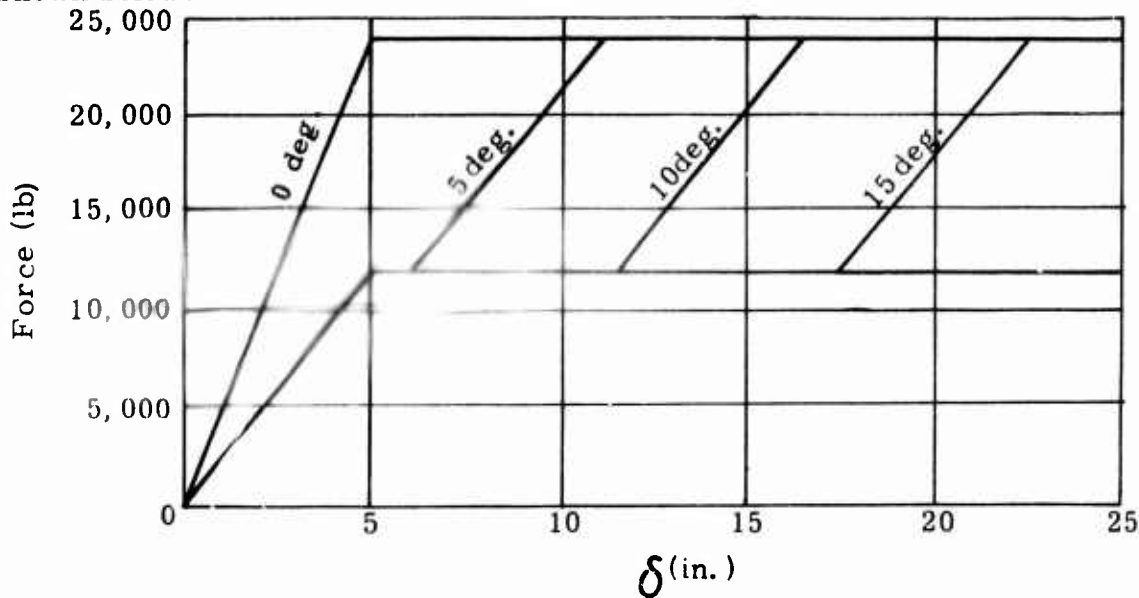
If an attitude exists at impact it is assumed that one set of struts will absorb its energy while the other will not do so until the attitude angle at impact has stroked the vehicle up to the remaining strut. Schematically,



The rear strut strokes as the vehicle descends at a fixed attitude. A span of 70 inches has been assumed as a nominal value. Therefore, the displacement required for a 5-degree impact to initiate the forward strut is $70 \sin(5 \text{ degrees})$ or 6.1 inches. The force-displacement curve developed is



This type of diagram was developed for several types of conventional skids at selected attitudes. The 3.5G and 8-foot-per-second skid curve is shown below.



By integrating beneath the curve, it is possible to calculate the energy dissipated during stroking of the skid system. This is shown in Figure 42. The curve developed is representative of a conventional skid system being compressed at various impact angles and having elastic and plastic deformation. For any stroke and attitude, it is possible to determine from the graph how much energy is dissipated by the conventional skid.

The weight of the skid is more easily determined than the energy capability, since tube failure is dictated by bending strength. Since the design 'G' level dictates a bending moment which requires a particular section modulus, the section modulus was increased in proportion with the 'G'

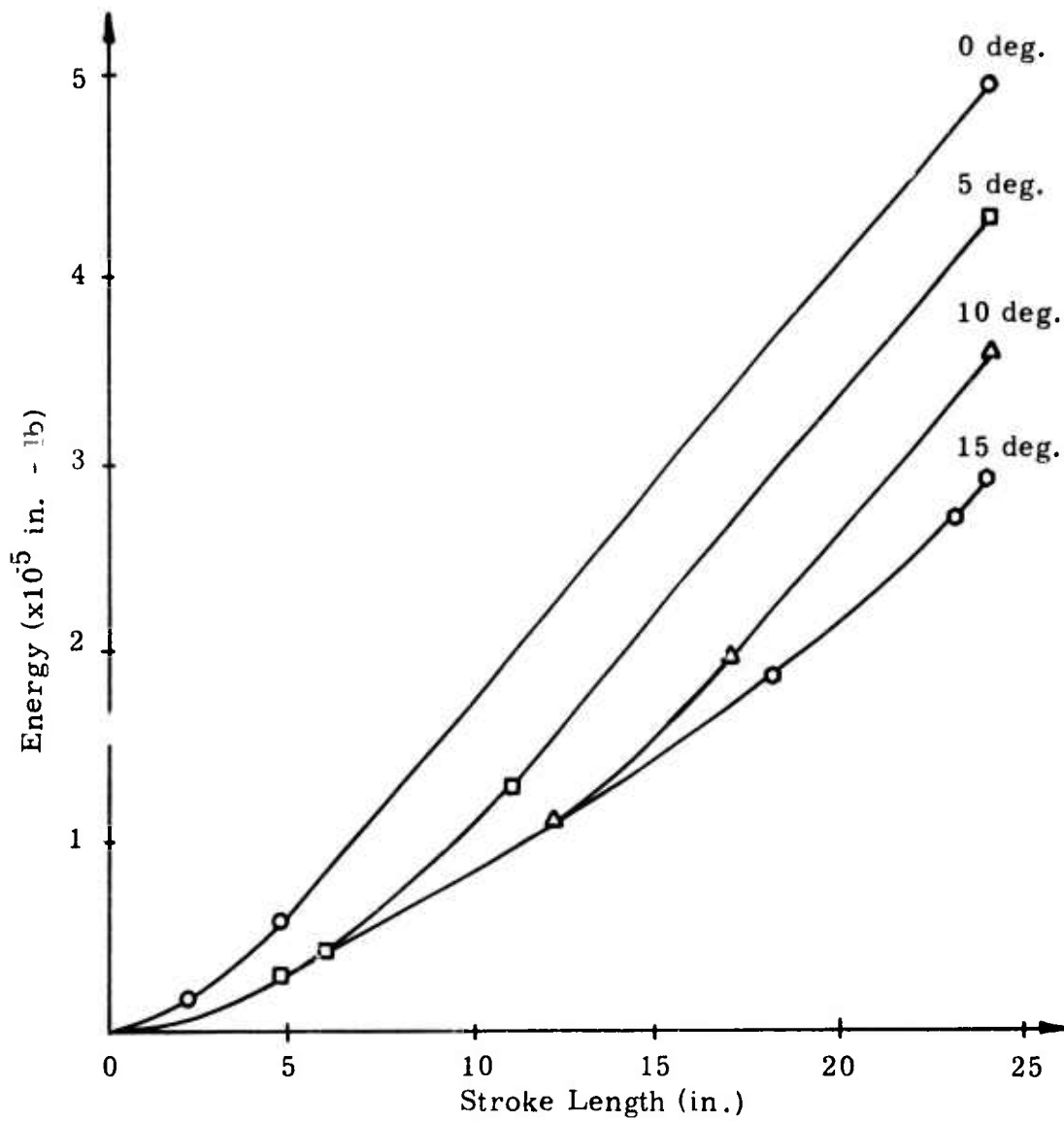


Figure 42. Energy Versus Stroke Length for Selected Attitudes
 $G = 3.5$ and $V = 8$ ft/sec.

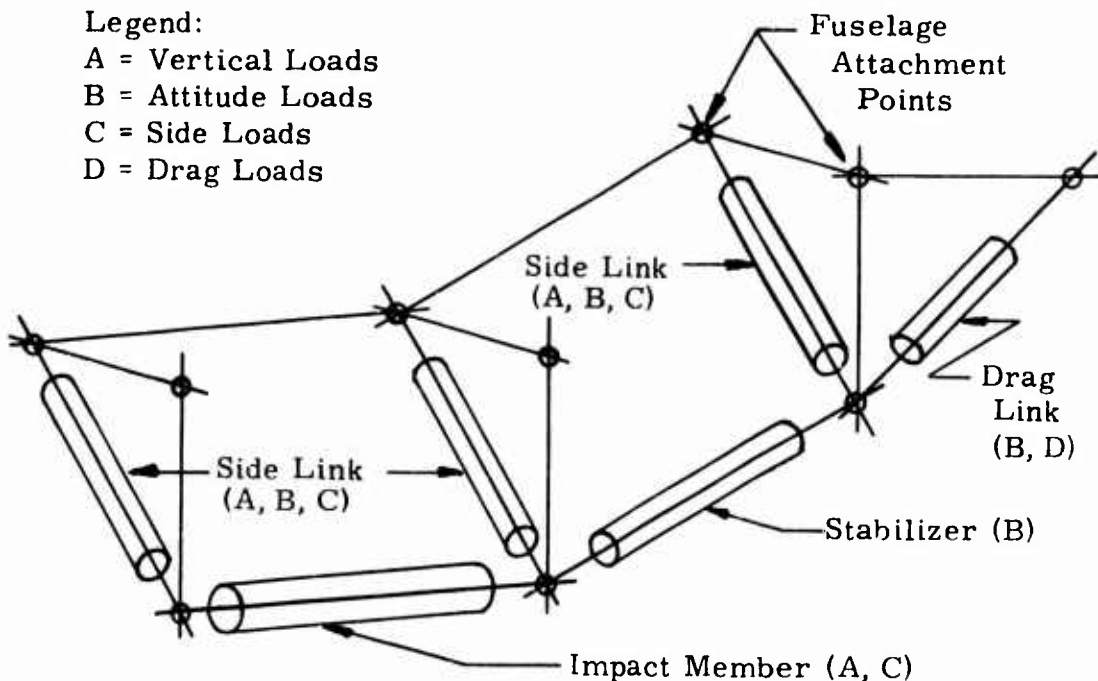
level. The section property of a tube was then found with minimum weight per foot. The skid size was estimated as 27.5 feet of tubing. The resulting skid weight versus design G limit is plotted in Figure 43 and indicates a basic skid weight of 93 pounds.

4.6.2.2 Energy-Absorbing Landing Gear Skid

The energy-absorbing landing gear skid concept used is shown schematically below.

Legend:

- A = Vertical Loads
- B = Attitude Loads
- C = Side Loads
- D = Drag Loads



There are several links, each designed for particular loads. That is, the lower member is always necessary to transmit ground impact into the absorbers for even the side or drag force, level impact condition. The other links are necessary to permit combined forces and attitudes to be attenuated.

The lower crossmember is a pinned-end member that must transmit running loads into the absorbers at the ends. The first question is that of which force levels to consider. If we consider applied forces of 50,000, 100,000, and 150,000 pounds, the fuselage acceleration would be from 10G to 28G when the force is added to a 3.5G conventional skid. These numbers were used to generate the data by calculating the applied loads in the links, that would occur due to 50,000, 100,000 and 150,000 pounds of force at the energy absorbing landing gear lower surface.

The maximum bending moments for vertical, and vertical plus side forces

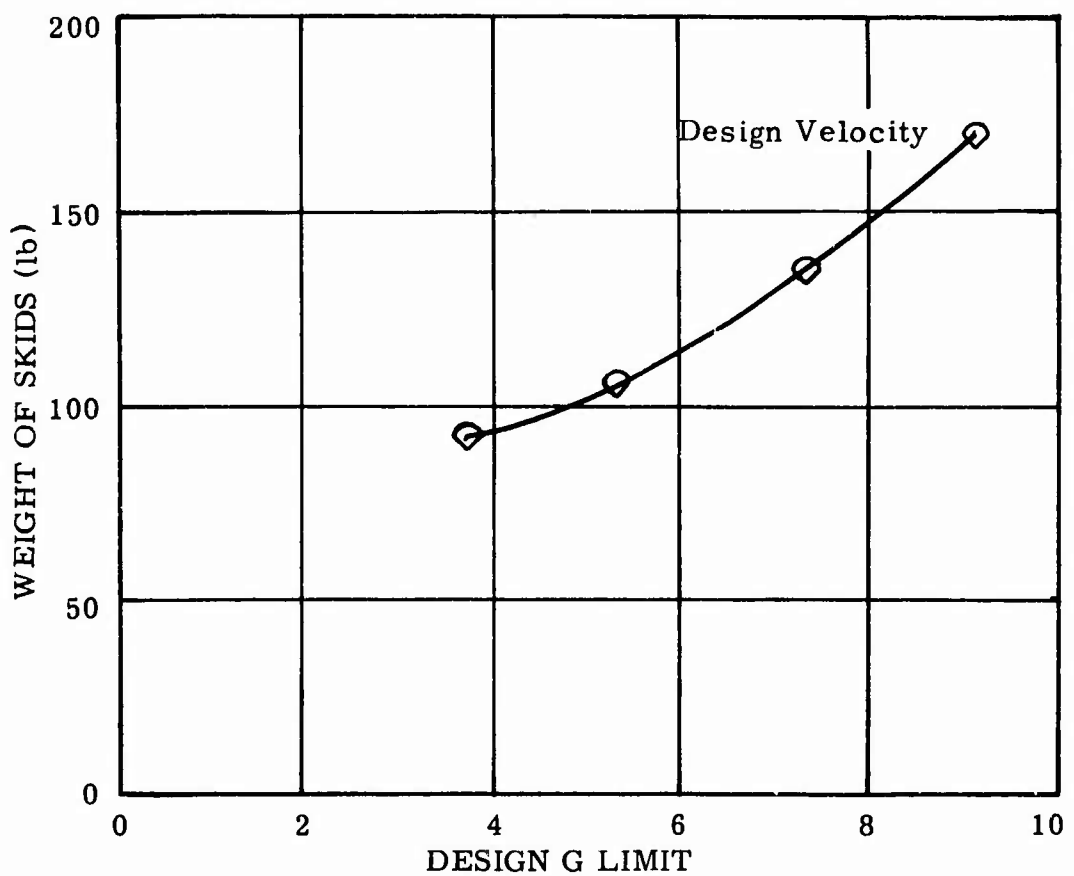


Figure 43. Skid Weight vs. G Limit.

were found and compared with an ultimate stress of 107,000 psi to determine section properties of tubes required. Again, minimum weight sections were found from commercially available stock sizes. The drag load applied axially to the selected tubes did not alter the section properties required enough to consider it necessary to change the weight. The weight requirements would be:

		Total Energy-Absorber Force (lb)		
		50,000	100,000	150,000
		Weight (lb)		
Vertical only		44.2	52.5	63.8
Vertical and side		51.0	63.7	92.6
Vertical, side & drag (weights shown are for both tubes)		51.0	63.7	92.6

The side and drag links would be necessary for at least 10 percent of the vertical force at the energy-absorber attachment point. That is, even if only a vertical impact is considered, some stabilizing members would be necessary. By using the 10 percent figure and the link lengths of the developed concept, it is possible to calculate the column required for a pinned-end configuration. The links required would be:

		Total Energy-Absorber Force (lb)		
		50,000	100,000	150,000
		Weight (lb)		
Side and drag links for vertical only (weight for all links)		3.18	7.78	10.40

If the side links are designed to carry side loads generated by frictional forces, the requirements are quite different. For an assumed 30-inch link that is attached 15 inches beneath the fuselage to the energy-absorber, the axial force in a side link is 8/10 of the force in the energy-absorber. Using the known axial load with a column configuration, the side link and drag links are:

		Total Energy-Absorber Force (lb)		
		50,000	100,000	150,000
		Weight (lb)		
Side & drag links for side & drag forces separately. (weight for all links)		8.10	17.30	25.00

A similar approach for combined loads acting on side and drag links indicates that the axial load generated is greater than the energy-absorber force by a factor of 1.26. The resulting weights are:

Total Energy-Absorber Force (lb)			
	50,000	100,000	150,000
Side & drag links, combined loads (weight/link)	Weight (lb)		
	1.59	3.46	5.20

The end fittings and attachments create an additional weight of approximately 40 percent for the hardware fabricated. This approximates the 100,000 pound force data; and hence, a 20,40,60, percent additional weight penalty was applied to the links for the force levels assumed. These are consistent with the ratios of the structural weights of the links.

By tabulating the four various configurations possible for the vertical impact only, the curves of Figure 44 were developed. For each configuration, two lower links, four side links, and four drag links are included. These are plotted against the force levels of the energy-absorber system. The acceleration felt by the fuselage would be generated by the assumed energy-absorber system and skids. Consequently, if the fuselage is "designed" later for 15G, the energy absorbers and conventional skid will both contribute to the total vehicle force required.

The curve generated was indicative of a vertical impact with or without side and drag forces assuming that the linkages necessary were provided at the energy-absorber attachments.

If the attitude is to be considered, additional structure is required. Stabilizing links are added to provide a means of distributing the impact forces, at up to 10 degrees of pitch, into the energy absorbers at both ends. The link between them is designed for calculating the maximum bending moment generated and calculating the tubular section required.

The size of the stabilizing link depends upon the attitude used as a design condition. A given attitude causes the conventional skid to absorb different amounts of energy. Assuming the conventional 3.5G, 8-foot-per-second skid, the energy dissipated at various attitudes was found and subtracted, and force estimates were made for the attenuators required for attitude attenuation. The forces dictate a particular center of pressure on the link, and from this the applied bending moment and bending stress are calculated. For impacts normal to the stabilizing link, the data are:

Total Energy-Absorber Force (lb)			
Attitude	50,000	100,000	150,000
5°	12.00	19.34	22.80
10°	14.78	22.80	28.71
12.5°	14.78	25.63	31.17

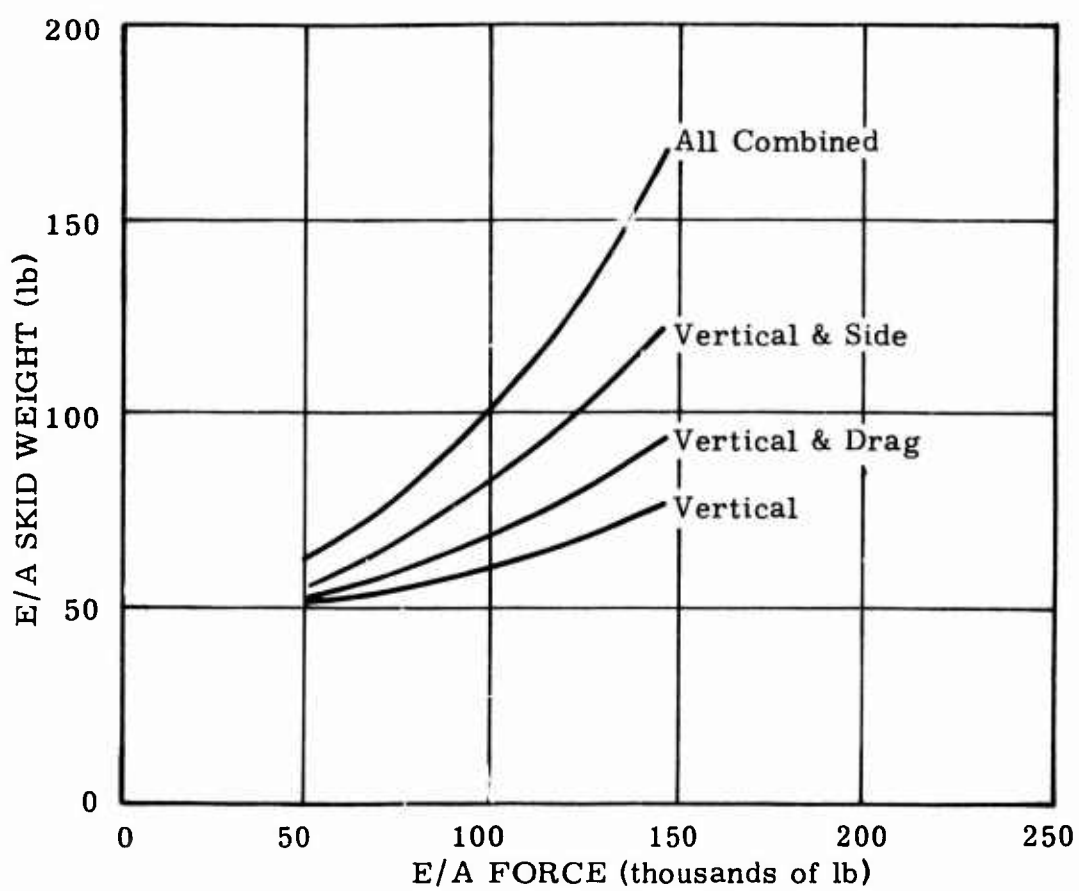


Figure 44. E/A Skid Weight vs. E/A Force (Total).

The addition of side forces due to friction generate:

Attitude	Total Energy-Absorber Force (lb)		
	50,000	100,000	150,000
5°	14.78	22.80	28.58
10°	17.35	28.58	36.72
15°	20.50	31.17	47.20

The entire assembly must have interface structure that permits the freedom of fore and aft motion within the lower skid. The tube required to permit a sliding motion (one tube within the other) is designed to carry the end moments of lower skid into the energy-absorber pivot point. The additional weight is:

Total Energy-Absorber Force (lb)	50,000	100,000	150,000
Weight (lb)	15.24	25.54	29.11

The additional weight required because of attitude requirement was determined by adding the tube interface hardware, stabilizing links, and side links for the selected combined load conditions. The drag links were not added because of their previous inclusion in the pure impact configuration. Figure 45 provides the summed data.

It is possible to obtain an estimate of the accuracy of these curves based upon the fabricated structure. For a 15G design with conventional skids, a vertical impact at 25 feet-per-second will require an energy-absorber force of approximately 75,000 pounds. From Figure 44, this requires 87 pounds of structure. The attitude of 10 degrees dictates 107,500 pounds of energy-absorber force and an additional 185 pounds for a total of 272 pounds. The measured weight was 440 pounds, or 62 1/2 percent higher than calculated. At this point all components were reviewed, and the calculated and measured design criteria were compared. The data show that all items are consistently 60 percent low. The end fittings, bearings, washers, bolts and specially machined parts contribute the difference between the ideal calculated for an element, and the practical hardware with appropriate attachments. The main bearings weigh 2 pounds apiece, tie rod ends weigh approximately 1 pound apiece, and the end fittings at each main bearing weigh 8 1/2 pounds. Consequently, although the structural elements were in agreement with fabricated hardware for the one set of criteria (tubing and joint structure), the end fittings and associated hardware contributed a considerable amount of weight. Since the same increment was apparent in all elements, the weight estimate curves were adjusted by adding a 60 percent factor to each curve shown in Figures 44 and 45.

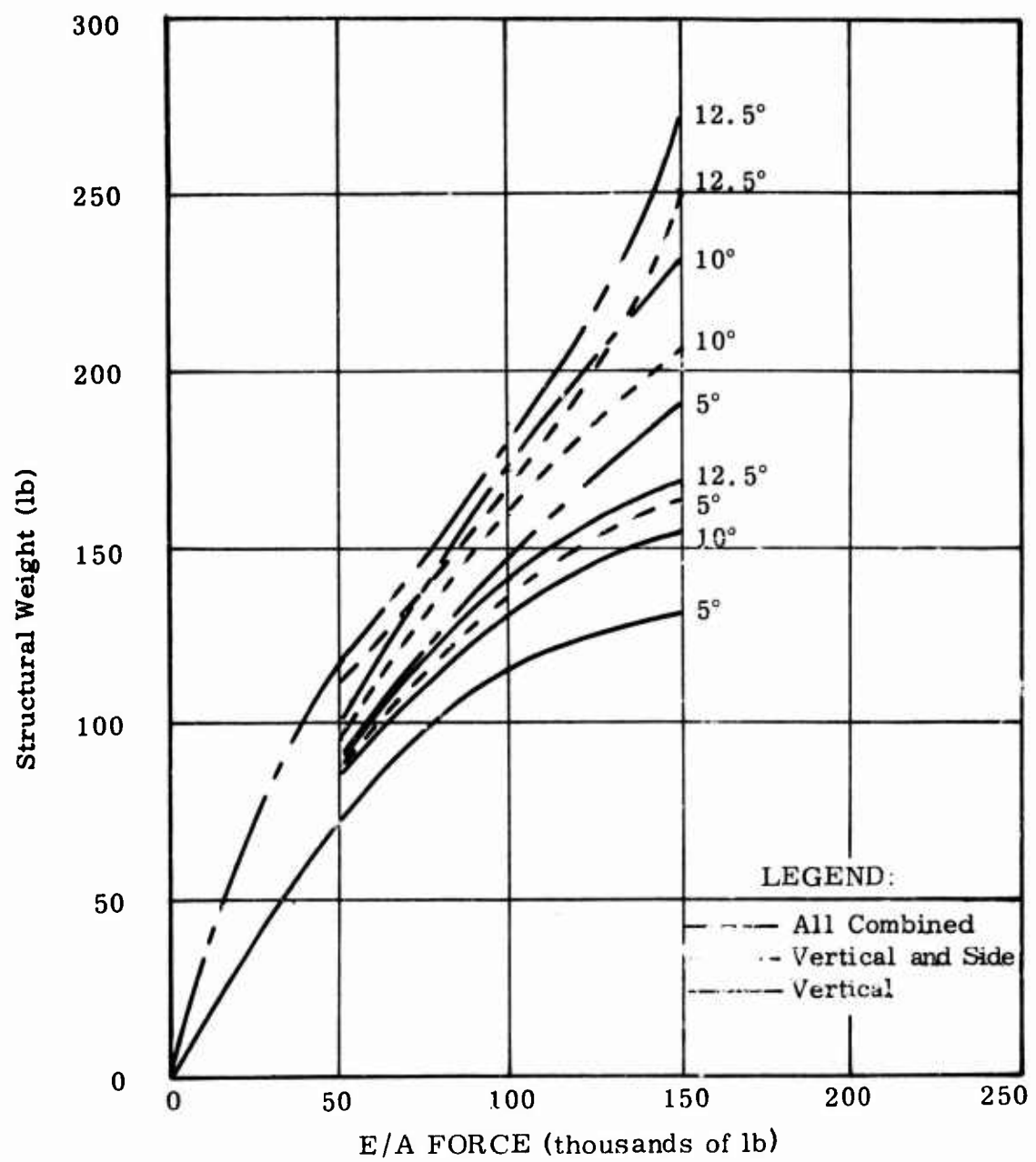


Figure 45. E/A Force (Total on Added Structure) vs. Structural Weight.

4.6.2.3 Energy-Absorber Weight

Data were collected from ARA Products data sheets and translated into parameter curves indicating SEA as a function of force and stroke required (see Figure 46).

4.6.2.4 Structural Weight of Fuselage

To obtain an estimate of the structural weight of the fuselage necessary for improved criteria, it was assumed that an estimated fuselage floor weight could be calculated and compared with measured data to establish a baseline condition.

The floor of the UH-1 was approximated by 4 shear beams of 12-inch height. The center of gravity for the 6600-pound condition is 1/5 of the distance between the skids and causes a maximum shear and bending moment of 42,200 pounds and 590,000 inch-pounds at ultimate load. Assuming a semimonocoque approximation

$$f_s = \frac{V}{ht} = 30,000 \text{ psi allowable} \quad (52)$$

$$f_b = \frac{My}{I} = 75,000 \text{ psi allowable} \quad (53)$$

From the data, the shear web thickness is 0.117 inch and the cap area is 0.184 square inch. The 4 beams assumed would then result in a floor weight of 131.3 pounds. Since this is for an 8.0G ultimate (3.5G x 1.5 factor of safety x 1.5 ultimate to yield), this implies a weight of 16.4 pounds per G.

As a check on the assumed structure, it was assumed that the crush strength of the fuselage would be inferred by the buckling strength of compression panels. For a 12-inch-deep panel with fixed edges and a thickness of 0.117 inch, the buckling stress is⁴¹

$$\sigma_{ct} = KE \left(\frac{t}{b} \right)^2 \quad (54)$$

where K is the buckling coefficient of the panel and the value of 6.35 is used. This is the asymptotic minimum value for a fixed-edge plate.

E is the modulus of elasticity of aluminum

t is the panel thickness

b is the minimum panel dimension

$$\sigma_{ct} = 6,030 \text{ psi}$$

or for the 0.117 inch thickness,

LEGEND
Specific Energy Absorption
(inch/lb /lb)

A - 3660	F - 9560
B - 4460	G - 11700
C - 4750	H - 14600
D - 5930	I - 17900
E - 7120	

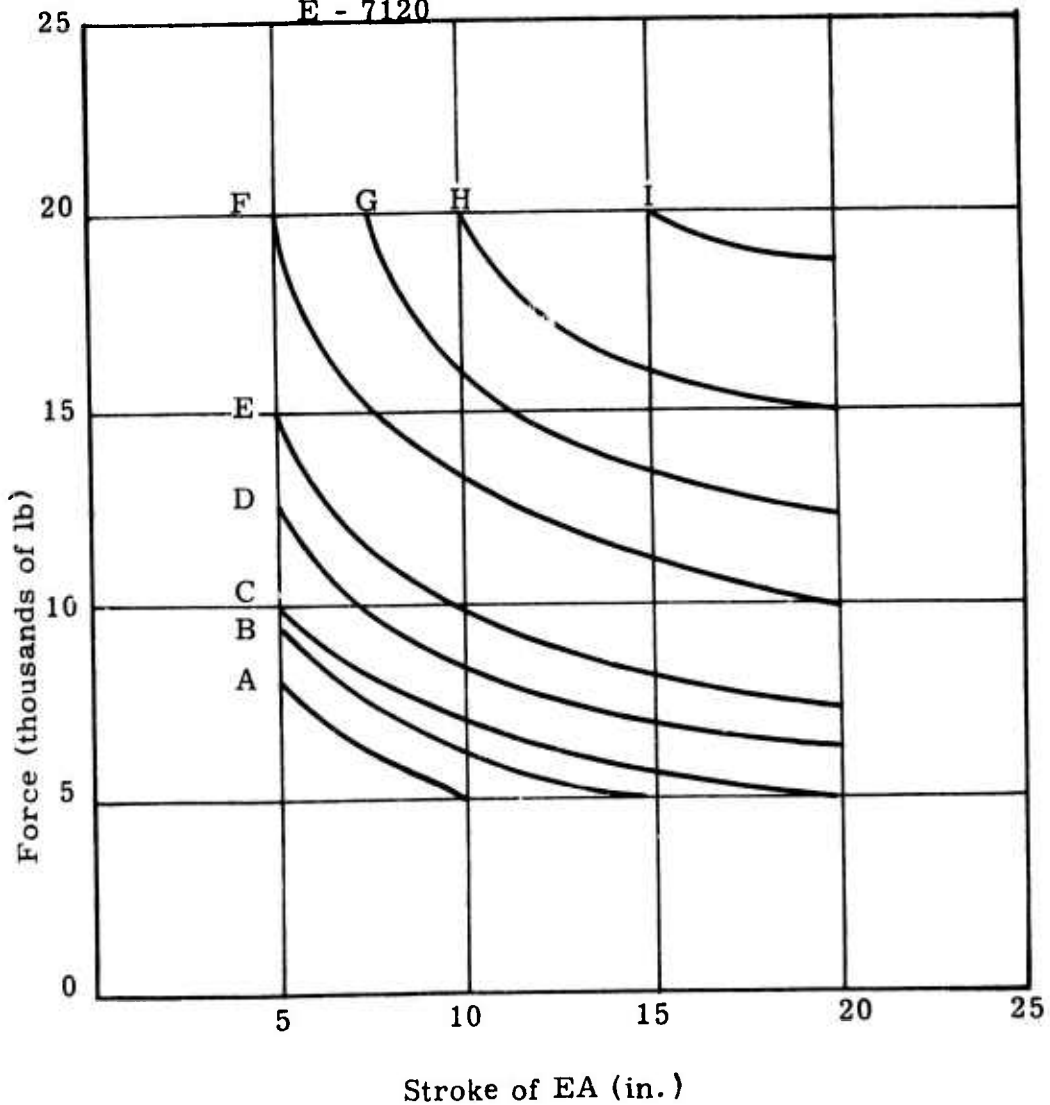


Figure 46. EA Force vs. Stroke.

$$q_{ct} = 706 \text{ pounds/inch}$$

For the assumed 4 beams of 70 inches, the crushing force of the fuselage would be 197,000 pounds. Reference 40 lists the crush strength as 22G for a 9,180 pound vehicle, or 202,000 pounds. It was therefore assumed that the weight estimate calculated indicates the additional weight required to strengthen a fuselage from the given 3.5G design level in bending up to any other level.

4.6.2.5 Seat Structure and Attenuators

The seat must attenuate any tendency for the seated man to exceed 15G. At the instant that the vehicle has dissipated as much energy as the skids will permit, a given amount of impact velocity remains. The seat and man must dissipate the energy dictated by that velocity in stroking a seat absorber. The weight of the seat will be dictated by the energy-absorption capability of the seat unit. That is, for the absorber there is a particular value and for the structural system that supports it another value which can be used to relate unit requirements to overall weight increase.

If 15G is developed by a 200 pound man (the 50th percentile plus 30 pounds of equipment and clothing), and an arbitrary 20-pound crew seat, the 3,300-pound force level dictates a minimal weight unit for 10 inches of stroke (specifically, a 13-pound unit with an SEA of 3,660 inch-pounds per pound). From the previous efforts using larger units, it is possible to evaluate the SEA applicable for seat structure added and absorber.

Vertical attenuation by the energy-absorbing landing gear required units with an SEA of 5,900 inch-pounds per pound. The weight of energy absorbing landing gear skid structure required to dissipate the vertical impact energy of 4.55×10^5 inch-pounds was 144 pounds, or an SEA of 3,160. Without additional data, it will be assumed that the ratio of structural weight to absorber weight will be constant and can be used for any absorber required. Hence, the energy to be dissipated is evaluated, a stroke is calculated, and the weight is calculated using a value of $(3160/5900 \times 3660)$, 1950 inch-pounds per pound for the structure. A 25-foot-per-second impact dissipated at 15G for the above weight would require 8.2 inches of stroke and a weight of 26.2 pounds. Hence, a weight of 26.2 pounds is required to provide the seat structure, energy-absorber attachment points, guides, structural interface, etc., in order to sustain 15G with a 200-pound payload.

4.6.3 Calculation Techniques and Resulting Data

The trade-off values were calculated by using a tabular approach which leads from initial criteria to total weight, acceleration response, and DRI, if applicable. The blocks of Figure 47 show the operations that were used to generate the required data.

I. Input Criteria

1. Vertical impact velocity $V_z =$ _____
2. Drag forces present Yes _____ No _____
3. Side forces present Yes _____ No _____
4. Attitude of pitch axis $\theta =$ _____
5. Fuselage height above ground at impact $\delta =$ _____
6. Vertical energy $E = 10.2V_z^2, E =$ _____

II. Conventional Landing Gear

1. Select configuration
Design acceleration $G_{LG} =$ _____
Design impact velocity $V_{LG} =$ _____
2. Calculate force $F_{LG} = 6600 G_{LG}$ $F_{LG} =$ _____
3. Calculate stroke of landing gear $\delta_{LG} =$ _____
Plastic stroke $\delta_{LGP} = 56_{LG}$ $\delta_{LGP} =$ _____
4. Calculate weight of landing gear $W_{LG} =$ _____
5. Calculate energy dissipated at δ $\delta < \delta_{LG}$ $E_{LG} =$ _____
6. Calculate remaining energy $E_{R1} = E - E_{LG}$ $E_{R1} =$ _____

IV. Attitude Requirement

1. Calculate energy of conventional skid at θ and δ $E_{\theta S} =$ _____
2. Calculate energy remaining $E_{\theta EA} = E - E_{\theta S}$ $E_{\theta EA} =$ _____
3. Calculate energy to be carried by absorbers $E_{\theta A} = P_{EA} \cdot E_{\theta EA}$ $E_{\theta A} =$ _____
4. Subtract contributions due to vertical attenuators $F_{\theta} = F - F/EA \cdot 2$ $F_{\theta} =$ _____
 $E_{\theta} = E_{\theta A} - E/EA \cdot 2$ $F_{\theta}/EA =$ _____
5. Calculate stroke required $E_{\theta} =$ _____
 $E_{\theta}/EA =$ _____
 $\delta_{\theta} = EA$ $\delta_{\theta} =$ _____
6. Assume same stroke as vertical, δ_{EA}
find $F_{\theta R}$ force required $F_{\theta R}/EA =$ _____
7. Calculate energy absorber weight $\Delta W_{\theta} =$ _____
8. Calculate system weight $\Delta W_{\theta S} =$ _____

V. Seat Structure

1. Calculate velocity change available $E_{R3} = 10.20 (\Delta V)^2$ $\Delta V =$ _____
2. Calculate incremental DRI $\Delta DRI =$ _____
3. Select peak acceleration $G_S =$ _____
4. Calculate force of seat $F_S = 250 G_S$ $F_S =$ _____
5. Calculate energy of seat $E_S = 389 (\Delta V)^2$ $E_S =$ _____
6. Calculate stroke required $\delta_S =$ _____
7. Calculate weight of seat E.A. $\Delta W_{SEA} =$ _____
8. Calculate weight of seat and structure $\Delta W_{SS} =$ _____

Figure 47. Calculation Procedure.

B

Conventional Landing Gear

Select configuration

Design acceleration

Design impact velocity

$$G_{LG} = \underline{\quad}$$

$$V_{LG} = \underline{\quad}$$

Calculate force

$$F_{LG} = 6600 G_{LG}$$

$$F_{LG} = \underline{\quad}$$

Calculate stroke of landing gear

$$\text{Plastic stroke } \delta_{LGP} = 55_{LG}$$

$$\delta_{LG} = \underline{\quad}$$

$$\delta_{LGP} = \underline{\quad}$$

Calculate weight of landing gear

$$W_{LG} = \underline{\quad}$$

Calculate energy dissipated at δ

$$\delta < \delta_{LG}$$

$$E_{LG} = \underline{\quad}$$

Calculate remaining energy

$$E_{R1} = E - E_{LG}$$

$$E_{R1} = \underline{\quad}$$

Seat Structure

Calculate velocity change available

$$E_{R3} = 10.20 (\Delta V)^2$$

$$\Delta V = \underline{\quad}$$

Calculate incremental DRI

$$\Delta DRI = \underline{\quad}$$

Select peak acceleration

$$G_S = \underline{\quad}$$

Calculate force of seat

$$F_S = 250 G_S$$

$$F_S = \underline{\quad}$$

Calculate energy of seat

$$E_S = 389 (\Delta V)^2$$

$$E_S = \underline{\quad}$$

Calculate stroke required

$$\delta_S = \underline{\quad}$$

Calculate weight of seat E.A.

$$\Delta W_{SEA} = \underline{\quad}$$

Calculate weight of seat and structure

$$\Delta W_{SS} = \underline{\quad}$$

III. Energy Absorbing Landing Gear

1. Select percent of energy to be dissipated

$$P_{EA} = \underline{\quad}$$

$$E_{EA} = P_{EA} \cdot E_{R1}$$

$$E_{EA} = \underline{\quad}$$

2. Calculate energy per absorber

$$E_{EA}/4$$

$$E_{EA} = \underline{\quad}$$

3. Select peak force to be carried by the structure

$$F = \underline{\quad}$$

4. Calculate force carried by energy absorbers

$$F_{EA} = F - F_{LG}$$

$$F_{EA} = \underline{\quad}$$

5. Calculate force per energy absorber

$$F_{EA} = \underline{\quad}$$

6. Calculate stroke of energy absorber

$$\delta_{EA} = \underline{\quad}$$

7. Calculate weight/EA and total weight

$$W_{EA} = \underline{\quad}$$

8. Calculate weight of energy absorbing system structure

$$W_{EAS} = \underline{\quad}$$

9. Calculate Remaining Energy

$$E_{R2} = E_{R1} - E_{EA}$$

$$E_{R2} = \underline{\quad}$$

VI. Fuselage Structure

1. Select fuselage design acceleration $G_{ST} = \underline{\quad}$

2. Calculate force level

$$F_{ST} = 6600 G_{ST}$$

$$F_{ST} = \underline{\quad}$$

3. Select limiting stroke to "bottom" structure

$$\delta_{ST} = \underline{\quad}$$

4. Calculate energy absorbed

$$E_{ST} = \underline{\quad}$$

5. Calculate residue $E_{R3} = E_{R2} - E_{ST}$

$$E_{R3} = \underline{\quad}$$

6. Calculate incremental weight penalty

$$\Delta W_{ST} = \underline{\quad}$$

The input criteria are selected to initiate a weight calculation. The vertical velocity at impact was, for example, 25 feet per second. If a lateral or longitudinal velocity existed, there were side or drag forces. The attitude originally assumed was 10 degrees. The fuselage is assumed to be 20 inches above the ground at impact. The total energy available is the kinetic energy of the entire vehicle.

The conventional landing gear energy-absorption characteristics have been calculated as functions of pitch attitude. For a selected skid, the elastic stroke is determined in order to be certain that the skid deforms plastically as much as the clearance between ground and fuselage. It is desired that the skid not rupture. If the skid does deform plastically over the range desired, the energy obtained is subtracted from that available to determine the portion available for energy-absorbing skids and seat energy absorbers. The weight of the skid comes from previously plotted data. The vertical impact data is calculated first in order to determine the energy absorbers required for vertical impact only. The energy absorbers determined for vertical attitudes exist for any attitude criteria specified and are supplemented by those required for attitude effects.

The energy-absorbing landing gear can have any arbitrary percent of remaining energy to be dissipated. Since the system is a 4 energy absorber system, the total remaining energy is divided by 4 to evaluate one unit. If the structure is to carry a given G level, the force the energy-absorbing system carries is in parallel with the conventional skid and must be accounted for. Knowing the force level and energy, the stroke is calculated to determine its acceptability. The weights of energy absorbers and skid structure are evaluated, one from SEA, the other from plotted data.

At this point the effects of attitude are evaluated. The energy dissipated by the conventional skid at a particular attitude is subtracted from the total to determine energy remaining. Since the vertical energy-absorption characteristics are known, the force and energy required by the "attitude" attenuators are calculated. The additional weight is taken from the plotted attitude weight increment curve.

The fuselage structural segment was not used since it was determined that the fuselage does not contribute significant energy absorption because of the fuselage strengths examined. However, an incremental weight penalty is required in going from the 3.5G bending criteria to any other level.

The seat structure is subjected to any input energy as an impulsive input. From the remaining energy at fuselage impact, it is possible to calculate the impact velocity. Each seat must dissipate the energy generated by the mass of occupant and seat. It was assumed that a 15G level was desirable since this should limit the DRI to a level of 18. The stroke, weight of the energy absorber, and structure are calculated using SEA values.

The results of several calculations for the 25-foot-per-second impact with conventional skid landing gear are shown on Figure 48. Six configurations were considered: energy-absorbing capability in the seats alone, energy-absorbing landing gear system alone, and a system wherein half of the energy was absorbed by the energy-absorbing landing gear and the remainder by the seats. Each of these was then examined for both vertical impacts only and combined loads.

4.6.4 Trade-Off Data Analysis

The data indicate that for the Phase III UH skid type energy-absorbing landing gear and the parameter values assumed, the 25-foot-per-second impact can best be attenuated by the seats alone if weight penalty is the only criterion. It can also be shown that the use of a stiffer landing skid creates even greater weight penalties.

Additional curves were generated for the remainder of the velocity, landing gear, attitude variations as compiled in Figure 49. There are several significant points of interest to be considered:

1. The curves are shown as functions of skid landing gear type (3.5G, 8 ft/sec, & 7.5G, 16 ft/sec) and attitude at impact. The curves are for minimum weight configurations. The minimum weight landing gear system to attenuate a 37.5-foot-per-second impact at 0 degrees is 370 pounds.
2. The detailed calculations indicate that all points at 25 ft/sec are for seat energy absorption only. No configuration of skid and energy-absorber system, with or without combined loads, has a lesser weight than seat energy absorption alone. At 37.5 ft/sec, the minimum weight is achieved by having an energy-absorbing landing gear system absorb as much as possible, limited by an assumed 15G fuselage and 15-inch stroke, and the remainder absorbed in the seat. At 50 feet-per-second, both energy-absorbing landing gear and energy-absorbing seats (12 inches of seat stroke) are required and cannot keep the DRI level below 22, which corresponds to approximately a 50-percent probability of spinal injury.

One of the prime objectives of the trade-off study was to quantitatively evaluate the effect of crash criteria upon energy-absorbing landing gear design. This is now partially possible in that we have data relating weight, simplicity, and performance for one particular design. The design and weight of the landing gear system is a function of impact velocity, attitude, type of conventional skid, and application of combined load.

As a gross approximation, the end points of the curves of Figure 49 were examined as if linearly related. That is, it was assumed that the weight curves are linearly related between 25 and 50 feet per second. If

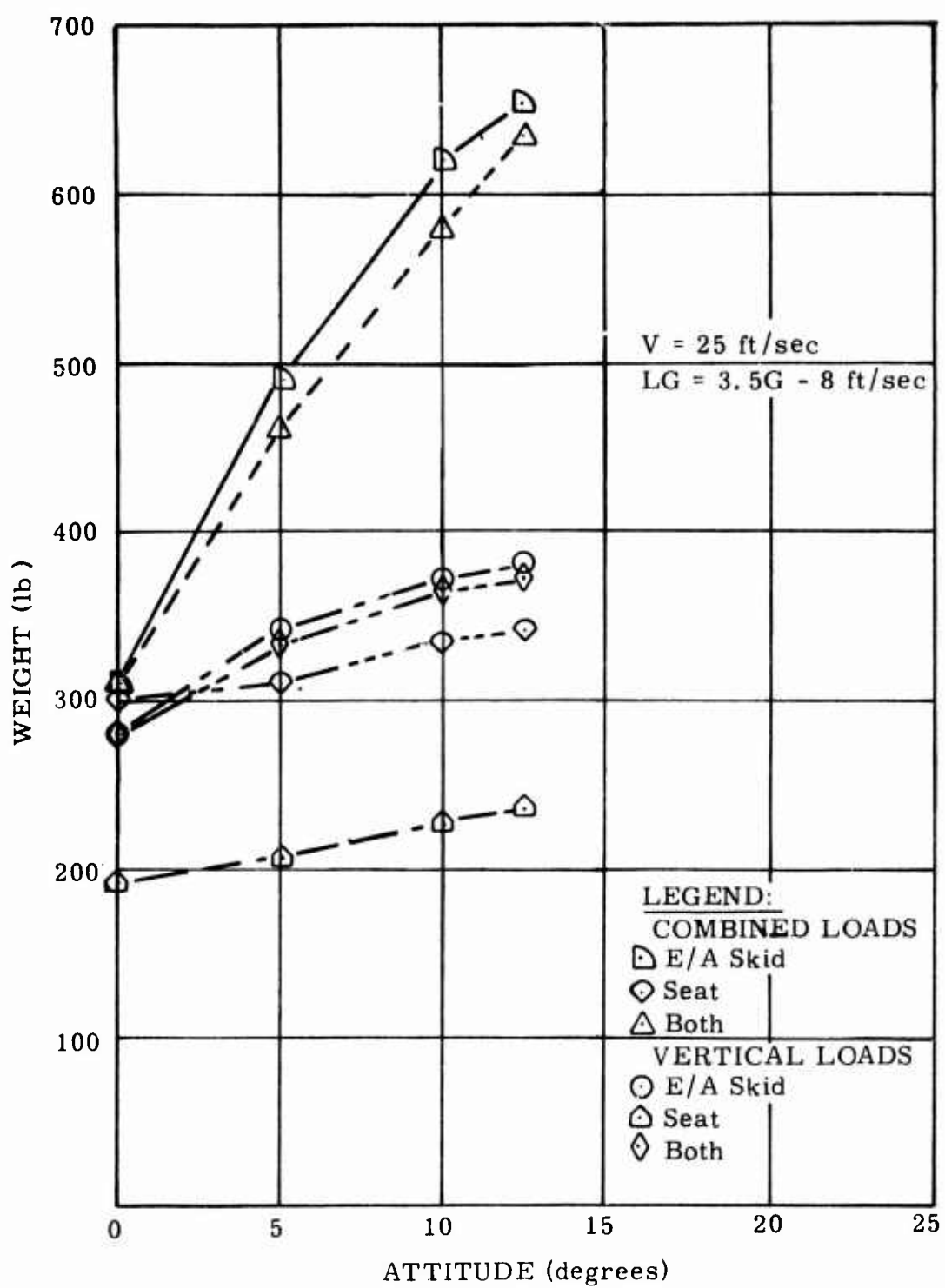


Figure 48. Weight Variations vs. Attitude.

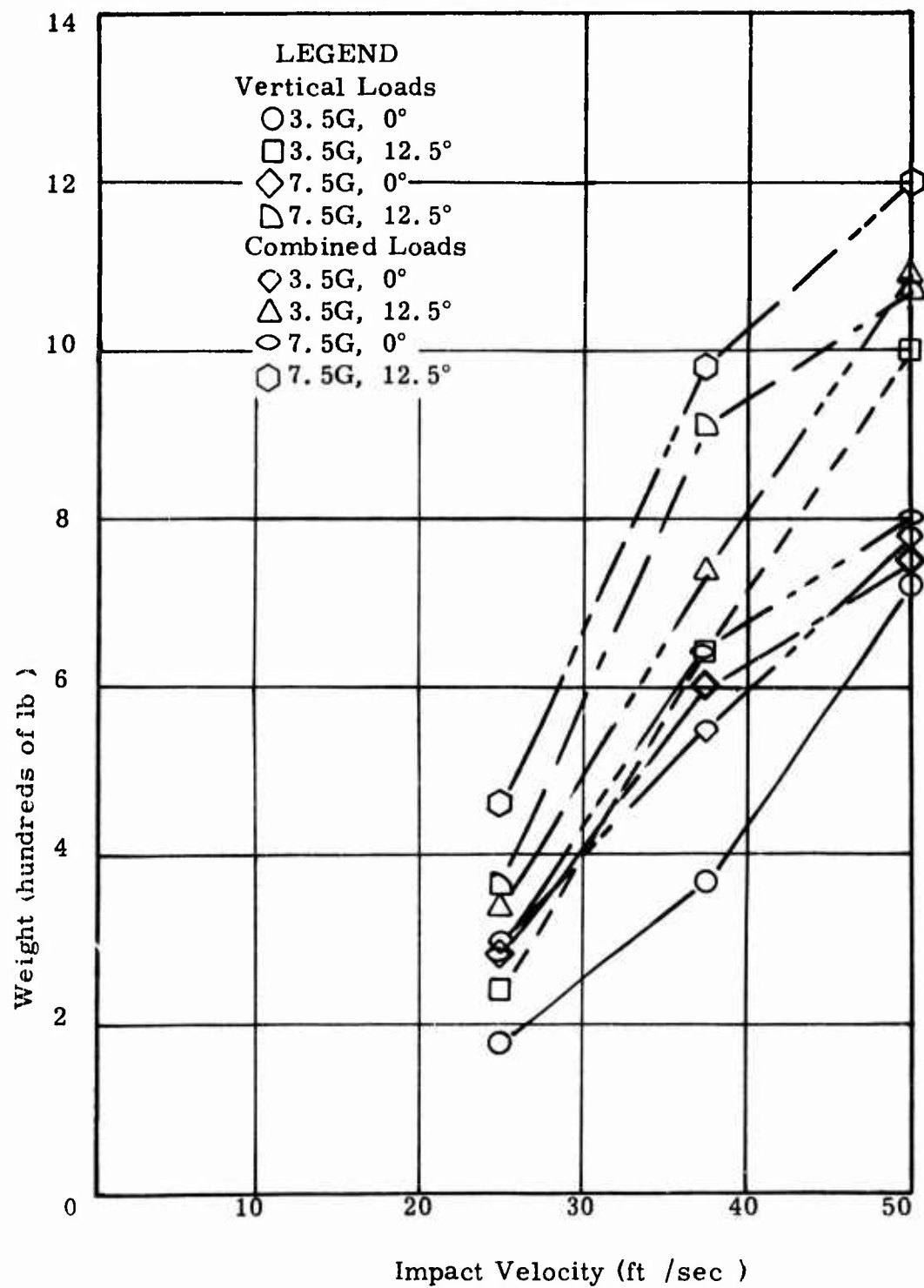


Figure 49. Weight Variations of Minimum Weight Systems.

this were true, then the skid configuration and addition or deletion of combined loads would result in a variation of approximately 20 pounds per degree of attitude over the entire velocity range:

$$\frac{\Delta W}{\Delta \theta} = 20 \text{ lb/deg.}$$

Similarly, if we examine the dependence upon velocity constant values of skid type and attitude,

$$\frac{\Delta W}{\Delta V} = 20 \text{ lb/ft/sec}$$

The effects of adding combined loads and increased skid strength are both approximately 110 pounds. Therefore, the minimum weight landing gear system has a weight of

$$W = W_0 + 20 (\Delta V) + 20 (\Delta \theta) + 110 (\Delta C) + 110 (\Delta G) \quad (55)$$

where W = landing gear system weight

W_0 = a reference weight which is that of a 3.5G skid designed for 0 degrees of attitude

ΔV = the incremental impact velocity over 25 feet per second

$\Delta \theta$ = the attitude angle

where ΔC and ΔG have values of 0 or 1 depending upon the existence of a combined load or stiff skid.

If the system is to be designed for minimum weight, it is reasonable to assume that a stiffer conventional skid will not be used. Additionally, it is quite probable that combined loads will exist since they are created either by velocity components or attitudes at impacts. The attitude may be vertical at impact, but there will probably be some drifting to generate lateral and longitudinal loads. With these assumptions, the equation reduces to a variation of weight with respect to velocity and attitude as shown in Figure 50.

The weight is shown as percent of aircraft design weight, 6,600 pounds. Hence, for 25 feet per second and a horizontal attitude, the weight of the system is about $(.05) \times (6,600)$ or 330 pounds.

Several other parameters are also shown in Figure 50. A limit for energy-absorbing landing gear is shown as 31 feet per second. For the stroke and height above the ground assumed for a utility class vehicle, an energy-absorbing landing gear can attenuate an impact up to only 31 feet-per-second without exceeding a DRI of 18. This would require failure of the

LEGEND

- Haley, J. L., NATO/AGARD Paper 3 (Ref 41)
- Turnbow, J. R., USAAVLABS-TR-70-22 (Ref 1)
- △ Carr, R. W., and Phillips, N. S., NADC-AC-7010 (Ref 28)
- ◇ Rich, M. J., SAE Paper 680673 (Ref 21)

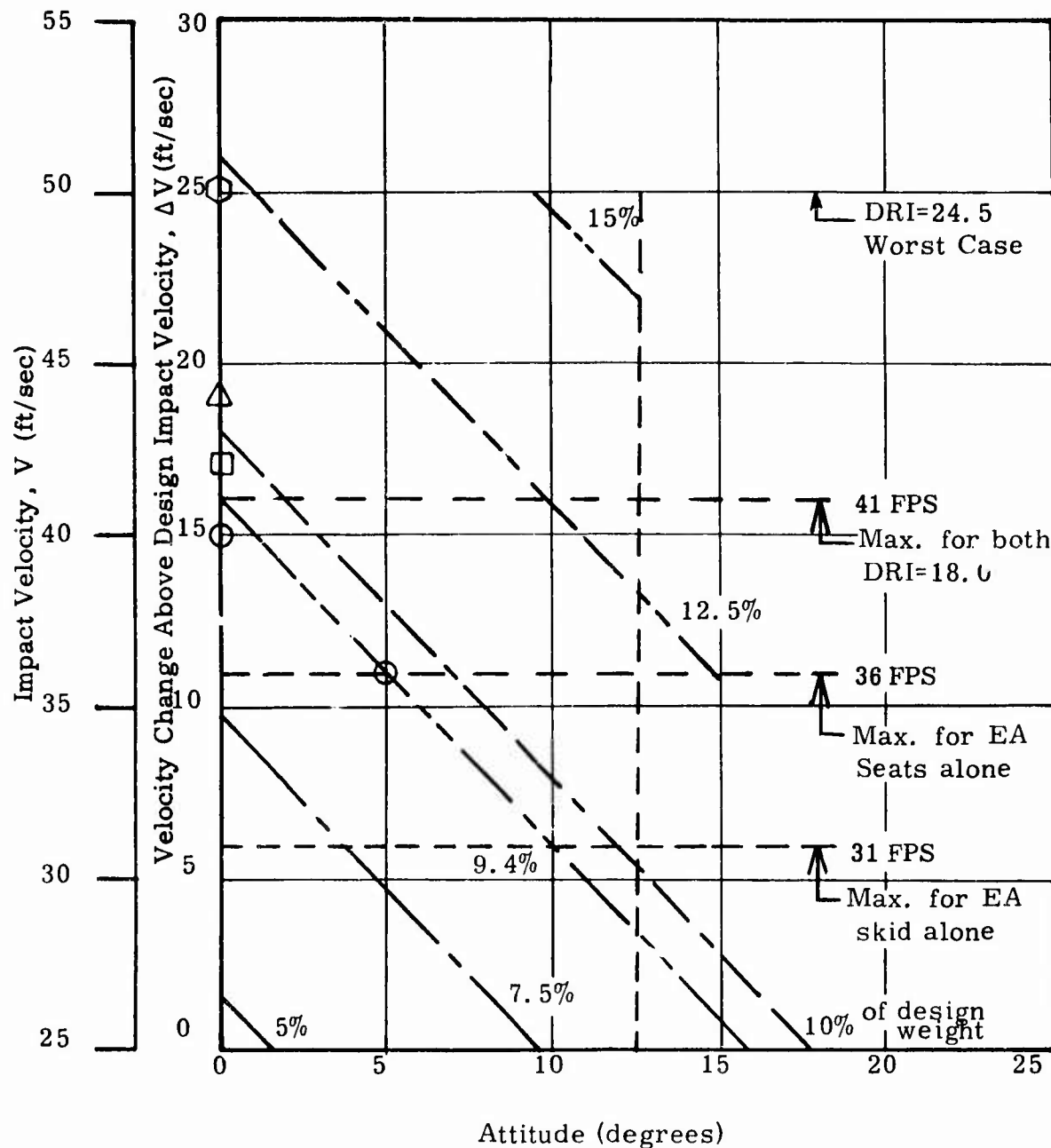


Figure 50. Weight Penalty vs. Velocity and Attitude.

conventional skid and would stroke the energy absorbers, but would not permit the fuselage to impact. For an impact of 36 feet-per-second, the limit for seat energy absorbers only, the conventional skid fails, the fuselage impacts, and the seats crush 12 inches. Both energy absorbing landing gear and seats will permit impacts up to 41 feet-per-second with failure of skids, energy absorbers, and seats. At the ultimate velocity considered (50 feet-per-second), the impact energy has been dissipated by increasing the force levels of the energy-absorbing landing gear. If the residue over 41 feet-per-second were carried through the structure and acted impulsively on the man, the DRI level would be severe. Hence, the total energy is dissipated by whatever force is required over the 15-inch stroke, and the resulting DRI is calculated. That is, the seat can dissipate a maximum amount of energy without causing the man to impact the floor structure. If the residue energy is reduced by the capability of the seat, the remainder is used to calculate the force needed by the energy-absorbing landing gear over the 15-inch stroke. This is then the minimum DRI level permitted by the seat and landing gear system assumed.

Several other points are plotted on Figure 50. The latest Crash Survival Design Guide²³ indicates that a design pulse for rotary-wing aircraft should have a vertical velocity change of 42 feet-per-second. A recent U.S. Army Agency for Aviation Safety paper⁴¹ indicates some tentative crashworthiness impact conditions for helicopters: 40 feet-per-second along the vertical axis of the vehicle; and a sink velocity of 36 feet-per-second flat impact, with sod-type terrain at an impact angle of up to 5 degrees. These are consistent with the combined loads assumption of Figure 50, in that they both nearly fall on a constant percent of gross weight line. This infers that both impact conditions will generate the same added weight for protection. The highest point shown (50 feet-per-second) is from the works of Rich²¹. He states that a combined 12-inch seat crush and 12-inch fuselage crush can provide an inertial response of 20G for a 50-foot-per-second impact. The inertial G will generate the DRI specified.

The last point shown is taken from Reference 28, and is indicative of the maximum velocity that can be dissipated by a "notched" energy absorber acting over 20 inches when subjected to a helicopter design pulse and supporting a seated subject.

The data shown indicate the values currently being examined by several authors using crash data, energy data, and computer oriented dynamic analysis to infer capability or desirability of attenuation or crashworthy systems.

The data indicate several aspects of the attenuation of crash forces. The 50-foot-per-second impact cannot be attenuated to a "tolerable" level for the E/A landing gear design assumed. If that level were to be protected against, additional stroke would have to be made available perhaps by raising the vehicle further off the ground for normal operations. Even if "optimal" characteristics were available for the seat structure and landing gear,

44 feet-per-second would be limiting. Therefore, it appears that the 40- to 42-foot-per-second regime, could be a realistic design level for energy-absorbing landing gear with seat absorption. The current study indicates a 41-foot-per-second limit for the utility class vehicle equipped with skid-type landing gear. The recent data of Haley⁴¹ establishes 40-foot-per-second based upon accident data, and theoretical studies²⁸ indicate that the 42-foot-per-second design pulse is compatible with the injury level and stroke length limits desired.

The current crashworthy crew seat specification MIL-S-58095 (AV) indicates that the design must have energy-absorbing capability for aircraft crash conditions. Hence, it is not unreasonable to require seat capability in a landing gear design specification. Secondly, the data indicate that the energy-absorbing landing gear system is only efficient at the higher impact velocities. At impacts below 36 feet-per-second, the seats will carry all of the impact energy of man and seat at minimum weight. This could be easily modified if the seat is also to be armored or otherwise increased in weight. The maximum additional seat weight with absorber for this analysis was 41 pounds. If a seat weight greater than 20 pounds basic is assumed, the dissipation of energy is less efficient, the input energy per seat absorber is increased, and (with a fixed force level and stroke) a more limited capability at greater weight is created.

Another aspect of seat energy absorption is that the seat, even if designed to the specification, cannot dissipate the impact over 12 inches without exceeding the 18 DRI value. It was shown in Reference 42 that a square wave absorber designed for a 20G plateau for the 95th percentile man requires 11.2 inches. If the force level is reduced to 15G, more stroke is required and the 12 inches will be exceeded.

From this information it appears that the energy-absorbing landing gear concept is most efficient, with respect to weight, in precisely the region where it is required, above 36 feet per second. The seat criteria currently specified provides protection up to that level with minimum weight. Above that velocity change, the landing gear and seat must both have attenuation capability. Therefore, since the design pulse of 42-foot-per-second velocity change is currently used as the basis for crashworthiness in both the Crash Survival Design Guide and seat specifications, it is now also consistent to use that as the design criterion for an energy-absorbing landing gear system. Indeed, for that pulse it is necessary to have structure, seat, and landing gear designed as a system to protect the crewmember. This type of systems approach to crashworthiness was pursued in the structural crashworthiness study described in Reference 40

A practical attitude requirement is more difficult to evaluate objectively. Hence, the attitude criterion is not specified, and instead Figure 50 is suggested as a means of evaluating the importance of attitude. The data indicate that the design pulse velocity and the USAAAVS flat impact criteria lie approximately on the 9 percent weight penalty line. If it is

later determined that the attitude is indeed more likely to exist at 10 degrees than the velocity at 42 feet per second, then the reduced velocity of 32 feet per second could be used for analysis. This should result in another configuration of the same weight with similar protection capability. The design would also revert from energy absorbing skid to improved seat structure. In a similar manner, if it is mandatory to consider a 10-degree attitude with the 42-foot-per-second velocity, then the 12.5 percent weight increase must be accepted.

CHAPTER 5 CONCLUSIONS AND RECOMMENDATIONS

5.1 CONCLUSIONS

5.1.1 Landing Gear Specifications

There are no quantitative specifications for crash loads or a crash environment for helicopter landing gear as a particular structural entity. Landing gear are designed to be compatible with the normal landing impact velocity and fuselage normal load factor limits of the particular procuring agency.

There are dynamic analysis techniques available to examine the response of elastic vehicles coupled with dynamic representation of landing gear elements. These are only used by a limited number of manufacturers and are proprietary. The dynamic analysis may not be necessary in most cases since the current specification can be satisfied by energy relations and parameters such as "efficiency" as measured during a drop test. Hence, through experience in orifice design and drop test data examination, the landing gear systems for wheel types only, can be designed without rigorous analyses.

5.1.2 Energy-Absorbing Devices

Many energy-absorbing devices have been tested under prototype development conditions. Data are available for the devices which establish the analytical relations and measured material "properties" required for design and analysis. However, the data have generally been collected over a limited range of forces and strokes with attendant difficulties in reliably extrapolating the data.

Three energy-absorbing devices are available that hold promise for incorporation within any conceptual system design. The liquid spring and cyclic strain devices can be obtained from commercial sources that have manufactured and delivered quantities of absorbers having sufficient energy dissipation, stroke, and force capability. Prestressed honeycomb within a telescoping tube has been used and has demonstrated operational capability. The use of this technique is dependent upon the trade-off between cost of design manufacture and maintenance of a "one-shot" absorber, and the purchase cost of a reusable commercially available unit.

5.1.3 Energy-Absorbing Landing Gear Concepts

It was possible, assuming a 25-foot-per-second impact, to develop several concepts for LOH, UH, and CH helicopter classes. The concepts were compatible with commercially available energy absorbers and could be developed to limit the fuselage acceleration to 15G with a reasonable stroke or static height above the ground.

The CH vehicle concepts were primarily truss arrangements wherein the side, drag, and vertical loads could be carried by appropriate linkages. It was shown that the addition of combined loads creates a problem in determining the particular truss elements that must provide vertical energy absorption. However, arrangements can be found to decouple the combined loads from the vertical and permit proper actuation.

The skid concepts are more dependent on attitude than was originally anticipated. The deformation of an elastic skid is dependent upon the point of load application and can introduce bending moment value reversals from pure vertical impact analyses. However the inherent flexibility of plastically deforming tubes tends to negate any strength or rupture problems at ultimate displacements. The tip load, or attitude at impact, significantly influences the energy capability of the skid energy-absorbing landing gear system.

Based upon the preliminary analyses conducted, the most promising concept of energy-absorbing landing gear for the utility class, skid-type helicopter was considered to be that using additional skids supported by energy absorbers beneath the fuselage. In this manner the existing skids could meet their design landing requirements without introducing problems of direct compatibility with high level impact attenuation systems. Other concepts investigated were originally judged to be of heavier weight, greater complexity and relied upon the motions of the conventional skids for activation. However, as the design for the "additional" skid system progressed this became more and more questionable.

It was originally assumed that the additional skid could function in guides that would carry the combined drag and side force effects. Several configurations examined eventually led to the addition of linkages necessary to carry the loads. The moments generated by the side and drag forces are so large that they force the design into that of axial load carrying members or extremely large reaction load attachment points. Consequently the finished design was extremely heavy, making it doubtful that the selected concept did indeed result in the least weight design.

5.1.4 Trade-Off Analysis

The trade-off conducted indicates the significance of the relationship between the energy-absorbing landing gear, fuselage strength stiffness and energy absorption capacity, and seat crash force attenuation capabilities. In order to protect the occupant at maximum expected acceleration levels, the analysis must consider all components acting together. It is difficult, maybe impossible, to determine a fixed contribution required from each element for all helicopters. It may be desirable to have a stiffer landing gear and a crushable fuselage, but the two may be structurally incompatible as well as heavier than necessary for a particular impact condition.

The trade-off analyses were conducted to establish the variations of crash

criteria parameters that would be associated with a 10 percent increase in structural weight. Based upon the UH additional skid design results, it appears that a 10-percent weight penalty could provide protection up to the 95th percentile vertical impact while permitting appreciable protection at realistic attitudes and proportionately reduced velocities.

5.2 RECOMMENDATIONS

1. Any future research into improved energy-absorbing landing gear should consider the landing gear as only one portion of a total impact protection system.
2. Design criteria for crashworthiness should be separated into various helicopter classes such as CH, UH, and LOH.

LITERATURE CITED

1. Turnbow, J. R., et al, CRASH SURVIVAL DESIGN GUIDE, USAAVLABS TR 70-22, U. S. Army Aviation Materiel Laboratories, Fort, Eustis, Virginia, Revised August 1969, AD 695648.
2. Chernoff, M., ANALYSIS AND DESIGN OF SKID GEARS FOR LEVEL LANDING, Journal of the American Helicopter Society, January 1961.
3. LANDING GEAR, AIRCRAFT SHOCK ABSORBER (AIR-OIL TYPE), MIL-S-8552C, Government Printing Office, December 1968.
4. TAXIING AND GROUND HANDLING, Report No. S-88, Kaman Aircraft Corporation, August 1958.
5. Walls, J. H., INVESTIGATION OF THE AIR-COMPRESSION PROCESS DURING DROP TESTS OF AN OLEO-PNEUMATIC LANDING GEAR, NACA TN 2477, 1951.
6. Ferguson, T. R., et al, A RATIONAL METHOD FOR PREDICTING ALIGHTING GEAR DYNAMIC LOADS, ASD-TDR-62-555, Vol 1, Air Force Systems Command, Wright-Patterson Air Force Base, Ohio, December 1963.
7. Conway, H. G., LANDING GEAR DESIGN, Chapman and Hall, Ltd., London, England, 1958.
8. Flugge, W., LANDING GEAR IMPACT, NACA TN 2743, 1954.
9. Yackle, A. R., Gaidelis, J. A., Perlmutter, A. A., STUDY OF HELICOPTER STRUCTURAL DESIGN CRITERIA, WADC Technical Report 58-336, ASTIA Document No. AD 202 531, Kellett Aircraft Corporation, May 1958.
10. Sahnoun, R., DROP TESTS OF SKID GEAR, SNCA-SE Document No. 46.005, SUD Aviation, January 1957.
11. Schwartz, Marcus, DYNAMIC TESTING OF ENERGY ATTENUATING DEVICES, NADC-AC-6905, USNADC, Johnsville, Pennsylvania, October 1969.
12. PROGRAM FOR THE EXPLOITATION OF THE UNUSED NASA PATENTS, NGL 06-004-078, University of Denver, NASA 1st Annual Report, May 1969.
13. PROGRAM FOR THE EXPLOITATION OF UNUSED NASA PATENTS, NGL 06-004-078, University of Denver, NASA 2nd Annual Report, May 1970.

14. McGehee, J. R., EXPERIMENTAL INVESTIGATION OF PARAMETER AND MATERIALS FOR FRAGMENTING TUBE ENERGY-ABSORPTION PROCESS, NASA TN-D3268, National Aeronautics and Space Administration, Washington, D. C., February 1966.
15. Balogh, Steve E., DESIGN PRINCIPLES FOR SHOCK LOAD PROTECTION THROUGH ENERGY ABSORPTION AND DISSIPATION METHODS, ASME Publication, ASME New York, New York, May 1969.
16. Kroell, C. K., A SIMPLE, EFFICIENT, ONE SHOT ENERGY ABSORBER, Part III, Bulletin 30, Shock, Vibration and Associated Environments, Symposium on Shock, Vibration, and Associated Environments, Detroit, Michigan, October 1961.
17. Guist, L. R., and Marble, D. P., PREDICTION OF THE INVERSION LOAD OF A CIRCULAR TUBE, NASA TND-3622, National Aeronautics and Space Administration, Washington, D. C., September 1966.
18. Ferguson, T. R., Mollick, J., and Kitts, W. W., A RATIONAL METHOD FOR PREDICTING ALIGHTING GEAR DYNAMIC LOADS, ASD TR 62-555, December 1963.
19. Platus, D. L., et al, CONCEPTS OF MULTIPLE-IMPACT STUDY OF ENERGY ABSORPTION, NASA CR-273, National Aeronautics and Space Administration, Washington, D. C., August 1965.
20. Platus, D. L., CYCLIC DEFORMATION CREW ATTENUATOR STRUTS FOR THE APOLLO COMMAND MODULE, Bulletin 38-Part 3, The Shock and Vibration Bulletin, USNRL, Washington, D. C., November 1968.
21. Rich, J. J., AN ENERGY ABSORPTION SAFETY ALIGHTING GEAR FOR HELICOPTERS AND VTOL AIRCRAFT, Paper 62-16, Institute of Aeronautics and Astronautics, January 1962.
22. Turnbow, J. W., A DYNAMIC CRASH TEST OF AN H-25 HELICOPTER, SAE Transactions, Vol 71, 1953, p 508-519.
23. CRASH SURVIVAL DESIGN GUIDE, USAAMRDL TR-71-22, Eustis Directorate, U. S. Army Air Mobility Research and Development Laboratory, Fort Eustis, Virginia, October 1971, AD 733358.
24. Weinberg, L. W. T., CRASHWORTHINESS EVALUATION OF AN ENERGY-ABSORPTION EXPERIMENTAL TROOP SEAT CONCEPT, AD 614-582.
25. Weinberg, L. W. T., and Turnbow, J. W., DYNAMIC TEST OF A COMMERCIAL TYPE PASSENGER SEAT INSTALLATION IN AN H-21 HELICOPTER, AD 416 298.
26. A STUDY OF HELICOPTER ACCIDENT DATA TO DETERMINE THE FEASIBILITY OF A SURVIVABLE ESCAPE SYSTEM, Boeing Company, Vertol Division for Naval Air Systems Command.

27. U. S. ARMY H-25 HELICOPTER TOP TEST, AVCIR, Division of Flight Safety Foundation, Inc., AD 804-147.
28. Carr, R. W. and Phillips, N. S., DESIGN CRITERIA FOR ENERGY ABSORPTION SYSTEMS, NADC-AC-7010, Naval Air Development Center, Johnsville, Pennsylvania, June 1970.
29. Turnbow, J. W., et al, FULL-SCALE DYNAMIC CRASH TEST OF A SMALL OBSERVATION TYPE HELICOPTER, Report AVSER-65-10, May 1966, AD 483-730L.
30. Smith, H. G., McDermott, J. M., DESIGNING FOR CRASHWORTHINESS AND SURVIVABILITY, Journal of the American Helicopter Society, October 1968.
31. Watson, W. R., Dunham, J. R., RESUME OF U. S. ARMY HELICOPTER OPERATIONS IN VIETNAM, Journal of American Helicopter Society, July 1968.
32. Eiband, A. M., HUMAN TOLERANCE TO RAPIDLY APPLIED ACCELERATIONS: A SUMMARY OF THE LITERATURE, NASA Memorandum 5-10-59E, National Aeronautics and Space Administration, Washington, D. C., June 1959.
33. Brinkley, James W., DEVELOPMENT OF AEROSPACE EXCAPE SYSTEM, Air University Review, Vol XIX (5), 34-49, July-August 1968.
34. JANE'S ALL THE WORLD'S AIRCRAFT, McGraw-Hill, 1969-1970.
35. STRUCTURAL ANALYSIS OF HELICOPTER COMPONENTS PECULIAR TO MODEL UH-1F, Report No. 204-099-691, Bell Helicopter Company, January 1964.
36. STRUCTURAL DESIGN REQUIREMENT, HELICOPTERS, MIL-S-8698, July 1959.
37. ALCOA STRUCTURAL HANDBOOK, Aluminum Company of America, 1958.
38. STRUCTURAL ANALYSIS OF HELICOPTER COMPONENTS PECULIAR TO MODEL UH-1F, Report No. 204-099-691, Bell Helicopter Company, January 1964.
39. Sansom, Frederick J. and Peterscn, H. E., MIMIC PROGRAMMING MANUAL, SEG TR 67-31, Aeronautical Systems Division, Wright-Patterson Air Force Base, Ohio, July 1967.
40. Clifford, I. G., Goehel, D. E., and Larren, S. E., ANALYSIS OF HELICOPTER STRUCTURAL CRASHWORTHINESS, USAAVLABS Technical Report 70-71A, Vol 1, Mathematical Simulation and Experimental Verification for Helicopter Crashworthiness, Eustis Directorate, U. S. Army Air Mobility Research and Development Laboratory, Fort Eustis, Virginia, January 1971, AD 880680.

41. Haley, J. T., ANALYSIS OF U. S. ARMY HELICOPTER ACCIDENTS TO DEFINE IMPACT INJURY PROBLEMS, AGARD Conference Preprint No. 88, June, 1971.
42. N. S. Phillips, et al, A STATISTICAL EVALUATION OF THE INJURY POTENTIAL OF CURRENT ENERGY ABSORBER DESIGN CRITERIA, November 1970.

APPENDIX I TEST VEHICLE DESIGN

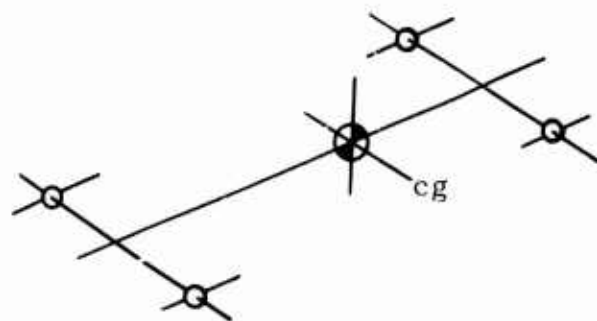
A full-scale test vehicle was required to conduct drop tests of the energy-absorbing landing gear. The selection of vehicle characteristics to be duplicated was dictated by data contained in "Structural Analysis of Helicopter Components Peculiar to Model UH-1F" ³⁸. Computer data were available for the following condition:

Gross Weight	6600 pounds
I_{yy}	$13.726 \times 10^4 \text{ lb-in.-sec}^2$
I_{xx}	$2.7815 \times 10^4 \text{ lb-in.-sec}^2$
I_{zz}	$11.9305 \times 10^4 \text{ lb-in.-sec}^2$
Center of Gravity	57.5 inches aft of forward strut at WL 58.65

This condition was used as the desired vehicle design.

The design was initiated by first finding a fore and aft weight distribution that would duplicate the longitudinal center-of-gravity location and the pitching moment of inertia.

The rolling moment was then duplicated by splitting the masses into two units equidistant from the centerline.



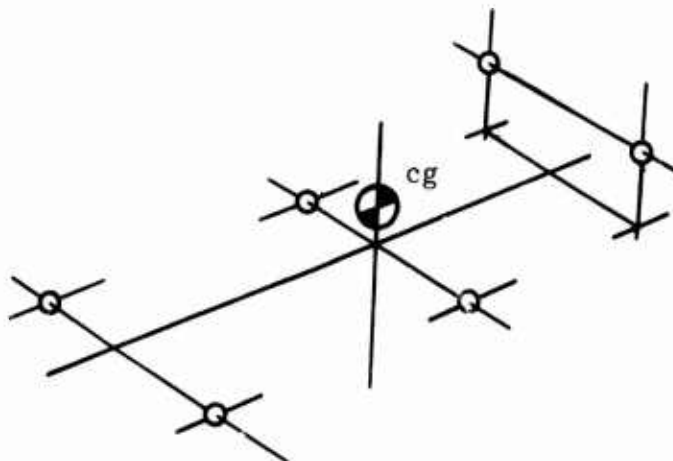
The yawing moment of this configuration was too great and required the provision of height in order to generate the proper vertical center of gravity and yawing moment. After several iterations, one configuration was found that approached the desired condition but would not duplicate the yawing moment of inertia:

$$I_{yy} = 13.47 \times 10^4 \text{ lb-in.-sec}^2$$

$$I_{xx} = 2.79 \times 10^4 \text{ lb-in.-sec}^2$$

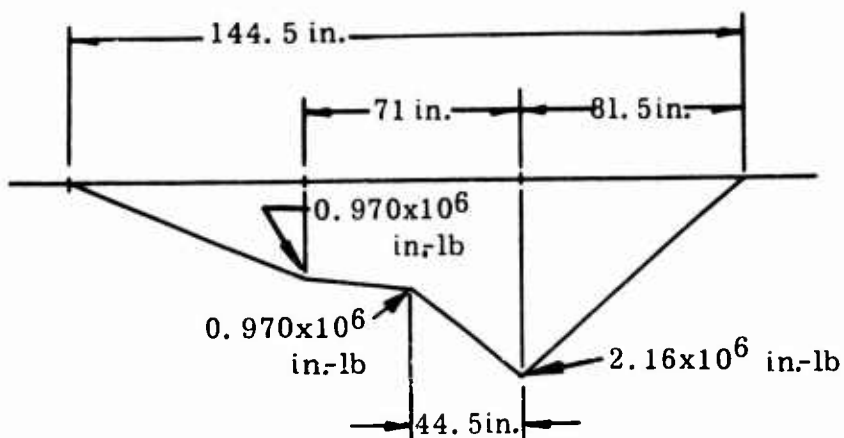
$$I_{zz} = 14.67 \times 10^4 \text{ lb-in.-sec}^2$$

This demonstrated that the four mass system could not duplicate all three correctly and that a different configuration would be required. This led to the concept of six masses as shown below:

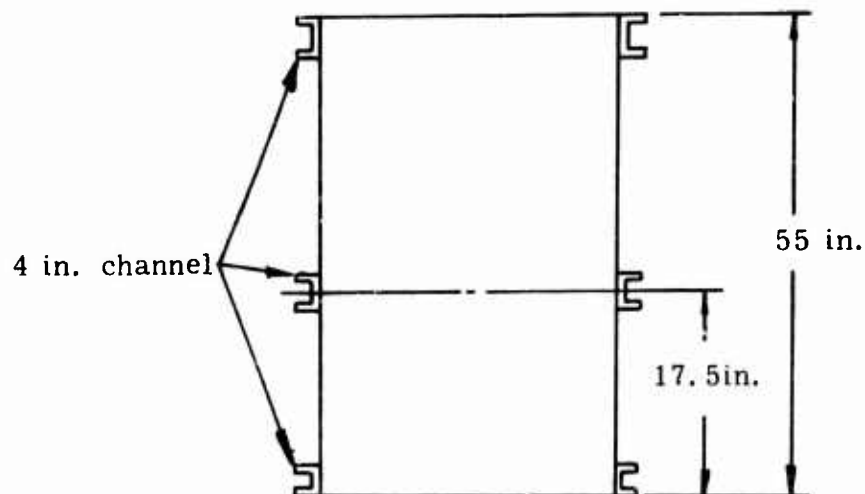


It was assumed that gravel at 100 pounds per cubic foot would be used to allow the capability of shifting the ballast as required by detailed design. The volume required to carry the weights selected was determined and a schematic was drawn.

An estimate of the structure required was obtained by assuming that two similar frames along the inside of the fuselage would carry the applied loads. The design acceleration level was 15G and an assumed factor of safety of 1.5 was used. The moment diagram developed is shown on the following page.



The structural configuration assumed was schematically



and the resulting structure consisted of 4-inch channel.

The analysis indicated

$$I = 4318 \text{ in.}^4$$

$$M = 2.16 \times 10^6 \text{ in.-lb}$$

$$Z = 24.2 \text{ in.}$$

$$f_B = \frac{MY}{I} = \frac{(2.16 \times 10^6)(30.8)}{4318} = 15,000 \text{ psi} \quad (56)$$

$$\text{For 6061 aluminum, M.S.} = 1 - \frac{15,000}{38,000} = +0.60$$

The structural schematic was then referred to and the lengths of the channel stock required to support the ballast and the landing gear were estimated. The result was an estimate of 124 feet of stock weighing 910 pounds. The weight of structure based upon the ballast weights used was approximately 800 pounds. Therefore, the weight, center of gravity, and inertial response characteristics for the assumed configuration, ballast, and structure seemed reasonable.

The applied loads due to a deceleration of 15G and a factor of safety of 1.5 were applied to the schematic configuration, and a truss analysis was conducted. The diagonal members were added as required in order to permit a statically determinate structural analysis. The internal loads carried are shown in Figure 51.

The worst conditions found were

37,300 lb (T)	L = 48 in.
47,000 lb (C)	L = 47 in.
35,265 lb (C)	L = 51 in.

These were examined to determine the design condition (47,000 lb - compression), and several standard structural sections were selected. After examining weight, strength, cost, and availability of the various sections, it was decided that steel angle stock would be used. For the primary longitudinal bending members, $\frac{1}{4}$ -inch-thick angle stock could be used. Secondary or diagonal structure could consist of 2-x-2-inch, $\frac{1}{4}$ -inch-thick angle stock. At this point the vehicle structure was drawn to indicate the overall configuration (see Figure 52).

A detailed weight analysis of the structure was conducted to determine the effect of a steel construction and the required location and amount of ballast. Using an 83-element representation of the structure, it was found that the total structural weight would be 2750 pounds, leaving 3850 pounds for ballast. If all sand were placed in a rectangle in the furthest corner from the center of gravity, the inertial characteristics would be

$$I_{xx} = 2.7 \times 10^4 \text{ lb-in.-sec}^2$$

$$I_{yy} = 13.0 \times 10^4 \text{ lb-in.-sec}^2$$

$$I_{zz} = 11.6 \times 10^4 \text{ lb-in.-sec}^2$$

$$cg = 13.6 \text{ in. forward of rear strut} \\ (\text{vs. } 13.5 \text{ desired})$$

At this point, the preliminary design was considered to be complete, and detailed analyses of joints, bulkheads and fittings were conducted as dictated by the landing gear systems. Additional drawings and analysis

CROSS MEMBER LOADS

(C) = Commission (T) = Transac-

(C)	= Compression	(1) = Tension
A.	3137 lb (C)	L. 10, 850 lb (T)
B.	5630 lb (T)	M. 47, 000 lb (C)
C.	4700 lb (C)	N. 32, 300 lb (T)
D.	13, 000 lb (C)	O. 35, 400 lb (T)
E.	16, 000 lb (T)	P. 35, 265 lb (C)
F.	13, 000 lb (T)	Q. 21, 200 lb (C)
G.	27, 400 lb (C)	R. 5, 560 lb (T)
H.	5, 960 lb (C)	S. 15, 900 lb (T)
I.	27, 400 lb (C)	T. 7, 150 lb (C)
J.	10, 850 lb (C)	U. 13, 650 lb (C)
K.	37, 300 lb (T)	V. 12, 200 lb (T)

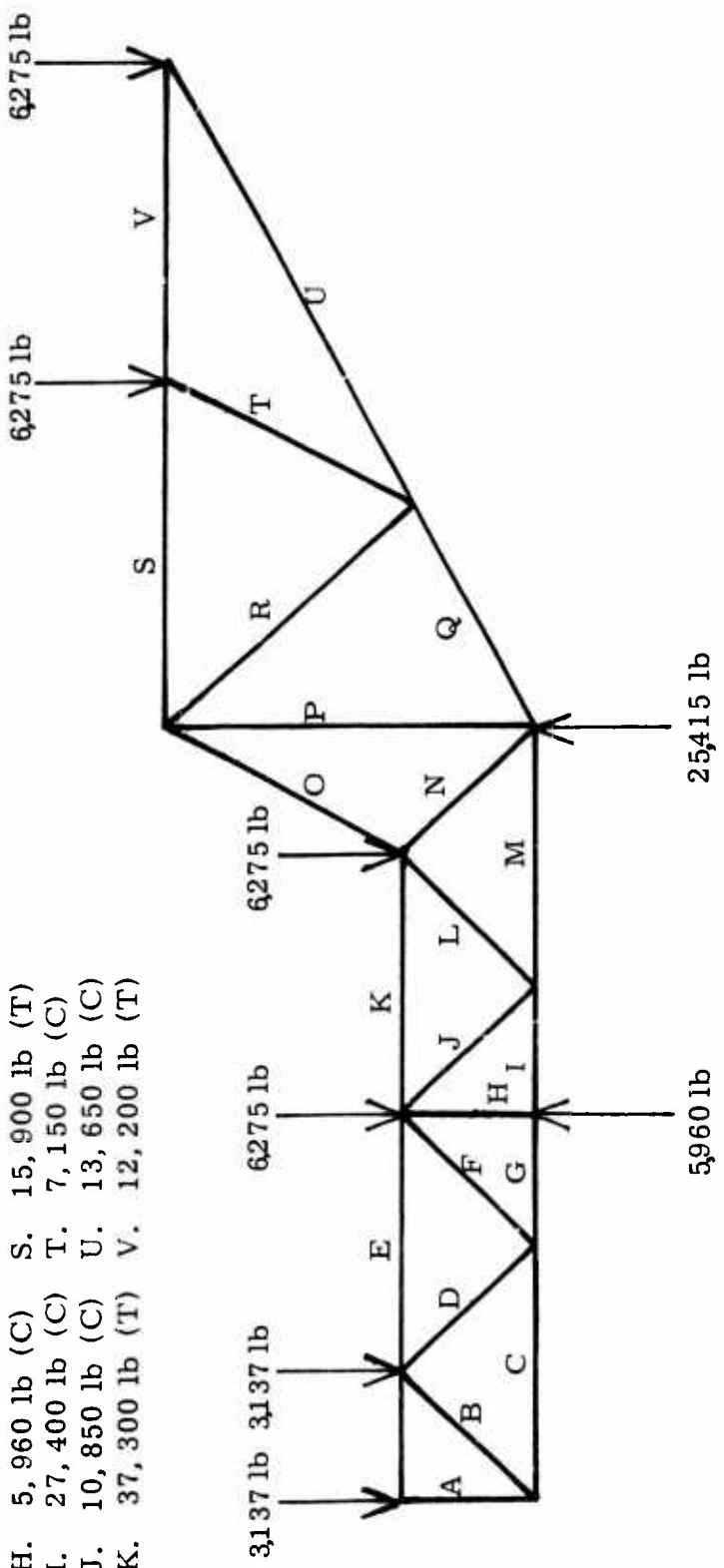


Figure 51. Truss Configuration.

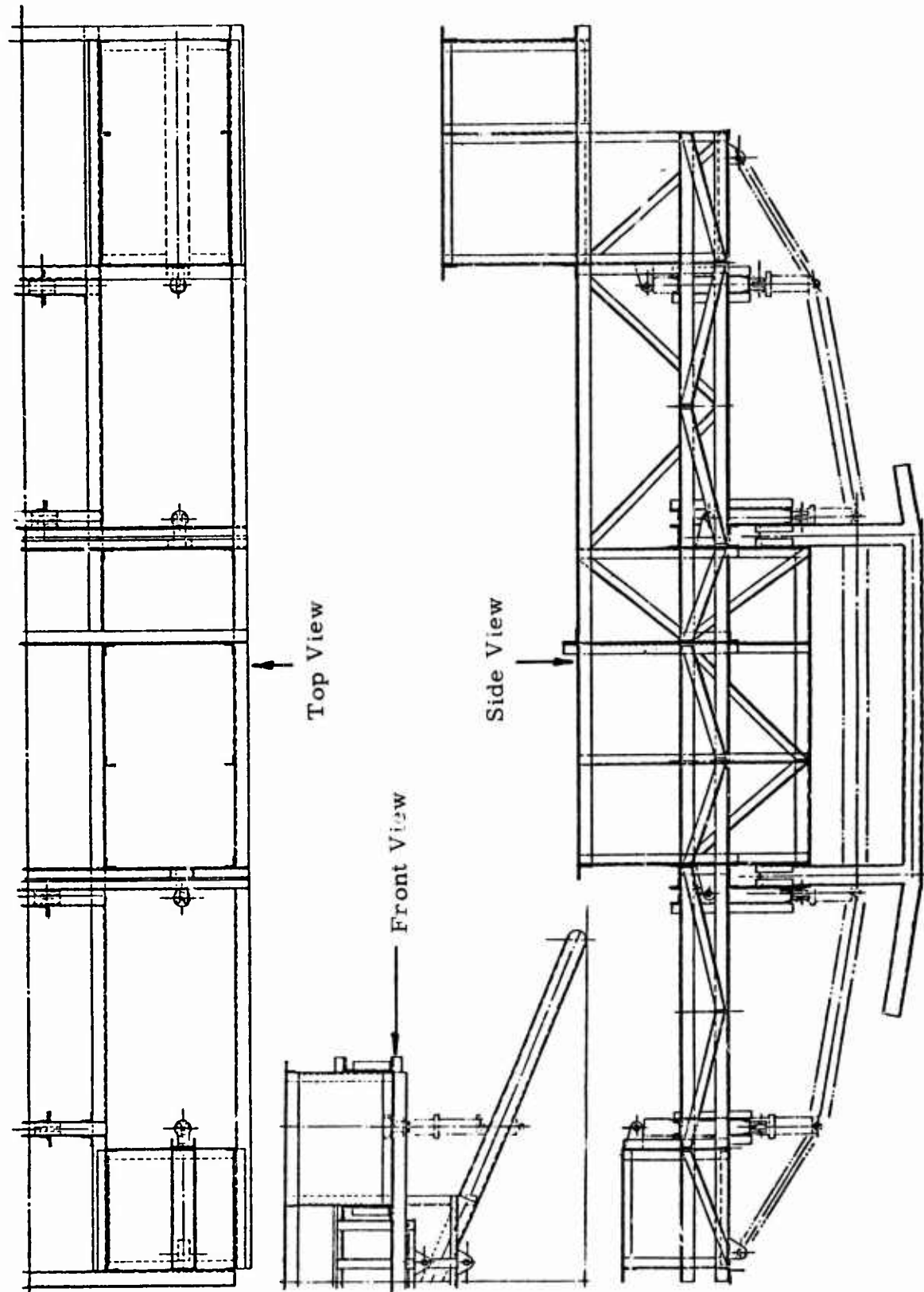


Figure 52. Final Vehicle Configuration.

were developed at each attachment point to determine that the load paths selected could indeed provide adequate strength from point of load application through the structure.

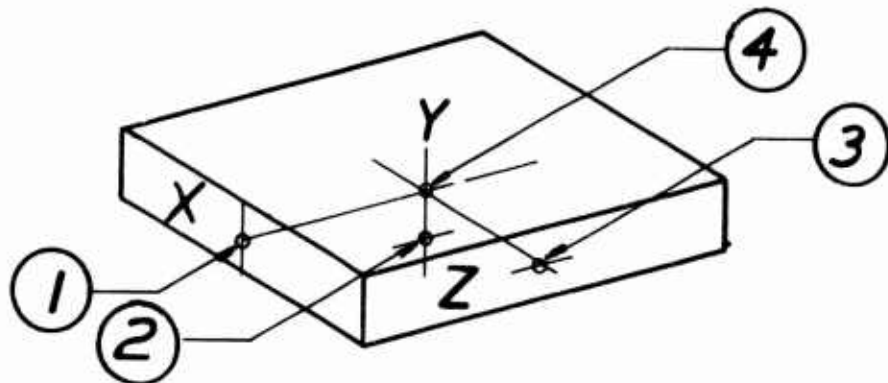
APPENDIX II

PARAMETERS MEASURED

Several parameters had to be measured to evaluate the system response: the accelerations of the vehicle and the skids, the forces in the skids, and the output of the energy absorbers. With these accurately measured, it is possible to have a measure of the inputs to the vehicle, force and acceleration, and the generated outputs, vehicle motion. It was intended to use the input accelerations measured as computer input to the digital routine developed.

If it is assumed that the vehicle is a rigid body with a plane of symmetry, it is possible to calculate the rigid body motions using three sets of biaxial accelerometers and one triaxial accelerometer.

The accelerometers were mounted as shown schematically below:



Accelerometer	Location	Sensitive Axes
1	$(X_1, 0, 0)$	(Y, Z)
2	$(0, 0, Z_2)$	(X, Y)
3	$(0, Y_3, 0)$	(X, Y)
4	$(0, 0, 0)$	(X, Y, Z)

By locating the accelerometers in the above manner, it is possible to insure that the value of all parameters $p, q, r, \dot{p}, \dot{q}$, and \ddot{r} can be calculated. The equations of motion are of the form

$$\ddot{Z}_1 = \ddot{Z}_{1cg} + Y_1 (\dot{p} + qr) - Z_1 (q - pt) - Z_1 (p^2 + q^2) \quad (57)$$

Locating the accelerometers at locations where two coordinates are 0 permits calculation of p, q, r, pq, qr , and pr from three linearly related equations. The values of p, q , and r can be calculated from the remaining equations. From the above equation,

$$\ddot{Z}_1 = \ddot{Z}_{cg} - X_1 (q-pr) \quad (58)$$

and similarly,

$$\ddot{X}_2 = \ddot{X}_{cg} + Z_3 (q+pr) \quad (59)$$

These are solved for q and pr .

For the locations and sensitive axes selected, there are always two accelerometers that permit the evaluation of one angular acceleration and a velocity product. The measurement at a point is a function of the center-of-gravity acceleration, measured, and the angular effects. Hence, there are a sufficient number of measurements to calculate all values required.

Corrections to the measured data due to the gravitational field will not be required. The equations are of the form such that the gravitational contribution is contained on both sides of the original equations and the subtraction of center-of-gravity acceleration from the accelerometer reading eliminates gravitational effects.

Four additional sets of triaxial accelerometers were required at the intersection of the landing gear struts and skids. In this manner the accelerations that act as inputs to the system can be evaluated. Regardless of the nature of the impact surface, the accelerations measured are indicative of the impulse desired.

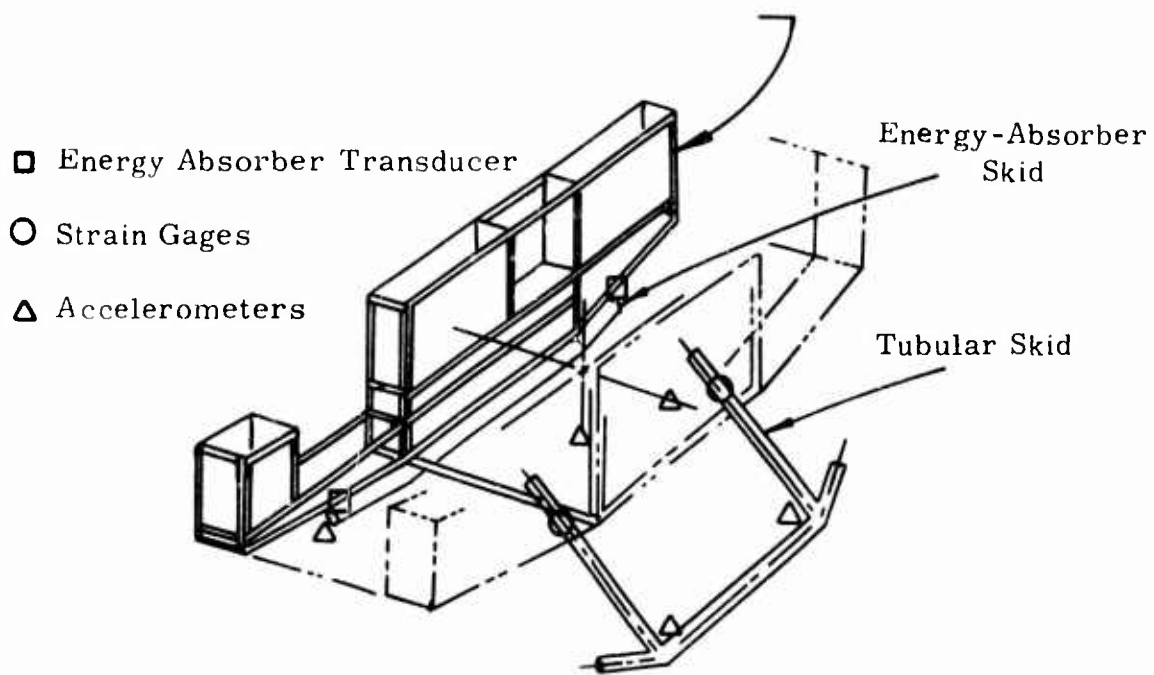
Additional measurements required are force levels developed. While the acceleration is indicative of the input, the forces developed also provide necessary comparative data. The accelerations of the vehicle could be used to calculate force levels, but could not distinguish energy-absorber force applied from skid force applied. Therefore, strain gages were applied to the skids and evaluated under loads up to failure during tests conducted by Bowser-Morner Testing Laboratories.

The ARA energy absorbers have force-displacement curves available for each unit, and it was decided to use displacement transducers to infer force levels, rather than measure the forces directly. Force transducers required for the force levels to be developed were very large and would create attachment problems in interfacing with the structure.

The transducers were located as shown schematically below. The estimated ranges for these are 200G for all vertical or Z-axis accelerometers on the skids and 25G for this component on the frame, 10-15G for all those sensing in the X and Y directions, 3600 pounds for the strain gaged struts,

and 8 inches of travel for the energy absorbers. The flat frequency response requirement for all of these is 100 Hz.

LEFT-SIDE STRUCTURAL FRAME



TRANSDUCERS

As determined, 21 acceleration measurements and 4 force measurements were made. Strain gage accelerometers were used since they provide adequate accuracy, frequency response, and insensitivity to transverse accelerations while still preserving the steady-state component of the transient data. An additional benefit was accrued from their usage in that the output of the strain gage bridge was sufficient to drive a low frequency recording galvanometer without requiring amplification.

The skid support tubes were strain gaged and calibrated by a local testing company. Preliminary tests were performed on a section of support tubing to determine what strains would be produced, and as a result, the strain gage configuration required.

The ARA energy absorbers were provided with calibration curves. Since these are resilient devices, a force-time relationship was determined by measuring the displacement as a function of time and referring to the calibration curves. This method was more economical than measuring the force directly. Linear potentiometers, Datacraft Model 400's were used to determine the displacement.

CONDITIONING AND RECORDING

Since we used all strain gage bridge type transducers and operated the linear potentiometers in bridge circuits, bridge balance and calibration circuitry were required. The Honeywell B-12 Excitation and Switching Units were used for this purpose. A regulated DC power supply provided the bridge excitation. The outputs from the B-12's were then recorded on two CEC 5-124 oscillograph recorders equipped with CEC 7-345 galvanometers.

A comparison of the various specifications and characteristics of the components involved indicated that galvanometer-driver amplifiers were not required.

The conditioning and recording components were rented.

PHOTOGRAPHY

The impact tests required two cameras for photometric purposes and one to provide the photographic measurements necessary to determine the impact attitude of the helicopter.

CALIBRATION AND CERTIFICATION

System components were calibrated, and certification to that effect was

provided. Datacraft provided calibrations for their transducers which are traceable to the National Bureau of Standards. The pertinent calibration data furnished was used as our calibration standard.

SYSTEM CONTROL

Due to the relatively short duration of the tests, provisions had to be made for synchronizing the various parts of the system. This was done to permit both the cameras and the oscilloscopes to attain their proper recording speeds prior to the time they were to start recording, yet without requiring the excessive use of film or oscilloscope paper. This is particularly important with regard to the cameras since they hold only 100 feet of film, yielding only about 2 seconds of recording time. The free fall time of the test vehicle was less than 1 second, based on the target impact velocity of 25 feet per second. As a result, manual control was used. The oscilloscope was started just prior to the drop and the cameras were begun once the vehicle had been observed. The release mechanism was manually actuated.

INSTRUMENTATION SYSTEM DESCRIPTION

The system is shown in block diagram form in Figure 53. An umbilical cable provided the transmission link between the test vehicle and the rest of the collection system. The signal conditioners and recorders were mounted in a panel truck which also served as a chase vehicle. System power was obtained from a portable generator mounted in the truck. A separate, self-contained power supply was provided for the cameras.

TEST VEHICLE PREPARATION

TRANSDUCER MOUNTING

The accelerometer assemblies were fabricated simply by using two or three accelerometers, as appropriate, mounted onto a metal cube. They were attached to the structure with machine screws. The strain gages were bonded to the landing gear struts. The linear potentiometers were mounted in parallel with the energy absorbers.

ATTACHMENT AND ORIENTATION

The release mechanism was then attached to the crane by a device. The jaws were opened and the vehicle dropped when the lever and cam release was manually actuated. The helicopter was supported by a sling arrangement designed such that the cables looped over the frame structures on both sides. By adjusting the cable lengths, the proper helicopter orientation was achieved. The net result was a mechanism which was completely independent of the hoist, simple in construction, and amenable to adjustment over a wide range of initial attitudes.

INSTRUMENTATION CAMERAS

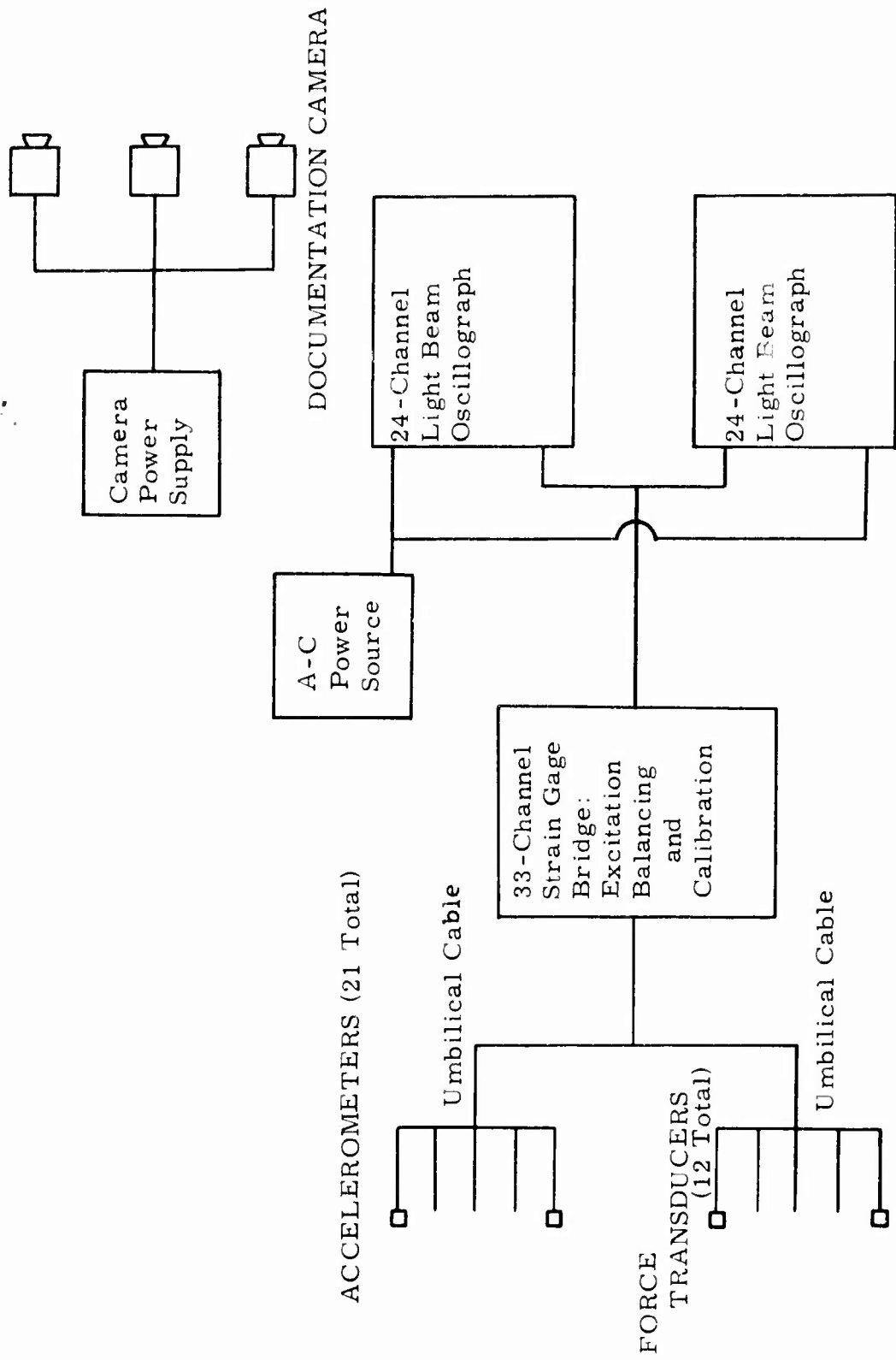


Figure 53. Instrumentation System.

TRANSPORTATION AND HANDLING

At the test site a crane was used for loading and unloading the test vehicle from the flat bed truck which was used to transport it to and from Beta.

WEIGHTING AND CENTER-OF-GRAVITY DETERMINATION

The test vehicle structure did not weigh the desired total weight of 6,600 pounds and some weighting was necessary. Sand was used to provide the desired weight, center of gravity, and moments of inertia. The total weight with ballast was verified by scales and the moment of inertia was based upon calculations previously established.

TEST SITE

The tests were conducted at the Springfield, Ohio, airport. The north-south runway was used for testing. This runway is not currently active and was available on a noninterference basis during the test period. The asphalt runway is 5,000 feet long. This provided a sufficient distance for the crane to get up to speed and an adequately rigid impact surface. The runway was scheduled to be repaved shortly after the drops, so no preparation was necessary. Coordination was effected with the airport authorities to insure that all local regulations were complied with. The tower chief was kept informed about the test operations at all times via using citizen band walkie-talkies.

APPENDIX III **COMPUTER PROGRAM DESCRIPTION**

A computer program that solves the equations of motion of a three-dimensional analytical model of a helicopter landing gear system is detailed below. The program is written using MIMIC³⁹ and is described by sections in the following paragraphs. The program printout is attached to this section

Section 1 (lines 1 through 14) Systems Constants

This part of the program reads in constants that define inertial, angular, and dimensional values for the vehicle model.

Inertia Constants

CON (M, JP, JQ, JR)

M = Mass

JP = Moment of inertia - x axis

JQ = Moment of inertia - y axis

JR = Moment of inertia - z axis

Initial angular rotations between body axis and component axis

CON (IA1, IB1, IC1)

CON (IA2, IB2, IC2)

CON (IA3, IB3, IC3)

CON (IA4, IB4, IC4)

IA_j = Initial rotation between body axis and j^{th} landing gear component.

IB_j = Initial rotation between body axis and j^{th} landing gear component.

IC_j = Initial rotation between body axis and j^{th} landing gear component.

Landing Gear Attachment Location - Body Axis

CON (AA, BA, CA, AB, BB, CB)

CON (AC, BC, CC, AD, BD, CD)

Aa = x dimension to ath landing gear attachment

Ba = y dimension to ath landing gear attachment

Ca = z dimension to ath landing gear attachment

Landing gear component letter to number correspondence

(A=1, B=2, C=3, D=4)

Landing gear attachment location component axis

CON (XC1, YC1, ZC1)

CON (XC2, YC2, ZC2)

CON (XC3, YC3, ZC3)

CON (XC4, YC4, ZC4)

XC_j = x dimension to j^{th} landing gear attachment
 YC_j = y dimension to j^{th} landing gear attachment
 ZC_j = z dimension to j^{th} landing gear attachment

The numerical values for these constants are coded on data cards with one data card for each CON card. The format for the data cards is 6 fields of 12 columns with each field corresponding to an argument in a CON statement. If the number of arguments is less than 6, then the data card fields corresponding to the missing arguments are not used. The constant values can be coded in decimal or exponential (E Format) form, however, the exponent must be right justified.

Section 2 (lines 16 thru 27) System Parameters

This section of the program reads in values for model parameters that change between program runs.

Initial velocities and displacements

PAR (IDB, IXB, IDYB, IYB, IDZB, IZB)
PAR (IP, IQ, IR)

PAR (IDXB1, IDYB1, IDZB1, IDXB2, IDYB2, IDZB2)

PAR (IDXB3, IDYB3, IDZB3, IDXB4, IDYB4, IDZB4)

IDa_B = Initial velocity of body CG - a $^{\text{th}}$ coordinate

Ia_E = Initial displacement of body CG - a $^{\text{th}}$ coordinate

Ia_A = Initial angular velocity of body CG - a $^{\text{th}}$ coordinate

IDa_Bj = Initial velocity of j^{th} landing gear attachment - a $^{\text{th}}$ coordinate
(body axis)

Landing gear component stiffness and damping terms

PAR (K11, K12, K13, B11, B12, B13)

PAR (K21, K22, K23, B21, B22, B23)

PAR (K31, K32, K33, B31, B32, B33)

PAR (K41, K42, K43, B41, B42, B43)

K_{ij} = Stiffness coefficient of i^{th} landing gear component along j^{th} coordinate
(component axis)

B_{ij} = Damping coefficient of i^{th} landing gear component along j^{th} coordinate
(component axis)

Landing gear touchdown - logic values

PAR (ZD1, ZD2, ZD3, ZD4)

ZD_j = Landing gear touchdown value j^{th} landing gear component

The program will not calculate any reaction forces in the j^{th} landing gear component if $ZD_j \leq 0$. If less than four point impact response is desired, then ZD_j for landing gear components not in initial contact with impact surface must be redefined as variables to be calculated by the program.

The numerical values for these parameters are coded and read in the same manner as the constant data cards. The parameter data cards are located directly behind the constant data cards.

Section 3 (lines 28 thru 50) - Landing Configuration Logic

The landing gear component that is in contact with the impact surface and its reaction forces are determined in this section of the program.

F_{ij} = Force developed in the i^{th} landing gear component along j^{th} coordinate (body axis)

Landing gear component number to coordinate correspondence

(1=x, 2=y, 3=z)

Section 4 (lines 52 thru 86) - Equations of Motion - Rigid Body CG

This portion of the program solves the six second order differential equations of motion for the rigid body's center of gravity.

$2D_{aB}$ = Linear acceleration of a $^{\text{th}}$ body axis coordinate
 D_a = Angular acceleration of a $^{\text{th}}$ body axis coordinate

Section 5 (lines 87 thru 137) - Equations of Motion - Landing Gear Attachment Points

The differential equations of motion for the landing gear attachment points are solved in this part of the program.

$2D_{aBj}$ = Acceleration of the a^{th} coordinate at the j^{th} attachment point.

Section 6 (lines 138 thru 162) - Rotation Angle Equations

This section of the program calculates the Euler angles between the body axis and each of the component axes.

$A_j = \psi$ rotation between the body axis and the j^{th} component axis
 $B_j = \theta$ rotation between body axis and the j^{th} component axis
 $C_j = \phi$ rotation between body axis and the j^{th} component axis

Section 7 (lines 163 thru 193) - Initial Coordinate Transformation

In this section of the program, the initial body axis coordinates are transformed into component axis coordinates.

X_j = Component axis X coordinate at j^{th} connection point
 Y_j = Component axis Y coordinate at j^{th} connection point
 Z_j = Component axis Z coordinate at j^{th} connection point
 DX_j = Velocity of component axis X coordinate at j^{th} connection point
 DY_j = Velocity of component axis Y coordinate at j^{th} connection point
 DZ_j = Velocity of component axis Z coordinate at j^{th} connection point

Section 8 (lines 194 thru 239) - Element Resultant Vector Magnitude - Component Component Coordinate System

Landing gear attachment point location vectors are calculated in this part of the program, and then used to determine the displacements and velocities of the attachment point.

ER_{ij} = The j^{th} component of the location vector at the i^{th} attachment point
D_{ij} = The j^{th} component of the displacement vector at the i^{th} attachment point
DD_{ij} = The j^{th} component of the velocity vector at the i^{th} attachment point

Section 9 (lines 240 thru 291) - Element Force Equations

This portion of the program calculates the landing gear forces in the component coordinate system.

FC_{jX} = Force in X direction at j^{th} attachment point
FC_{jY} = Force in Y direction at j^{th} attachment point
FC_{jZ} = Force in Z direction at j^{th} attachment point

Section 10 (lines 202 thru 345) - Back Transformation Component Axis to Body Axis

In this section of the transformation matrix that transforms component coordinates into body coordinates is calculated and used to determine the landing gear forces in the body coordinate system.

T_{aij} = The ij^{th} element of the matrix that transforms the a^{th} component

Landing gear component letter to number correspondence

(A=1, B=2, C=3, D=4)

F_{aj} = Force in the a^{th} direction at the j^{th} attachment

The remaining portions of the program are used to determine:

Print interval

Integration step interval

End of run

Variable to be printed and/or plotted

The instructions for changing any of the statements in this section can be found in the Mimic Programming Manual³⁹.

MIMIC SOURCE-LANGUAGE PROGRAM
VERSION 1 10/01/68 MOD LEVEL 0001

SYSTEM CONSTANTS

```
CON(M,JP,JQ,JR)
CON(IA1,IB1,IC1)
CON(IA2,IB2,IC2)
CON(IA3,IB3,IC3)
CON(IA4,IB4,IC4)
CON(AA,BA,CA,AB,BB,CB)
CON(AC,BC,CC,AD,BD,CD)
CON(XC1,YC1,ZC1)
CON(XC2,YC2,ZC2)
CON(XC3,YC3,ZC3)
CON(XC4,YC4,ZC4)
```

SYSTEM PARAMETERS

```
PAR(IDXB,IXB,IDX8,IX8,IDX9,IX9)
PAR(IP,IQ,IR)
PAR(IDXB1,IDX81,IDX91,IDXB2,IDX82,IDX92)
PAR(IDXB3,IDX83,IDX93,IDXB4,IDX84,IDX94)
PAR(K11,K12,K13,B11,B12,B13)
PAR(K21,K22,K23,B21,B22,B23)
PAR(K31,K32,K33,B31,B32,B33)
PAR(K41,K42,K43,B41,B42,B43)
PAR(ZD1,ZD2,ZD3,ZD4)
```

LANDING CONFIGURATION LOGIC

LV1	FSW(ZD1, FALSE, FALSE, TRUE)
LV2	FSW(ZD2, FALSE, FALSE, TRUE)
LV3	FSW(ZD3, FALSE, FALSE, TRUE)
LV4	FSW(ZD4, FALSE, FALSE, TRUE)
I	LSW(LV1,1.,0.)
J	LSW(LV2,1.,0.)
K	LSW(LV3,1.,0.)
L	LSW(LV4,1.,0.)
F11	FX1*I
F12	FY1*I
F13	FZ1*I
F21	FX2*J
F22	FY2*J
F23	FZ2*J
F31	FX3*K

F32	FY3*K
F33	FZ3*K
F41	FX4*L
F42	FY4*L
F43	FZ4*L

EQUATIONS OF MOTION - BODY CRDT. SYSTEM

G	32.2
2DXB	(+F11+F21+F31+F41)/M
1DXB	INT(2DXB,IDX8)
XB	INT(1DXB,IXB)
2DYB	(+F12+F22+F32+F42)/M
1DYB	INT(2DYB,IDX8)
YB	INT(1DYB,IYB)
2DZB	(+F13+F23+F33+F43+M*G)/M
1DZB	INT(2DZB,IDX8)
ZB	INT(1DZB,IZB)
DP1	(BA*F13+BB*F23+BC*F33+BD*F43)/JP
DP2	(-CA*F12-CB*F22-CC*F32-CD*F42)/JP
DP	DP1+DP2
P	INT(DP,IP)
PDISP	INT(P,0.)
DQ1	(-AA*F13-AB*F23-AC*F33-AD*F43)/JQ
DQ2	(CA*F11+CB*F21+CC*F31+CD*F41)/JQ
DQ	DQ1+DQ2
Q	INT(DQ,IQ)
QDISP	INT(Q,0.)
DR1	(-BA*F11-BB*F21-BC*F31-BD*F41)/JR
DR2	(AA*F12+AB*F22+AC*F32+AD*F42)/JR
DR	DR1+DR2
R	INT(DR,IR)
RDISP	INT(R,0.)
DU	2DXB
U	1DXB
DV	2DYB
V	1DYB
DW	2DZB
W	1DZB
2DXB1	DU+Q*W-R*V+CA*(DQ+R*P)-BA*(DR-Q*P)-AA*(Q*Q+R*R)
1DXB1	INT(2DXB1,IDX8)
XB1	INT(1DXB1,IXB)
IXB1	INT(1DXB1,0.,TRUE,LV1)
2DYB1	DV+R*U-P*W+AA*(DR+P*Q)-CA*(DP-R*Q)-BA*(R*R+P*P)
1DYB1	INT(2DYB1,IDX8)
YB1	INT(1DYB1,IYB)
IYB1	INT(1DYB1,0.,TRUE,LV1)
2DZB1	DW+P*V-Q*U+BA*(DP+Q*R)-AA*(DQ-P*R)-CA*(P*P+Q*Q)
1DZB1	INT(2DZB1,IDX8)
ZB1	INT(1DZB1,IZB)
IZB1	INT(1DZB1,0.,TRUE,LV1)

2DXB2 $DU + Q*W - R*V + CB * (DQ + R*P) - BB * (DR - Q*P) - AB * (Q*Q + R*R)$
 1DXB2 INT(2DXB2,IDX82)
 XB2 INT(1DXB2,IXB)
 IXB2 INT(1DXB2,0.,TRUE,LV2)
 2DYB2 DV + R*U - P*W + AB * (DR + P*Q) - CB * (DP - R*Q) - BB * (R*R + P*P)
 1DYB2 INT(2DYB2,IDX82)
 YB2 INT(1DYB2,IYB)
 IYB2 INT(1DYB2,0.,TRUE,LV2)
 2DZB2 DW + P*V - Q*U + BB * (DP + Q*R) - AB * (DQ - P*R) - CB * (P*P + Q*Q)
 1DZB2 INT(2DZB2,IDX82)
 ZB2 INT(1DZB2,IZB)
 IZB2 INT(1DZB2,0.,TRUE,LV2)
 2DXB3 DU + Q*W - R*V + CC * (DQ + R*P) - BC * (DR - Q*P) - AC * (Q*Q + R*R)
 1DXB3 INT(2DXB3,IDX83)
 XB3 INT(1DXB3,IXB)
 IXB3 INT(1DXB3,0.,TRUE,LV3)
 2DYB3 DV + R*U - P*W + AC * (DR + P*Q) - CC * (DP - R*Q) - BC * (R*R + P*P)
 1DYB3 INT(2DYB3,IDX83)
 YB3 INT(1DYB3,IYB)
 IYB3 INT(1DYB3,0.,TRUE,LV3)
 2DZB3 DW + P*V - Q*U + BC * (DP + Q*R) - AC * (DQ - P*R) - CC * (P*P + Q*Q)
 1DZB3 INT(2DZB3,IDX83)
 ZB3 INT(1DZB3,IZB)
 IZB3 INT(1DZB3,0.,TRUE,LV3)
 2DXB4 DU + Q*W - R*V + CD * (DQ + R*P) - BD * (DR - Q*P) - AD * (Q*Q + R*R)
 1DXB4 INT(2DXB4,IDX84)
 XB4 INT(1DXB4,IXB)
 IXB4 INT(1DXB4,0.,TRUE,LV4)
 2DYB4 DV + R*U - P*W + AD * (DR + P*Q) - CD * (DP - R*Q) - BD * (R*R + P*P)
 1DYB4 INT(2DYB4,IDX84)
 YB4 INT(1DYB4,IYB)
 IYB4 INT(1DYB4,0.,TRUE,LV4)
 2DZB4 DW + P*V - Q*U + BD * (DP + Q*R) - AD * (DQ - P*R) - CD * (P*P + Q*Q)
 1DZB4 INT(2DZB4,IDX84)
 ZB4 INT(1DZB4,IZB)
 IZB4 INT(1DZB4,0.,TRUE,LV4)
 ROTATION ANGLE EQUATIONS
 A - PS1
 B - THETA
 C - PH1

DA $Q * \text{SIN}(A) / \text{COS}(B) + R * \text{COS}(A) / \text{COS}(B)$
 A INT(DA,0.)
 DB $Q * \text{COS}(C) - R * \text{SIN}(C)$
 B INT(DB,0.)
 DC $P + Q * \text{SIN}(B) * \text{SIN}(C) / \text{COS}(B) + R * \text{SIN}(B) * \text{COS}(C) / \text{COS}(B)$
 C INT(DC,0.)
 PI 3.141592653
 A1 A + IA1
 A2 A + IA2 - PI
 A3 A + IA3
 A4 A + IA4 + PI

B1	B+IB1
B2	B+IB2
B3	B+IB3
B4	B+IB4
C1	C+IC1
C2	C+IC2
C3	C+IC3
C4	C+IC4
INITIAL COORDINATE TRANSFORMATION	
DISPLACEMENT TRANSFORMATION	
X1	COS(IA1)*IXB1+SIN(IA1)*IYB1
Y1	-SIN(IA1)*IXB1+COS(IA1)*IYB1
Z1	IZB1
X2	COS(IA2)*IXB2+SIN(IA2)*IYB2
Y2	-SIN(IA2)*IXB2+COS(IA2)*IYB2
Z2	IZB2
X3	COS(IA3)*IXB3+SIN(IA3)*IYB3
Y3	-SIN(IA3)*IXB3+COS(IA3)*IYB3
Z3	IZB3
X4	COS(IA4)*IXB4+SIN(IA4)*IYB4
Y4	-SIN(IA4)*IXB4+COS(IA4)*IYB4
Z4	IZB4
VELOCITY TRANSFORMATION	
DX1	(COS(IA1)*1DXB1+SIN(IA1)*1DYB1)*I
DY1	(-SIN(IA1)*1DXB1+COS(IA1)*1DYB1)*I
DZ1	(1DZB1)*I
DX2	(COS(IA2)*1DXB2+SIN(IA2)*1DYB2)*J
DY2	(-SIN(IA2)*1DXB2+COS(IA2)*1DYB2)*J
DZ2	(1DZB2)*J
DX3	(COS(IA3)*1DXB3+SIN(IA3)*1DYB3)*K
DY3	(-SIN(IA3)*1DXB3+COS(IA3)*1DYB3)*K
DZ3	(1DZB3)*K
DX4	(COS(IA4)*1DXB4+SIN(IA4)*1DYB4)*L
DY4	(-SIN(IA4)*1DXB4+COS(IA4)*1DYB4)*L
DZ4	(1DZB4)*L
ELEMENT RESULTANT VECTOR MAGNITUDE	
COMPONENT CRDT. SYSTEM	
ER11	SQR((XC1+X1)*(XC1+X1)+Y1*Y1+Z1*Z1)
ER12	SQR(X1*X1+(YC1+Y1)*(YC1+Y1)+Z1*Z1)
ER13	SQR(X1*X1+Y1*Y1+(ZC1-Z1)*(ZC1-Z1))
ER21	SQR((XC2+X2)*(XC2+X2)+Y2*Y2+Z2*Z2)
ER22	SQR(X2*X2+(YC2+Y2)*(YC2+Y2)+Z2*Z2)
ER23	SQR(X2*X2+Y2*Y2+(ZC2-Z2)*(ZC2-Z2))
ER31	SQR((XC3+X3)*(XC3+X3)+Y3*Y3+Z3*Z3)
ER32	SQR(X3*X3+(YC3+Y3)*(YC3+Y3)+Z3*Z3)
ER33	SQR(X3*X3+Y3*Y3+(ZC3-Z3)*(ZC3-Z3))
ER41	SQR((XC4+X4)*(XC4+X4)+Y4*Y4+Z4*Z4)
ER42	SQR(X4*X4+(YC4+Y4)*(YC4+Y4)+Z4*Z4)
ER43	SQR(X4*X4+Y4*Y4+(ZC4-Z4)*(ZC4-Z4))
DISPLACEMENT EQUATIONS	
D11	XC1-ER11

D12	YC1-ER12
D13	ER13-ZC1
D21	XC2-ER21
D22	YC2-ER22
D23	ER23-ZC2
D31	XC3-ER31
D32	YC3-ER32
D33	ER33-ZC3
D41	XC4-ER41
D42	YC4-ER42
D43	ER43-ZC4

VELOCITY EQUATIONS

DD11	-(DX1*(XC1+X1)+DY1*Y1+DZ1*Z1)/ER11
DD12	-(DX1*X1+DY1*(YC1+Y1)+DZ1*Z1)/ER12
DD13	-(DX1*X1+DY1*Y1+DZ1*(ZC1-Z1))/ER13
DD21	-(DX2*(XC2+X2)+DY2*Y2+DZ2*Z2)/ER21
DD22	-(DX2*X2+DY2*(YC2+Y2)+DZ2*Z2)/ER22
DD23	-(DX2*X2+DY2*Y2+DZ2*(ZC2-Z2))/ER23
DD31	-(DX3*(XC3+X3)+DY3*Y3+DZ3*Z3)/ER31
DD32	-(DX3*X3+DY3*(YC3+Y3)+DZ3*Z3)/ER32
DD33	-(DX3*X3+DY3*Y3+DZ3*(ZC3-Z3))/ER33
DD41	-(DX4*(XC4+X4)+DY4*Y4+DZ4*Z4)/ER41
DD42	-(DX4*X4+DY4*(YC4+Y4)+DZ4*Z4)/ER42
DD43	-(DX4*X4+DY4*Y4+DZ4*(ZC4-Z4))/ER43

ELEMENT FORCE EQUATIONS

COMPONENT CRDT SYSTEM

FC1XA	(K11*D11+B11*DD11)*(XC1+X1)/ER11
FC1XB	(K12*D12+B12*DD12)*X1/ER12
FC1XC	(K13*D13+B13*DD13)*X1/ER13
FC2XA	(K21*D21+B21*DD21)*(XC2+X2)/ER21
FC2XB	(K22*D22+B22*DD22)*X2/ER22
FC2XC	(K23*D23+B23*DD23)*X2/ER23
FC3XA	(K31*D31+B31*DD31)*(XC3+X3)/ER31
FC3XB	(K32*D32+B32*DD32)*X3/ER32
FC3XC	(K33*D33+B33*DD33)*X3/ER33
FC4XA	(K41*D41+B41*DD41)*(XC4+X4)/ER41
FC4XB	(K42*D42+B42*DD42)*X4/ER42
FC4XC	(K43*D43+B43*DD43)*X4/ER43
FC1X	FC1XA+FC1XB+FC1XC
FC2X	FC2XA+FC2XB+FC2XC
FC3X	FC3XA+FC3XB+FC3XC
FC4X	FC4XA+FC4XB+FC4XC
FC1YA	(K11*D11+B11*DD11)*Y1/ER11
FC1YB	(K12*D12+B12*DD12)*(YC1+Y1)/ER12
FC1YC	(K13*D13+B13*DD13)*Y1/ER13
FC2YA	(K21*D21+B21*DD21)*Y2/ER21
FC2YB	(K22*D22+B22*DD22)*(YC2+Y2)/ER22
FC2YC	(K23*D23+B23*DD23)*Y2/ER23
FC3YA	(K31*D31+B31*DD31)*Y3/ER31
FC3YB	(K32*D32+B32*DD32)*(YC3+Y3)/ER32
FC3YC	(K33*D33+B33*DD33)*Y3/ER33

FC4YA $(K41*D41+B41*DD41)*Y4/ER41$
 FC4YB $(K42*D42+B42*DD42)*(YC4+Y4)/ER42$
 FC4YC $(K43*D43+B43*DD43)*Y4/ER43$
 FC1Y $FC1YA+FC1YB+FC1YC$
 FC2Y $FC2YA+FC2YB+FC2YC$
 FC3Y $FC3YA+FC3YB+FC3YC$
 FC4Y $FC4YA+FC4YB+FC4YC$
 FC1ZA $(K11*D11+B11*DD11)*Z1/ER11$
 FC1ZB $(K12*D12+B12*DD12)*Z1/ER12$
 FC1ZC $(K13*D13+B13*DD13)*(ZC1-Z1)/ER13$
 FC2ZA $(K21*D21+B21*DD21)*Z2/ER21$
 FC2ZB $(K22*D22+B22*DD22)*Z2/ER22$
 FC2ZC $(K23*D23+B23*DD23)*(ZC2-Z2)/ER23$
 FC3ZA $(K31*D31+B31*DD31)*Z3/ER31$
 FC3ZB $(K32*D32+B32*DD32)*Z3/ER32$
 FC3ZC $(K33*D33+B33*DD33)*(ZC3-Z3)/ER33$
 FC4ZA $(K41*D41+B41*DD41)*Z4/ER41$
 FC4ZB $(K42*D42+B42*DD42)*Z4/ER42$
 FC4ZC $(K43*D43+B43*DD43)*(ZC4-Z4)/ER43$
 FC1Z $FC1ZA+FC1ZB+FC1ZC$
 FC2Z $FC2ZA+FC2ZB+FC2ZC$
 FC3Z $FC3ZA+FC3ZB+FC3ZC$
 FC4Z $FC4ZA+FC4ZB+FC4ZC$
 BACK TRANSFORMATION COMPONENT AXIS TO BODY AXIS
 TA11 $\cos(B1)*\cos(A1)$
 TA12 $\cos(B1)*\sin(A1)$
 TA13 $-\sin(B1)$
 TA21 $\sin(C1)*\sin(B1)*\cos(A1)-\cos(C1)*\sin(A1)$
 TA22 $\sin(C1)*\sin(B1)*\sin(A1)+\cos(C1)*\cos(A1)$
 TA23 $\sin(C1)*\cos(B1)$
 TA31 $\cos(C1)*\sin(B1)*\cos(A1)+\sin(C1)*\sin(A1)$
 TA32 $\cos(C1)*\sin(B1)*\sin(A1)-\sin(C1)*\cos(A1)$
 TA33 $\cos(C1)*\cos(B1)$
 TB11 $\cos(B2)*\cos(A2)$
 TB12 $\cos(B2)*\sin(A2)$
 TB13 $-\sin(B2)$
 TB21 $\sin(C2)*\sin(B2)*\cos(A2)-\cos(C2)*\sin(A2)$
 TB22 $\sin(C2)*\sin(B2)*\sin(A2)+\cos(C2)*\cos(A2)$
 TB23 $\sin(C2)*\cos(B2)$
 TB31 $\cos(C2)*\sin(B2)*\cos(B2)+\sin(C2)*\sin(A2)$
 TB32 $\cos(C2)*\sin(B2)*\sin(A2)-\sin(C2)*\cos(A2)$
 TB33 $\cos(C2)*\cos(B2)$
 TRANSFORMATION MATRIX ELEMENTS
 TC11 $\cos(B3)*\cos(A3)$
 TC12 $\cos(B3)*\sin(A3)$
 TC13 $-\sin(B3)$
 TC21 $\sin(C3)*\sin(B3)*\cos(A3)-\cos(C3)*\sin(A3)$
 TC22 $\sin(C3)*\sin(B3)*\sin(A3)+\cos(C3)*\cos(A3)$
 TC23 $\sin(C3)*\cos(B3)$
 TC31 $\cos(C3)*\sin(B3)*\cos(B3)+\sin(C3)*\sin(A3)$
 TC32 $\cos(C3)*\sin(B3)*\sin(A3)-\sin(C3)*\cos(A3)$

```

TC33    COS(C3)*COS(B3)
TD11    COS(B4)*COS(A4)
TD12    COS(B4)*SIN(A4)
TD13    -SIN(B4)
TD21    SIN(C4)*SIN(B4)*COS(A4)-COS(C4)*SIN(A4)
TD22    SIN(C4)*SIN(B4)*SIN(A4)+COS(C4)*COS(A4)
TD23    SIN(C4)*COS(B4)
TD31    COS(C4)*SIN(B4)*COS(B4)+SIN(C4)*SIN(A4)
TD32    COS(C4)*SIN(B4)*SIN(A4)-SIN(C4)*COS(A4)
TD33    COS(C4)*COS(B4)
FORCE EQUATIONS - BODY CRDT. SYSTEM
FX1     TA11*FC1X+TA12*FC1Y+TA13*FC1Z
FY1     TA21*FC1X+TA22*FC1Y+TA23*FC1Z
FZ1     TA31*FC1X+TA32*FC1Y+TA33*FC1Z
FX2     TB11*FC2X+TB12*FC2Y+TB13*FC2Z
FY2     TB21*FC2X+TB22*FC2Y+TB23*FC2Z
FZ2     TB31*FC2X+TB32*FC2Y+TB33*FC2Z
FX3     TC11*FC3X+TC12*FC3Y+TC13*FC3Z
FY3     TC21*FC3X+TC22*FC3Y+TC23*FC3Z
FZ3     TC31*FC3X+TC32*FC3Y+TC33*FC3Z
FX4     TD11*FC4X+TD12*FC4Y+TD13*FC4Z
FY4     TD21*FC4X+TD22*FC4Y+TD23*FC4Z
FZ4     TD31*FC4X+TD32*FC4Y+TD33*FC4Z
DT     .01
DTMIN   .0001
FIN(T,2.)
OUT(T,Z1,Z2,Z3,Z4)
OUT(FX1,FY1,FZ1,FX3,FY3,FZ3)
OUT(FX2,FY2,FZ2,FX4,FY4,FZ4)
OUT(FC1X,FC1Y,FC1Z,FC3X,FC3Y,FC3Z)
OUT(FC2X,FC2Y,FC2Z,FC4X,FC4Y,FC4Z)
OUT(XB,YB,ZB,PDISP,QDISP,RDISP)
OUT(2DXB,1DXB,2DYB,1DYB,2DZB,1DZB)
OUT(P,Q,R,A,B,C)
PL0(T,ZB,PDISP,FZ1,FZ3)
END

```